

Mathematics 18.337
(Cross listed as 18.337/6.338 in 1997)

Parallel Scientific Computing
Spring 1996

Lecturer: Alan Edelman¹
MIT

¹Department of Mathematics and Laboratory for Computer Science. Room 2-380, Massachusetts Institute of Technology, Cambridge, MA 02139, Email: edelman@math.mit.edu, <http://theory.lcs.mit.edu/~edelman>

Preface

These lecture notes (under development and constant revision, like the field itself) have been used at MIT in a graduate course first offered by Alan Edelman and Shang-Hua Teng during the spring of 1994 (MIT 18.337, Parallel Scientific Computing). This first class had about forty students from a variety of disciplines which include Applied Mathematics, Computer Science, Mechanical Engineering, Chemical Engineering, Aeronautics and Aerospace, and Applied Physics. Because of the diverse backgrounds of the students, the course, by necessity, was designed to be of interest to engineers, computer scientists, and applied mathematicians.

Our course covers a mixture of material that we feel students should be exposed to. Our primary focus is on modern numerical algorithms for scientific computing, and also on the historical trends in architectures. At the same time, we have always felt that students (and the professors) must suffer through hands-on experience with modern parallel machines. Some students enjoy fighting new machines; others scream and complain. This is the reality of the subject. In 1995, the course was taught again by Alan Edelman with an additional emphasis on the use of portable parallel software tools. The sad truth was that there were not yet enough fully developed tools to be used. The situation is currently improving.

During 1994 and 1995 our students programmed the 128 node Connection Machine CM5. This machine was the 35th most powerful computer in the world in 1994, then the very same machine was the 74th most powerful machine in the spring of 1995. At the time of writing, December 1995, this machine has sunk to position 136. The fastest machine in the world is currently in Japan. In the upcoming 1996 course we plan to use a new machine.

In addition to coauthors Shang-Hua Teng and Robert Schreiber, I would like to thank our numerous students who have written and commented on these notes and have also prepared many of the diagrams. We also thank the students from Minnesota SCIC 8001 and the summer course held at MIT, Summer 6.50s (also taught by Rob Schreiber) for all of their valuable suggestions. These notes will probably evolve into a book which will eventually be coauthored by Rob Schreiber and Shang-Hua Teng. Meanwhile, we are fully aware that the 1996 notes are incomplete, contain mathematical and grammatical errors, and do not cover everything we wish. They are an improvement over the 1995 notes, but not as good as the 1997 notes will be. I view these notes as a basis on which to improve, not as a completed book.

It has been our experience that some students of pure mathematics and theoretical computer science are a bit fearful of programming real parallel machines. Students of engineering and computer science are sometimes intimidated by mathematics. The most successful students understand that computing is not “dirty” and mathematical knowledge is not “scary” or “useless,” but both require hard work and maturity to master. The good news is that there are many jobs both in the industrial and academic sectors for experts in the field!

A good course should have a good theme. We try to emphasize the fundamental algorithmic ideas and machine design principles. We have seen computer vendors come and go, but we believe that the mathematical, algorithmic, and numerical ideas discussed in these notes provide a solid foundation that will last for many years.

Contents

1	Introduction	1
1.1	A General Look at the Industry	1
1.2	The Web as a Tool for Tracking Machines	3
1.3	Scientific Computing and High Performance Computing	3
1.4	A Natural 3D Problem	3
1.5	Components of a Parallel System	4
1.6	Scientific Algorithms	4
1.7	Applications	5
1.8	History, State-of-Art, and Perspective	5
1.9	Parallel Computing: An Example	6
1.10	Exercises	7

I Mathematical Foundations **9**

2	Linear Algebra	11
2.1	Linear Algebra	11
3	Function Expansions	13
3.1	Function Representation and Expansions	13
3.2	A close look at shifts and flips	14
3.3	Harmonic expansions in 3-dimensions	14
3.4	Exercises	14
4	Graph Theory	17
5	Elementary Geometry	19
6	Probability Theory	21

II Parallelism **22**

7	Parallel Machines	23
7.1	Characteristics of Parallel Computers	23
7.1.1	SIMD v. MIMD	25

7.1.2	Programming Model	25
7.1.3	Machine Topology	26
7.1.4	Homogeneous and heterogeneous machines	27
7.2	Architecture of the CM-5	29
8	Parallel Programming	31
8.1	Programming style	31
8.2	Data Parallel Programming in High Performance Fortran	32
8.2.1	Parallelism	35
8.2.2	Intrinsics	35
8.2.3	Extended data parallelism	36
8.3	Message Passing	36
8.3.1	Sending and receiving	37
8.3.2	Tags and communicators	39
8.3.3	Who am I?	40
8.3.4	Performance, and tolerance	41
8.3.5	Who's got the floor?	42
8.4	Message Passing in PVM	44
8.4.1	PVM Basics	44
8.5	More on Message Passing	46
8.5.1	Nomenclature	46
8.5.2	The Development of Message Passing	47
8.5.3	Machine Characteristics	47
8.5.4	CM-5 /CMOST Environment:	48
8.6	Mechanics of Message Passing :	48
8.6.1	Sending and receiving	48
8.6.2	Bidirectional transfers:	50
8.6.3	Adding send side buffering:	50
8.6.4	'One touch' non blocking messaging	50
8.6.5	Optimizing for repetitive communications patterns: channels.	51
8.6.6	Observations on standard message passing:	52
8.7	Non-traditional messaging: Active Messages and Ports	52
8.7.1	Active Messages:	53
8.7.2	Observations on Active messages:	53
8.7.3	Rports	54
8.7.4	Observations on Rports:	55
8.7.5	Miscellaneous caveats regarding Active Messages and Rports:	55
8.7.6	Conclusions on message passing	56
9	Modeling Parallel Algorithms	57
10	Primitives	59
10.1	Parallel Prefix	59
10.2	Segmented Scan	61
10.3	Sorting and Selection	61
10.4	FFT	63
10.4.1	Data motion	64
10.4.2	FFT on parallel machines	65

10.4.3 Exercise	66
10.5 Matrix Multiplication	66
10.6 Basic Data Communication Operations	67

III Multipole Methods 68

11 Particle Methods	69
11.1 Reduce and Broadcast: A function viewpoint	69
11.2 Particle Methods: An Application	70
11.3 Outline	70
11.4 What is N-Body Simulation?	70
11.5 Examples	70
11.6 The Basic Algorithm	71
11.6.1 Finite Difference and the Euler Method	72
11.7 Methods for Force Calculation	73
11.7.1 Direct force calculation	73
11.7.2 Potential based calculation	73
11.7.3 Poisson Methods	74
11.7.4 Hierarchical methods	75
11.8 Quadtree (2D) and Octree (3D) : Data Structures for Canonical Clustering	76
11.9 Barnes-Hut Method (1986)	77
11.9.1 Approximating potentials	79
11.10 Outline	80
11.11 Introduction	80
11.12 Multipole Algorithm: An Overview	81
11.13 Multipole Expansion	81
11.14 Taylor Expansion	83
11.15 Operation No.1 — SHIFT	84
11.16 Operation No.2 — FLIP	86
11.17 Application on Quad Tree	87
11.18 Expansion from 2-D to 3-D	89
11.19 Parallel Implementation	90

IV Numerical Linear Algebra 91

12 Numerical Discretization	93
12.1 Mathematical Modeling and Numerical Methods	93
12.1.1 PDEs for Modeling	93
12.1.2 Numerical Methods	94
12.2 Well-Shaped Meshes	95
12.3 From PDEs to Systems of Linear Equations	96
12.3.1 Finite Difference Approximations	96
12.3.2 Finite Element Approximations	97

13	Dense Linear Algebra	101
13.1	Outline	101
13.2	Introduction	101
13.3	Applications	101
13.4	Records	102
13.5	Software Libraries	102
13.6	Software Engineering	103
14	Sparse Linear Algebra	107
14.1	Cyclic Reduction for Structured Sparse Linear Systems	107
14.2	Sparse Direct Methods	109
14.2.1	LU Decomposition and Gaussian Elimination	109
14.2.2	Parallel Factorization: the Multifrontal Algorithm	112
14.3	Basic Iterative Methods	113
14.3.1	Jacobi Method	114
14.3.2	Gauss-Seidel Method	114
14.3.3	Splitting Matrix Method	114
14.3.4	Weighted Splitting Matrix Method	115
14.4	Red-Black Ordering for parallel Implementation	115
14.5	Conjugate Gradient Method	116
14.6	Preconditioning	116
14.7	Main Issues	118
14.8	Efficient sparse matrix algorithms	118
14.8.1	Scalable algorithms	118
14.8.2	Cholesky factorization	120
14.8.3	Distributed sparse Cholesky and the model problem	121
14.8.4	Parallel Block-Oriented Sparse Cholesky Factorization	122
14.9	Load balance with cyclic mapping	122
14.9.1	Empirical Load Balance Results	122
14.10	Heuristic Remapping	124
14.11	Scheduling Local Computations	126
15	Domain Decomposition for PDE	127
15.1	Geometric Issues	129
15.1.1	Overlapping vs Non-overlapping regions	129
15.1.2	Geometric Discretization	130
15.2	Algorithmic Issues	130
15.2.1	Schwarz approaches: additive vs multiplicative	131
15.2.2	Substructuring Approaches	133
15.2.3	Accerlerants	135
15.3	Theoretical Issues	136
15.4	A Domain Decomposition Assignment: Decomposing MIT	136
16	Multilevel Methods	139
16.1	Multigrids	139
16.1.1	The Basic Idea	139
16.1.2	Restriction and Interpolation	139
16.1.3	The Multigrid Scheme	141

V	Graph and Geometric Algorithms	142
17	Partitioning and Load Balancing	143
17.1	Motivation from the Parallel Sparse Matrix Vector Multiplication	143
17.2	Separators	144
17.3	Spectral Partitioning – One way to slice a problem in half	144
17.3.1	Electrical Networks	144
17.3.2	Laplacian of a Graph	145
17.3.3	Spectral Partitioning	146
17.4	Geometric Methods	148
17.4.1	Geometric Graphs	153
17.4.2	Geometric Partitioning: Algorithm and Geometric Modeling	154
17.4.3	Other Graphs with small separators	156
17.4.4	Other Geometric Methods	157
17.4.5	Partitioning Software	158
17.5	Load-Balancing N-body Simulation for Non-uniform Particles	158
17.5.1	Hierarchical Methods of Non-uniformly Distributed Particles	158
17.5.2	The Communication Graph for N-Body Simulations	159
17.5.3	Near-Field Graphs	163
17.5.4	N-body Communication Graphs	164
17.5.5	Geometric Modeling of N-body Graphs	164
18	Mesh Generation	165
18.1	How to Describe a Domain?	166
18.2	Types of Meshes	167
18.3	Refinement Methods	168
18.3.1	Hierarchical Refinement	168
18.3.2	Delaunay Triangulation	169
18.3.3	Delaunay Refinement	170
VI	Selected Topics	172
19	The Pentium Bug	173
19.1	About These Notes on The Pentium Bug	173
19.2	The Discovery of The Bug	173
19.3	The Pentium Bug	173
19.4	Introduction	174
19.5	SRT Division	175
19.6	Understanding why SRT works	175
19.7	Quotient digit selection on the Pentium	176
19.8	Analyzing the bug	179
19.8.1	It is not easy to reach the buggy entry	179
19.9	The “Send More Money” Puzzle for the Pentium	181
19.10	At least nine steps to failure	182

19.11	Acknowledgement	183
19.12	Conclusions	183
20	Network Topologies	185
21	Topology Based Parallel Algorithms	187
21.1	Overview	187
21.2	Interprocessor Communication and the Hypercube Graph	187
21.2.1	The Gray Code and Other Embeddings of the Hypercube	188
21.2.2	Going Beyond Embedded Cycles	189
21.2.3	Hypercube theory: Unique Edge-Disjoint Hamiltonian Cycles in a Hypercube	190
21.2.4	An Application: Matrix Multiplication on a Grid	191
21.2.5	The Direct N-Body problem on a Hypercube	195
21.2.6	The Hamming Sum	196
21.2.7	Extending Gray Code-directed Body Movement to Multiple Sets of Bodies .	196
21.2.8	Matrix Multiplication using all Hypercube Wires	198
21.2.9	Matrix Multiplication using the Cartesian Product	198
21.3	References	198
22	Scalable Algorithms	201
22.1	Scalability, Communication Cost, and Matrix-Vector Product	201
22.1.1	Sparse Matrices	204
22.1.2	Parallel iterative Solvers	204
23	Scheduling on Parallel Machines	207
24	Shared Memory Computations	209
25	Scientific Libraries	211
25.1	Scientific Libraries	211

Chapter 1

Introduction

This class strives to study that elusive mix of theory and practice so important for understanding modern scientific computing. We try to cover it all, from the engineering aspects of computer science (parallel architectures, vendors, parallel languages, and tools) to the mathematical understanding of numerical algorithms, and also certain aspects from theoretical computer science.

1.1 A General Look at the Industry

This is a science course at MIT, but somehow it seems appropriate to wonder how special purpose parallel computation really is. Maybe this sort of analysis more properly belongs in the introduction to a business school case study.

Is it correct to conclude that there will never be an enormous market for parallel computers? We are certain that parallel computers will be everywhere. The editorial below may not immediately substantiate my conclusion, but it does illustrate the famous quote (Kipling?) that many people look at what is and ask why, while it is wiser to look at what isn't and ask why not.

Editorial on markets for technology: We probably all have our favorite examples. How many of us have heard that there will never be a large market for computers. Only “nerds” would have a computer in the living room. I for one have systematically heard that 1) only nerds would communicate by electronic mail, 2) French people would never embrace electronic mail, and 3) lawyers would never accept electronic mail. I suspect that 100 years ago people might have thought that nobody would want a telephone in their living rooms. The surest way to be wrong is to reason that nobody is buying it now hence nobody will ever buy it.

Some books might start with a machine and a programming language. This is a mistake. The machines have been changing and the programming languages are maturing, but still in 1996 the subject is in a state of flux. Many machines are still not as usable as people would want. Quite likely, too many companies have been trying to create their own proprietary products.

Editorial on proprietary products: Look at the fast evolving world wide web. For years we wondered why we were all content to live with `ftp`. One of us used to ask why my bank account balance was unavailable from my workstation. The other now wonders why his telephone is not an integrated part of his workstation. Somehow, just now, the infrastructure and the public's perception is right for the internet to catch on, not only for techies, but for everybody.

However, an interesting phenomenon is developing. Various internet providers are attempting to be the sole owners of the internet. They are learning the hard way that attempts to own the market are doomed to failure. The realists will understand that the web is public, and a common infrastructure benefits all. Attempts to dominate the internet are doomed to failure. Bill Gates, beware!

Parallel computers do not yet have a common infrastructure, but things are improving. Nevertheless parallel machines continue to be more painful to use than serial machines.

Editorial: What do scientists and students with scientific applications want on a parallel machine? People get religious about programming languages, and among the students, even the engineering students, C is growing in importance over Fortran. Nevertheless if we had to pick four things that would make a large number of people very happy we would have to list

- A reliable High Performance Fortran Compiler
- No difficulties using the Message Passing Interface MPI
- A high quality portable common debugging and visualizing mechanism such as Thinking Machines Corporation's Prism product. It is crucial that every machine support the same product.
- A non-proprietary performance monitoring interface whose timings one can trust and allow for predictions. Vendors just do not seem to be able to solve the engineering question of providing the user with the answer to the question of just how long did the program take to execute.

[To be written: discussions about parallel libraries]

Which specific machines did we use in our class? Last year (1995) we used MIT's 128 processor CM-5, and a 12 processor SP-2. This year we expect to use the SP-2 and some Silicon Graphics machines currently located at Boston University. If we are lucky, the MIT lab for Computer Science will receive a donation of an interesting symmetric multiprocessor that we will use in our class.

Most of you may have either seen the 1993 movie or read the 1990 Michael Crichton novel *Jurassic Park*. The 1993 movie shows the CM-5 in the background of the control center and even mentions the Thinking Machines Computer, but you could easily miss it if you do not pay attention. The older novel has the dinosaur theme park controlled by a Cray vector supercomputer. Many in this field believe that the Cray belonged on the dinosaur side of the *Jurassic Park* fence!

In fact, in 1996, both vector supercomputers and proprietary, custom-engineered parallel computers may be on their way to extinction. The investments required to keep pace with evolving hardware technology can't be justified by the size of the market. At Cray, for example, the vector supercomputer (the T90) at 60 gigaflops and 8 gigabytes, is overshadowed by the new parallel machine (the T3E), based on the DEC alpha chip, which offers up to 1.2 teraflops and 4 terabytes. Kendall Square Research designed its machine from the ground up in order to exploit novel ideas about caching and memory architecture: they are now out of business. Tera Computer Company, which has followed the same business model as KSR, will very likely suffer the same fate. And the first big parallel computer company, Thinking Machines Corporation, once located on expensive Cambridge real estate near MIT, has trimmed itself, moved to less-expensive Bedford, and has emerged from bankruptcy protection. Their latest announcement has them teaming up with Sun Microsystems for software for the next generation of machines.

1.2 The Web as a Tool for Tracking Machines

For the latest info on the parallel machine market, the World Wide Web is unmatched. The address <http://www.cs.cmu.edu/~scandal/vendors.html> currently (January 1996) points to Alta Technology. Chen Systems, Convex Computer Corporation, Cray Research, Digital Equipment Corporation, Fujitsu, Hewlett-Packard, Hitachi, IBM, ICE, Intel, Meiko, NEC, Parsytec, Siemens Nixdorf, TERA Computer, and Thinking Machines Corporation.

1.3 Scientific Computing and High Performance Computing

There is no formal definition of *parallel scientific computing* and we do not intend to give one here. However, the goal of parallel scientific computing is very well defined, that is, to find faster solutions to larger and more complex problems. Parallel scientific computing is a highly interdisciplinary area ranging from numerical analysis and algorithm design to programming languages, computer architectures, software, and real applications. The participants include engineers, computer scientists, applied mathematicians, and physicists, and this team is growing.

High-performance parallel computers have become a fundamental tool for computation intensive tasks in real applications. Computer architecture is driven by technology. The advance of very large scale integration (VLSI) makes it possible to develop faster computers that have smaller physical volume. The new technology makes feasible massive parallelism. To sustain increases in computation demands, the industry must embrace multiprocessing in almost all computers, either in the format of tightly coupled multiprocessor supercomputers, or loosely coupled workstation clusters.

Scientific numerical computing plays a critical role in the development of high-performance parallel computers. It provides a class of problems that are so demanding of computational cycles, a class of problems that do not require completely “general purpose” machine, yet are rich in content and in real applications, and a class of problems that give raise challenging scientific and engineering activities ranging from mathematical modeling, algorithmic design to software/hardware/architecture development. Scientific applications were the main motivation for the development of supercomputers in the past decade. Now, parallel machines have begun to find more applications in symbolic computing, large-scale databases, and multimedia environments.

Conversely, parallel computers are the most important platforms for scientific simulation. To perform meaningful simulation within a reasonable time-span computational scientists have to make trade-offs between accuracy, time, and space. The larger memory a machine has, the more powerful it is, the less restriction and simplification we need to impose on the numerical approximation of real problems and their physical domains, and the more accurately we can solve real problems.

1.4 A Natural 3D Problem

The most challenging problems in parallel scientific computing are those in three or higher dimensions. One simple reason is that problems in higher dimensions are of a very large scale.

Parallel scientific computing itself is a three dimensional discipline whose three major dimensions are

- x = scientific and engineering applications
- y = mathematical algorithms

z = parallel architecture and programming

Our goal in the course is to provide a reliable road map to the projection of our field into the (y, z) plane!

1.5 Components of a Parallel System

The components of a parallel system are not just its hardware, architecture, and network topology. They include its operating system, parallel languages and their compilers, scientific libraries and other software tools.

Most parallel languages are defined by adding parallel extensions to well-established sequential languages, such as C and Fortran. Such extensions allow user to specify various levels of parallelism in an application program, to define and manipulate parallel data structures, and to specify message passing among parallel computing units.

Compilation has become more important for parallel systems. The purpose of a compiler is not just to transform a parallel program in a high-level description into machine-level code. The role of compiler optimization is more important. We will always have discussions about: *Are we developing methods and algorithms for a parallel machine or are we designing parallel machines for algorithm and applications?* Compiler are meant to bridge the gap between algorithm design and machine architectures. Extension of compiler techniques to run time libraries will further reduce users' concern in parallel programming.

Software libraries are important tools in the use of computers. The purpose of libraries is to enhance the productivity by providing preprogrammed functions and procedures. Software libraries provide even higher level support to programmers than high-level languages. Parallel scientific libraries embody expert knowledge of computer architectures, compilers, operating systems, numerical analysis, parallel data structures, and algorithms. They systematically choose a set of basic functions and parallel data structures, and provide highly optimized routines for these functions that carefully consider the issues of data allocation, data motion, load balancing, and numerical stability. Hence scientists and engineers can spend more time and be more focused on developing efficient computational methods for their problems. Another goal of scientific libraries is to make parallel programs portable from one parallel machine platform to another. Because of the lack, until very recently, of non-proprietary parallel programming standards, the development of portable parallel libraries has lagged far behind the need for them. There is good evidence now, however, that scientific libraries will be made more powerful in the future and will include more functions for applications to provide a better interface to real applications.

Due to the generality of scientific libraries, their functions may be more complex than needed for a particular application. Hence, they are less efficient than the best codes that take advantage of the special structure of the problem. So a programmer needs to learn how to use scientific libraries. A pragmatic suggestion is to use functions available in the scientific library to develop the first prototype and then to iteratively find the bottleneck in the program and improve the efficiency.

1.6 Scientific Algorithms

The multidisciplinary aspect of scientific computing is clearly visible in algorithms for scientific problems. A scientific algorithm can be either sequential or parallel. In general, algorithms in scientific software can be classified as graph algorithms, geometric algorithms, and numerical algorithms, and most scientific software calls on algorithms of all three types. Scientific software also makes use of advanced data structures and up-to-date user interfaces and graphics.

1.7 Applications

Parallel (numerical) methods have been used to solve problems in virtually all areas of science and engineering:

- Structural analysis and mechanical engineering.
- Computational chemistry and material science
- Computational particle physics
- Computational fluid and plasma dynamics, air and space vehicle design, and space science.
- Environment and Earth science: climate modeling, glaciology, weather forecasting, an ocean modeling.
- Structure biology and medical imaging, signal processing, drug design
- ECAD and circuit validation
- Economics and finance
- Optimization, searching and databases
- Oil and gas exploration

1.8 History, State-of-Art, and Perspective

The supercomputer industry started when Cray Research developed the Cray-1, in 1975. The massively parallel processing (MPP) industry emerged with the introduction of the CM-2 by Thinking Machines in 1985. The industry is represented by several companies including Cray Research (the T90 and the T3E), Intel Supercomputer System Division (the Paragon), Thinking Machines Corporation (the CM-5 and the Global), IBM (the SP-2), HP (the Convex Exemplar), MasPar (the MP-2), Tera (the MTA, which is also the subway system in Boston), and Silicon Graphics (the PowerChallenge). The MPP industry has received substantial support from the U.S. government. The *US High Performance Computing and Communication* program was designed to explore technologies for building and using such machines. Most MPP installations are at government research centers (e.g., NASA Ames and Los Alamos) and universities and supercomputer centers (NCSA, Pittsburgh, MSI, etc).

Achieving high performance for numerical computing for scientific applications are the main goals. Indeed, most of the benchmarks are numeric oriented such as dense linear algebra computations, as represented by the heated race for the top of Linpack benchmarks between Intel and Thinking Machines.

High performance parallel computers have begun to play an important role in science and engineering development. At the same time, the vendors of parallel supercomputers have engaged in a brand of hype unusual in science and engineering. Now that the cold war has ended, the supercomputing market in major universities and government centers is close to being saturated, at least for the moment. (Nevertheless, the U.S. Department of Energy has, this past year, purchased a massively parallel supercomputer that far exceeds the capacity of any previously built.) The parallel computing industry is evolving. There are more and more “real” demands from commercial companies. Hence the cost/efficiency trade-off is more relevant. More friendly programming environments

are desired. Other non-numeric applications such as in large databases, optimization, business and finance are in greater demand. And of course the parallel computing industry is more competitive. Workstation clusters bring new challenges to tightly coupled MPP. The parallel computing field and industry are maturing. The application domain of parallel computing is expanding.

1.9 Parallel Computing: An Example

Here is an example of a problem that one can easily imagine being performed in parallel:

A rudimentary parallel problem: Compute

$$x_1 + x_2 + \dots + x_P,$$

where x_i is a floating point number and for purposes of exposition, let us assume P is a power of 2.

Obviously, the sum can be computed in $\log P$ (base 2 is understood) steps, simply by adding neighboring pairs recursively. (The algorithm has also been called *pairwise summation* and *cascade summation*). The data flow in this computation can be thought of as a binary tree.

(Illustrate on tree.)

Nodes represent values, either input or the result of a computation. Edges communicate values from their definition to their uses.

This is an example of what is often known as a *reduce* operation. We can replace the addition operation with any associative operator to generalize. (Actually, floating point addition is not associative, leading to interesting numerical questions about the best order in which to add numbers. This is studied by Higham [46, See p. 788].)

There are so many questions though. How would you write a program to do this on P processors? Is it likely that you would want to have such a program on P processors? How would the data (the x_i) get to these processors in the first place? Would they be stored there or result from some other computation? It is far more likely that you would have $10000P$ numbers on P processors to add.

A correct parallel program is often not an efficient parallel program. A flaw in a parallel program that causes it to get the right answer *slowly* is known as a performance bug. Many beginners will write a working parallel program, obtain poor performance, and prematurely conclude that either parallelism is a bad idea, or that it is the machine that they are using which is slow.

What are the sources of performance bugs? We illustrate some of them with this little, admittedly contrived example. For this example, imagine four processors, numbered zero through three, each with its own private memory, and able to send and receive message to/from the others. As a simple approximation, assume that the time consumed by a message of size n words is $A + Bn$.

Four Bad Parallel Algorithms for Computing $1 + 2 + 3 + \dots + 10^6$ on Four Processors

1. Load imbalance. One processor has too much to do, and the others sit around waiting for it. For our problem, we could eliminate all the communication by having processor zero do all the work; but we won't see any parallel speedup with this method!
2. Excessive communication.

Processor zero has all the data which is divided into four equally sized parts each with a quarter of a million numbers. It ships three of the four parts to each of

the other processors for proper load balancing. The results are added up on each processor, and then processor 0 adds the final four numbers together.

True, there is a tiny bit of load imbalance here, since processor zero does those few last additions. But that is nothing compared with the cost it incurs in shipping out the data to the other processors. In order to get that data out onto the network, it incurs a large cost that does not drop with the addition of more processors. (In fact, since the number of messages it sends grows like the number of processors, the time spent in the initial communication will actually increase.)

3. A sequential bottleneck. Let's assume the data are initially spread out among the processors; processor zero has the numbers 1 through 250,000, etc. Assume that the owner of i will add it to the running total. So there will be no load imbalance. But assume, further, that we are constrained to add the numbers in their original order! (Sounds silly when adding, but other algorithms require exactly such a constraint.) Thus, processor one may not begin its work until it receives the sum $0 + 1 + \dots + 250,000$ from processor zero!

We are thus requiring a sequential computation: our binary summation tree is maximally unbalanced, and has height 1,000,000. It is always useful to know the critical path – the length of the longest path in the dataflow graph – of the computation being parallelized. If it is excessive, change the algorithm!

4. A scheduling problem. For this kind of performance bug, we get a better illustration by changing the problem. Let there be a 1000×1000 matrix, distributed to the four processors by columns, so that processor zero owns all of columns 1 through 250. The job is to add the columns, producing a vector of length 1000. The constraint, which makes this problem interesting, is that within each row we are required to do the addition left-to-right! So the computation in each matrix row is sequential, and the parallelism comes from the fact that there are 1000 independent row sums to be computed.

The bad algorithm has processor zero do all of its row sums, then send them all in a message of 1000 words to processor one, etc. We have chosen to defer sending the sum of the first rows until we compute the sum of the last rows, thereby sequentializing an otherwise parallel task. The right idea is to schedule high-priority tasks (the sending of sums to the next processor) sooner than lower priority tasks. The fact of the latency term A in message cost makes the optimum scheduling here tricky – single-word messages may not be ideal either.

1.10 Exercises

1. Compute the sum of 1 through 1,000,000 using HPF. This amounts to a “hello world” program on whichever machine you are using. We are not currently aware of any free distributions of HPF for workstations, so your instructor will have to suggest a computer to use.
2. Download MPI to your machine and compute the sum of 1 through 1,000,000 using C or Fortran with MPI. A number of MPI implementations may be found at <http://www.mcs.anl.gov/Projects/mpi/implementations.html> The easy to follow ten step quick start on <http://www.mcs.anl.gov/mpi/mpiinstall/node1.html#Node1> worked very easily on the MIT mathematics department's SUN network.

3. In HPF, generate 1,000,000 real random numbers and sort them. (Use `RANDOM_NUMBER` and `GRADE_UP`.)
4. (Extra Credit) Do the same in C or Fortran with MPI.
5. Set up the excessive communication situation described as the second bad parallel algorithm. Place the numbers 1 through one million in a vector on one processor. Using four processors see how quickly you can get the sum of the numbers 1 through one million.

I Mathematical Foundations

Modeling and solving complex scientific problems requires a large class of mathematical machinery. In this part of the book, we will review mathematical basics and notations in linear algebra, function expansions, and probability theory. We will also present some materials in graph theory and geometry that are important for the design and analysis of scientific algorithms.

In our course, we do not formally review this material, but we place these sections prominently in the front of the book (rather than in an appendix, say) so as to emphasize the importance of mathematical foundations.

Chapter 2

Linear Algebra

2.1 Linear Algebra

Linear algebraists often like to believe that every scientific application, once discretized, becomes a linear algebra problem. Though many applications have no linear algebra at all in them, there is no question that linear algebra at least covers a very large fraction of applications. Here we intend to review the most important ideas of the field that are needed to follow the lecture notes. Meanwhile, a good text such as the elementary treatment by Strang or the numerical coverage by Golub and van Loan [40] should be consulted.

Experience has taught me that the first idea that students forget is the concept of eigenvalues. An eigenvalue is simply a number λ such that $Ax = \lambda x$. If a matrix has a full set of eigenvectors, this can be expressed with the notation $AX = X\Lambda$, where the columns of X are the eigenvectors, and the diagonal matrix Λ contains the eigenvalues.

Once linear algebra was taught more abstractly than it usually is now. In a classical course, a matrix A is a linear operator on a vector space. Now it is usually an $n \times n$ array of numbers. For the largest applications, the old fashioned way of thinking may be more the right way. It is probably best to think of a matrix A as a black-box whose input x (call it a vector if you like) gets transformed into the output Ax . The student who understands that polynomials form a vector space and differentiation is a perfectly legitimate linear operator (with determinant 0) understands the concept.

For more medium sized problems, the n by n array point of view makes sense, and then this black box may be thought of as “matrix–vector” multiplication in the usual component sense.

Chapter 3

Function Expansions

3.1 Function Representation and Expansions

How should we represent functions? Much of the history of mathematics or at least what we now call analysis might be traced to this very question.

We hardly ever think of a power series as a definition of a function, but it is certainly true that $\sum_{k=0}^{\infty} z^k/k!$ defines the exponential function. Even $\sum_{k=0}^{\infty} z^k$ defines $1/(1-z)$, and although the power series has no meaning for $|z| > 1$, we somehow feel that the power series is somehow good enough to capture the function $f(z) = 1/(1-z)$ everywhere, even though technically the series does not converge for $|z| > 1$.

So what is a power series? From the calculus point of view, it is always presented as a representation of a function which lets you plug in a number z , and if z is within this radius of convergence the function seems well defined. Another point of view is that a power series is a linear combination of the “basis” functions $f(z) = z^k$, $k = 0, \dots, \infty$.

There is yet another point of view which is not considered nearly as often. Any function can be interpolated with an n th degree polynomial given values at $n+1$ points. (I always like to remember the $n = 1$ story that “two points determine a line.”) If those $n+1$ points all coalesce into the same point, the polynomial is the leading segment of the Taylor series. Therefore if we can imagine interpolating a function using “infinitely” many points at the origin, we get the Taylor or power series. A Taylor series about another point z_c has the form

$$f(z) = \sum_{k=0}^{\infty} a_k (z - z_c)^k$$

Another basis for functions that is natural may be derived by taking one generating function and using all of its derivatives as the basis. For example if we start with $f(z) = 1/z$, then we obtain series expansions of the form $\sum_{k=0}^{\infty} a_k/z^k$. This is called a *multipole expansion* centered at $z = 0$. More generally, if our generator is $1/(z - z_c)$, then we have the general form of the multipole expansion of a function $f(z)$

$$f(z) = \sum_{k=1}^{\infty} a_k \frac{1}{(z - z_c)^k}.$$

If the generator is $\log(z - z_c)$ then of course the multipole expansion has one more term:

$$f(z) = a_0 \log(z - z_0) + \sum_{k=1}^{\infty} a_k \frac{1}{(z - z_c)^k}.$$

Multipole expansions converge outside of a disk in the complex plane. By contrast, the more familiar Taylor series converge within a disk.

We can take any function $f(z)$ and write it as a Taylor series about an arbitrary point z_c . Forgetting for a moment what the pure mathematicians might think, let us agree that at least psychologically, all such Taylor series are just multiple ways of representing the same function. Also, the same $f(z)$ may be written as a multipole expansion; each different center z_c gives a different representation with different convergence properties.

If

$$f(z) = \sum_{k=1}^{\infty} a_k \frac{1}{(z - z_c)^k} = \sum_{k=1}^{\infty} a'_k \frac{1}{(z - z'_c)^k} \quad (3.1)$$

then the linear operator that takes the a_k to the a'_k is known as a shift. Similarly if

$$f(z) = \sum_{k=0}^{\infty} a_k (z - z_c)^k = \sum_{k=0}^{\infty} a'_k (z - z'_c)^k \quad (3.2)$$

this operator is also known as a shift. Finally, if

$$f(z) = \sum_{k=1}^{\infty} a_k \frac{1}{(z - z_c)^k} = \sum_{k=0}^{\infty} a'_k (z - z'_c)^k \quad (3.3)$$

then the operator that converts the a_k to an a'_k is known as a flip. We will see that multipole expansions serve the purpose of broadcasting the news about a body to far away locations efficiently. On the other hand, Taylor expansions serve the purpose of locally computing all the needed information. The shifts allow the computations to occur on common ground.

3.2 A close look at shifts and flips

Given fixed values of z_c and z'_c , the equations (3.1), (3.2), and (3.3) define linear operators from the infinite a vector to the infinite a' vector.

In a moment we will work out an explicit form for the operators, but mathematics students should be able to see the linearity from a slightly abstract viewpoint. Ignoring issues of infinity and convergence, the operator from a and a' vectors to formal functions is clearly linear. Since the zero function has only one formal representation, the map from a to a' must be linear.

[work out explicit formulas and remove from the particle section]

3.3 Harmonic expansions in 3-dimensions

[This is a specialized optional topic and is usually omitted from the course]

3.4 Exercises

1. For a general derivative series work out the shift formula. Are you surprised?
2. Work out the flip formula from a general derivative series to a general integral series.
3. Work out the shift formula from a general integral series to another integral series.

4. Numerically shift and flip the field due to one charge. Compare the absolute and relative errors with that of the true shifted or flipped field. Difficult: Derive a theoretical estimate for the difference and compare with what is seen.

Chapter 4

Graph Theory

Ask a student from an engineering discipline what a *graph* is. The student will probably right away say something about the plot of a function with axes and a curve that represents the graph of a function.

If you ask a computer scientist or a mathematician, you find out that a *graph* is a collection of vertices and edges that indicate connections between the vertices. Mathematically, a graph $G = (V, E)$ consists a set V of vertices that are connected by a set E of edges. A typical graph is given in Figure ??.

A graph can be either directed or undirected. In an *undirected graph*, E is a set of unordered pairs of vertices. In contrast, in a *directed graph* $G = (V, E)$, E is a set of ordered pairs of vertices, where the order indicates the direction of an edge.

Trees, planar graphs, an example of a non-planar graph.

Graphs may be represented in many ways: edge lists; it's Laplacian (see Chapter ??); adjacent matrices, node edge incident matrices.

Basic concepts: degrees, paths, cycles, independent sets, colorings, connected components,

For many applications, we can associate weights with edges and vertices to define a weighted graph.

Chapter 5

Elementary Geometry

Chapter 6

Probability Theory

II Parallelism

Chapter 7

Parallel Machines

A parallel computer contains a collection of processors connected in a certain configuration. Different machines choose different interconnection network topologies, different node processors, different address-space organizations and memory structures. These choices are based on the parallel computation model, the current technology, and marketing decisions.

7.1 Characteristics of Parallel Computers

In Flynn's traditional classification of machines, there are two binary criteria, leading to four phyla: machines have one or many loci of control, and they operate simultaneously on one or many operands. Hence, the classes **Single Instruction Single Data** or SISD, which contains the sequential (or Van Neumann) machines; **Single Instruction Multiple Data** or SIMD, a class of parallel machines that perform one operation on a vector or array of data in parallel. It includes single vector processor machines as well as the Maspar machines and the first Connection Machines (the CM-1 and CM-2); **Multiple Instruction Multiple Data** or MIMD, a class now usually viewed as being synonymous with "parallel", which spans the gamut from workstation farms to shared-memory parallel (SMP) to distributed memory multiprocessors like the IBM SP-2; **Multiple Instruction Single Data** or MISD, a class which seems to be without and extant member unless one wants to consider the systolic arrays that were briefly of interest. Flynn's classification dates back to 1972. In the late 1980's, there were arguments about whether SIMD or MIMD would win. When Thinking Machines switched from a mostly SIMD to a mostly MIMD architecture when going from the CM-2 to the CM-5, people used that as an excuse to declare the argument over.

For most of our course, we will take the view that parallel means MIMD; but the principles we discuss will usually apply to SIMD as well. Indeed, a number of machines are MIMD collections of SIMD machines – notably the multiple vector processor supercomputers.

The memory architecture of all machines, and especially of parallel machines, is a central issue in their design; it plays a dominant role in determining both performance and the natural, low-level programming model for the machine.

The usual terminology in this area is also two-sided: *shared* versus *distributed*. Nothing leads to more confusion about parallel machines than this, because the terminology is not sufficiently precise; in fact, there are several issues and we need to be careful about using just two terms to describe a larger variety of possible designs. We'll define two other terms here: "central" (the opposite of distributed) and "private" (the opposite of shared). The central/distributed distinction will be one of system architecture, and the shared/private distinction will refer to addressing.

We will view the physical memory architecture as distributed if the memory is packaged with

the processors in such a way that some parts of the memory are substantially “farther” (in the sense of lower bandwidth or greater access latency) from a processor than other parts. If all the memory is nearly equally expensive to access, the system has central memory. The vector supercomputers are genuine central memory machines. A network of workstations has distributed memory. What is typical now in MIMD machines based on microprocessors, and this seems to be the “wave of the future” in machine design, is that each processor has its own cache. Even when the main memory is central, as in the SMP machines like the PowerChallenge, these caches act like distributed, low-latency, high-bandwidth memories, giving the system most of the important performance characteristics of distributed memory. Such systems are said to have non-uniform memory access (NUMA).

An equally important question is the addressing architecture. If all the P processors in the system can address all the memory, we have a “shared address” machine; if on the other hand the memory is divided into P chunks, and each processor gets the right to address locations in one and only one chunk, we have a “private address space”. In such a machine, the only way a process can read or write the contents of a memory location not in its chunk is to get the cooperation of the owning processor. The Cray T3E and the Silicon Graphics PowerChallenge are shared address, as are the vector supercomputers; the IBM SP-2 and the SIMD Maspar and Thinking Machines systems have private address spaces.

One important machine class, then, is the distributed memory, private address machines. These are collections of independent computers, equipped with a communication network and a software layer that allows the programs running on them to send messages to one another. The network is a shared resource, and some form of parallel file system may be added in software, too. These machines are often called “multicomputers”. Another important class are the shared address MIMD machines, which may or may not have physically distributed, NUMA memory and, again, may or may not have coherent caches on each processor. These wide range of machines are often called “multiprocessors.”

Both forms of addressing lead to difficulties for the programmer. In a shared address system, the programmer must insure that any two processors that access the same memory location do so in the correct order: for example, processor one should not load a value from location N until processor zero has stored the appropriate value there (this is called a “true” or “flow” dependence); in another situation, it may be necessary that processor one not store a new value into location N before processor zero loads the old value (this is an “anti” dependence); finally, if multiple processors write to location N , it’s final value is determined by the last writer, so the order in which they write is significant (this is called “output” dependence). The fourth possibility, a load followed by another load, is called an “input” dependence, and can generally be ignored. Thus, the programmer can get incorrect code do to “data races”. Also, performance bugs due to too many accesses to the same location (the memory bank that holds a given location becomes the sequential bottleneck) are common. ¹

The big problem created by private memory is that the programmer has to distribute the data. “Where’s the matrix?” becomes a key issue in building a LINPACK style library for private memory machines. And communication cost, whenever there is NUMA, is also a critical issue. It has been said that the three most important issues in parallel algorithms are “locality, locality, and locality”.²

One factor that complicates the discussion is that a layer of software, at the operating system level or just above it, can provide virtual shared addressing on a private address machine by using

¹It is an important problem of the “PRAM” model used in the theory of parallel algorithms that it does not capture this kind of performance bug, and also does not account for communication in NUMA machines.

²For those too young to have suffered through real estate transactions, the old saw in that business is that the three most important factors in determining the value of a property are “location, location, and location”.

interrupts to get the help of an owning processor when a remote processor wants to load or store data to its memory. And a different piece of software can also segregate the shared address space of a machine into chunks, one per processor, and confine all loads and stores by a processor to its own chunk, while using private address space mechanisms like message passing to access data in other chunks. (As you can imagine, hybrid machines have been built, with some amount of shared and private memory.)

The student reading this for the first time may find the various possibilities bewildering. As we write this in 1996, it is probably fair to say that there are only two important styles of architectures to keep in mind. One comes from the workstation vendors. These machines all have shared address spaces but because of the caches (sometimes more than one level) they are NUMA machines. Of course, people will start hooking these machines together, hence from the top level the machine is distributed. The other sort of machine, the kind built with government money, will tend to be private address space distributed machines.

7.1.1 SIMD v. MIMD

Concerning the control aspect of parallel machines, the SIMD/MIMD distinction does not tell the whole story. In fact among SIMD machines, there is considerable variability. Such issues as whether a processor can elect *not* to execute the current instruction, and whether the memory addresses used must be the same in all processors or can be the per processor result of a computation or a memory reference, divide the world of SIMD machines into subsets.

The distinction between SIMD and Vector Computer is not so clear and belongs to folklore. The idea is that when you think of SIMD you have in mind many many processors, while Vector Computer usually means a small number of arithmetic pipelines driven by a central processor, and having only one memory.

SIMD is cheaper (for example, the CM2 had a single sequencer sending out instructions to as many as 16k 1 bit processors³); in general the hardware for fetching and decoding instructions can be shared among several processors. In some important respects SIMD machines are also faster: they can communicate with minimal latency and very high bandwidth, because the processors are always in synch. For example, a Maspar can do a circular shift of a distributed array, or a broadcast, in less time than it take to do a floating point addition. SIMD machines employ custom processors, while MIMD have the advantage of the ability to use the fastest off-the-shelf processors. (It is evidently not feasible to run a collections of microprocessors in lock step, even when they have the same code.)

There have also been hybrids; the PASM Project has investigated the problem of running MIMD applications on SIMD hardware! There is, of course, some performance penalty.

7.1.2 Programming Model

The programming model used may seem to be natural for one style of machine; data parallel programming seems to be an SIMD shared memory style, and message passing seems to favor distributed memory MIMD.

Nevertheless, it is quite feasible to implement data parallelism on distributed memory MIMD machines. For example, on the Thinking Machines CM-5, a user can program in CM-Fortran an array data parallel language, or program in node programs such as C and Fortran with message

³A not so well known secret is that the 64k machine (and even some smaller machines) had four different sequencers and in principle could have executed four different instructions.

passing system calls, in the style of MIMD computing. We will discuss the pros and cons of SIMD and MIMD models in the next section when we discuss parallel languages and programming models.

7.1.3 Machine Topology

The two things processors need to do in parallel machines that they do not do when all alone are communication (with other processors) and coordination (again with other processors). Communication is obviously needed: one computes a number that the other requires, for example. Coordination is important for sharing a common pool of resources, whether they are hardware units, files, or a pool of work to be performed. The usual mechanisms for coordination, moreover, involve communication.

Parallel machines differ in their underlying hardware for supporting message passing and data routing.

In a shared memory parallel machine, communication between processors is achieved by access to common memory locations. Access to the common memory is supported by a switch network that connects the processors and memory modules. The set of proposed switch network for shared parallel machines includes crossbars and multistage networks such as the butterfly network. One can also connect processors and memory modules by a bus, and this is done when the number of processors is limited to ten or twenty.

An interconnection network is normally used to connect the nodes of a multicomputer as well. Again, the the network topology varies from one machine to another. Due to technical limitations, most commercially used topologies are of small node degree. Commonly used network topologies include (not exclusively) linear arrays, ring, hierarchical rings, two or three dimension grids or tori, hypercubes, fat trees.

The performance and scalability of a parallel machine in turn depend on the network topology. For example, a two dimensional grid of p nodes has diameter \sqrt{p} , on the other hand, the diameter of a hypercube or fat tree of p nodes is $\log p$. This implies that the number of physical steps to send a message from a processor to its most distant processor is \sqrt{p} and $\log p$, respectively, for 2D grid and hypercube of p processors. The node degree of a 2D grid is 4, while the degree of a hypercube is $\log p$. Another important criterion for the performance of a network topology is its *bisection bandwidth*, which is the minimum communication capacity of a set of links whose removal partitions the network into two equal halves. Assuming unit capacity of each direct link, a 2D and 3D grid of p nodes has bisection bandwidth \sqrt{p} and $p^{2/3}$ respectively, while a hypercube of p nodes has bisection bandwidth $\Theta(p/\log p)$. (See FTL page 394)

There is an obvious cost / performance trade-off to make in choosing machine topology. A hypercube is much more expensive to build than a two dimensional grid of the same size. An important study done by Dally at Caltech showed that for randomly generated message traffic, a grid could perform better and be cheaper to build. Dally assumed that the number of data signals per processor was fixed, and could be organized into either four “wide” channels in a grid topology or $\log n$ “narrow” channels (in the first hypercubes, the data channels were bit-serial) in a hypercube. The grid won, because too the average utilization of the hypercube channels was too low: the wires, probably the most critical resource in the parallel machine, were sitting idle. Furthermore, the work on routing technology at Caltech and elsewhere in the mid 80’s resulted in a family of hardware routers that delivered messages with very low latency even though the length of the path involved many “hops” through the machines. For the earliest multicomputers used “store and forward” networks, in which a message sent from A through B to C was copied into and out of the memory of the intermediate node B (and any others on the path): this causes very large latencies that grew in proportion to the number of hops. Later routers, including those used in

today's networks, have a “virtual circuit” capability that avoids this copying and results in small latencies.

Does topology make any real difference to the performance of parallel machines in practice? Some may say “yes” and some may say “no”. Due to the small size (less than 512 nodes) of most parallel machine configurations and large software overhead, it is often hard to measure the performance of interconnection topologies at the user level.

7.1.4 Homogeneous and heterogeneous machines

Another example of cost / performance trade-off is the choice between tightly coupled parallel machines and workstation clusters, workstations that are connected by fast switches or ATMs. The networking technology enables us to connect heterogeneous machines (including supercomputers) together for better utilization. Workstation clusters may have better cost/efficient trade-offs and are becoming a big market challenger to “main-frame” supercomputers.

A parallel machine can be *homogeneous* or *heterogeneous*. A homogeneous parallel machine uses identical node processors. Almost all tightly coupled supercomputers are homogeneous. Workstation clusters may often be heterogeneous. The Cray T3D is in some sense a heterogeneous parallel system which contains a vector parallel computer C90 as the front end and the massively parallel section of T3D. (The necessity of buying the front-end was evidently not a marketing plus: the T3E does not need one.) A future parallel system may contain a cluster of machines of various computation power from workstations to tightly coupled parallel machines. The scheduling problem will inevitably be much harder on a heterogeneous system because of the different speed and memory capacity of its node processors.

More than 1000 so called supercomputers have been installed worldwide. In US, parallel machines have been installed and used at national research labs (Los Alamos National Laboratory, Sandia National Labs, Oak Ridge National Laboratory, Lawrence Livermore National Laboratory, NASA Ames Research Center, US Naval Research Laboratory, DOE/Battis Atomic Power Laboratory, etc) supercomputing centers (Minnesota Supercomputer Center, Urbana-Champaign NCSA, Pittsburgh Supercomputing Center, San Diego Supercomputer Center, etc) US Government, and commercial companies (Ford Motor Company, Mobil, Amoco, Alliant echsystems Inc) and major universities. Machines from different supercomputing companies look different, are priced differently, and are named differently. Here are the names and birthplaces of some of them.

- Cray T3E (MIMD, distributed memory, 3D torus, uses Digital Alpha microprocessors), C90 (vector), Cray YMP, from Cray Research, Eagan, Minnesota.
- Thinking Machine CM-2 (SIMD, distributed memory, almost a hypercube) and CM-5 (SIMD and MIMD, distributed memory, Sparc processors with added vector units, fat tree) from Thinking Machines Corporation, Cambridge, Massachusetts.
- Intel Delta, Intel Paragon (mesh structure, distributed memory, MIMD), from Intel Corporation, Beaverton, Oregon. Based on Intel i860 RISC, but new machines based on the P6. Recently sold world's largest computer (over 6,000 P6 processors) to the US Dept of Energy for use in nuclear weapons stockpile simulations.
- IBM SP-1, SP2, (clusters, distributed memory, MIMD, based on IBM RS/6000 processor), from IBM, Kingston, New York.
- MasPar, MP-2 (SIMD, small enough to sit next to a desk), by MasPar, Santa Clara, California.

- KSR-2 (global addressable memory, hierarchical rings, SIMD and MIMD) by Kendall Square, Waltham, Massachusetts. Now defunct. They seem to have committed corporate suicide by deceiving Wall Street about their sales.
- Fujitsu VPX200 (multi-processor pipeline), by Fujitsu, Japan.
- NEC SX-4 (multi-processor vector, shared and distributed memory), by NEC, Japan.
- Tera MTA (MPP vector, shared memory, multithreads, 3D torus), by Tera Computer Company, Seattle, Washington. A novel architecture which uses the ability to make very fast context switches between threads to hide latency of access to the memory.
- Meiko CS-2HA (shared memory, multistage switch network, local I/O device), by Meiko Concord, Massachusetts and Bristol UK.
- Cray-3 (gallium arsenide integrated circuits, multiprocessor, vector) by Cray Computer Corporation, Colorado Spring, Colorado. Now defunct.

Additional comments by Alan Edelman on the past evolution:

CM-2 seemed to be a success ... initiates parallel computing excitement and legitimizes parallel computing as an academic discipline. SIMD worked well with many applications, but was not fully multipurpose.

Maspar decides that the SIMD CM-2 is the way to go and builds machines based on the CM-2 model, but with their own improvements.

Intel has commodity chips available so uses them. Never really came up with the nice software that the CM-2 had. Now, with the HPF from Portland Group, it can finally be programmed in data parallel mode.

CM-5 Goes for the commodity chips and gets MIMD for free. Therefore can program either as data parallel or message passing. That the machine was a "fat tree," never seemed to be so relevant. Vector units were slapped on as an afterthought when they realized the machine would not be competitive. Had short term success by beating Intel to market, but the machine became difficult to program for performance. (Message passing did not access vector units.)

In the end, rumor has it that management got into squabbles, and perhaps got greedy, the company fell into bankruptcy protection. At the time of writing (1995) morale appears to be so down, and so many people are leaving, it would be hard to imagine a turn-around. Nevertheless a core group of people remain, and though the odds look bad, maybe they can find a way to buck the trend.

Cray Entered the market in 1994 with the T3D, which has some shared address capabilities, unlike the CM-5, SP-2 and Paragon. The new T3E, which is a revision of the T3D, is one of the most powerful machines on the market. In the full 2048 processor model it peaks at over one teraflop.

IBM then joined with the SP-2. There is still some hope, but this machine still does not have anything like the software environment of the CM-5. Hardware is quite good, however, and MPI implementation is ready, HPF is on the way.

Silicon Graphics Has machines based on FDDI and HPPI interconnected 16 way multiprocessor machines, a hybrid of shared and private NUMA.

7.2 Architecture of the CM-5

The machine need not have 2^n processors (128 in the machine at MIT), each one is in turn a small SIMD machine: there are 4 Vector Units per processors, and a RISC chip to feed them with instructions and data. Each VU achieves about 120 MFLOPS. VU were a later add-on for competitive performance.

The processors are connected by a fat tree, something like a binary tree but whose bandwidth grows as height grows, avoiding therefore the bottleneck at the root. The fat tree looked promising because of good theoretical properties, and they didn't build it as a fat tree anyway (the actual network is a mixture of a fat tree and a butterfly).

The real bottleneck is the interface between the CPU and the network, the actual topology of the network is not very important. Some hacker (Charles Leiserson) suggested to dedicate the CM5 SPARC CPUs to communication, and perform calculations on the vector units.

On the top of the tree sits a front end, a normal sparcstation downloading programs and data to the processors, performing diagnostic checks, and so on.

Chapter 8

Parallel Programming

A parallel language must provide mechanisms for implementing parallel algorithms, i.e., to specify various levels of parallelism and define parallel data structures for distributing and sharing information among processors.

Most current parallel languages add parallel constructs for standard sequential languages. Different parallel languages provide different basic constructs. The choice largely depends on the parallel computing model the language means to support.

There are two basic parallel computation models other than vector and pipeline model: *message passing* and *data parallel*.

8.1 Programming style

Data-Parallel vs. Message Passing: the explicit communication can be somewhat hidden if one wants to program in a Data-Parallel style; it's something like SIMD: you specify a single action to execute on all processors. Example: if **A**, **B** and **C** are matrices, you can write **C=A+B** and let the compiler do the hard work of accessing remote memory locations, partition the matrix among the processors, etc. Guy Blelloch's doctoral dissertation wants to show that you can take your favorite algorithm and program it in HPF (High Performance Fortran), a data-parallel language with a clever set of primitives.

By contrast, the explicit message passing gives the programmer careful control over the communication, but programming requires a lot of knowledge and is much more difficult (as you probably understood from the previous section).

There are uncountable other alternatives, still academic at this point (in the sense that no commercial machine comes with them bundled). A great deal of research has been conducted on multithreading; the idea is that the programmer expresses the computation graph in some appropriate language and the machine executes the graph, and potentially independent nodes of the graph can be executed in parallel. Example in Cilk (multithreaded C, developed at MIT by Charles Leiserson and his students):

```
thread int fib(int n)
{
    if (n<2)
        return n;
    else {
        cont int x, y;
```

```

        x = spawn fib (n-2);
        y = spawn fib (n-1);
        sync;
        return x+y;
    }
}

```

Actually Cilk is a little bit different right now, but this is the way the program will look like when you read these notes. The whole point is that the two computations of `fib(n-1)` and `fib(n-2)` can be executed in parallel. As you might have expected, there are dozens of multithreaded languages (functional, imperative, declarative) and implementation techniques; in some implementations the thread size is a single-instruction long, and special processors execute this kind of programs. Ask Arvind at LCS for details.

Writing a good HPF compiler is difficult and not every manufacturer provides one; actually for some time TMC machines were the only machines available with it. The first HPF compiler for the Intel Paragon dates December 1994.

Why SIMD is wrong: consider the following fragment, where `x` and `y` are vectors:

```

    if (x > 0)
        y = x + 2;
    else
        y = -x + 5;

```

A SIMD machine will execute both cases, and discard one of the results; it does twice the needed work (see why? there is a single flow of instructions).

Moral: even if the programming model is that there is one processor per data element, the programmer must be aware that it's not true.

8.2 Data Parallel Programming in High Performance Fortran

The idea in data parallel programming is to make parallel programming look almost the same as sequential programming. As in a sequential program, there is one thread of control. There can be no race conditions, and the results of a program are only indeterminate if the programmer wants them to be (via a random number generator, for example). There are no synchronization constructs. There is only one “name space” for variables; the declarations of variables in a data parallel program describe their actual shape, and they are accessible on all processors. Unlike other parallel programming dialects, like message passing, there are no private variables that are seen only by an owning processor. Users of CM Fortran and Maspar Fortran have found data parallel programming to be quite useful and relatively easy, compared to lower level parallel programming.

As you know, most scientific software is written in Fortran, and for good reasons: stable and effective compilers, a good base of libraries, reasonable support for single and double precision and complex arithmetic, and for multidimensional arrays, and good performance on uniprocessors. Programmers also hate Fortran, and for equally good reasons: no dynamic storage allocation, no function prototypes, no reasonable scoping and no real global variables, no structs, no recursion, no standard random number generator or system clock. Fortunately, Fortran 90 *has* all these desirable features. Some of the bizarre and archaic features of Fortran are labeled “obsolescent” in Fortran 90 and will be purged in Fortran 95 and later revisions. In addition, Fortran 90 allows operations on whole arrays and sections of arrays, greatly improved facilities for passing arrays or subarrays

to subprograms, as well as array-valued constants, array-valued functions, and a number of new intrinsic functions and subroutines that operate on arrays. The array features are a simple way to specify data parallel computation as the concurrent application of a function to all the elements of an array.

High Performance Fortran (HPF) was developed during 1992 – 1993 by a group of volunteers that included representatives of users, researchers, and vendors of parallel machines. The goal was to define a standard, non-proprietary dialect of Fortran 90 for distributed memory machines that would allow programmers to write portable, high-level data parallel code. The HPF standard can be downloaded; the URL is

<http://www.erc.msstate.edu/hpff/home.html>. A good reference is “The High Performance Fortran Handbook,” by Charles Koelbel, David Loveman, Robert Schreiber, Guy L. Steele Jr., and Mary Zosel, published by MIT Press.

HPF is Fortran 90 with a few additions. The added language features are a `FORALL` construct and a new attribute for subprograms, `PURE`. In addition, in HPF the mapping of the data to the processors can be specified.

Here is how the mapping of data is specified. All mappings are described by what are technically comments in the program. Fortran 90 comments begin with `!`. HPF directives begin with the string `!HPF$`. Thus, a Fortran 90 compiler that is liberal enough to allow `FORALL` and `PURE` (and these are to be included in the next generation, Fortran 95) will accept HPF programs! You can debug them on one processor this way. In fact, DEC has taken the obvious step of having one compiler, which accepts both Fortran 90 and HPF programs.

Thus the data mapping directives *do not change the meaning of the program*. By “meaning” I mean the relation between the output and the input. Changing the mapping of the data has no effect on *what* is computed, only on *where* it is computed.

First, one can give the machine a shape, as a multidimensional processor grid. Example:

```
!HPF$ PROCESSORS PROCS(2, NUMBER_OF_PROCESSORS() / 2)
```

`NUMBER_OF_PROCESSORS()` is an HPF intrinsic that returns, you guessed it, the number of processors that the program is running on. So we’re saying with the statement above that `PROCS` is a virtual grid of processors that is $2 \times p/2$. We use `PROCS` to describe the mapping of data with the `DISTRIBUTE` directive. Example:

```
REAL A(10,20), B(10,20,10)
!HPF$ DISTRIBUTE A(BLOCK, CYCLIC) ONTO PROCS
!HPF$ DISTRIBUTE B(BLOCK, *, CYCLIC)
```

`A(i,j)` is mapped to processor `PROCS(1 + (i-1)/5, 1 + mod(j, p/2))`. The array `B` is mapped to *some* two dimensional processors arrangement, whose shape is determined by the compiler. `B(i,j,k)` is mapped to a processor that depends on `i` and `k`, but not `j` — the second axis of `B` is mapped to processor memory. Block mappings chop an array axis up into contiguous hunks that are given one to each processor along an axis of the processor grid. Cyclic mappings deal the array out to the processors just as one deals cards to card players. Finally, HPF allows `CYCLIC(k)` mappings, where `k` is an integer, which deal out contiguous groups of `k` indices. So, if a 10 element array has a cyclic(3) distribution onto 2 processors, then processor 1 gets array elements 1, 2, 3, 7, 8, and 9 and processor 2 gets array elements 4, 5, 6, and 10.

One may replicate data and one may align arrays with other arrays using the `ALIGN` directive. Example:

```

      REAL A(10,20), C(10), D(20), E(5,5), F(20,10), S
!HPF$  ALIGN C(I) WITH A(I, 4)      ! C aligned to 4th column
!HPF$  ALIGN D(J) WITH A(*, J)     ! Replicate D across the rows of A
!HPF$  ALIGN E(I,J) WITH A(2*I, 4*J) ! Non-unit stride
!HPF$  ALIGN F(J,I) WITH A(I,J)   ! Note the transposition
!HPF$  ALIGN WITH A(*,*) :: S     ! Replicate the scalar variable.
!HPF$  DISTRIBUTE A(BLOCK, BLOCK) ! An align target, but not an
                                     ! alignee, may be distributed.
                                     ! The aligned elements
                                     ! are "carried along".

```

Here you see a Fortran 90 variant of a declaration in which all the attributes of an object or objects are listed, then a double colon (::) then a list of the objects that have those attributes. I like it, because I can go to one place to find all that I need to know about a given variable. HPF allows this style in directives too, as the example shows.

If we wanted to get the same mapping of C, D, E, and F, but didn't have a convenient 10×20 array like A to align them to, we can use, instead, an HPF thing called a *template*, which is an array without any data, just subscripts! (Guy Steele says that if an array is a cat, then a template is a Cheshire Cat and the index set is its smile. $\hat{\smile}$) Thus:

```

!HPF$  TEMPLATE, DIMENSION(10,20) :: T
!HPF$  ALIGN E(J,I) WITH T(I,J)
!HPF$  DISTRIBUTE T(BLOCK, BLOCK)

```

Where does one put the mapping directives, and what is their scope? In general, they go in the same place one puts variable declarations. The mappings apply for the life of the object. Some programmers, however, want to be able to change a mapping during the computation, and HPF allows this. To do so, there are “executable” forms called **REALIGN** and **REDISTRIBUTE** that may appear in the executable part of a program. When control reaches the directive, the indicated remapping takes place. Any object that is remapped this way, wither directly or indirectly (by virtue of its alignment to a redistributed target) has to be given the **DYNAMIC** attribute. Example:

```

!HPF$  TEMPLATE, DYNAMIC, DIMENSION(2*NUMBER_OF_PROCESSORS()) :: T
!HPF$  DISTRIBUTE T(CYCLIC)
!HPF$  ALIGN (I) WITH A(I) :: B, C
!HPF$  ALIGN (I) WITH T(I) :: A
!HPF$  DYNAMIC :: A, B, C

! Executable Statements ....

!HPF$  REDISTRIBUTE T(BLOCK) !Remaps A, B, and C
!HPF$  REALIGN A(I) WITH T(*) !Replicates A

```

Note that A, B, and C are aligned to T, although in the case of B and C, two directives are used to specify the alignment. Alignment is always simplified to an alignment to an *ultimate align target*. This, the redistribution of T carries all three arrays with it. The realignment of A does not affect B or C. Finally, note that A, B, and C are all required to have the **DYNAMIC** attribute, even though B and C do not explicitly appear in a **REALIGN**.

8.2.1 Parallelism

There are some instances in which the Fortran 90 array syntax cannot express a simple data parallel operation, or at least not conveniently. One of the most important is when each processor uses the elements of an array that it owns as indices into some other array that it owns or of which it owns a copy. For these, one can use the HPF `FORALL` assignment statement. Example

```

    INTEGER, PARAMETER :: NPROCS = NUMBER_OF_PROCESSORS()
    REAL TABLE(NPROCS, 100), RESULT(NPROCS)
    INTEGER INDEX(NPROCS)
    !HPF$ DISTRIBUTE (CYCLIC) :: INDEX, RESULT
    !HPF$ DISTRIBUTE (CYCLIC,*) :: TABLE
    FORALL (P = 1:NPROCS) RESULT(P) = TABLE(P, INDEX(P))

```

Note that the Fortran 90 expression `TABLE(:,INDEX)` does not produce the rank-one result we need. Another `FORALL` example:

```

    FORALL (I = 1:N) A(I,I) = 2*I !Access a diagonal of an array

```

The right hand sides of all instances of the `FORALL` are evaluated before any of the left hand sides is changed. The following are therefore equivalent:

```

    A(2:N) = A(1:N-1)
    FORALL (I = 1:N-1) A(I+1) = A(I)

```

8.2.2 Intrinsic

Fortran 90's intrinsic subprograms are a big improvement on Fortran 77. There are random number and system clock subroutines, array inquiry functions, and many array-valued operations, like `SUM`, `TRANPOSE`, and `MATMULT`.

A few important data-parallel array operators were left out of Fortran 90, and are added to HPF in the HPF library. These include parallel prefix functions, combining send functions, and sorting.

Here is an example of parallel prefix. Suppose we want to enumerate the elements of a logical vector that are true. This is accomplished by `COUNT_PREFIX`. In Fortran 90, `(/ 1, 2, 3 /)` is a rank one integer array constant of size 3. Let `T` denote the value true and `F` denote false. Then `COUNT_PREFIX((/F, T, T, F, T, F/))` has the value `(/ 0, 1, 2, 2, 3, 3)`.

The combining send functions perform a scatter, much as the Fortran 90 vector-valued subscript does if used on the left side of an assignment statement:

```

    INTEGER, DIMENSION(:) :: A, B, V
    B(V) = A

```

The Fortran 90 fragment is meaningful only when the elements of `V` are all different, and are all legitimate subscripts for `B`. What if there are duplicate elements of `V`, so that several elements of `A` are associated with one element of `B`? If we specify that this element of `B` is to get, for example, the sum of the associated elements of `A`, then the program again makes sense. This is accomplished with

```

    B = SUM_SCATTER(ARRAY = A, BASE = B, INDX1 = V)

```

Note the use of Fortran 90 keyword arguments (which can occur in any order). The result of any of the scatter functions has the same shape as its **BASE** argument. The value of an element of the result is the corresponding element of the base unless it is associated with a set of elements of **ARRAY**. Element k of the result is associated with and (in the case of **SUM_SCATTER** is set to the sum of the elements **ARRAY**(i) for which **V**(i) is equal to k .

8.2.3 Extended data parallelism

Is data parallelism the same as array-based parallelism? Some think so, but this is a misconception. The key idea is the application of a function simultaneously to a collection of arguments. HPF allows one to specify this in a very flexible way with the **INDEPENDENT DO** loop

```
!HPF$ INDEPENDENT
  DO I = 1, 1024
    ...
  ENDDO
```

The independent directive does not change what is computed. It just advises the compiler that the loop iterations may be executed in parallel, with no contention for or race conditions involving shared variables. When the use of some variable by multiple iterations of a loop renders this false, we can still use the **INDEPENDENT** directive, as long as the use of the variable is essentially local to each iteration and it does not carry information from one iteration to another. For example,

```
DO I = 1, N
  DO J = 1, 3
    ...
  ENDDO
ENDDO
```

Ordinarily, the variable **J** is not used to carry information between iterations of the **I** loop. We can assert that the outer loop is independent *if* the variable **J** is made local to each outer iteration by use of the directive

```
!HPF$ INDEPENDENT, NEW J
```

just before the **DO I** statement; this has the same effect as replacing the shared scalar **J** with an array, and using **J**(**I**) at iteration **I**, but it uses less storage.

8.3 Message Passing

In the SISD, SIMD, and MIMD computer taxonomy, SISD machines are conventional uniprocessors, SIMD are single instruction stream machines that operate in parallel on ensembles of data, like arrays or vectors, and MIMD machines have multiple active threads of control (processes) that can operate on multiple data in parallel. How do these threads share data and how do they synchronize? For example, suppose two processes have a producer/consumer relationship. The producer generates a sequence of data items that are passed to the consumer, which processes them further. How does the producer deliver the data to the consumer?

If they share a common memory, then they agree on a location to be used for the transfer. In addition, they have a mechanism that allows the consumer to know when that location is full, *i.e.* it has a valid datum placed there for it by the producer, and a mechanism to read that location and

change its state to empty. A full/empty bit is often associated with the location for this purpose. The hardware feature that is often used to do this is a “test-and-set” instruction that tests a bit in memory and simultaneously sets it to one. The producer has the obvious dual mechanisms.

Many highly parallel machines have been, and still are, just collections of independent computers on some sort of a network. Such machines can be made to have just about any data sharing and synchronization mechanism; it just depends on what software is provided by the operating system, the compilers, and the runtime libraries. One possibility, the one used by the first of these machines (The Caltech Cosmic Cube, from around 1984) is message passing. (So it’s misleading to call these “message passing machines”; they are really multicomputers with message passing library software.)

From the point of view of the application, these computers can send a message to another computer and can receive such messages off the network. Thus, a process cannot touch any data other than what is in its own, private memory. The way it communicates is to send messages to and receive messages from other processes. Synchronization happens as part of the process, by virtue of the fact that both the sending and receiving process have to make a call to the system in order to move the data: the sender won’t call send until its data is already in the send buffer, and the receiver calls receive when its receive buffer is empty and it needs more data to proceed.

Message passing systems have been around since the Cosmic Cube, about ten years. In that time, there has been a lot of evolution, improved efficiency, better software engineering, improved functionality. Many variants were developed by users, computer vendors, and independent software companies. Finally, in 1993, a standardization effort was attempted, and the result is the Message Passing Interface (MPI) standard. MPI is flexible and general, has good implementations on all the machines one is likely to use, and is almost certain to be around for quite some time. We’ll use MPI in the course.

In print, the best MPI reference is the handbook *Using MPI*, by William Gropp, Ewing Lusk, and Anthony Skjellum, published by MIT Press ISBN 0-262-57104-8.

The standard is on the World Wide Web. The URL is <http://www.mcs.anl.gov/mpi/mpi-report/mpi-report.html>. An updated version is at <ftp://ftp.mcs.anl.gov/pub/mpi/mpi-1.jun95/mpi-report.ps>

8.3.1 Sending and receiving

In order to get started, let’s look at the two most important MPI functions, `MPI_Send` and `MPI_Recv`.

The call

```
MPI_Send(void *buf, int count, MPI_Datatype datatype, int dest,
         int tag, MPI_Comm comm)
```

sends `count` items of data of type `datatype` starting at the location `buf`. In all message passing systems, the processes have identifiers of some kind. In MPI, the process is identified by its `rank`, an integer. The data is sent to the processes whose rank is `dest`. Possible values for `datatype` are `MPI_INT`, `MPI_DOUBLE`, `MPI_CHAR` *etc.* `tag` is an integer used by the programmer to allow the receiver to select from among several arriving messages in the `MPI_Recv`. Finally, `comm` is something called a communicator, which is essentially a subset of the processes. Ordinarily, message passing occurs within a single subset. The subset `MPI_COMM_WORLD` consists of all the processes in a single parallel job, and is predefined.

A receive call matching the send above is

```
MPI_Recv(void *buf, int count, MPI_Datatype datatype, int source,
         int tag, MPI_Comm comm, MPI_Status *status)
```

`buf` is where the data is placed once it arrives. `count`, an input argument, is the size of the buffer; the message is truncated if it is longer than the buffer. Of course, the receive has to be executed by the correct destination process, as specified in the `dest` part of the send, for it to match. `source` must be the rank of the sending process. The communicator and the tag must match. So must the datatype.

The purpose of the datatype field is to allow MPI to be used with heterogeneous hardware. A process running on a little-endian machine may communicate integers to another process on a big-endian machine; MPI converts them automatically. The same holds for different floating point formats. Type conversion, however, is not supported: an integer must be sent to an integer, a double to a double, *etc.*

Suppose the producer and consumer transact business in two word integer packets. The producer is process 0 and the consumer is process 1. Then the send would look like this:

```
int outgoing[2];
MPI_Send(outgoing, 2, MPI_INT, 1 100, MPI_COMM_WORLD)
```

and the receive like this:

```
MPI_Status stat;
int incoming[2];
MPI_Recv(incoming, 2, MPI_INT, 0 100, MPI_COMM_WORLD, &stat)
```

What if one wants a process to which several other processes can send messages, with service provided on a first-arrived, first-served basis? For this purpose, we don't want to specify the source in our receive, and we use the value `MPI_ANY_SOURCE` instead of an explicit source. The same is true if we want to ignore the tag: use `MPI_ANY_TAG`. The basic purpose of the status argument, which is an output argument, is to find out what the tag and source of such a received message are. `status.MPI_TAG` and `status.MPI_SOURCE` are components of the struct `status` of type `int` that contain this information after the `MPI_Recv` function returns.

This form of send and receive are “blocking”, which is a technical term that has the following meaning. for the send, it means that `buf` has been read by the system and the data has been moved out as soon as the send returns. The sending process can write into it without corrupting the message that was sent. For the receive, it means that `buf` has been filled with data on return. (A call to `MPI_Recv` with no corresponding call to `MPI_Send` occurring elsewhere is a very good and often used method for hanging a message passing application.)

MPI implementations may use buffering to accomplish this. When send is called, the data are copied into a system buffer and control returns to the caller. A separate system process (perhaps using communication hardware) completes the job of sending the data to the receiver. Another implementation is to wait until a corresponding receive is posted by the destination process, then transfer the data to the receive buffer, and finally return control to the caller. MPI provides two variants of send, `MPI_Bsend` and `MPI_Ssend` that force the buffered or the rendezvous implementation. Lastly, there is a version of send that works in “ready” mode. For such a send, the corresponding receive must have been executed previously, otherwise an error occurs. On some systems, this may be faster than the blocking versions of send. All four versions of send have the same calling sequence.

NOTE: MPI allows a process to send itself data. Don't try it. On the SP-2, if the message is big enough, it doesn't work. Here's why. Consider this code:

```
if (myrank == 0)
    for(dest = 0; dest < size; dest++)
```

```

    MPI_Send(sendbuf+dest*count, count, MPI_INT, dest, tag, MPI_COMM_WORLD);
    MPI_Recv(recvbuf, count, MPI_INT, 0, tag, MPI_COMM_WORLD, &stat);

```

The programmer is attempting to send data from process zero to all processes, including process zero; $4 \cdot \text{count}$ bytes of it. If the system has enough buffer space for the outgoing messages, this succeeds, but if it doesn't, then the send blocks until the receive is executed. But since control does not return from the blocking send to process zero, the receive never does execute. If the programmer uses buffered send, then this deadlock cannot occur. An error will occur if the system runs out of buffer space, however:

```

    if (myrank == 0)
        for(dest = 0; dest < size; dest++)
            MPI_Bsend(sendbuf+dest*count, count, MPI_INT, dest, tag, MPI_COMM_WORLD);
    MPI_Recv(recvbuf, count, MPI_INT, 0, tag, MPI_COMM_WORLD, &stat);

```

8.3.2 Tags and communicators

Tags are used to keep messages straight. An example will illustrate how they are used. Suppose each process in a group has one integer and one real value, and we wish to find, on process zero, the sum of the integers and the sum of the reals. Lets write this:

```

    itag = 100;
    MPI_Send(&intvar, 1, MPI_INT, 0, itag, MPI_COMM_WORLD);
    ftag = 101;
    MPI_Send(&floatvar, 1, MPI_FLOAT, 0, ftag, MPI_COMM_WORLD);
    /**** Sends are done.   Receive on process zero   ****/
    if (myrank == 0) {
        intsum = 0;
        for (kount = 0; kount < nprocs; kount++) {
            MPI_Recv(&intrecv, 1, MPI_INT, MPI_ANY_SOURCE, itag, MPI_COMM_WORLD, &stat);
            intsum += intrecv;
        }
        fltsum = 0;
        for (kount = 0; kount < nprocs; kount++) {
            MPI_Recv(&fltrecv, 1, MPI_FLOAT, MPI_ANY_SOURCE, ftag, MPI_COMM_WORLD, &stat);
            fltsum += fltrecv;
        }
    }
}

```

It looks simple, but there are a lot of subtleties here! First, note the use of `MPI_ANY_SOURCE` in the receives. We're happy to receive the data in the order it arrives. Second, note that we use two different tag values to distinguish between the int and the float data. Why isn't the `MPI_TYPE` field enough? Because MPI does not include the type as part of the message "envelope". The envelope consists of the source, destination, tag, and communicator, and these must match in a send-receive pair. Now the two messages sent to process zero from some other process are guaranteed to arrive in the order they were sent, namely the integer message first. But that does not mean that all of the integer message precede all of the float messages! So the tag is needed to distinguish them.

This solution creates a problem. Our code, as it is now written, sends off a lot of messages with tags 100 and 101, then does the receives (at process zero). Suppose we called a library routine written by another user before we did the receives. What if that library code uses the same message

tags? Chaos results. We've "polluted" the tag space. Note, by the way, that synchronizing the processes before calling the library code does not solve this problem.

MPI provides communicators as a way to prevent this problem. The communicator is a part of the message envelope. So we need to change communicators while in the library routine. To do this, we use `MPI_Comm_dup`, which makes a new communicator with the same processes in the same order as an existing communicator. For example

```
void safe_library_routine(MPI_Comm oldcomm)
{
    MPI_Comm mycomm;
    MPI_Comm_dup(oldcomm, &mycomm);
    <library code using mycomm for communication>
    MPI_Comm_free(&mycomm);
}
```

The messages sent and received inside the library code cannot interfere with those sent outside.

8.3.3 Who am I?

On the SP-2 and other multicomputers, one usually writes one program which runs on all the processors. In order to differentiate its behavior, (like producer and consumer) a process usually first finds out at runtime its rank within its process group, then branches accordingly. The calls

```
MPI_Comm_size(MPI_Comm comm, int *size)
```

sets `size` to the number of processes in the group specified by `comm` and the call

```
MPI_Comm_rank(MPI_Comm comm, int *rank)
```

sets `rank` to the rank of the calling process within the group (from 0 up to $n - 1$ where n is the size of the group). Usually, the first thing a program does is to call these using `MPI_COMM_WORLD` as the communicator, in order to find out the answer to the *big* questions, "Who am I?" and "How many other 'I's are there?".

Okay, I lied. That's the second thing a program does. Before it can do anything else, it has to make the call

```
MPI_Init(int *argc, char ***argv)
```

where `argc` and `argv` should be pointers to the arguments provided by UNIX to `main()`. While we're at it, let's not forget that one's code needs to start with

```
#include "mpi.h"
```

The *last* thing the MPI code does should be

```
MPI_Finalize()
```

No arguments.

Here's an MPI multi-process "Hello World":

```

#include <stdio.h>
#include "mpi.h"

main(int argc, char** argv) {
    int i, myrank, nprocs;
    double a = 0, b = 1.1, c = 0.90;

    MPI_Init(&argc, &argv);
    MPI_Comm_rank(MPI_COMM_WORLD, &myrank);
    MPI_Comm_size(MPI_COMM_WORLD, &nprocs);
    printf("Hello world! This is process %d out of %d\n",myrank, nprocs);
    if (myrank == 0) printf("Some processes are more equal than others.");
    MPI_Finalize();
} /* main */

```

which is compiled and executed on the SP-2 at Ames by

```

babbage1% mpicc -O3 example.c
babbage1% a.out -procs 2

```

and produces (on the standard output)

```

0:Hello world! This is process 0 out of 2
1:Hello world! This is process 1 out of 2
0:Some processes are more equal than others.

```

Another important thing to know about is the MPI wall clock timer:

```
double MPI_Wtime()
```

which returns the time in seconds from some unspecified point in the past.

8.3.4 Performance, and tolerance

Try this exercise. See how long a message of length n bytes takes between the call time the send calls send and the time the receiver returns from receive. Do an experiment and vary n . Also vary the rank of the receiver for a fixed sender. Does the model

$$\text{Elapsed_Time}(n, r) = \alpha + \beta n$$

work? (r is the receiver, and according to this model, the cost is receiver independent.)

In such a model, the latency for a message is α seconds, and the bandwidth is $1/\beta$ bytes/second. Other models try to split α into two components. The first is the time actually spent by the sending processor and the receiving processor on behalf of a message. (Some of the per-byte cost is also attributed to the processors.) This is called the overhead. The remaining component of latency is the delay as the message actually travels through the machines interconnect network. It is ordinarily much smaller than the overhead on modern multicomputers (ones, rather than tens of microseconds).

A lot has been made about the possibility of improving performance by “tolerating” communication latency. To do so, one finds other work for the processor to do while it waits for a message to arrive. The simplest thing is for the programmer to do this explicitly. For this purpose, there are “nonblocking” versions of send and receive in MPI and other dialects.

Nonblocking send and receive work this way. A nonblock **send start** call initiates a send but returns before the data are out of the send buffer. A separate call to **send complete** then blocks the sending process, returning only when the data are out of the buffer. The same two-phase protocol is used for nonblocking receive. The **receive start** call returns right away, and the **receive complete** call returns only when the data are in the buffer.

The simplest mechanism is to match a nonblocking receive with a blocking send. To illustrate, we perform the communication operation of the previous section using nonblocking receive.

```
MPI_Request request;
MPI_IRecv(recvbuf, count, MPI_INT, 0, tag, MPI_COMM_WORLD, &request);
if (myrank == 0)
    for(dest = 0; dest < size; dest++)
        MPI_Send(sendbuf+dest*count, count, MPI_INT, dest, tag, MPI_COMM_WORLD);
MPI_Wait(&request, &stat);
```

`MPI_Wait` blocks until the nonblocking operation identified by the handle `request` completes. This code is correct regardless of the availability of buffers. The sends will either buffer or block until the corresponding **receive start** is executed, and all of these will be.

Before embarking on an effort to improve performance this way, one should first consider what the payoff will be. In general, the best that can be achieved is a two-fold improvement. Often, for large problems, it's the bandwidth (the βn term) that dominates, and latency tolerance doesn't help with this. Rearrangement of the data and computation to avoid some of the communication altogether is required to reduce the bandwidth component of communication time.

8.3.5 Who's got the floor?

We usually think of send and receive as the basic message passing mechanism. But they're not the whole story by a long shot. If we wrote codes that had genuinely different, independent, asynchronous processes that interacted in response to random events, then send and receive would be used to do all the work. Now consider computing a dot product of two identically distributed vectors. Each processor does a local dot product of its pieces, producing one scalar value per processor. Then we need to add them together and, probably, broadcast the result. Can we do this with send and receive? Sure. Do we want to? No. No because it would be a pain in the neck to write and because the MPI system implementor may be able to provide the two necessary, and generally useful collective operations (sum, and broadcast) for us in a more efficient implementation.

MPI has lots of these "collective communication" functions. (And like the sum operation, they often do computation as part of the communication.)

Here's a sum operation, on doubles. The variable `sum` on process `root` gets the sum of the variables `x` on all the processes.

```
double x, sum;
int root, count = 1;
MPI_Reduce(&x, &sum, count, MPI_DOUBLE, MPI_SUM, root, MPI_COMM_WORLD);
```

The fifth argument specifies the operation; other possibilities are `MPI_MAX`, `MPI_LAND`, `MPI_BOR`, ... which specify maximum, logical AND, and bitwise OR, for example.

The semantics of the collective communication calls are subtle to this extent: nothing happens except that a process stops when it reaches such a call, until *all* processes in the specified group reach it. Then the reduction operation occurs and the result is placed in the `sum` variable on the `root` processor. Thus, reductions provide what is called a *barrier* synchronization.

There are quite a few collective communication operations provided by MPI, all of them useful and important. We will use several in the assignment. To mention a few, `MPI_Bcast` broadcasts a vector from one process to the rest of its process group; `MPI_Scatter` sends different data from one process to each process in its a group; `MPI_Gather` is the inverse of a scatter: one process receives and concatenates data from all processes in its group; `MPI_Allgather` is like a gather followed by a broadcast: all processes receive the concatenation of data that are initially distributed among them; `MPI_Reduce_scatter` is like reduce followed by scatter: the result of the reduction ends up distributed among the process group. Finally, `MPI_Alltoall` implements a very general communication in which each process has a separate message to send to each member of the process group.

Often the process group in a collective communication is some subset of all the processors. In a typical situation, we may view the processes as forming a grid, let's say a 2d grid, for example. We may want to do a reduction operation within rows of the process grid. For this purpose, we can use `MPI_Reduce`, with a separate communicator for each row.

To make this work, each process first computes its coordinates in the process grid. MPI makes this easy, with

```
int nprocs, myproc, procdims[2], myproc_row, myproc_col;
MPI_Dims_create(nprocs, 2, procdims);
myproc_row = myrank / procdims[1];
myproc_col = myrank % procdims[1];
```

Next, one creates new communicators, one for each process row and one for each process column. The calls

```
MPI_Comm my_prow, my_pcol;
MPI_Comm_split(MPI_COMM_WORLD, myproc_row, 0, &my_prow);
MPI_Comm_split(MPI_COMM_WORLD, myproc_col, 0, &my_prow);
```

create them and

```
MPI_Comm_free(&my_prow);
MPI_Comm_free(&my_pcol);
```

free them. The reduce-in-rows call is then

```
MPI_Reduce(&x, &sum, count, MPI_DOUBLE, MPI_SUM, 0, my_prow);
```

which leaves the sum of the vectors `x` in the vector `sum` in the process whose rank in the group is zero: this will be the first process in the row. The general form is

```
MPI_Comm_split(MPI_Comm comm, int color, int key, MPI_Comm newcomm)
```

As in the example above, the group associated with `comm` is split into disjoint subgroups, one for every different value of `color`; the communicator for the subgroup that this process belongs to is returned in `newcomm`. The argument `key` determines the rank of this process within `newcomm`; the members are ranked according to their value of `key`, with ties broken using the rank in `comm`.

8.4 Message Passing in PVM

PVM is a popular message passing system that allows a user to treat a heterogeneous collection of networked machines as a single “parallel virtual machine”. It was developed at Oak Ridge National Lab, beginning in 1989, and it continues to evolve and improve. It is freely available, easy to download and install, and it runs in user mode; any user can configure any set of machines on which he has accounts into a PVM using PVM. PVM handles all communication and synchronization, as well as format conversion for machines with different internal representations of integers, floating point values, and strings.

PVM allows the virtual machine to be configured dynamically: computers can be added to or deleted from the VM during the course of a computation. Very useful if someone switches off one of the machines! A PVM computation consists of a number of separate programs, called tasks, that use the PVM library to communicate. Tasks can be created and can drop out, also dynamically.

To obtain PVM and the documentation, one can use the web:

http://www.epm.ornl.gov/pvm/pvm_home.html

The book, *PVM: Parallel Virtual Machine A Users' Guide and Tutorial for Networked Parallel Computing* by Al Geist Adam Beguelin Jack Dongarra Weicheng Jiang Robert Manchek, and Vaidy Sunderam, is the best reference on PVM. It too has a home page and can be downloaded:

<http://www.netlib.org/pvm3/book/pvm-book.html>

8.4.1 PVM Basics

Once one makes PVM, there are two relevant pieces of software. One is the pvm daemon (called pvmd). You start it on any machine that it has been compiled for, and it then allows you to give commands to add other machines to the current *configuration*, which is the virtual parallel machine. The user's command interface to PVM is called the PVM console, and there is also an X Windows version of it, XPVM.

Here is an example session, running at HP Labs. The machine will include two HP workstations:

```
hplpp3% pvm
new pvm shell
t40001
pvm> add hplpp4
1 successful
          HOST      DTID
          hplpp4    80000
pvm> conf
2 hosts, 1 data format
          HOST      DTID      ARCH    SPEED
          hplpp3    40000     HPPA    1000
          hplpp4    80000     HPPA    1000
pvm>
```

The machine configuration commands can also be given by function calls from a running PVM application.

A PVM application is just a C or Fortran 77 program compiled and linked against the PVM library. Here is a sample:

```

#include <stdio.h>
#include "pvm3.h"

main()
{
    int cc, tid;
    char buf[100];

    printf("i'm t%x\n", pvm_mytid());

    cc = pvm_spawn("hello_other", (char**)0, 0, "", 1, &tid);

    if (cc == 1) {
        cc = pvm_recv(-1, -1);
        pvm_bufinfo(cc, (int*)0, (int*)0, &tid);
        pvm_upkstr(buf);
        printf("from t%x: %s\n", tid, buf);
    } else
        printf("can't start hello_other\n");

    pvm_exit();
    exit(0);
}

```

This example illustrates some of PVM's outstanding features. First, once begun, this task first finds its own PVM task identifier (or *tid*) by calling the PVM library function `pvm_mytid`.

Next, it starts another PVM task, leaving it up to `pvm` to decide which actual processor to run it on. The other task's executable file is called `hello_other`, the source for which appears below. Its `tid` is kept in order to use it for communication, later. In the `if` construct, we see the basics of PVM message passing. In PVM, a send is a three step process. First, one allocates a buffer using `pvm_initsend`; next, one packs data into the buffer using `pvm_pk*` routines, which specify datatype. When there are multiple machines in the configuration, this is where data format conversions occur. Last, after its contents are all packed in, the buffer is sent with `pvm_send`, which gives the destination `tid` and a message tag. The receive is a similar process. The `pvm_recv` (which allows specification of source `tid` and message tag) returns a receive buffer identifier. This is then used to unpack the data with `pvm_upk*`.

Here is the code for `hello_other`. Notice the call to `pvm_parent` which returns the `tid` of the task that spawned this one.

```

#include "pvm3.h"

main()
{
    int ptid;
    char buf[100];

```

```

    ptid = pvm_parent();

    strcpy(buf, "hello, world from ");
    gethostname(buf + strlen(buf), 64);

    pvm_initsend(PvmDataDefault);
    pvm_pkstr(buf);
    pvm_send(ptid, 1);

    pvm_exit();
    exit(0);
}

```

After compiling and linking both programs, I can log into either of the two workstations and start `hello` from the UNIX prompt. Also, using the PVM console, I configure the two machines as above. The result is this:

```

hplpp4% hello
i'm t80001
from t40002: hello, world from hplpp3
hplpp4%

```

The ability to configure heterogeneous networks and use them as a parallel processor is a very impressive capability. It's what makes PVM so popular. As a message passing dialect, however, PVM lacks the power and sophistication of MPI: it has only one send mode, no asynchronous receive, no communication contexts, and limited collective communication functions. Thus, we expect MPI and PVM to evolve towards one another, each importing the strengths of the other in time.

Performance is another issue. PVM is a user application, and as such it is forced to use the communication facilities of UNIX, which add latency and limit bandwidth. Vendor supported MPI implementations appear to have significantly better performance at this time.

8.5 More on Message Passing

8.5.1 Nomenclature

- Performance:

Latency: the time it takes to send a zero length message (overhead)

Bandwidth: the rate at which data can be sent

- Synchrony:

Synchronous: sending function returns when a matching receiving operation has been initiated at the destination.

Blocking: sending function returns when the message has been safely copied.

Non-blocking (asynchronous): sending function returns immediately. Message buffer must not be changed until it is safe to do so

- Miscellaneous:

Interrupts: if enabled, the arrival of a message interrupts the receiving processor

Polling: the act of checking the occurrence of an event

Handlers: code written to execute when an interrupt occurs

Critical sections: sections of the code which cannot be interrupted safely

Scheduling: the process of determining which code to run at a given time

Priority: a relative statement about the ranking of an object according to some metric

8.5.2 The Development of Message Passing

- Early Multicomputers:

UNIVAC

Goodyear MPP (SIMD.)

Denelcor HEP (Shared memory)

- The Internet and Berkeley Unix (High latency, low bandwidth)

Support for communications between computers is part of the operating system (sockets, ports, remote devices)

Client/server applications appear

- Parallel Machines (lowest latency, high bandwidth - dedicated networks)

Ncube

Intel (Hypercubes, Paragon)

Meiko (CS1, CS2)

TMC (CM-5)

- Workstation clusters (lower latency, high bandwidth, popular networks)

IBM (SP1,2) - optional proprietary network

- Software (libraries):

CrOS, CUBIX, NX, Express

Vertex

EUI/MPL (adjusts to the machine operating system)

CMMD

PVM (supports heterogeneous machines; dynamic machine configuration)

PARMACS, P4, Chamaleon

MPI (analogum of everything above and adjusts to the operating system)

- Systems:

Mach

Linda (object-based system)

8.5.3 Machine Characteristics

- Nodes:

CPU, local memory, perhaps local I/O

- Networks:
 - Topology: Hypercube, Mesh, Fat-Tree, other
 - Routing: circuit, packet, wormhole, virtual channel random
 - Bisection bandwidth (how much data can be sent along the net)
 - Reliable delivery
 - Flow Control
 - “State” : Space sharing, timesharing, stateless
- Network interfaces:
 - Dumb: Fifo, control registers
 - Smart: DMA (Direct Memory Access) controllers
 - Very Smart: handle protocol management

8.5.4 CM-5 /CMOST Environment:

- Sparc (or sparc superscalar) nodes (optional vector units). 32-128 MB memory
- Sparc (or sparc superscalar) control processor.
- Dedicated Network (Fat-tree). Two data router links per node, 20 MB/s each.
- Separate cooperative communications support in network
- Bisection Bandwidth is 5 MB/s/node (higher on CM-5E)
- Network support for all timesharing (all fall down)
- CMOST operating system:
 - Unix (SunOS) derived
 - Time sharing
 - Data Parallel antecedents
 - Single process model
 - Memory mapped NI

8.6 Mechanics of Message Passing :

8.6.1 Sending and receiving

Sending and receiving:

- CMMD_send_block (destination, tag, buffer, len)
CMMD_receive_block(source, tag, buffer, len)
- A pairwise synchronizing operation
- High level “Heavyweight” functions
- Designed to prevent network deadlock if used properly (“Safe”)
- Relatively high latency:
 - Handshaking protocol used

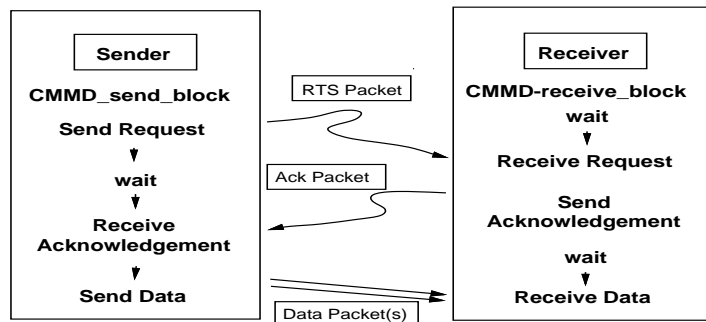


Figure 8.1: CMMD Cooperative Message Passing Protocol

- Bandwidth limited to unidirectional rates
- Resources:
 - Messages buffered by sender
 - Send side queue: waiting ACK
 - Receive side queues: ready to send, waiting to receive
- Interrupts used but not required (not a user concern)
- All packets managed by the system
- Send and receive must match characteristics:
 - tag match (or wildcard on receive)
 - source match (or wildcard on receive)
 - Only $\min(\text{slen}, \text{dlen})$ bytes actually sent

Receiving considerations:

- Can post receive before send
- Can query the ready to receive queue for specific messages:
 - `CMMD_msg_pending (src, tag)`
- If a desired message is pending, can query for characteristics:
 - `CMMD_bytes_received()`
 - `CMMD_msg_sender()`
 - `CMMD_msg_tag()`
- Can then allocate desired buffer size and post a receive

8.6.2 Bidirectional transfers:

- `CMMD_send_and_receive (source,tag,inbuf,len,dest,tag,outbuf,len)`
- Higher latency (setup both in and out transactions)
- Higher bandwidth (don't have to reenter inner kernel twice)
- Allows for more data parallel like communication (cshifts etc.)

8.6.3 Adding send side buffering:

- `CMMD_send_noblock (dest, tag, buf, len)`
- Returns immediately (either sends message or copies it into a system buffer)
- Copying data can be expensive.
- Dangerous - system buffer space may not be available.
- Provides behavior compatible with `NX_csend`
- Europeans frequently expect/request this style of messaging.
- Hides latency?
- Same protocol as `CMMD_send_block`

8.6.4 'One touch' non blocking messaging

- `CMMD_send_async (dest, tag, buffer, length, handler, h-arg)`
`CMMD_receive_async(source, tag, buffer, length, handler, h-arg)`
- Returns a message Control Block (MCB) immediately
- Contract: no user buffer changes until MCB indicates operation is done
- Handlers are invoked when operation is complete:
 - Handler is a function of two arguments: MCB and h-arg.
 - Handler is executed with interrupts disabled.
- Handlers are invoked 'asynchronously' with respect to the main user thread of control. Introduces the notion of a critical section.
- Query functions required:
 - `CMMD_mcb_node(mcb)`
 - `CMMD_mcb_source(mcb)`
 - `CMMD_mcb_tag(mcb)`
 - `CMMD_mcb_bytes(mcb)`
- Querying for message arrival:
 - `CMMD_mcb_pending(source, tag)`

- Querying for completion:
 - `CMMD_msg_done(mcb)`
 - `CMMD_all_msgs_done()`
- Waiting for message completion:
 - `CMMD_msg_wait(mcb)`
 - `CMMD_all_msgs_wait()`
- Resources:
 - Same queues as non-blocking functions
 - MCBs are a finite resource: `CMMD_mcb_free(mcb)`;
 - Dependence on interrupts.
- Actual transaction is synchronizing, but user code does not wait for synchronization (latency hiding).

8.6.5 Optimizing for repetitive communications patterns: channels.

- Saves latency: handshake is performed only once. Resources reused.
- Channel state: a slightly different view of communication management.
- Behavior is asynchronous
- Channels are unidirectional.
- Establishing a channel:
 - `CMMD_open_send_channel(dest, tag, buffer, len)`.
 - `CMMD_open_receive_channel(source, tag, buffer, len)`.
 - Sending and receiving functions must agree in tag and buffer length.
 - A Channel Descriptor $xcd|x = (r, s)$ is returned by each function.
 - This is similar, in constitution and function, to an MCB.
- Operation on a channel:
 - `CMMD_write_channel(scd)`
 - Sends a message when the channel is writable.
 - Message arrives in receiver's buffer without notice.
- Querying channel state:
 - `CMMD_send_channel_status(scd)`
 - `CMMD_receive_channel_status(rcd)`
 - `CMMD_is_channel_writable(scd)`
 - `CMMD_is_channel_readable(rcd)`
- Allows user to structure code to avoid latency. Check for message arrival only when algorithmically necessary. Wait only when necessary.
- Closing channels. Freeing resources:
 - `CMMD_close_send_channel(scd)`
 - `CMMD_close_receive_channel(rcd)`
 - `CMMD_all_channels_free()`
 - `CMMD_all_channels_free_wait()`

- Channel descriptors are a finite resource in the same sense as MCBs. They are freed automatically when both the send and receive descriptors are in the closed state.
- Channels are somewhat lower level, less 'safe' functions. There is more than can go wrong, more state to check. The user must trade off the additional performance and flexibility against the additional responsibility.

8.6.6 Observations on standard message passing:

- Some sort of synchronization or rendezvous is required.
- Programmer must schedule both ends of each transaction. That is, a send must be matched by a receive somewhere (slightly relaxed in case of a channel).
- Overheads (latencies) are relatively high. This encourages the programmer to view communications as expensive to very expensive operations.
- To counter this expense, latency hiding is attempted. The success of such strategies varies widely depending on the behavior (sophistication) of the underlying hardware (DMA or co-processor available?).
- Latency hiding affects code structure. This effect has already been noticed by programmers and compiler writers who have had to deal with the ever increasing distance between fast processors and their memories. Operand prefetch and instruction scheduling become at once important and more difficult (many more cycles to hide).
- Proposed alternative? Reduce message latency as much as possible. Get rid of extraneous protocol. Don't preclude the user from gaining performance in the gain of safety.

8.7 Non-traditional messaging: Active Messages and Ports

- An active message is conceptually similar to a UNIX remote procedure call.

It is a single packet message.

The first word contains the address of a function.

The remaining words contain arguments to which the function is to be applied.

When the message is sent, the function pointer and arguments are copied from registers to the network interface (no unnecessary memory use).

Upon receipt, the receiving processor immediately constructs a stack frame with the received arguments and executes the function at the address specified by the pointer.

- Extremely lightweight (low latency)
- Designed as a compiler target (an assembly language for communication). Allows communication to be better integrated with computation
- Ideas borrowed from dataflow philosophy.
- Work done by von Eicken, Culler et al at UC Berkeley (Threaded Abstract Machine project)

8.7.1 Active Messages:

Active message variants:

- CMAML_requests(dest, ptr, arg1, arg2, arg3, arg4)
CMAML_reply(dest, ptr, arg1, arg2, arg3, arg4)
CMAML_rpc(dest, ptr, arg1, arg2, arg3, arg4)
- Pointer arguments specify destination handlers. Handlers execute in interrupt scope.
- Request sends on left DR channel. Interrupt status of sender is not important.
- Reply can only occur in the handler of a request. It is sent on the right DR channel.
- RPC can only be sent with the interrupts disabled. In its handler, any communication can be initiated.
- On CM-5E, longer packet variants of these will be available.

Interrupt control and polling functions:

- CMAML_enable_interrupts()
CMAML_disable_interrupts()
CMAML_poll()
- Many polling variants (with unusual semantics)

8.7.2 Observations on Active messages:

- Original intent was to provide 'surgical' communications control. Handlers are expected to be short. Get the data out of the network and into the destination as quickly as possible.
- Originally designed to work only with a polling interface (compiler would have complete knowledge of communications schedule).
- Extended (bastardized) by TMC to work in the context of interrupts. Also to be used by mere mortals.
- Speed is all. Safety is nonexistent. User control of interrupts allows for all sorts of potential problems. E.g. router deadlock, critical section violations.
- Extremely flexible. Other protocols can be built on top of these. E.g. CMMD.
- Request/reply protocol was implemented to use the CM-5 network in such a way as to prevent deadlock. Blumofe (MIT) notes that this is overly restrictive.
- Can think of active messages invoking new threads of control upon arrival. When combined with interrupts, this may complicate some code (user must consider safety issues).
- The idea of active messages seems simple, but it's actually very recent.

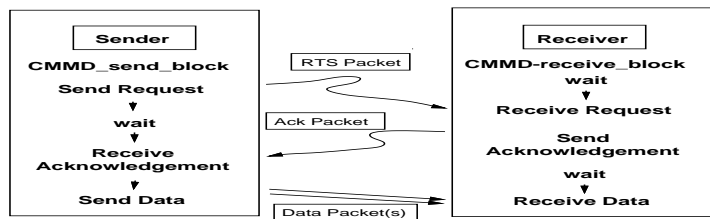


Figure 8.2: Rport structure

8.7.3 Rports

- Active messages are good for moving small amounts of data. What about moving large amounts?
- Desire transport with several properties:
 - Latency be kept at a minimum as if with active messages
 - Protocol should be kept to a minimum. This allows policy to be moved up to higher levels (simplifies design). As much as possible, the mechanism should not prevent the user from doing anything.
- Solution (also from UC Berkeley)
 - An rport is a sized destination for data. Once established by the receiver, data may be deposited at the destination by any sender. Once the destination has received the expected amount of data, the optional handler may be invoked.

Allocation and release:

- `CMAML_allocate_rport()`
- `CMAML_allocate_this_rport(rport_id)`
- `CMAML_free_rport(rport_id)`

Setting rport characteristics:

- `CMAML_set_rport_addr(rport_id, *buffer)`
- `CMAML_set_rport_byte_counter(rport_id, count)`
- `CMAML_set_rport_handler(rport_id, *handler)`
- `CMAML_set_rport_handler_arg2(rport_id, arg)`
- `CMAML_set_rport_total_nbytes(rport_id, size)`
- Total_nbytes is the size of the rport (the amount of data expected)
- Byte_counter is the size less the number of bytes already received

- Query functions exist as well
- Limited number of rports:
 - CMAML_number_of_rports()
 - CMAML_number_of_free_rports()

Sending to an rport:

- CMAML_scopy(dest, rport_id, dest_align, dest_offset, *buffer, nbytes, *handler, arg).
- Rport_id is the identity of the rport at the destination.
- Dest_align indicates alignment of start of buffer at destination.
- Dest_offset indicates how far into the buffer to start.
- Nbytes is the number of bytes to send.

8.7.4 Observations on Rports:

- Receiver controls the size of the rport (it can be changed after allocation).
- Receiver must reset byte_counter before rport reuse.
- Senders may execute a handler after sending has been completed.
- Up to the user to create a protocol based on these primitives.
- Many ways to go wrong.
- Very flexible. Can implement many-to-one patterns as well as point-to-point patterns.
- With interrupts enabled, operation is completely asynchronous. No rendezvous or synchronization is required.

8.7.5 Miscellaneous caveats regarding Active Messages and Rports:

- Remember to poll
- Be careful with interrupts. Be sure to preserve floating point state if necessary:
 - CMAML_save_fpu_regs()
 - CMAML_restore_fpu_regs()
- Interrupts are expensive.
- Beware of handler recursion. CMMD assigns priorities to message types and handlers:
 - Request, Reply
 - RPC
 - Scopy
 - Handlers
 - Main thread

- Lower priority items are queued when a higher priority event occurs. The queue is drained (in queue order) before control is return to the main thread. There is limited queue space.
- Flags are volatile. Compilers need to be told that.
- Message order is not preserved (one active message may overtake another).

8.7.6 Conclusions on message passing

There are dozens of libraries to perform such natural actions as **send** and **receive**. A standard library emerged for message passing (PVM), if you are willing to pay its performance cost. Also, PVM runs on networks of workstations, enabling another form of parallelism; PVM takes care of such issues as different endianity of the processors. Another standard library seems to emerge, called MPI; therefore neither is standard.

Chapter 9

Modeling Parallel Algorithms

To model and evaluate a parallel algorithm we need to analyze its performance. Two important parameters are *speedup* and *efficiency*. For each problem, there is a parameter n that describes the size of the problem. For example, n can be the number of particles in a particle simulation problem, or n can be the number of nonzero entries of a sparse matrix. Suppose we solve it on one processor in time $T(n, 1)$ and on p processors in time $T(n, p)$. Then the speedup is

$$S(n, p) = \frac{T(n, 1)}{T(n, p)}$$

and the efficiency is

$$E(n, p) = S(n, p)/p.$$

The sequential time $T(n, 1)$ in some sense give the total work needed to be done to solve the problem. On p machines, the total work given by $p \cdot T(n, p)$ and hence the overhead of the parallelization $H(n, P)$ is equal to $pT(n, p) - T(n, 1)$.

Chapter 10

Primitives

We now discuss a set of primitive functions that are frequently used in parallel programming. Many Scientific libraries support these functions.

10.1 Parallel Prefix

An important primitive for (data) parallel computing is the *scan operation*, also called *prefix sum* which takes an associated binary operator \oplus and an ordered set $[a_1, \dots, a_n]$ of n elements and returns the ordered set

$$[a_1, (a_1 \oplus a_2), \dots, (a_1 \oplus a_2 \oplus \dots \oplus a_n)].$$

For example,

$$\text{plus_scan}([1, 2, 3, 4, 5, 6, 7, 8]) = [1, 3, 6, 10, 15, 21, 28, 36].$$

Notice that computing the scan of an n -element array requires $n - 1$ serial operations.

Suppose we have n processors, each has a element of the array. If we are interested only in the last element, namely the total sum of the arrays, then it is easy to see how to compute it efficiently in parallel: we can just break the array recursively into two halves, and add the sums of the two halves, recursively. Associated with the computation is a complete binary tree. With n processors, this takes $O(\log n)$ steps. If we have only $p < n$ processors, we can break the array into p subarray, each has roughly $\lceil n/p \rceil$ elements. At the first step, each processor adds its own elements. The problem is then reduced to one with p elements. So we can perform the $\log p$ time algorithm. The total time is clearly $O(n/p + \log p)$ and communication only occur in the second step. For architecture like hypercube and fat tree, we can embed the complete binary tree so that the communication is performed by communication link directly.

Now we discuss a parallel method of finding *all* elements $[b_1, \dots, b_n] = \oplus_scan[a_1, \dots, a_n]$ in $O(\log n)$ time assume we have n processors each has an element of the array. The following is a Parallel Prefix algorithm to compute the scan of an array.

Function `scan`($[a_i]$):

1. $c_{2i} := a_{2i-1} \oplus a_{2i}$ (all i)
2. $[b_{2i}] := \text{scan}([c_{2i}])$ (all i)
3. $b_{2i+1} := b_{2i} \oplus a_{2i+1}$ (all i) Return $[b_i]$

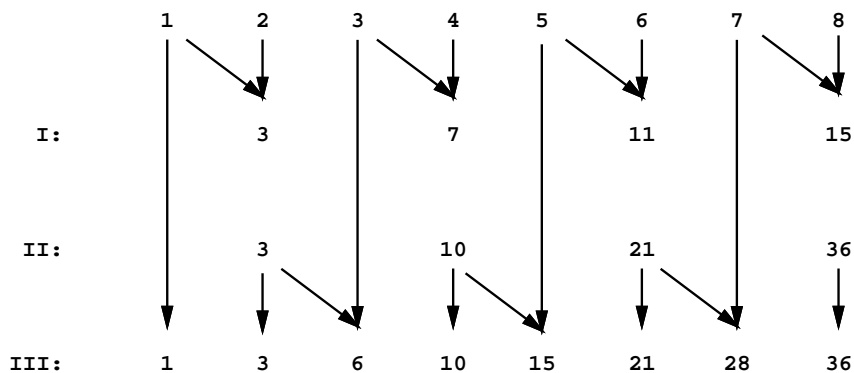


Figure 10.1: Action of the Parallel Prefix algorithm. The array in II comes from running `scan` recursively on the array in I.

The total number of \oplus operations performed by this algorithm is (ignoring a constant term of ± 1):

$$\begin{aligned}
 T_n &= \underbrace{\frac{n}{2}}^{\text{I}} + \underbrace{T_{n/2}}^{\text{II}} + \underbrace{\frac{n}{2}}^{\text{III}} \\
 &= n + T_{n/2} \\
 &= 2n
 \end{aligned}$$

If there is a processor for each array element, then the number of parallel operations is:

$$\begin{aligned}
 T_n &= \underbrace{1}^{\text{I}} + \underbrace{T_{n/2}}^{\text{II}} + \underbrace{1}^{\text{III}} \\
 &= 2 + T_{n/2} \\
 &= 2 \lg n
 \end{aligned}$$

In practice, we usually do not have a processor for each array element. Instead, there will likely be many more array elements than processors. If we have 32 processors and an array of 32000 numbers, then each processor should store a contiguous section of 1000 array elements. Suppose we have n element and p processors. In the following assume $k = n/p$, then the procedure to compute the scan is:

1. At each processor i , compute a local scan serially, for n/p consecutive elements, giving result $[d_1^i, d_2^i, \dots, d_k^i]$. Notice that this step vectorizes over processors.
2. Use the parallel prefix algorithm to compute $\text{scan}([d_k^1, d_k^2, \dots, d_k^p]) = [b_1, b_2, \dots, b_p]$
3. At each processor $i > 1$, add b_{i-1} to all elements d_j^i .

The time taken for the will be

$$T = 2 \cdot \left(\begin{array}{l} \text{time to add and store} \\ n/p \text{ numbers serially} \end{array} \right) + 2 \cdot (\log p) \cdot \left(\begin{array}{l} \text{Communication time} \\ \text{up and down a tree,} \\ \text{and a few adds} \end{array} \right)$$

10.2 Segmented Scan

We can extend the parallel scan algorithm to perform segmented scan. In *segmented scan* the original sequence is used along with an additional sequence of booleans. These booleans are used to identify the start of a new segment. Segmented scan is simply prefix scan with the additional condition the the sum starts over at the beginning of a new segment (which is indicated by a one in the string of booleans). Thus the following inputs would produce the following result when applying segmented plus scan on the array A and boolean array C .

$$\begin{aligned} A &= [1\ 2\ 3\ 4\ 5\ 6\ 7\ 8\ 9\ 10] \\ C &= [1\ 0\ 0\ 0\ 1\ 0\ 1\ 1\ 0\ 1] \\ \text{plus_scan}(A, C) &= [\underline{1}\ \underline{3}\ \underline{6}\ \underline{10}\ \underline{5}\ \underline{11}\ \underline{7}\ \underline{8}\ \underline{17}\ \underline{10}] \end{aligned}$$

We now show how to reduce segmented scan to simple scan. We define an operator (\oplus_2) that combines the vectors A and C (see above) which takes 2 operands x and y . These operands are simply 2 element column vectors where the first entry is from vector (A) and the second entry is from vector (C). Thus the 2-element representation of the example above is given as:

$$\begin{pmatrix} 1 \\ 1 \end{pmatrix} \begin{pmatrix} 2 \\ 0 \end{pmatrix} \begin{pmatrix} 3 \\ 0 \end{pmatrix} \begin{pmatrix} 4 \\ 0 \end{pmatrix} \begin{pmatrix} 5 \\ 1 \end{pmatrix} \begin{pmatrix} 6 \\ 0 \end{pmatrix} \begin{pmatrix} 7 \\ 1 \end{pmatrix} \begin{pmatrix} 8 \\ 1 \end{pmatrix} \begin{pmatrix} 9 \\ 0 \end{pmatrix} \begin{pmatrix} 10 \\ 1 \end{pmatrix}$$

The operator (\oplus_2) is defined as follows:

$$\begin{array}{c|cc} \oplus_2 & \begin{pmatrix} y \\ 0 \end{pmatrix} & \begin{pmatrix} y \\ 1 \end{pmatrix} \\ \hline \begin{pmatrix} x \\ 0 \end{pmatrix} & \begin{pmatrix} x+y \\ 0 \end{pmatrix} & \begin{pmatrix} y \\ 1 \end{pmatrix} \\ \begin{pmatrix} x \\ 1 \end{pmatrix} & \begin{pmatrix} x+y \\ 1 \end{pmatrix} & \begin{pmatrix} y \\ 1 \end{pmatrix} \end{array}$$

As an easy assignment, we can show that the binary operator \oplus_2 defined above is associative and satisfies has the following property: For each vector A and each boolean vector C , let AC be the 2-element representation of A and C . For each binary associative operator \oplus , the \oplus_2 -scan(AC) gives a 2-element vector whose first row is equal to the vector computed by segmented \oplus -scan(A, C); whose second vector is the all 1's vector. Therefore, we can apply the parallel scan algorithm to compute the segmented scan.

Notice that the method of assigning each segment to a separate processor may results in load imbalance.

10.3 Sorting and Selection

Sorting is one of the most important operations in computations. The problem is defined as: given an array of n elements $S = \{s_1, \dots, s_n\}$, transform S into an array $S' = \{s_{\pi(1)}, \dots, s_{\pi(n)}\}$ by permutation such that $s_{\pi(i)} \leq s_{\pi(i+1)}$ for all $1 \leq i \leq n - 1$. The rank of the element $s_{\pi(i)}$ is i . The problem of finding the rank of all element (without permuting) is called the *ranking problem*.

The k th element selection problem is defined as: given an array of n elements $S = \{s_1, \dots, s_n\}$ and an integer k , find the element of rank k . The k smallest elements selection problem is to find the set of all elements whose rank is no more than k .

Sorting and selection on parallel computers have been studied intensively. Efficient algorithms are given in the forms of sorting networks, shared memory algorithms, as well as sorting algorithms on particular parallel architectures such as hypercubes, lines and meshes. We refer the reader to the book of Tom Leighton for more complete covering. Here we present an algorithm that use parallel scan for the selection problem.

The algorithm is based on “quick selection”, a variant of quick sort (which is available in the Unix library). The quick selection algorithm can be described as following:

Algorithm: *Quick-Selection*(A, k)

1. Choose a random index i . We call $A[i]$ the sample.
2. Compute the number $m_{<}$ of the elements that are smaller than $A[i]$ and the number $m_{=}$ of elements that are equal to $A[i]$.
3. If $m_{<} < k$ and $m_{<} + m_{=} \geq k$, return $A[i]$.
4. If $m_{\leq} = m_{<} + m_{=} < k$, find the set $A_{>}$ of all elements that are larger than $A[i]$ and recursively call *Quick-Selection*($A_{>}, k - m_{\leq}$).
5. Else find the set $A_{<}$ of all elements that are less than $A[i]$ and recursively call *Quick-Selection*($A_{<}, k$).

The expected sequential time of *Quick-Selection* is $O(n)$. In parallel, the key computational steps are the computation of $m_{<}$, $m_{=}$, $A_{<}$ or $A_{>}$. The $m_{<}$ can be found by a reduction operation as following. Generate a 0-1 array C such that $C[j] = 0$ if $A[j] < A[i]$. On a parallel machine, we need to “broadcast” $A[i]$ to all the processors. The $m_{<}$ is equal to the sum of elements in C which can be found by a reduction. Similarly, we can compute $m_{=}$. To construct $A_{<}$ in an array representation, we also use the C vector. By applying prefix sum on C , i.e., $B = \text{plus-scan}(C)$, if $C[j] = 1$ then $A_{<}[B[j]] = A[j]$. So a parallel prefix sum following by an “array indexing” will allow to construct $A_{<}$. Therefore, the expect number of prefix sum operations needed by *Quick-Selection* is $O(\log n)$.

Similar prefix sum based quick sort, shells sort, and bucket sort can be developed. Interested readers can find some of them and some other applications of prefix sum in the book by Guy Blelloch.

With the help of randomization, we can selection with constant number of parallel scans. This is the first time we publish this selection algorithm.

Select the k th smallest element.

- Select a random $m = \sqrt{n}$ elements $S = \{s_1, \dots, s_m\}$.
- Sort the sample S into $s_{\pi(1)} < s_{\pi(2)} < \dots < s_{\pi(m)}$ using the parallelization of the all-pairs comparison algorithm.
- Using parallel scan to find all element A' in the interval $[s_{\pi(\lfloor k/p \rfloor - 1)}, s_{\pi(\lfloor k/p \rfloor + 1)}]$ as well as the number $m_{<}$ the number of elements that are smaller than $s_{\pi(\lfloor k/p \rfloor - 1)}$ and the number $m_{>}$ the number of elements that are larger than $s_{\pi(\lfloor k/p \rfloor + 1)}$.

- From $m_<$ and $m_>$, we can decide whether the k th smallest element is the A' . If it is not in A' or $|A| > 2\sqrt{n}$, we repeat the algorithm, else we sort A' using the parallelization of the all-pairs comparison algorithm and return the proper element.

We can show that the expected number of tries in the above algorithm is bounded by a constant and hence only a constant number of prefix sums are needed.

10.4 FFT

The *Fast Fourier Transform* is perhaps the most important subroutine in scientific computing. It has applications ranging from multiplying numbers and polynomials to image and signal processing, time series analysis, and the solution of linear systems and PDEs. There are tons of books on the subject including two recent wonderful ones by Charles van Loan and Briggs.

The Fourier transform of a vector x is $y = F_n x$, where F_n is the $n \times n$ matrix whose entry $(F_n)_{jk} = e^{-2\pi ijk/n}$, $j, k = 0 \dots n-1$. It is nearly always a good idea to use 0 based notation (as with the C programming language) in the context of the discrete Fourier transform. The negative exponent corresponds to Matlab's definition. Indeed in matlab we obtain `fn=fft(eye(n))`.

A good example is

$$F_4 = \begin{pmatrix} 1 & 1 & 1 & 1 \\ 1 & -i & -1 & i \\ 1 & -1 & 1 & -1 \\ 1 & i & -1 & -i \end{pmatrix}.$$

Sometimes it is convenient to denote $(F_n)_{jk} = \omega_n^{jk}$, where $\omega_n = e^{-2\pi i/n}$.

The Fourier matrix has more interesting properties than any matrix deserves to have. It is symmetric (but not Hermitian). It is Vandermonde (but not ill-conditioned). It is unitary except for a scale factor ($\frac{1}{\sqrt{n}}F_n$ is unitary). In two ways the matrix is connected to group characters: the matrix itself is the character table of the finite cyclic group, and the eigenvectors of the matrix are determined from the character table of a multiplicative group.

The trivial way to do the Fourier transform is to compute the matrix-vector multiply requiring n^2 multiplications and roughly the same number of additions. Cooley and Tukey gave the first $O(n \log n)$ time algorithm (actually the algorithm may be found in Gauss' work) known today as the FFT algorithm. We shall assume that $n = 2^p$ and let $m = n/2$. Then [This will be rewritten in matrix notation]

$$y_j = (F_n x)_j = \sum_{k=0}^{n-1} \omega_n^{jk} x_k$$

can be cut into the even and the odd parts:

$$y_j = \sum_{k=0}^{m-1} \omega_n^{2jk} x_{2k} + \omega_n^j \left(\sum_{k=0}^{m-1} \omega_n^{2jk} x_{2k+1} \right) ;$$

since $\omega_n^2 = \omega_m$, the two sums are just $\text{FFT}(x_{\text{even}})$ and $\text{FFT}(x_{\text{odd}})$. With this remark (see Fig. 1),

$$\begin{aligned} y_j &= \sum_{k=0}^{m-1} \omega_m^{jk} x_{2k} + \omega_n^j \left(\sum_{k=0}^{m-1} \omega_m^{jk} x_{2k+1} \right) \\ y_{j+m} &= \sum_{k=0}^{m-1} \omega_m^{jk} x_{2k} - \omega_n^j \left(\sum_{k=0}^{m-1} \omega_m^{jk} x_{2k+1} \right) . \end{aligned}$$

Then the algorithm keeps recurring; the entire "communication" needed for an FFT on a vector of length 8 can be seen in Fig. 2

The number of operations for an FFT on a vector of length n equals to twice the number for an FFT on length $n/2$ plus $n/2$ on the top level. As the solution of this recurrence, we get that the total number of operations is $\frac{1}{2}n \log n$.

Now we analyze the data motion required to perform the FFT. First we assume that to each processor one element of the vector x is assigned. Later we discuss the “real-life” case when the number of processors is less than n and hence each processor has some subset of elements. We also discuss how FFT is implemented on the CM-2 and the CM-5.

The FFT always goes from high order bit to low order bit, i.e., there is a fundamental asymmetry that is not evident in the figures below. This seems to be related to the fact that one can obtain a subgroup of the cyclic group by alternating elements, but not by taking, say, the first half of the elements.

10.4.1 Data motion

Let $i_p i_{p-1} \dots i_2 i_1 i_0$ be a bit sequence. Let us call $i_0 i_1 i_2 \dots i_{p-1} i_p$ the **bit reversal** of this sequence. The important property of the FFT network is that if the i -th input is assigned to the i -th processor for $i \leq n$, then the i -th output is found at the processor with address *the bit-reverse of i* . Consequently, if the input is assigned to processors with bit-reversed order, then the output is in standard order. The inverse FFT reverses bits in the same way.

To see why FFT reverses the bit order, let us have a look at the i -th segment of the FFT network (Fig. 3). The input is divided into parts and the current input (top side) consists of FFT's of these parts. One “block” of the input consists of the same fixed output element of all the parts. The $i - 1$ most significant bits of the input address determine this output element, while the least significant bits the the part of the original input whose transforms are at this level.

The next step of the FFT computes the Fourier transform of twice larger parts; these consist of an “even” and an “odd” original part. Parity is determined by the i -th most significant bit.

Now let us have a look at one unit of the network in Fig. 1; the two inputs correspond to the same even and odd parts, while the two outputs are the possible “farthest” vector elements, they differ in the most significant bit. What happens is that the i -th bit jumps first and becomes most significant (see Fig. 3).

Now let us follow the data motion in the entire FFT network. Let us assume that the i -th input element is assigned to processor i . Then after the second step a processor with binary address $i_p i_{p-1} i_{p-2} \dots i_1 i_0$ has the $i_{p-1} i_p i_{p-2} \dots i_1 i_0$ -th data, the second bit jumps first. Then the third, fourth, \dots , p -th bits all jump first and finally that processor has the $i_0 i_1 i_2 \dots i_{p-1} i_p$ -th output element.

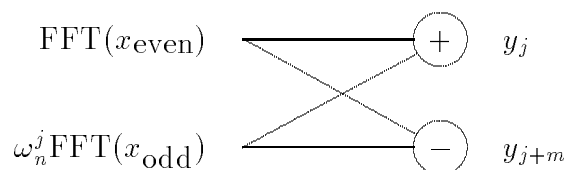


Figure 10.2: Recursive block of the FFT.

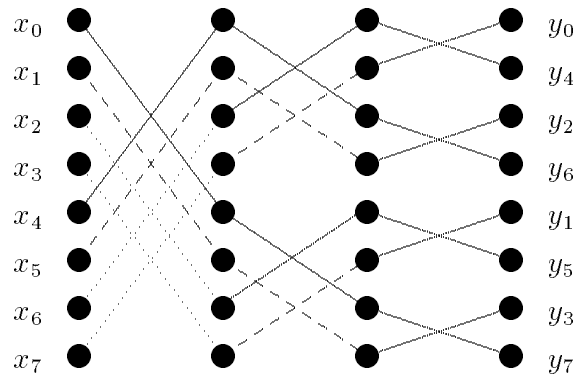


Figure 10.3: FFT network for 8 elements. (Such a network is not built in practice)

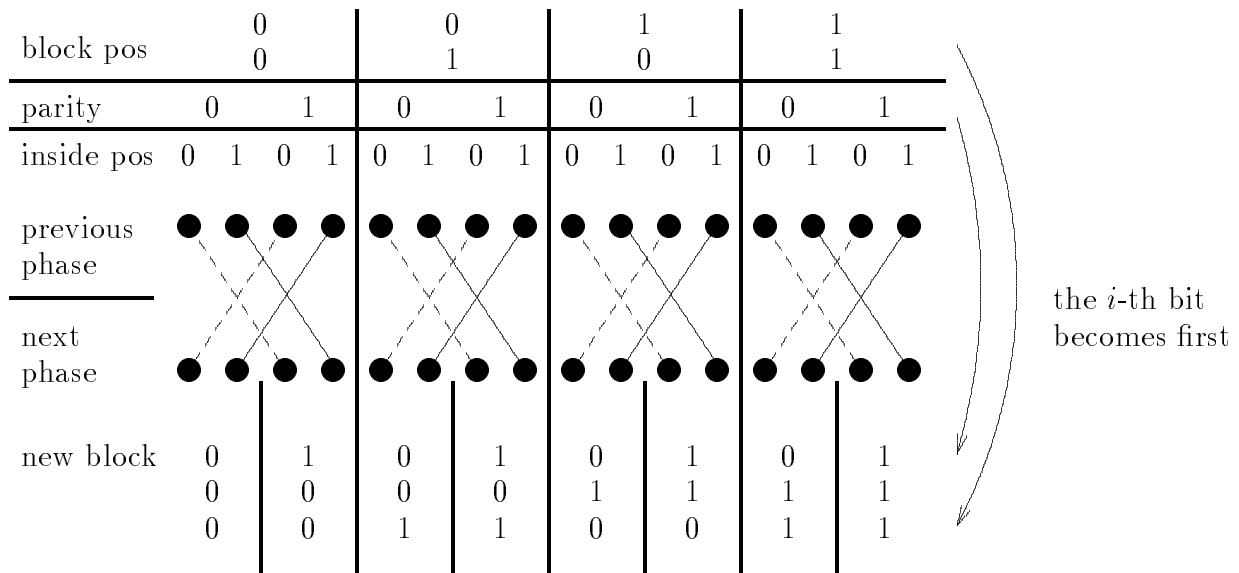


Figure 10.4: The output of FFT is in bit-reversed order.

10.4.2 FFT on parallel machines

In a realistic case, on a parallel machine some bits in the input address are local to one processor. The communication network can be seen in Fig. 4, left. FFT requires a large amount of communication; indeed it has fewer operations per communication than usual dense linear algebra. One way to increase this ratio is to *combine some layers* into one, as in Fig. 4, right. If s consecutive layers are combined, in one step a $2^s \times 2^s$ matrix multiplication must be performed. Since matrix multiplication vectorizes and usually there are optimized routines to do it, such a step is more efficient than communicating all small parts. Such a modified algorithm is called the *High Radix FFT*.

The FFT algorithm on the CM-2 is basically a High Radix FFT. However, on the CM-5 data motion is organized in a different way. The idea is the following: if s bits of the address are local to one processor, the last s phases of the FFT do not require communication. Let 3 bits be local

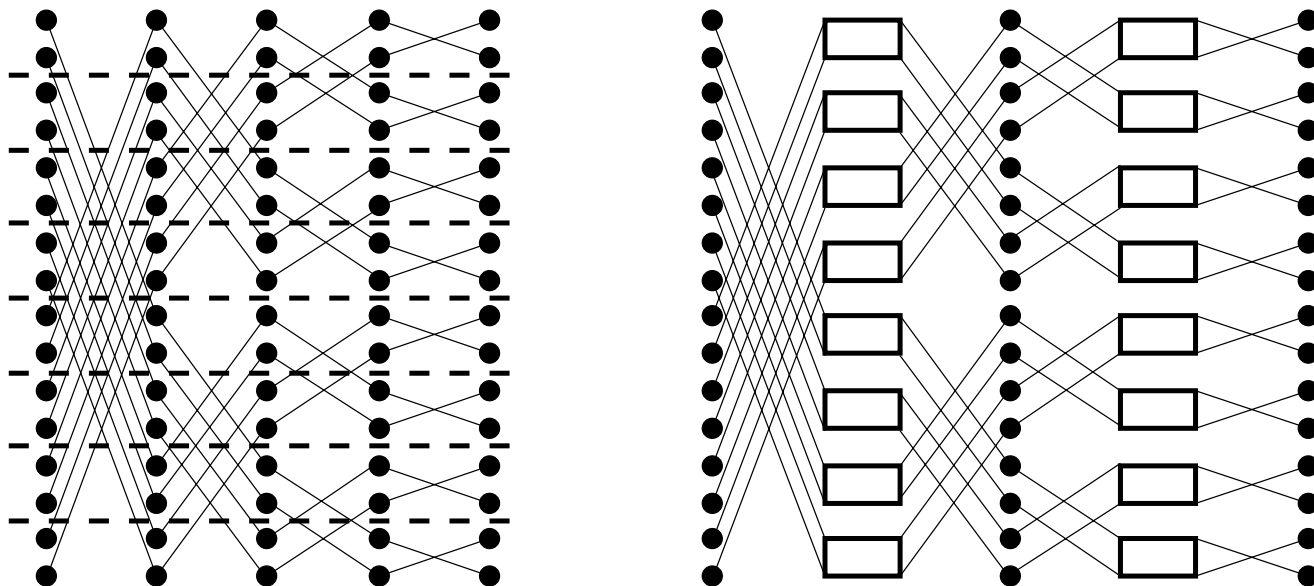


Figure 10.5: Left: more than one element per processor. Right: one box is a 4×4 matrix multiply.

to one processor, say. On the CM-5 the following data rearrangement is made: the data from the

$$i_p i_{p-1} i_{p-2} \dots i_3 | i_2 i_1 i_0 \text{-th}$$

processor is moved to the

$$i_2 i_1 i_0 i_{p-3} i_{p-4} \dots i_3 | i_p i_{p-1} i_{p-2} \text{-th!}$$

This data motion can be arranged in a clever way; after that the next 3 steps are local to processors. Hence the idea is to perform all communication at once *before* the actual operations are made.

10.4.3 Exercise

1. In Matlab use the `flops` function to obtain a flops count for FFT's for different power of 2 size FFT's. Make you input complex. Guess a flop count of the form $a + bn + c \log n + dn \log n$. Remembering that Matlab's `\` operator solves least squares problems, find a, b, c and d . Guess whether Matlab is counting flops or using a formula.

10.5 Matrix Multiplication

Everyone thinks that to multiply two 2-by-2 matrices requires 8 multiplications. However, Strassen gave a method, which requires only 7 multiplications! Actually, compared to the 8 multiplies and 4 adds of the traditional way, Strassen's method requires only 7 multiplies but 18 adds. Nowadays when multiplication of numbers is as fast as addition, this does not seem so important. However when we think of block matrices, matrix multiplication is very slow compared to addition. Strassen's method will give an $O(n^{2.8074})$ algorithm for matrix multiplication, in a recursive way very similar to the FFT.

First we describe Strassen's method for two block matrices:

$$\begin{pmatrix} A_{1,1} & A_{1,2} \\ A_{2,1} & A_{2,2} \end{pmatrix} \times \begin{pmatrix} B_{1,1} & B_{1,2} \\ B_{2,1} & B_{2,2} \end{pmatrix} = \begin{pmatrix} P_1 + P_4 - P_5 + P_7 & P_3 + P_5 \\ P_2 + P_4 & P_1 + P_3 - P_2 + P_6 \end{pmatrix}$$

where

$$\begin{aligned}
 P_1 &= (A_{1,1} + A_{1,2})(B_{1,1} + B_{2,2}) , \\
 P_2 &= (A_{2,1} + A_{2,2})B_{1,1} , \\
 P_3 &= A_{1,1}(B_{1,2} - B_{2,2}) , \\
 P_4 &= A_{2,2}(B_{2,1} - B_{1,1}) , \\
 P_5 &= (A_{1,1} + A_{1,2})B_{2,2} , \\
 P_6 &= (A_{2,1} - A_{1,1})(B_{1,1} + B_{1,2}) , \\
 P_7 &= (A_{1,2} - A_{2,2})(B_{2,1} + B_{2,2}) .
 \end{aligned}$$

If, as in the FFT algorithm, we assume that $n = 2^p$, the matrix multiply of two n -by- n matrices calls 7 multiplications of $(n/2)$ -by- $(n/2)$ matrices. Hence the time required for this algorithm is $O(n^{\log_2 7}) = O(n^{2.8074})$. Note that Strassen's idea can further be improved (of course, with the loss that several additions have to be made and the constant is impractically large) the current such record is an $O(n^{2.376})$ -time algorithm.

A final note is that, again as in the FFT implementations, we do not recur and use Strassen's method with 2-by-2 matrices. For some sufficient p , we stop when we get $2^p \times 2^p$ matrices and use direct matrix multiply which vectorizes well on the machine.

10.6 Basic Data Communication Operations

We conclude this section by list the set of basic data communication operations that are commonly used in a parallel program.

- **Single Source Broadcast:**
- **All-to-All Broadcast:**
- **All-to-All Personalized Communication:**
- **Array Indexing or Permutation:** There are two types of array indexing: the *left* array indexing and the *right* array indexing.
- **Polyshift:** SHIFT and EOSHIFT.
- **Sparse Gather and Scatter:**
- **Reduction and Scan:**

III Multipole Methods

Differential-equation based numerical methods are very important and have been applied to a large class of scientific problems. “However, not everyone has a complete faith in differential-equation based methods. Particles methods provide them with an alternative numerical approach to formulate and solve their problems from first principles” – paraphrased from Ahmed Sameh.

Chapter 11

Particle Methods

11.1 Reduce and Broadcast: A function viewpoint

[This section is being rewritten with what we hope will be the world's clearest explanation of the fast multipole algorithm. Readers are welcome to take a quick look at this section, or pass to the next section which leads up to the multipole algorithm through the particle method viewpoint]

Imagine we have P processors, and P functions $f_1(z), f_2(z), \dots, f_P(z)$, one per processor. Our goal is for every processor to know the sum of the functions $f(z) = f_1(z) + \dots + f_P(z)$. Really this is no different from the reduce and broadcast situation given in the introduction.

As a practical question, how can functions be represented on the computer? Probably we should think of Taylor series or multipole expansion. If all the Taylor series or multipole expansions are centered at the same point, then the function reduction is easy. Simply reduce the corresponding coefficients. If the pairwise sum consists of functions represented using different centers, then a common center must be found and the functions must be transformed to that center before a common sum may be found.

Example: Reducing Polynomials Imagine that processor i contains the polynomial $f_i(z) = (z - i)^3$. The coefficients may be expanded out as $f_i(z) = a_0 + a_1z + a_2z^2 + a_3z^3$. Each processor i contains a vector (a_0, a_1, a_2, a_3) . The sum of the vectors may be obtained by a usual reduce algorithm on vectors.

An alternative that may seem like too much trouble at first is that every time we make a pairwise sum we shift to a common midpoint. For example,

An example will go here

There is another complication that occurs when we form pairwise sums of functions. If the expansions are multipole or Taylor expansions, we may shift to a new center that is outside the region of convergence. The coefficients may then be meaningless. Numerically, even if we shift towards the boundary of a region of convergence, we may well lose accuracy, especially since most computations choose to fix the number of terms in the expansion to keep.

Difficulties with shifting multipole or Taylor Expansions

The fast multipole algorithm accounts for these difficulties in a fairly simple manner. Instead of computing the sum of the functions all the way up the tree and then broadcasting back, it saves the intermediate partial sums summing them in only when appropriate. The figure below indicates when this is appropriate.

11.2 Particle Methods: An Application

Imagine we want to model the basic mechanics of our solar system. We would probably start with the sun, somehow representing its mass, velocity, and position. We might then add each of the nine planets in turn, recording their own masses, velocities, and positions at a point in time. Let's say we add in a couple of hundred of the larger asteroids, and a few of our favorite comets. Now we set the system in motion. Perhaps we would like to know where Pluto will be in a hundred years, or whether a comet will hit us soon. To solve Newton's equations directly with more than even two bodies is intractably difficult. Instead we decide to model the system using discrete time intervals, and computing at each time interval the force that each body exerts on each other, and changing the velocities of the bodies accordingly. This is an example of an N-body problem. To solve the problem in a simple way requires $O(n^2)$ time for each time step. With some considerable effort, we can reduce this to $O(n)$ (using the fast multipole algorithm to be described below). A relatively simple algorithm the Barnes-Hut Algorithm, to be described below) can compute movement in $O(n \log(n))$ time.

11.3 Outline

- Formulation and applications
- “The easiest part”: the Euler method to move bodies.
- Direct methods for force computation.
- Hierarchical methods (*Barnes-Hut, Appel, Greengard and Rokhlin*)

11.4 What is N-Body Simulation?

We take n bodies (or particles) with state describing the initial position $\vec{x}_1, \vec{x}_2, \dots, \vec{x}_n \in \mathbb{R}^k$ and initial velocities $\vec{v}_1, \vec{v}_2, \dots, \vec{v}_n \in \mathbb{R}^k$.

We want to simulate the evolution of such a system, i.e., to compute the trajectories of each body, under an interactive force: the force exerted on each body by the whole system at a given point. For different applications we will have different interaction forces, such as gravitational or Coulombic forces. We could even use these methods to model spring systems, although the advanced methods, which assume forces decreasing with distance, do not work under these conditions.

11.5 Examples

- **Astrophysics:** The bodies are stars or galaxies, depending on the scale of the simulation. The interactive force is gravity.
- **Plasma Physics:** The basic particles are ions, electrons, etc; the force is Coulombic.

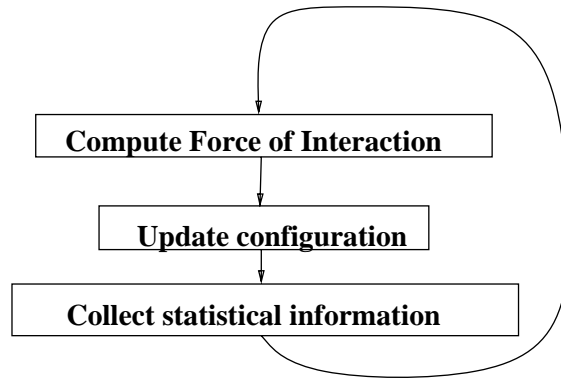


Figure 11.1: Basic Algorithm of N-body Simulation

- **Molecular Dynamics:** Particles are atoms or clusters of atoms; the force is electrostatic.
- **Fluid Dynamics:** Vortex method where particle are fluid elements (fluid blobs).

Typically, we call this class of simulation methods, the **particle methods**. In such simulations, it is important that we choose both spatial and temporal scales carefully, in order to minimize running time and maximize accuracy. If we choose a time scale too large, we can lose accuracy in the simulation, and if we choose one too small, the simulations will take too long to run. A simulation of the planets of the solar system will need a much larger timescale than a model of charged ions. Similarly, spatial scale should be chosen to minimize running time and maximize accuracy. For example, in applications in fluid dynamics, molecular level simulations are simply too slow to get useful results in a reasonable period of time. Therefore, researchers use the vortex method where bodies represent large aggregates of smaller particles. Hackney and Eastwood's book **Computer Simulations Using Particles**, McGraw Hill (1981), explores the applications of particle methods applications, although it is somewhat out of date.

11.6 The Basic Algorithm

Figure 11.1 illustrates the key steps in n -body simulation. The step of collecting statistical information is application dependent, and some of the information gathered at this step may be used during the next time interval.

We will use gravitational forces as an example to present N-body simulation algorithms. Assume there are n bodies with masses m_1, m_2, \dots, m_n , respectively, initially located at $\vec{x}_1, \dots, \vec{x}_n \in \mathbb{R}^3$ with velocity $\vec{v}_1, \dots, \vec{v}_n$. The gravitational force exert on the i th body by the j th body is given by

$$\vec{F}_{ij} = G \frac{m_i m_j}{r^2} = G \frac{m_i m_j}{|\vec{x}_j - \vec{x}_i|^3} (\vec{x}_j - \vec{x}_i),$$

where G is the gravitational constant. Thus the total force on the i th body is the vector sum of all these forces and is give by,

$$\vec{F}_i = \sum_{j \neq i} \vec{F}_{ij}.$$

Let $\vec{a}_i = d\vec{v}_i/dt$ be the acceleration of the body i , where where $\vec{v}_i = d\vec{x}_i/dt$. By Newton's second law of motion, we have $\vec{F}_i = m_i \vec{a}_i = m_i d\vec{v}_i/dt$.

11.6.1 Finite Difference and the Euler Method

In general, the force calculation is the most expensive step for N-body simulations. We will present several algorithms for this later on, but first assume we have already calculated the force \vec{F}_i acting on each body. We can use a numerical method (such as the Euler method) to update the configuration.

To simulate the evolution of an N -body system, we decompose the time interval into discretized time steps: $t_0, t_1, t_2, t_3, \dots$. For uniform discretizations, we choose a Δt and let $t_0 = 0$ and $t_k = k\Delta t$. The Euler method approximates the derivative by finite difference.

$$\begin{aligned}\vec{a}_i(t_k) &= \vec{F}_i/m_i = \frac{\vec{v}_i(t_k) - \vec{v}_i(t_k - \Delta t)}{\Delta t} \\ \vec{v}_i(t_k) &= \frac{\vec{x}_i(t_k + \Delta t) - \vec{x}_i(t_k)}{\Delta t},\end{aligned}$$

where $1 \leq i \leq n$. Therefore,

$$\vec{v}_i(t_k) = \vec{v}_i(t_{k-1}) + \Delta t(\vec{F}_i/m_i) \quad (11.1)$$

$$\vec{x}_i(t_{k+1}) = \vec{x}_i(t_k) + \Delta t\vec{v}_i(t_k). \quad (11.2)$$

From the given initial configuration, we can derive the next time step configuration using the formulae by first finding the force, from which we can derive velocity, and then position, and then force at the next time step.

$$\vec{F}_i \rightarrow v_i(t_k) \rightarrow x_i(t_k + \Delta t) \rightarrow F_{i+1}.$$

High order numerical methods can be used here to improve the simulation. In fact, the Euler method that uses uniform time step discretization performs poorly during the simulation when two bodies are very close. We may need to use non-uniform discretization or a sophisticated time scale that may vary for different regions of the N-body system.

In one region of our simulation, for instance, there might be an area where there are few bodies, and each is moving slowly. The positions and velocities of these bodies, then, do not need to be sampled as frequently as in other, higher activity areas, and can be determined by extrapolation. See figure 11.2 for illustration.¹

How many floating point operations (flops) does each step of the Euler method take? The velocity update (step 1) takes $2n$ floating point multiplications and one addition and the position updating (step 2) takes 1 multiplication and one addition. Thus, each Euler step takes $5n$ floating point operations. In Big-O notation, this is an $O(n)$ time calculation with a constant factor 5.

Notice also, each Euler step can be parallelized without communication overhead. In data parallel style, we can express steps (1) and (2), respectively, as

$$\begin{aligned}V &= V + \Delta t(F/M) \\ X &= X + \Delta tV,\end{aligned}$$

where V is the velocity array; X is the position array; F is the force array; and M is the mass array. V, X, F, M are $3 \times n$ arrays with each column corresponding to a particle. The operator $/$ is the elementwise division.

¹In figure 11.2 we see an example where we have some close clusters of bodies, and several relatively disconnected bodies. For the purposes of the simulation, we can ignore the movement of relatively isolated bodies for short periods of time and calculate more frames of the proximate bodies. This saves computation time and grants the simulation more accuracy where it is most needed. In many ways these sampling techniques are a temporal analogue of the later discussed Barnes and Hut and Multipole methods.

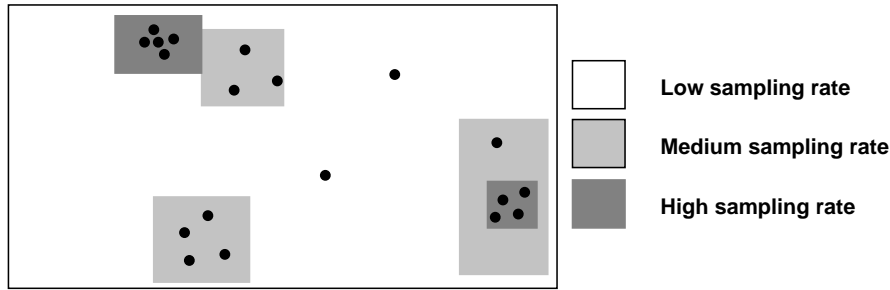


Figure 11.2: Adaptive Sampling Based on Proximity

11.7 Methods for Force Calculation

Computationally, the force calculation is the most time expensive step for N-body simulation. We now discuss some methods for computing forces.

11.7.1 Direct force calculation

The simplest way is to calculate the force directly from the definition.

$$\vec{F}_{ij} = G \frac{m_i m_j}{r^2} = G \frac{m_i m_j}{|\vec{x}_j - \vec{x}_i|^3} (\vec{x}_j - \vec{x}_i),$$

Note that the step for computing \vec{F}_{ij} takes 9 flops. It takes n flops to add \vec{F}_{ij} ($1 \leq j \leq n$). Since $\vec{F}_{ij} = -\vec{F}_{ji}$, the total number of flops needed is roughly $5n^2$. In Big-O notation, this is an $O(n^2)$ time computation. For large scale simulation (e.g., $n = 100$ million), the direct method is impractical with today's level of computing power.

It is clear, then, that we need more efficient algorithms. The one fact that we have to take advantage of is that in a large system, the effects of individual distant particles on each other may be insignificant and we may be able to disregard them without significant loss of accuracy. Instead we will cluster these particles, and deal with them as though they were one mass. Thus, in order to gain efficiency, we will approximate in space as we did in time by discretizing.

11.7.2 Potential based calculation

For N-body simulations, sometimes it is easier to work with the (gravitational) potential rather than with the force directly. The force can then be calculated as the gradient of the potential.

In three dimensions, the gravitational potential at position \vec{x} defined by n bodies with masses m_1, \dots, m_n at position $\vec{x}_1, \dots, \vec{x}_n$, respectively is equal to

$$\Phi(\vec{x}) = \sum_{i=1}^n G \frac{m_i}{\|\vec{x} - \vec{x}_i\|}.$$

The force acting on a body with unit mass at position \vec{x} is given by the *gradient* of Φ , i.e.,

$$F = -\nabla\Phi(x).$$

The potential function is a sum of local potential functions

$$\phi(\vec{x}) = \sum_{i=1}^n \phi_{\vec{x}_i}(\vec{x}) \quad (11.3)$$

where the local potential functions are given by

$$\phi_{\vec{x}_i}(\vec{x}) = \frac{G * m_i}{\|\vec{x} - \vec{x}_i\|} \quad \text{in } \mathfrak{R}^3 \quad (11.4)$$

11.7.3 Poisson Methods

The earlier method from 70s is to use Poisson solver. We work with the gravitational potential field rather than the force field. The observation is that the potential field can be expressed as the solution of a Poisson equation and the force field is the gradient of the potential field.

The gravitational potential at position \vec{x} defined by n bodies with masses m_1, \dots, m_n at position $\vec{x}_1, \dots, \vec{x}_n$, respectively is equal to

$$\Phi(\vec{x}) = \sum_{i=1}^n G \frac{m_i}{|\vec{x} - \vec{x}_i|}.$$

The force acting on a body with unit mass at position \vec{x} is given by the gradient of Φ :

$$\vec{F} = -\nabla\Phi(\vec{x}).$$

So, from Φ we can calculate the force field (by numerical approximation).

The potential field Φ satisfies a Poisson equation:

$$\nabla^2\Phi = \frac{\partial^2\Phi}{\partial x^2} + \frac{\partial^2\Phi}{\partial y^2} + \frac{\partial^2\Phi}{\partial z^2} = \rho(x, y, z),$$

where ρ measures the mass distribution can be determined by the configuration of the N -body system. (The function Φ is harmonic away from the bodies and near the bodies, $\text{div}\nabla\Phi = \nabla^2\Phi$ is determined by the mass distribution function. So $\rho = 0$ away from bodies).

We can use finite difference methods to solve this type of partial differential equations. In three dimensions, we discretize the domain by a structured grid.

We approximate the Laplace operator ∇^2 by finite difference and obtain from $\nabla^2\Phi = \rho(x, y, z)$ a system of linear equations. Let h denote the grid spacing. We have

$$\begin{aligned} \Phi(x_i, y_j, z_k) &= \frac{1}{h^2} (\Phi(x_i + h, y_j, z_k) + \Phi(x_i - h, y_j, z_k) + \Phi(x_i, y_j + h, z_k) \\ &\quad + \Phi(x_i, y_j - h, z_k) + \Phi(x_i, y_j, z_k + h) + \Phi(x_i, y_j, z_k - h) - 6\phi(x_i, y_j, z_k)) \\ &= \rho(x_i, y_j, z_k). \end{aligned}$$

The resulting linear system is of size equal to the number of grid points chosen. This can be solved using methods such as FFT (fast Fourier transform), SOR (successive overrelaxation), multigrid methods or conjugate gradient. If n bodies give a relatively uniform distribution, then we can use a grid which has about n grid points. The solution can be fairly efficient, especially on parallel machines. For highly non-uniform set of bodies, hybrid methods such as finding the potential induced by bodies within near distance by direct method, and approximate the potential field induced by distant bodies by the solution of a much smaller Poisson equation discretization. More details of these methods can be found in Hockney and Eastwood's book.

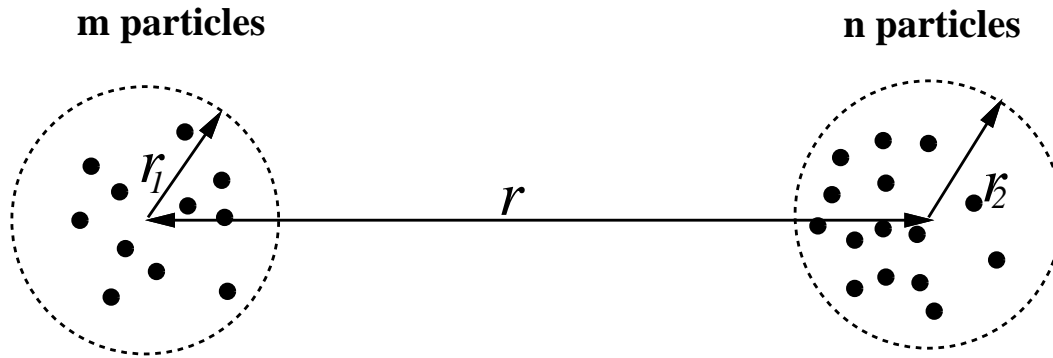


Figure 11.3: Well-separated Clusters

11.7.4 Hierarchical methods

We now discuss several methods which use a hierarchical structure to decompose bodies into clusters. Then the force field is approximated by computing the interaction between bodies and clusters and/or between clusters and clusters. We will refer this class of methods *hierarchical methods* or *tree-code methods*.

The crux of hierarchical N-body methods is to decompose the potential at a point x , $\phi(x)$, into the sum of two potentials: $\phi_N(x)$, the potential induced by “neighboring” or “near-field” particles; and $\phi_F(x)$, the potential due to “far-field” particles [5, 41]. In hierarchical methods, $\phi_N(x)$ is computed exactly, while $\phi_F(x)$ is computed approximately.

The approximation is based on a notion of well-separated clusters [5, 41]. Suppose we have two clusters A and B , one of m particles and one of n particles, the centers of which are separated by a distance r . See Figure 11.3.

Suppose we want to find the force acting on all bodies in A by those in B and vice versa. A direct force calculation requires $O(mn)$ operations, because for each body in A we need to compute the force induced by every body in B .

Notice that if r is much larger than both r_1 and r_2 , then we can simplify the calculation tremendously by replacing B by a larger body at its center of mass and replacing A by a larger body at its center of mass. Let M_A and M_B be the total mass of A and B , respectively. The center of mass c_A and c_B is given by

$$c_A = \frac{\sum_{i \in A} m_i x_i}{M_A}$$

$$c_B = \frac{\sum_{j \in B} m_j x_j}{M_B}.$$

We can approximate the force induced by bodies in B on a body of mass m_x located at position s by viewing B as a single mass M_B at location c_B . That is,

$$F(x) \approx \frac{G m_x M_B (x - c_B)}{\|x - c_B\|^3}.$$

Such approximation is second order: The relative error introduced by using center of mass is bounded by $(\max(r_1, r_2)/r)^2$. In other words, if $f(x)$ be the true force vector acting on a body at

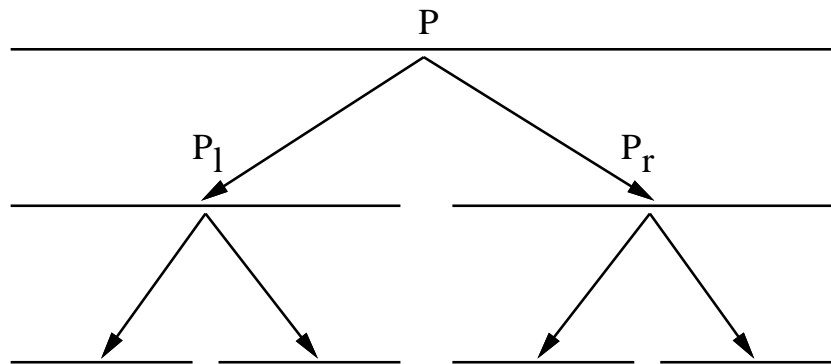


Figure 11.4: Binary Tree (subdivision of a straight line segment)

x , then

$$F(x) = f(x) \left(1 + O \left(\left(\frac{\max(r_1, r_2)}{r} \right)^2 \right) \right).$$

This way, we can find all the interaction forces between A and B in $O(n + m)$ time. The force calculations between one m particle will be computed separately using a recursive construction. This observation gives birth to the idea of hierarchical methods.

We can also describe the method in terms of potentials. If r is much larger than both r_1 and r_2 , i.e., A and B are “well-separated”, then we can use the p th order multipole expansion (to be given later) to express the p th order approximation of potential due to all particles in B . Let $\Phi_B^p(x)$ denote such a multipole expansion. To (approximately) compute the potential at particles in A , we simply evaluate $\Phi_B^p()$ at each particle in A . Suppose $\Phi_B^p()$ has $g(p, d)$ terms. Using multipole expansion, we reduce the number of operations to $g(p, d)(|A| + |B|)$. The error of the multipole expansion depends on p and the ratio $\max(r_1, r_2)/r$. We say A and B are β -well-separated, for a $\beta > 2$, if $\max(r_1, r_2)/r \leq 1/\beta$. As shown in [41], the error of the p th order multipole expansion is bounded by $(1/(\beta - 1))^p$.

11.8 Quadtree (2D) and Octtree (3D) : Data Structures for Canonical Clustering

Hierarchical N-body methods use quadtree (for 2D) and octtree (for 3D) to generate a canonical set of boxes to define clusters. The number of boxes is typically linear in the number of particles, i.e., $O(n)$.

Quadtrees and octtrees provide a way of hierarchically decomposing two dimensional and three dimensional space. Consider first the one dimensional example of a straight line segment. One way to introduce clusters is to recursively divide the line as shown in Figure 11.4.

This results in a binary tree².

In two dimensions, a *box* decomposition is used to partition the space (Figure 11.5). Note that a box may be regarded as a “product” of two intervals. Each partition has at most one particle in it.

²A tree is a graph with a single *root* node and a number of subordinate nodes called *leaves* or *children*. In a binary tree, every node has at most two children.

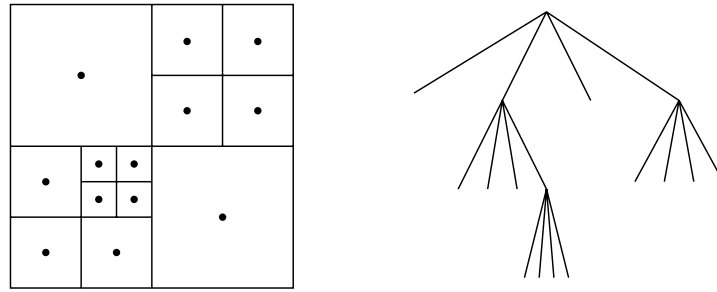


Figure 11.5: Quadtree

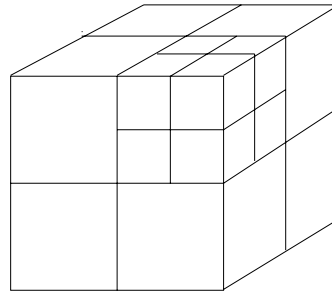


Figure 11.6: Octree

A *quadtree* [83] is a recursive partition of a region of the plane into axis-aligned squares. One square, the *root*, covers the entire set of particles. It is often chosen to be the smallest (up to a constant factor) square that contains all particles. A square can be divided into four *child* squares, by splitting it with horizontal and vertical line segments through its center. The collection of squares then forms a tree, with smaller squares at lower levels of the tree. The recursive decomposition is often adaptive to the local geometry. The most commonly used termination condition is: the division stops when a box contains less than some constant (typically $m = 100$) number of particles (See Figure 11.5).

Octtree is the three-dimension version of quadtree. The root is a box covering the entire set of particles. Octtree are constructed by recursively and adaptively dividing a box into eight child-boxes, by splitting it with hyperplanes normal to each axes through its center (See Figure 11.6).

11.9 Barnes-Hut Method (1986)

The Barnes-Hut method uses these clustered data structures to represent the bodies in the simulation, and takes advantage of the distant-body simplification mentioned earlier to reduce computational complexity to $O(n \log(n))$.

The method of Barnes and Hut has two steps.

1. Upward evaluation of center of mass

Refer to Figure 11.5 for the two dimensional case. Treating each box as a uniform cluster, the center of mass may be hierarchically computed. For example, consider the four boxes shown in Figure 11.7.

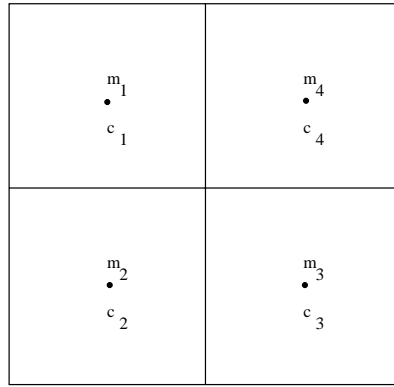


Figure 11.7: Computing the new Center of Mass

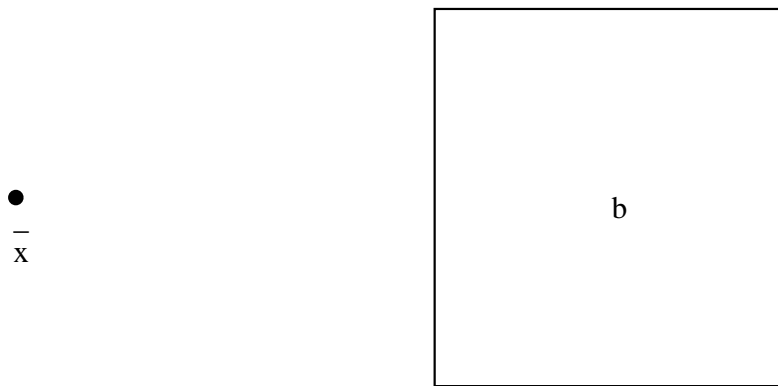


Figure 11.8: Pushing the particle down the tree

The total mass of the system is

$$m = m_1 + m_2 + m_3 + m_4 \quad (11.5)$$

and the center of mass is given by

$$\vec{c} = \frac{m_1\vec{c}_1 + m_2\vec{c}_2 + m_3\vec{c}_3 + m_4\vec{c}_4}{m} \quad (11.6)$$

The total time required to compute the centers of mass at all layers of the quadtree is proportional to the number of nodes, or the number of bodies, whichever is greater, or in Big-O notation, $O(n + v)$, where v is for *vertex*.

This result is readily extendible to the three dimensional case.

2. Pushing the particle down the tree

Consider the case of the octtree i.e. the three dimensional case. In order to evaluate the potential at a point \vec{x}_i , start at the top of the tree and move downwards. At each node, check whether the corresponding box, b , is well separated with respect to \vec{x}_i (Figure 11.8).

Let the force at point \vec{x}_i due to the cluster b be denoted by $\vec{F}(i, b)$. This force may be calculated using the following algorithm:

- if b is “far” i.e. well separated from \vec{x}_i , then

$$\vec{F}(\vec{x}_i) := \vec{F}(\vec{x}_i) + \frac{Gm_x M_b (\vec{x} - \vec{c}_b)}{\|\vec{x}_i - \vec{c}_b\|^3} \quad \text{in } \mathfrak{R}^3 \quad (11.7)$$

- else if b is “close” to \vec{x}_i

for $k = 1$ to 8

$$\vec{F}(\vec{x}_i) = \vec{F}(\vec{x}_i) + \vec{F}(i, \text{child}(b, k)) \quad (11.8)$$

$$(11.9)$$

The computational complexity of pushing the particle down the tree has the upper bound $9hn$, where h is the height of the tree and n is the number of particles. (Typically, for more or less uniformly distributed particles, $h = \log_4 n$.)

11.9.1 Approximating potentials

We now rephrase Barnes and Hut scheme in term of potentials. Let

$$\begin{aligned} m_A &= \text{total mass of particles in } \mathbf{A} \\ m_B &= \text{total mass of particles in } \mathbf{B} \\ \vec{c}_A &= \text{center of mass of particles in } \mathbf{A} \\ \vec{c}_B &= \text{center of mass of particles in } \mathbf{B} \end{aligned}$$

The potential at a point \vec{x} due to the cluster \mathbf{B} , for example, is given by the following second order approximation:

$$\phi(\vec{x}) \approx \frac{m_B}{\|\vec{x} - \vec{c}_B\|} \left(1 + \frac{1}{\delta^2}\right) \quad \text{in } \mathfrak{R}^3 \quad (11.10)$$

In other words, each cluster may be regarded as an individual particle when the cluster is sufficiently far away from the evaluation point \vec{x} .

A more advanced idea is to keep track of a higher order (Taylor expansion) approximation of the potential function induced by a cluster. Such an idea provides better tradeoff between time required and numerical precision. The following sections provide the two dimensional version of the fast multipole method developed by Greengard and Rokhlin.

The Barnes-Hut method discussed above uses the *particle-cluster* interaction between two well-separated clusters. Greengard and Rokhlin showed that the *cluster-cluster* intersection among well-separated clusters can further improve the hierarchical method. Suppose we have k clusters $B_1 \dots, B_k$ that are well-separated from a cluster A . Let $\Phi_i^p()$ be the p th order multipole expansion of B_i . Using particle-cluster interaction to approximate the far-field potential at A , we need to perform $g(p, d)|A|(|B_1| + |B_2| + \dots + |B_k|)$ operations. Greengard and Rokhlin [41] showed that from $\Phi_i^p()$ we can efficiently compute a Taylor expansion $\Psi_i^p()$ centered at the centroid of A that approximates $\Phi_i^p()$. Such an operation of transforming $\Phi_i^p()$ to $\Psi_i^p()$ is called a *FLIP*. The cluster-cluster interaction first flips $\Phi_i^p()$ to $\Psi_i^p()$; we then compute $\Psi_A^p() = \sum_{i=1}^k \Psi_i^p()$ and use $\Psi_A^p()$ to evaluate the potential at each particle in A . This reduces the number of operations to the order of

$$g(p, d)(|A| + |B_1| + |B_2| + \dots + |B_k|).$$

11.10 Outline

- Introduction
- Multipole Algorithm: An Overview
- Multipole Expansion
- Taylor Expansion
- Operation No. 1 — SHIFT
- Operation No. 2 — FLIP
- Application on Quad Tree
- Expansion from 2-D to 3-D

11.11 Introduction

For N-body simulations, sometimes, it is easier to work with the (gravitational) potential rather than with the force directly. The force can then be calculated as the gradient of the potential.

In two dimensions, the potential function at z_j due to the other bodies is given by

$$\begin{aligned}\phi(z_j) &= \sum_{i=1, i \neq j}^n q_i \log(z_j - z_i) \\ &= \sum_{i=1, i \neq j}^n \phi_{z_i}(z_j)\end{aligned}$$

with

$$\phi_{z_i}(z) = q_i \log |z - z_i|$$

where z_1, \dots, z_n the position of particles, and q_1, \dots, q_n the strength of particles. The potential due to the bodies in the rest of the space is

$$\phi(z) = \sum_{i=1}^n q_i \log(z - z_i)$$

which is *singular* at each potential body. (Note: actually the potential is $\text{Re } \phi(z)$ but we take the complex version for simplicity.)

With the Barnes and Hut scheme in term of potentials, each cluster may be regarded as an individual particle when the cluster is sufficiently far away from the evaluation point. The following sections will provide the details of the fast multipole algorithm developed by Greengard and Rokhlin.

Many people are often mystified why the Green's function is a logarithm in two dimensions, while it is $1/r$ in three dimensions. Actually there is an intuitive explanation. In d dimensions the Green's function is the integral of the force which is proportional $1/r^{d-1}$. To understand the $1/r^{d-1}$ just think that the lines of force are divided "equally" on the sphere of radius r . One might wish to imagine an d dimensional ball with small holes on the boundary filled with d dimensional water. A hose placed at the center will force water to flow out radially at the boundary in a uniform manner. If you prefer, you can imagine 1 ohm resistors arranged in a polar coordinate manner, perhaps with higher density as you move out in the radial direction. Consider the flow of current out of the circle at radius r if there is one input current source at the center.

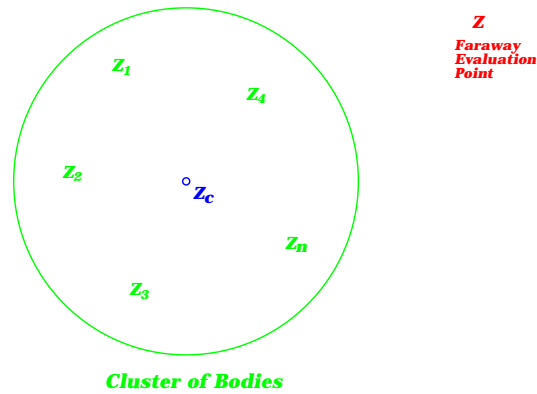


Figure 11.9: Potential of Faraway Particle due to Cluster

11.12 Multipole Algorithm: An Overview

There are three important concepts in the multipole algorithm:

- function representations (multipole expansions and Taylor series)
- operators to change representations (SHIFTs and FLIPs)
- the general tree structure of the computation

11.13 Multipole Expansion

The multipole algorithm flips between two point of views, or to be more precise, two representations for the potential function. One of them, which considers the cluster of bodies corresponding to many far away evaluation points, is treated in detail here. This part of the algorithm is often called the Multipole Expansion.

In elementary calculus, one learns about Taylor expansions for functions. This power series represents the function perfectly within the radius of convergence. A multipole expansion is also a perfectly valid representation of a function which typically converges *outside* a circle rather than inside. For example, it is easy to show that

$$\begin{aligned}\phi_{z_i}(z) &= q_i \log(z - z_i) \\ &= q_i \log(z - z_c) + \sum_{k=1}^{\infty} -\frac{q_i}{k} \left(\frac{z_i - z_c}{z - z_c} \right)^k\end{aligned}$$

where z_c is any complex number. This series converges in the region $|z - z_c| > |z - z_i|$, i.e., outside of the circle containing the singularity. The formula is particularly useful if $|z - z_c| \gg |z - z_i|$, i.e., if we are far away from the singularity.

Note that

$$\begin{aligned}\phi_{z_i}(z) &= q_i \log(z - z_i) \\ &= q_i \log[(z - z_c) - (z_i - z_c)] \\ &= q_i \left[\log(z - z_c) + \log\left(1 - \frac{z_i - z_c}{z - z_c}\right) \right]\end{aligned}$$

The result follows from the Taylor series expansion for $\log(1-x)$. The more terms in the Taylor series that are considered, the higher is the order of the approximation.

By substituting the single potential expansion back into the main equation, we obtain the multipole expansion as following

$$\begin{aligned}\phi(z) &= \sum_{i=1}^n \phi_{z_i}(z) \\ &= \sum_{i=1}^n q_i \log(z - z_c) + \sum_{i=1}^n \sum_{k=1}^{\infty} q_i \left(-\frac{1}{k} \left(\frac{z_i - z_c}{z - z_c} \right)^k \right) \\ &= Q \log(z - z_c) + \sum_{k=1}^{\infty} a_k \left(\frac{1}{z - z_c} \right)^k\end{aligned}$$

where

$$a_k = - \sum_{i=1}^n \frac{q_i (z_i - z_c)^k}{k}$$

When we truncate the expansion due to the consideration of computation cost, an error is introduced into the resulting potential. Consider a p -term expansion

$$\phi_p(z) = Q \log(z - z_c) + \sum_{k=1}^p a_k \frac{1}{(z - z_c)^k}$$

An error bound for this approximation is given by

$$\|\phi(z) - \phi_p(z)\| \leq \frac{A}{\left(\left|\frac{z-z_c}{r}\right| - 1\right)} \left|\frac{r}{z-z_c}\right|^p$$

where r is the radius of the cluster and

$$A = \sum_{i=1}^n |q_i|$$

This result can be shown as the following

$$\begin{aligned}\text{Error} &= \left| \sum_{k=p+1}^{\infty} a_k \frac{1}{(z - z_c)^k} \right| \\ &= \left| - \sum_{k=p+1}^{\infty} \sum_{i=1}^n \frac{q_i}{k} \left(\frac{z_i - z_c}{z - z_c} \right)^k \right| \\ &\leq \sum_{k=p+1}^{\infty} \sum_{i=1}^n |q_i| \left| \frac{r}{z - z_c} \right|^k \\ &\leq A \sum_{k=p+1}^{\infty} \left| \frac{r}{z - z_c} \right|^k \\ &\leq A \frac{\left| \frac{r}{z - z_c} \right|^{p+1}}{1 - \left| \frac{r}{z - z_c} \right|} \\ &\leq \frac{A}{\left(\left|\frac{z-z_c}{r}\right| - 1\right)} \left|\frac{r}{z-z_c}\right|^p\end{aligned}$$

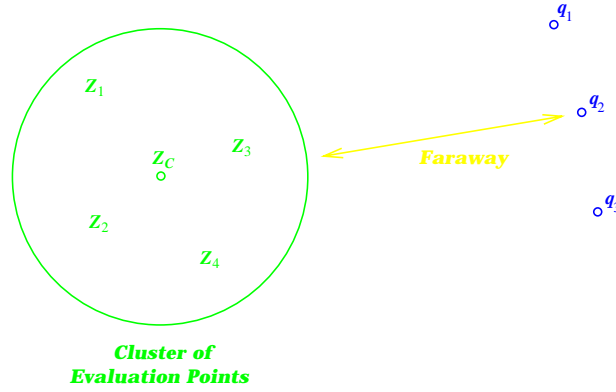


Figure 11.10: Potential of Particle Cluster

At this moment, we are able to calculate the potential of each particle due to cluster of far away bodies, through multipole expansion.

11.14 Taylor Expansion

In this section, we will briefly discuss the other point of view for the multipole algorithm, which considers the cluster of evaluation points with respect to many far away bodies. It is called Taylor Expansion. For this expansion, each processor "ownes" the region of the space defined by the cluster of evaluation points, and compute the potential of the cluster through a Taylor series about the center of the cluster z_c .

Generally, the local Taylor expansion for cluster denoted by C (with center z_c) corresponding to some body z has the form

$$\phi_{C,z_c}(z) = \sum_{k=0}^{\infty} b_k (z - z_c)^k$$

Denote $z - z_i = (z - z_c) - (z_i - z_c) = -(z_i - z_c)(1 - \xi)$. Then for z such that $|z - z_c| < \min(z_c, C)$, we have $|\xi| < 1$ and the series $\phi_{C,z_c}(z)$ converge:

$$\begin{aligned} \phi_{C,z_c}(z) &= \sum_C q_i \log(-(z_i - z_c)) + \sum_C q_i \log(1 - \xi) \\ &= \sum_C q_i \log(-(z_i - z_c)) + \sum_{k=1}^{\infty} \left(\sum_C q_i \right) k^{-1} (z_i - z_c)^{-k} (z - z_c)^k \\ &= b_0 + \sum_{k=1}^{\infty} b_k (z - z_c)^k \end{aligned}$$

where formulæ for coefficients are

$$b_0 = \sum_C q_i \log(-(z_i - z_c)) \quad \text{and} \quad b_k = k^{-1} \sum_C q_i (z_i - z_c)^{-k} \quad k > 0.$$

Define the p -order truncation of local expansion ϕ_{C,z_c}^p as follows

$$\phi_{C,z_c}^p(z) = \sum_{k=0}^p b_k (z - z_c)^k.$$

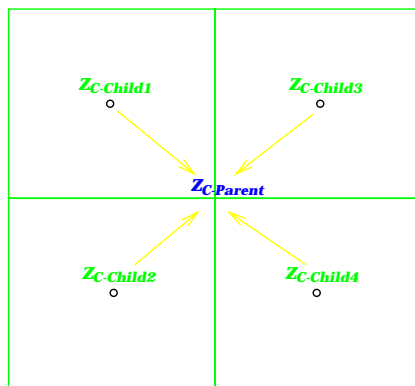


Figure 11.11: SHIFT the Center of Reference

We have error bound

$$\begin{aligned} \left| \phi_{C, z_c}(z) - \phi_{C, z_c}^p(z) \right| &= \left| \sum_{k=p+1}^{\infty} k^{-1} \sum_C q_i \left(\frac{z - z_c}{z_i - z_c} \right)^k \right| \\ &\leq \frac{1}{p+1} \sum_C |q_i| \sum_{k=p+1}^{\infty} \left| \frac{z - z_c}{\min(z_c, C)} \right|^k = \frac{A}{(1+p)(1-c)} c^{p+1}, \end{aligned}$$

where $A = \sum_C |q_i|$ and $c = |z - z_c| / \min(z_c, C) < 1$.

By now, we can also compute the local potential of the cluster through the Taylor expansion. During the process of deriving the above expansions, it is easy to see that

- Both expansions are singular at the position of any body;
- Multipole expansion is valid outside the cluster under consideration;
- Taylor expansion converges within the space defined the cluster.

At this point, we have finished the basic concepts involved in the multipole algorithm. Next, we will begin to consider some of the operations that could be performed on and between the expansions.

11.15 Operation No.1 — SHIFT

Sometimes, we need to change the location of the center of the reference for the expansion series, either the multipole expansion or the local Taylor expansion. To accomplish this goal, we will perform the SHIFT operation on the expansion series.

For the multipole expansion, consider some far away particle with position z such that both series ϕ_{z_0} and ϕ_{z_1} , corresponding to different center of reference z_0 and z_1 , converge: $|z - z_0| > \max(z_0, C)$ and $|z - z_1| > \max(z_1, C)$. Note that

$$z - z_0 = (z - z_1) - (z_0 - z_1) = (z - z_1) \left(1 - \frac{z_0 - z_1}{z - z_1} \right) = (z - z_1)(1 - \xi)$$

for appropriate ξ and if we also assume z sufficiently large to have $|\xi| < 1$, we get identity

$$(1 - \xi)^{-k} = \left(\sum_{l=0}^{\infty} \xi^l \right)^k = \sum_{l=0}^{\infty} \binom{k+l-1}{l} \xi^l.$$

Now, we can express the SHIFT operation for multipole expansion as

$$\begin{aligned}
\phi_{z_1}(z) &= \text{SHIFT}(\phi_{z_0}(z), z_0 \Rightarrow z_1) \\
&= \text{SHIFT}\left(a_0 \log(z - z_0) + \sum_{k=1}^{\infty} a_k (z - z_0)^{-k}, z_0 \Rightarrow z_1\right) \\
&= a_0 \log(z - z_1) + a_0 \log(1 - \xi) + \sum_{k=1}^{\infty} a_k (1 - \xi)^{-k} (z - z_1)^{-k} \\
&= a_0 \log(z - z_1) - a_0 \sum_{k=1}^{\infty} k^{-1} \xi^k + \sum_{k=1}^{\infty} \sum_{l=1}^{\infty} a_k \binom{k+l-1}{l} \xi^l (z - z_1)^{-k} \\
&= a_0 \log(z - z_1) + \sum_{l=1}^{\infty} \left(\sum_{k=1}^l a_k (z_0 - z_1)^{l-k} \binom{l-1}{k-1} - a_0 l^{-1} (z_0 - z_1)^l \right) (z - z_1)^{-l}
\end{aligned}$$

We can represent $\phi_{z_1}(z)$ as a sequence of its coefficients a'_k :

$$a'_0 = a_0 \quad \text{and} \quad a'_l = \sum_{k=1}^l a_k (z_0 - z_1)^{l-k} \binom{l-1}{k-1} - a_0 l^{-1} (z_0 - z_1)^l \quad l > 0.$$

Note that a'_l depends only on a_0, a_1, \dots, a_l and not on the higher coefficients. It shows that given $\phi_{z_0}^p$ we can compute $\phi_{z_1}^p$ exactly, that is without any further error! In other words, operators SHIFT and truncation commute on multipolar expansions:

$$\text{SHIFT}(\phi_{z_0}^p, z_0 \Rightarrow z_1) = \phi_{z_1}^p.$$

Similarly, we can obtain the SHIFT operation for the local Taylor expansion, by extending the operator on the domain of local expansion, so that $\text{SHIFT}(\phi_{C,z_0}, z_0 \Rightarrow z_1)$ produces ϕ_{C,z_1} . Both series converges for z such that $|z - z_0| < \min(z_0, C)$, $|z - z_1| < \min(z_1, C)$. Then

$$\begin{aligned}
\phi_{C,z_1}(z) &= \text{SHIFT}(\phi_{C,z_0}(z), z_0 \Rightarrow z_1) \\
&= \sum_{k=0}^{\infty} b_k ((z - z_1) - (z_0 - z_1))^k \\
&= \sum_{k=0}^{\infty} b_k \sum_{l=0}^{\infty} (-1)^{k-l} \binom{k}{l} (z_0 - z_1)^{k-l} (z - z_1)^l \\
&= \sum_{l=0}^{\infty} \left(\sum_{k=l}^{\infty} b_k (-1)^{k-l} \binom{k}{l} (z_0 - z_1)^{k-l} \right) (z - z_1)^l
\end{aligned}$$

Therefore, formula for transformation of coefficients b_k of ϕ_{C,z_0} to b'_l of ϕ_{C,z_1} are

$$b'_l = \sum_{k=l}^{\infty} a_k (-1)^{k-l} \binom{k}{l} (z_0 - z_1)^{k-l}.$$

Notice that in this case, b'_l depends only on the higher coefficients, which means knowledge of the coefficients b_0, b_1, \dots, b_p from the truncated local expansion in z_0 does *not* suffice to recover the coefficients b'_0, b'_1, \dots, b'_p at another point z_1 . We do incur an error by the SHIFT operation applied to truncated local expansion:

$$\left| \text{SHIFT}(\phi_{C,z_0}^p, z_0 \Rightarrow z_1) - \phi_{C,z_1}^p \right| = \left| \sum_{l=0}^{\infty} \left(\sum_{k=p+1}^{\infty} b_k (-1)^{k-l} (z_0 - z_1)^{k-l} \right) (z - z_1)^l \right|$$

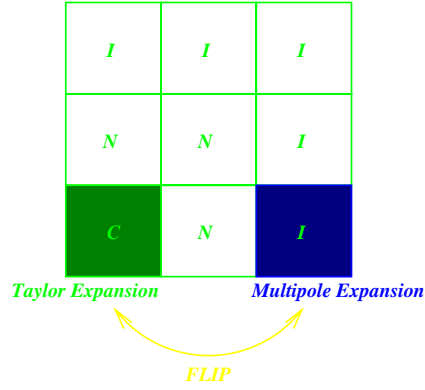


Figure 11.12: FLIP from Multipole to Taylor Expansion

$$\begin{aligned}
 &\leq \left| \sum_{k=p+1}^{\infty} b_k (z_1 - z_0)^k \right| \left| \sum_{l=0}^{\infty} \left(\frac{z - z_1}{z_1 - z_0} \right)^l \right| \\
 &= \left| \sum_{k=p+1}^{\infty} k^{-1} \sum_C q_i \left(\frac{z_1 - z_0}{z_i - z_0} \right)^k \right| \left| \sum_{l=0}^{\infty} \left(\frac{z - z_1}{z_0 - z_1} \right)^l \right| \\
 &\leq \frac{A}{(p+1)(1-c)(1-D)} c^{p+1},
 \end{aligned}$$

where $A = \sum_C |q_i|$. $c = |z_1 - z_0| / \min(z_0, C)$ and $D = |z - z_1| / |z_0 - z_1|$.

At this moment, we have obtained all the information needed to perform the SHIFT operation for both multipole expansion and local Taylor expansion. Next, we will consider the operation which can transform multipole expansion to local Taylor expansion.

11.16 Operation No.2 — FLIP

At this section, we will introduce the more powerful operation in multipole algorithm, namely the FLIP operation. For now, we will consider only the transformation in the direction from the multipole expansion $\phi_{z_0}(z)$ to the local Taylor expansion $\phi_{C, z_1}(z)$, denoted by

$$FLIP(\phi_{z_0}, z_0 \Rightarrow z_1) = \phi_{C, z_1}$$

For $|z - z_0| > \max(z_0, C)$ and $|z - z_1| < \min(z_1, C)$ both series converge. Note that

$$z - z_0 = -(z_0 - z_1) \left(1 - \frac{z - z_1}{z_0 - z_1} \right) = -(z_0 - z_1)(1 - \xi)$$

and assume also $|\xi| < 1$. Then,

$$\begin{aligned}
 \phi_{z_0}(z) &= a_0 \log(z - z_0) + \sum_{k=1}^{\infty} a_k (z - z_0)^{-k} \\
 &= a_0 \log(-(z_0 - z_1)) + a_0 \log(1 - \xi) + \sum_{k=1}^{\infty} a_k (-1)^k (z_0 - z_1)^{-k} (1 - \xi)^{-k}
 \end{aligned}$$

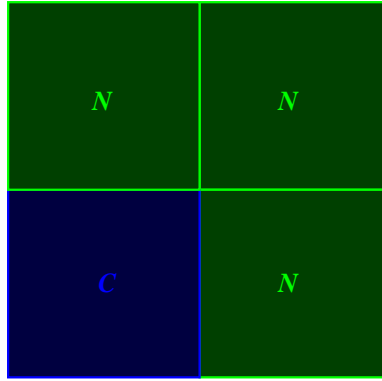


Figure 11.13: First Level of Quad Tree

$$\begin{aligned}
&= a_0 \log(-(z_0 - z_1)) + \sum_{l=1}^{\infty} -a_0 l^{-1} \xi^l + \sum_{k=1}^{\infty} (-1)^k a_k (z_0 - z_1)^{-k} \sum_{l=0}^{\infty} \binom{k+l-1}{l} \xi^l \\
&= \left(a_0 \log(-(z_0 - z_1)) + \sum_{k=1}^{\infty} (-1)^k a_k (z_0 - z_1)^{-k} \right) + \\
&\quad \sum_{l=1}^{\infty} \left(a_0 l^{-1} (z_0 - z_1)^{-l} + \sum_{k=1}^{\infty} (-1)^k a_k \binom{k+l-1}{l} (z_0 - z_1)^{-(k+l)} \right) (z - z_1)^l.
\end{aligned}$$

Therefore coefficients a_k of ϕ_{z_0} transform to coefficients b_l of ϕ_{C,z_1} by the formula

$$\begin{aligned}
b_0 &= a_0 \log(-(z_0 - z_1)) + \sum_{k=1}^{\infty} (-1)^k a_k (z_0 - z_1)^{-k} \\
b_l &= a_0 l^{-1} (z_0 - z_1)^{-l} + \sum_{k=1}^{\infty} (-1)^k a_k \binom{k+l-1}{l} (z_0 - z_1)^{-(k+l)} \quad l > 0
\end{aligned}$$

Note that FLIP does *not* commute with truncation since one has to know all coefficients a_0, a_1, \dots to compute b_0, b_1, \dots, b_p exactly. For more information on the error in case of truncation, see Greengard and Rokhlin (1987).

11.17 Application on Quad Tree

In this section, we will go through the application of multipole algorithm on quad tree in detail. During the process, we will also look into the two different operations *SHIFT* and *FLIP*, and gain some experience on how to use them in real situations.

We will start at the lowest level h of the tree. For every node of the tree, it computes the multipole expansion coefficients for the bodies inside, with origin located at the center of the cell. Next, it will shift all of the four centers for the children cells into the center of the parent node, which is at the $h - 1$ level, through the SHIFT operation for the multipole expansion. Adding up the coefficients from the four shifted expansion series, the multipole expansion of the whole parent node is obtained. And this SHIFT and ADD process will continue upward for every level of the tree, until the multipole expansion coefficients for each node of the entire tree are stored within that node. The computational complexity for this part is $O(N)$.

Before we go to the next step, some terms have to be defined first.

<i>I</i>	<i>I</i>	<i>I</i>	<i>I</i>
<i>I</i>	<i>I</i>	<i>I</i>	<i>I</i>
<i>N</i>	<i>N</i>	<i>I</i>	<i>I</i>
<i>C</i>	<i>N</i>	<i>I</i>	<i>I</i>

Figure 11.14: Second Level of Quad Tree

<i>F</i>	<i>F</i>	<i>F</i>	<i>F</i>	<i>F</i>	<i>F</i>
<i>F</i>	<i>F</i>	<i>F</i>	<i>F</i>	<i>F</i>	<i>F</i>
<i>I</i>	<i>I</i>	<i>I</i>	<i>I</i>	<i>F</i>	<i>F</i>
<i>I</i>	<i>I</i>	<i>I</i>	<i>I</i>	<i>F</i>	<i>F</i>
<i>N</i>	<i>N</i>	<i>I</i>	<i>I</i>	<i>F</i>	<i>F</i>
<i>C</i>	<i>N</i>	<i>I</i>	<i>I</i>	<i>F</i>	<i>F</i>

Figure 11.15: Third Level of Quad Tree

- NEIGHBOR — a neighbor N to a cell C is defined as any cell which shares either an edge or a corner with C
- INTERACTIVE — an interactive cell I to a cell C is defined as any cell whose parent is a neighbor to parent of C , excluding those which are neighbors to C
- FARAWAY — a faraway cell F to a cell C is defined as any cell which is neither a neighbor nor an interactive to C

Now, we start at the top level of the tree. For each cell C , FLIP the multipole expansion for the interactive cells and combine the resulting local Taylor expansions into one expansion series. After all of the FLIP and COMBINE operations are done, SHIFT the local Taylor expansion from the node in this level to its four children in the next lower level, so that the information is conserved from parent to child. Then go down to the next lower level where the children are. To all of the cells at this level, the faraway field is done (which is the interactive zone at the parent level). So we will concentrate on the interactive zone at this level. Repeat the FLIP operation to all of the interactive cells and add the flipped multipole expansion to the Taylor expansion shifted from parent node. Then repeat the COMBINE and SHIFT operations as before. This entire process will continue from the top level downward until the lowest level of the tree. In the end, add them together when the cells are *close* enough.

11.18 Expansion from 2-D to 3-D

For 2-D N-body simulation, the potential function is given as

$$\phi(z_j) = \sum_{i=1}^n q_i \log(z_j - z_i)$$

where z_1, \dots, z_n the position of particles, and q_1, \dots, q_n the strength of particles. The corresponding multipole expansion for the cluster centered at z_c is

$$\phi_{z_c}(z) = a_0 \log(z - z_c) + \sum_{k=1}^{\infty} a_k \frac{1}{(z - z_c)^k}$$

The corresponding local Taylor expansion looks like

$$\phi_{C,z_c}(z) = \sum_{k=0}^{\infty} b_k \frac{1}{(z - z_c)^k}$$

In three dimensions, the potential as well as the expansion series become much more complicated. The 3-D potential is given as

$$\Phi(x) = \sum_{i=1}^n q_i \frac{1}{\|x - x_i\|}$$

where $x = f(r, \theta, \phi)$. The corresponding multipole expansion and local Taylor expansion as following

$$\begin{aligned} \Phi_{multipole}(x) &= \sum_{n=0}^{\infty} \frac{1}{r^{n+1}} \sum_{m=-n}^n a_n^m Y_n^m(\theta, \phi) \\ \Phi_{Taylor}(x) &= \sum_{n=0}^{\infty} \sum_{m=-n}^n r^n b_n^m Y_n^m(\theta, \phi) \end{aligned}$$

where $Y_n^m(\theta, \phi)$ is the Spherical Harmonic function. For a more detailed treatment of 3-D expansions, see Nabors and White (1991).

11.19 Parallel Implementation

In Chapter 17.2, we will discuss issues on parallel N-body implementation.

IV Numerical Linear Algebra

Chapter 12

Numerical Discretization

12.1 Mathematical Modeling and Numerical Methods

The complex mathematical models for scientific problems are typically governed by partial differential equations. Therefore, at the center of scientific computing is the numerical solution of differential equations. To “solve” PDEs on computer, we need to discretize the continuous problem and approximate it by a finite representation, usually, in the form of system of equations.

12.1.1 PDEs for Modeling

To motivate, we now list three basic partial differential equations and briefly mention the physical problems modeled by the equations. For a scalar function u (in two or three dimensions), let ∇u denote the *gradient* of u . Let $\nabla^2 u$ be the *Laplacian* of u , i.e., for two dimensional function u ,

$$\nabla^2 u = \frac{\partial^2 u}{\partial x^2} + \frac{\partial^2 u}{\partial y^2}.$$

- **Poisson’s equation** in a domain Ω with boundary $\partial\Omega$,

$$-\nabla^2 u = f \quad \text{in } \Omega$$

The boundary value condition can be given as $u = c$ on $\partial\Omega$, where $c = 0$ for many problems (known as *Dirichlet condition*) or $\nabla u = g$ on $\partial\Omega$, (known as *Neumann condition*).

A number of problems in physics and mechanics are modeled by Poisson equation; u may represent for example a temperature, an electro-magnetic potential or the displacement of an elastic membrane fixed at the boundary under a transversal load of intensity f .

Laplace’s equation is a special case Poisson’s equation with $f = 0$.

- **Navier-Stokes’ equation** in a domain Ω in \mathbb{R}^d with boundary $\partial\Omega$, for incompressible flow.

$$\frac{\partial u_i}{\partial t} + u \cdot \nabla u_i = -\frac{\partial p}{\partial x_i} \frac{1}{\rho} + \nu \nabla^2 u_i + f_i, \quad \text{in } \Omega, i = 1, 2, \dots, d$$
$$\nabla \cdot u = 0 \text{ in } \Omega,$$

where $u(x, t)$ is the velocity, $p(x, t)$ is the pressure, x and t are space and time, respectively, $f(x, t)$ is the prescribed force, ρ is the fluid density, and ν is the fluid kinematic viscosity. Initial conditions are given to u and boundary conditions $u \cdot n$ and no-slip condition $u \cdot s = 0$ are given to u .

- **Schrödinger's equation** for quantum chemistry.

$$H\Psi = E\Psi,$$

where H is the *Hamiltonian operator*, given below, which has a Laplacian term, representing the electron kinetic energy, and a second term representing potential energy.

$$H = -\sum_a \frac{1}{2m_a} \nabla_a^2 + \frac{1}{2} \sum_{a,b} \frac{Q_a Q_b}{|r_a - r_b|}$$

Other important PDEs include the **Maxwell's equation** for electromagnetic, **Euler's equation** for an incompressible inviscid fluid in a domain, etc. We will discuss the application of numerical methods at the end of the tutorial.

12.1.2 Numerical Methods

There are two basic schools of numerical approaches: *equation based methods* and *particle methods*. We will cover the particle methods in Chapter ???. In this chapter, we discuss the set of key problems in the first approach. The basic scheme of equation based numerical methods has five steps.

1. **Problem Formulation and Geometric Modeling:** describe the geometry and the boundary of a continuous domain D and the governing partial differential equations.
2. **Mesh Generation:** generate a well-shaped mesh M to approximate the domain.
3. **Numerical System Formulation:** generate a system of equations over M for the governing PDEs, for example, assemble the stiffness matrix and the right hand vector.
4. **Solution to Numerical Systems:** solve the system of equations.
5. **Adaptive Refinement:** adaptively refine the mesh based on the estimated errors (for boundary value problems) or properly move the mesh (for initial value problems), and then return to Step 3 to reduce the error or to do the next time step simulation.

We start from a continuous problem which is described by a set of PDEs on a continuous domain. We must first arrive to a discretized problem. To obtain a proper discretize problem, we need first discretize the continuous domain by a step of mesh generation. The purpose of mesh generation is to decompose the domain into a collection of simple geometric elements such as squares, boxes, or triangles.

From the discretization, we derive a finite approximation of the PDEs. There are two leading numerical formulations: Finite difference and Finite element formulations. Both methods construct a system of linear equations to approximate the PDEs.

We then need to solve the linear equations and, if necessary, adaptively refine the discretization and approximation to achieve more accurate numerical solutions.

This tutorial will discuss each of the above steps with focus on the parallel implementation. One fundamental problem that will be called upon in the parallel implementation of each of the above steps in the partitioning problem, that is how to divide a large complex problem into relatively independent ones so that we can map them on a parallel machine to achieve load balancing and to reduce communication overhead. We will discuss several practically used partitioning methods and show how to use them to support the five steps above.

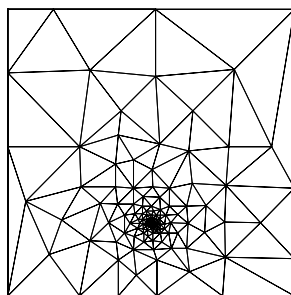


Figure 12.1: Triangulation of well-spaced point set around a singularity

12.2 Well-Shaped Meshes

Numerical methods approximate a continuous physical problem by discretizing the geometric domain into simple *cells* or *elements*. The resulting *mesh* is a graph embedded in two or three dimensions. The most versatile type of mesh is the unstructured triangular mesh in which each element is a simplex, i.e., a triangle in 2D or a tetrahedron in 3D. However, not all discretizations serve equally well. Numerical and discretization errors depend on the geometric *quality* of the mesh, which is often measured by the size and shape of the elements. A typical quality guarantee gives a lower bound on the minimum angle (e.g., greater than 30 degree). A mesh with such a quality guarantee is called a *well-shaped mesh*.

The simplest mesh is the regular Cartesian grid, which is used in finite difference methods. However, regular grids are only useful in practice for problems whose domain is simple and whose solution changes slowly. For problems with complex geometry whose solution changes rapidly, we need to use an *unstructured mesh* to reduce the problem size. For example, when modeling earthquake we want a dense discretization near the quake center and a sparse discretization in the regions with low activities. It would be waste to give regions with low activities as fine a discretization as the regions with high activities. See figure 12.1.

One important aspect that distinguishes a finite element or finite difference mesh from a regular graph is that it has two structures: the combinatorial structure and the geometric structure. In general, it can be represented by a pair (G, xyz) where G describes the combinatorial structure of the mesh and xyz gives the geometric information.

To properly approximate a continuous function, in addition to the conditions that a mesh must conform to the boundaries of the region and be fine enough, each individual element of the mesh must be *well shaped*. A common shape criterion for elements is the condition that the angles of each element are not too small, or the aspect ratio of each element is bounded [6, 33].

Several definitions of the *aspect ratio* have been used in literature. We list some of them.

1. The ratio of the longest dimension to the shortest dimension of the simplex S , denoted by $A_1(S)$. For a triangle in \mathbb{R}^2 , it is the ratio of the longest side divided by the altitude from the longest side.
2. The ratio of the radius of the smallest containing sphere to the radius of the inscribed sphere of S , denoted by $A_2(S)$.
3. The ratio of the radius of the circumscribing sphere to the radius of the inscribed sphere of S , denoted by $A_3(S)$.

4. The ratio of the diameter to the d th root of the volume of the simplex S , denoted by $A_d(S)$, where the *diameter* of a d -simplex S is the maximum distance between any pair of points in S .

12.3 From PDEs to Systems of Linear Equations

12.3.1 Finite Difference Approximations

Finite difference uses pointwise approximation to construct a linear system $AU = F$ for PDEs $Lu = f$. In its simplest form, finite difference uses a regular grid to discretize a continuous physical domain and replace derivatives by difference quotients.

Let us first consider the two-point boundary value problem:

$$\begin{aligned} -u(x)'' &= f(x) & 0 < x < 1 \\ u(0) &= u(1) = 0 \end{aligned}$$

The finite difference method discretizes the domain $[0, 1]$ into n intervals by introducing the grid points $x_j = jh$, where $h = 1/n$. At each $n - 1$ internal grid points, we approximate $u''(x_i)$ by $(u(x_{i-1}) - 2u(x_i) + u(x_{i+1}))/h^2$. Let $F = (f_1, \dots, f_{n-1})$ and $U = (u_1, \dots, u_{n-1})$, where $f_i = f(x_i)$ and $u_i = u(x_i)$. The finite difference approximation results an linear system $A^h U^h = F^h$ for the original PDE, where

$$A_h = \frac{1}{h^2} \begin{pmatrix} 2 & -1 & & & \\ -1 & 2 & -1 & & \\ & \ddots & \ddots & \ddots & \\ & & -1 & 2 & 1 \\ & & & -1 & 2 \end{pmatrix}.$$

The linear system has $n - 1$ variables and $n - 1$ equation and its matrix A_h is symmetric positive definite.

Analogously, we can use finite difference method for approximating two dimensional PDEs. We consider the *Poisson's equation* on a Ω with boundary $\partial\Omega$, which is given by

$$\begin{aligned} -u_{xx} - u_{yy} &= f(x, y) & (x, y) \in \Omega \\ u(x, y) &= 0 & (x, y) \in \partial\Omega \end{aligned}$$

We will illustrate the basic formulation on the unit square, i.e., $\Omega = [0, 1] \times [0, 1]$.

The finite difference discretizes the domain Ω by a regular $n \times n$ grid. So each grid point is of format (x_i, y_j) where $x_i = ih$ and $y_j = jh$, and where $h = 1/n$. Replacing $-u_{xx} - u_{yy} = f(x, y)$ by finite difference, we have obtain $(n - 1)^2$ linear equations of form

$$\begin{aligned} \frac{-u_{i-1,j} + 2u_{i,j} - u_{i+1,j}}{h^2} + \frac{-u_{i,j-1} + 2u_{i,j} - u_{i,j+1}}{h^2} &= f_{i,j} \\ u_{i,j} &= 0 \text{ if } i = 0 \text{ or } i = n \text{ or } j = 0 \text{ or } j = n, \text{ and } 0 < i < n, 0 < j < n. \end{aligned}$$

If we order the vertices by the lexicographic ordering of their coordinates, we can express the above linear system in form of $A_{hh}U_{hh} = F_{hh}$, where

$$A_{hh} = \frac{1}{h^2} \begin{pmatrix} A_h & -I & & & \\ -I & A_h & -I & & \\ & \ddots & \ddots & \ddots & \\ & & -I & A_h & I \\ & & & -I & A_h \end{pmatrix},$$

where A_h is the one dimensional finite difference matrix with space h .

Computationally we need to solve the linear system described above. Finite difference has also be extended to unstructured discretization. Mathematically, there are two key steps in the numerical analysis of the finite difference approximation:

1. Use a Taylor series expansion to bound the discretization error.
2. Show that the discretization solution U_{hh} is globally stable, that is U_{hh} depends continuously on F_{hh} as the mesh space h approach to zero.

The pointwise discretization error $E_{i,j}^{hh} = u_{x_i, x_j} - u_{i,j}^{hh}$, where $u_{i,j}$ is the exact solution of the finite difference linear system. We can show that the finite difference is a second order approximation in the sense that norm of the the discretization error is bounded as

$$\|E^{hh}\| \leq Ch^2, \text{ for a constant } C \text{ independent of } h.$$

12.3.2 Finite Element Approximations

As we have seen, finite difference methods approximate PDEs by pointwise approximation. This is one of the basic approaches to make a continuous problem discrete. The other way is choose a finite number of functions T_1, \dots, T_n , called *basis functions*. We approximate the continuous function u as a linear combination of T_i 's, that is, find the set of coefficients u_i ($1 \leq i \leq n$) so that the function $\sum_{i=1}^n u_i T_i$ is as close as to the continuous function u as possible.

Clearly, the choice of the basis functions is very important to the second approach. If these functions are sines and cosines, then we approximate the continuous function by finite Fourier series. *Finite element methods* use piecewise polynomials (or even linear functions) as basis functions. It starts with a discretization of a physical domain by a mesh (structured or unstructured). Then it generates a polynomial (or linear) basis function for each mesh point, which takes value zero outside the mesh elements that are incident to the mesh points. Therefore, we can choose basis functions that fit the geometry of the problem. The choice of polynomials or linear basis functions is to ensure that such basis functions can be generated automatically by computer from the mesh. The decision that a basis function is zero outside the neighboring elements is to reduce the complexity of the linear system generated by the finite element method, so that we only need to solve a sparse linear system as in the finite difference methods.

Galerkin Variational Formulation

To illustrate the basic idea of using basis functions, we first consider the two-point boundary value problem discussed in the previous subsection. We can show that the two-point boundary value problem is equivalent to the following variational form, known as *weak Galerkin form*: Find an u with $u(0) = u(1) = 0$ such that $\int_0^1 -u''(x)v(x)dx = \int_0^1 f(x)v(x)dx$, for all v that satisfies $v(0) = v(1) = 0$.

By integration by part, we have $\int_0^1 u''(x)v(x)dx = \int_0^1 u'(x)v'(x)dx$. Let $(u, v) = \int_0^1 u(x)v(x)dx$. So we are looking for a function u such that $(u', v') = (f, v)$ for all v that satisfies $v(0) = v(1) = 0$.

The basic idea of finite element formulation is to construct a set of basis functions T_1, \dots, T_n and find the solution to the following set of equations:

$$\left(\left(\sum_{i=1}^n u_i T_i \right)', (T_j)' \right) = (f, T_j) \quad 1 \leq j \leq n. \quad (12.1)$$

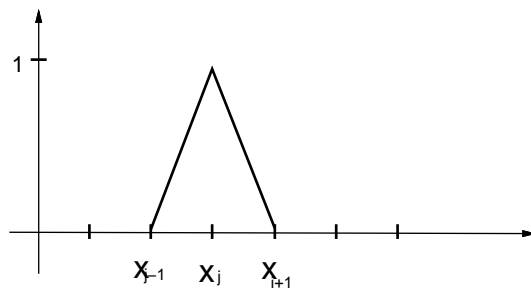


Figure 12.2: A basis function for 1D finite element

The approximation to the continuous problem is then given as $u = \sum_{i=1}^n u_i T_i$. Clearly, given T_1, \dots, T_n , equations (12.1) yield a linear system $Au = b$ in variables u_1, \dots, u_n . We call A the *stiffness matrix* and b the right hand vector or *load vector*.

The Choice of Basis Functions

The choice of the basis functions is essential in finite element formulation. The set of basis functions need to satisfy the following conditions.

1. *Small Discretization Error:* The solution $u = \sum_{i=1}^n u_i T_i$ for Equations (12.1) approximates the solution to the PDEs closely.
2. *Efficient Solution:* The resulting linear system $Ax = b$ can be solved efficiently.

Similar to the finite difference method, the finite element method first discretizes the domain. In its simplest format, it generates a linear function T_i for each mesh point p_i so that the function T_i takes value 1 at the mesh point and 0 at all other mesh points. T_i is linear in the elements that adjacent to the mesh point p_i .

We first illustrate the basic idea by the two-point boundary value problem. In one dimension, we discretize the interval $[0, 1]$ into a collection of subintervals. The basis function at a mesh point is the continuous piecewise linear function as shown in the following Figure 12.2

The final solution from the finite element formulation is also a piecewise linear function.

It is important to notice that the stiffness matrix so generated is very sparse. For one dimensional problem, it is a triangular matrix. The basis function of a mesh point only overlap with the basis functions its neighboring mesh points. In the special case of the uniform discretization of the interval, the stiffness matrix is the same as the matrix generated by the finite difference method. The stiffness matrix over a two dimension regular grid will be different from the matrix generated by the finite difference method.

Two dimensional finite element formulation is similar to its one dimensional formulation. We use the *Poisson's equation* on a domain Ω to illustrate. Recall that the Poisson's equation one Ω with boundary $\partial\Omega$, which is given by

$$\begin{aligned} -u_{xx} - u_{yy} &= f(x, y) & (x, y) \in \Omega \\ u(x, y) &= 0 & (x, y) \in \partial\Omega \end{aligned}$$

The finite element method constructs a mesh M of the domain Ω and use M to generate the basis and trial function.

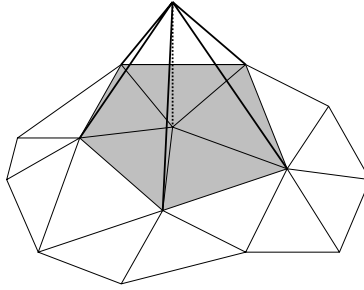


Figure 12.3: A basis function for 2D finite element

The Galerkin variational formulation of the Poisson equation become: *Find an u which is equal to zero on Γ_D , such that $\int_{\Omega} -(u_x x(x, y) + u_y y(x, y))v(x, y) dx dy = \int_{\Omega} f(x, y)v(x, y) dx dy$, for all v on Ω that satisfies the condition that v is equal to zero on Γ_D .*

Integrating by part, we have

$$\int \int_{\Omega} (u_x x(x, y) + u_y y(x, y))v(x, y) dx dy = \int \int_{\Omega} (u_x(x, y)v_x(x, y) + u_y(x, y)v_y(x, y)) dx dy.$$

So the formulation is symmetric with respect to both u and v . For each mesh point p_i of M we construct a basis function f_i which is a piecewise linear function that takes value 1 at p_i and 0 in all other mesh points. The function f_i is nonzero only in the elements that incident to p_i . See Figure 12.3 for illustration.

Again, we assume $u = \sum_{i=1}^n u_i T_i$ and use $\{T_1, \dots, T_n\}$ as trial functions to generate n linear equations as following.

$$\int \int_{\Omega} \sum_{i=1}^n u_i ((T_i)_x(x, y)(T_j)_x(x, y) + (T_i)_y(x, y)(T_j)_y(x, y)) dx dy \quad 1 \leq j \leq n.$$

From the integration formulation, we obtain a linear system $Au = b$ where A is the stiffness matrix. Notice that $A_{i,j}$ is nonzero iff p_i and p_j share an element. Therefore if we use the regular two dimensional grid as the mesh, the stiffness matrix is different from the matrix generated by the finite difference method in that each mesh point is connected to its eight nearest mesh points instead of the four as the in the finite difference method.

The finite element basis functions are more flexible than the pointwise difference formulae. For PDEs with complex geometry domain, the finite element approximation enables us to design a mesh that conform to the geometry so that we can approximate the continuous problem with smaller number of mesh points and hence with smaller number of linear equations. The Finite element method will be more important for 3D simulation where the scale of simulation is normally determined by the memory size and I/O capacity of a parallel machines.

We refer interested read to the Book of Johnson and Strang and Fix for more detailed discussion.

Year	Size of Dense System	Machine
1950's	≈ 100	
1991	55,296	
1992	75,264	Intel
1993	75,264	Intel
1993	76,800	CM
1993	128,600	Intel

Table 13.1: Largest Dense Matrices Solved

algebra libraries. Medium sized problems are most easily solved with these libraries, and the first pass at larger problems are best done with the libraries. Dense methods are the easiest to use, reliable, predictable, easiest to write, and work best for small to medium problems. For large problems, it is not clear whether dense methods are best, but other approaches often require far more work.

- “Law of Nature”: Nature does not throw n^2 numbers at us haphazardly, therefore there are few dense matrix problems. Some believe that there are no real problems that will turn up n^2 numbers to populate the $n \times n$ matrix without exhibiting some form of underlying structure. This implies that we should seek methods to identify the structure underlying the matrix. This becomes particularly important when the size of the system becomes large.

13.4 Records

Table 13.1 shows the largest dense matrices solved. Problems that warrant such huge systems to be solved are typically things like the Stealth bomber and large Boundary Element codes¹. We see here that space considerations, *not* processor speeds, are what bound the ability to tackle such large systems. Another application for large dense problems arise in the “methods of moments”, electro-magnetic calculations used by the military.

Memory is the bottleneck in solving these large dense systems. Only a tiny portion of the matrix can be stored inside the computer at any one time.

13.5 Software Libraries

There are libraries of routines that provide standard algorithms used in scientific computing. These routines are meant to be fast, accurate, and portable.

History of Library Development:

- *LINPACK* - Linear Systems
- *EISPACK* - Eigenvalue Problems

¹Typically this method involves a transformation using Greens Theorem from 3D to a dense 2D representation of the problems. This is where the large data sets are generated.

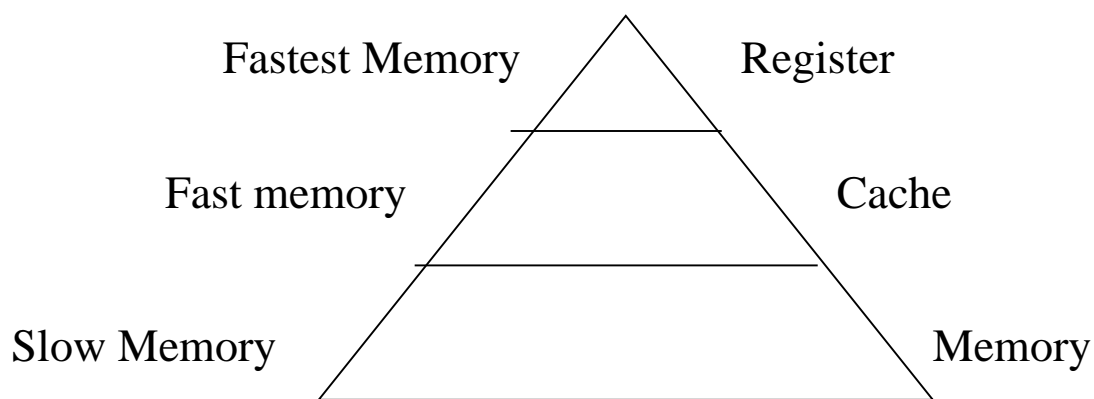


Figure 13.1: Matrix Operations on 1 processor

- *LAPACK* - Combination of LinPack and EisPack that takes advantage of vectorization
- *scaLAPACK* - Linear Algebra Pack for Parallel Machines (2/28/95)

LINPACK is high quality numerical software, but has no knowledge of blocking or layout. *EISPACK* enhanced *LINPACK* by adding the power of eigenvalues. Both packages are outdated by *LAPACK*. *scaLAPACK* is the current package under development.

Extensions to Scalapack:

- *BLACS* - C stands for communication
- *PB - BLACS* - Parallel Block *BLAS*
- *PBLAS* - basic *BLAS* plus communication tied together

Other packages include *IMSL* and *NAG*.

There is a library specially made for the CM machines -

- *CMSSL* - Connection Machine Scientific Software Libraries.

13.6 Software Engineering

Wrong View of linear algebra on parallel machines:

- one element per processor
- lots of processors
- communication is instantaneous

This is taught frequently in theory classes, but has no practical application.

Right View

- Large Chunks of each matrix on each processor

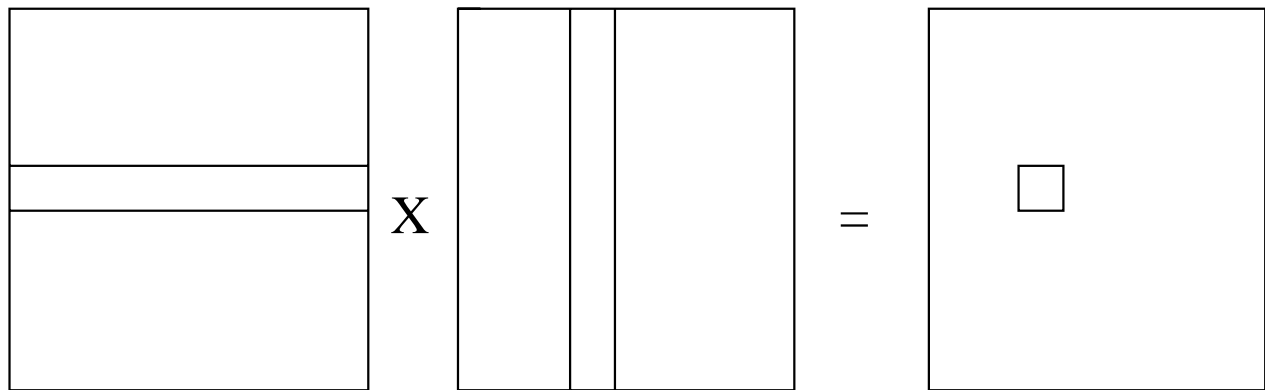


Figure 13.2: Matrix Multiply

Instruction	Operations	Memory Accesses (load/stores)	Ops /Mem Ref
BLAS1: SAXPY (Single Precision \mathbf{Ax} Plus \mathbf{y})	$2n$	$3n$	$\frac{2}{3}$
BLAS1: SAXPY $\alpha = x \cdot y$	$2n$	$2n$	1
BLAS2: Matrix-vec $y = Ax + y$	$2n^2$	n^2	2
BLAS3: Matrix-Matrix $C = AB + C$	$2n^3$	$4n^2$	$\frac{1}{2}n$

Table 13.2: Basic Linear Algebra Subroutines (BLAS)

Time to execute an arithmetic operation depends on the number of accesses to slow memory. In Figure 13.1, the amount of memory is proportional to the area in the triangle. As seen, there is only a small amount of fast memory, and larger amounts of slower memory. The need for many memory references to slow memory slows down many computations.

An example is Matrix Multiply as shown in Figure 13.2.

This pseudo code produces terrible performance because too many memory references are needed to do the column times row vector calculation.

Table 2 shows why people vectorize. Blocking calculations are faster. The lesson of vector computers is that computations should be blocked to maximize efficiency.

The grand plan is that manufacturers would write fast *BLAS* (not quite successful). *LAPACK* would write codes that calls the *BLAS*.

Load Balancing:

We will use Gaussian Elimination to demonstrate the advantage of cyclic order in dense linear algebra. In consecutive order, as the computation proceeds, processors in the lower triangular part become idle. In Figure 13.3, the lower processors would become idle as specified by the shaded processors, 4 and 7. Thus, this is bad load-balancing. While in cyclic order, we eliminate the same load for each processor, and the load remains balanced as the computation proceeds (See Figure 13.4) .

There are two methods to eliminate load imbalances:

1	2	3
4	5	6
7	8	9

Figure 13.3: Gaussian Elimination With Bad Load Balancing

1	2	3						
4	5	6						
	8	9						

Figure 13.4: Row and Column Block Cyclic Ordering of Data

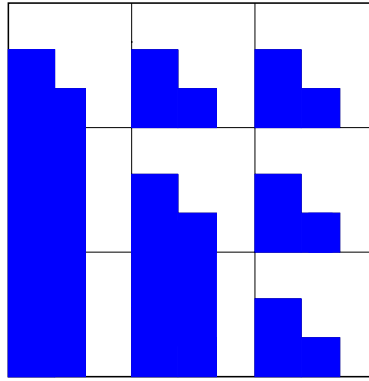


Figure 13.5: A stage in Gaussian elimination using cyclic order, where the shaded portion refers to the zeros and the unshaded refers to the non-zero elements

- Rearrange the data for better load balancing (costs: communication).
- Rearrange the calculation: eliminate in unusual order.

So, should we convert the data from consecutive to cyclic order and from cyclic to consecutive when we are done? The answer is “no”, and the better approach is to reorganize the algorithm rather than the data. The idea behind this approach is to regard matrix indices as a set (not necessarily ordered) instead of an ordered sequence.

In general if you have to rearrange the data, maybe you can rearrange the calculation.

Lesson of Computation Ordering: Matrix indices are a set (unordered), not a sequence (ordered). We have been taught in school to do operations in a linear order, but there is no mathematical reason to do this.

As Figure 13.5 demonstrates, we store data consecutively but do Gaussian Elimination cyclicly. In particular, if the block size is 10×10 , the pivots are 1, 11, 21, 31, ..., 2, 22, 32, ...

We can apply the above reorganized algorithm in block form, where each processor does one block at a time and cycles through.

Here we are using all of our lessons, blocking for vectorization, and rearrangement of the calculation, not the data.

Chapter 14

Sparse Linear Algebra

The solution of a linear system $Ax = b$ is one of the most important computational problems in scientific computing. As we shown in the previous section, these linear systems are often derived from a set of *differential equations*, by either finite difference or finite element formulation over a discretized mesh.

The matrix A of a discretized problem is usually very *sparse*, namely it has enough zeros that can be taken advantage of algorithmically. Sparse matrices can be divided into two classes: *structured sparse matrices* and *unstructured sparse matrices*. A structured matrix is usually generated from a structured regular grid and an unstructured matrix is usually generated from a non-uniform, unstructured grid. Therefore, sparse techniques are designed in the simplest case for structured sparse matrices and in the general case for unstructured matrices.

14.1 Cyclic Reduction for Structured Sparse Linear Systems

The simplest structured linear system is perhaps the tridiagonal system of linear equations $Ax = b$ where A is symmetric and positive definite and of form

$$A = \begin{pmatrix} b_1 & c_1 & & & \\ c_1 & b_2 & c_2 & & \\ & \ddots & \ddots & \ddots & \\ & & c_{n-2} & b_{n-1} & c_{n-1} \\ & & & c_{n-1} & b_n \end{pmatrix}$$

For example, the finite difference formulation of the one dimensional model problems

$$-u''(x) + \sigma u(x) = f(x), \quad 0 < x < 1, \sigma \geq 0 \quad (14.1)$$

subject to the boundary conditions $u(0) = u(1) = 0$, on a uniform discretization of spacing h yields of a triangular linear system of $n = 1/h$ variables, where $b_i = 2 + \sigma h^2$ and $c_i = -1$ for all $1 \leq i \leq n$.

Sequentially, we can solve a triangular linear system $Ax = b$ by factor A into $A = LDL^T$, where D is a diagonal matrix with diagonal (d_1, d_2, \dots, d_n) and L is of form

$$L = \begin{pmatrix} 1 & 0 & & & \\ e_1 & 1 & 0 & & \\ & \ddots & \ddots & \ddots & \\ & & e_{n-1} & 1 & \end{pmatrix}.$$

The factorization can be computed by the following simple algorithm.

Algorithm Sequential Tridiagonal Solver

1. $d_1 = b_1$
2. $e_1 = c_1/d_1$
3. for $i = 2 : n$
 - (a) $d_i = b_i - e_{i-1}c_{i-1}$
 - (b) if $i < n$ then $e_i = c_i/d_i$

The number float point operations is $3n$ upto a additive constant. With such factorization, we can then solve the tridiagonal linear system in additional $5n$ float point operations. However, this method is very reminiscent to the naive sequential algorithm for the prefix sum whose computation graph has a critical path of length $O(n)$. The cyclic reduction, developed by Golub and Hockney [?], is very similar to the parallel prefix algorithm presented in Section ?? and it reduces the length of dependency in the computational graph to the smallest possible.

The basic idea of the cyclic reduction is to first eliminate the odd numbered variables to obtain a tridiagonal linear system of $\lceil n/2 \rceil$ equations. Then we solve the smaller linear system recursively. Note that each variable appears in three equations. The elimination of the odd numbered variables gives a tridiagonal system over the even numbered variables as following:

$$c'_{2i-2}x_{2i-2} + b'_{2i}x_{2i} + c'_{2i}x_{2i+2} = f'_{2i},$$

for all $2 \leq i \leq n/2$, where

$$\begin{aligned} c'_{2i-2} &= -(c_{2i-2}c_{2i-1}/b_{2i-1}) \\ b'_{2i} &= (b_{2i} - c_{2i-1}^2/b_{2i-1} - c_{2i}^2/b_{2i+1}) \\ c'_{2i} &= c_{2i}c_{2i+1}/b_{2i+1} \\ f'_{2i} &= f_{2i} - c_{2i-1}f_{2i-1}/b_{2i-1} - c_{2i}f_{2i+1}/b_{2i+1} \end{aligned}$$

Recursively solving this smaller linear tridiagonal system, we obtain the value of x_{2i} for all $i = 1, \dots, n/2$. We can then compute the value of x_{2i-1} by the simple equation:

$$x_{2i-1} = (f_{2i-1} - c_{2i-2}x_{2i-2} - c_{2i-1}x_{2i})/b_{2i-1}.$$

By simple calculation, we can show that the total number of float point operations is equal to $16n$ upto an additive constant. So the amount of total work is doubled compare with the sequential algorithm discussed. But the length of the critical path is reduced to $O(\log n)$. It is worthwhile to point out the the total work of the parallel prefix sum algorithm also double that of the sequential algorithm. Parallel computing is about the trade-off of parallel time and the total work. The discussion show that if we have n processors, then we can solve a tridiagonal linear system in $O(\log n)$ time.

When the number of processor p is much less than n , similar to prefix sum, we hybrid the cyclic reduction with the sequential factorization algorithm. We can show that the parallel float point operations is bounded by $16n(n + \log n)/p$ and the number of round of communication is bounded by $O(\log p)$. The communication pattern is the nearest neighbor.

Cyclic Reduction has been generalized to two dimensional finite difference systems where the matrix is a block tridiagonal matrix.

14.2 Sparse Direct Methods

Direct methods for solving sparse linear systems are important because of their generality and robustness. For linear systems arising in certain applications, such as linear programming and some structural engineering applications, they are the only feasible methods for numerical factorization.

14.2.1 LU Decomposition and Gaussian Elimination

The basis of direct methods for linear system is Gaussian Elimination, a process where we zero out certain entry of the original matrix in a systematically way. Assume we want to solve $Ax = b$ where A is a sparse $n \times n$ symmetric positive definite matrix. The basic idea of direct method is to factor A into the product of triangular matrices $A = LL^T$. Such a processor is called *Cholesky factorization*.

The first step of Cholesky factorization is given by the following matrix equation:

$$A = \begin{pmatrix} d & v^T \\ v & C \end{pmatrix} = \begin{pmatrix} \sqrt{d} & 0 \\ v/\sqrt{d} & I \end{pmatrix} \begin{pmatrix} 1 & 0 \\ 0 & C - (vv^T)/d \end{pmatrix} \begin{pmatrix} \sqrt{d} & v^T/\sqrt{d} \\ 0 & I \end{pmatrix}$$

where v is $n - 1 \times 1$ and C is $n - 1 \times n - 1$. Note that d is positive since A is positive definite. The term $C - \frac{vv^T}{d}$ is the Schur complement of A . We call this step the elimination with the first row as the pivot. The above decomposition is now carried out on the Schur complement recursively. We therefore have the following algorithm for the Cholesky decomposition.

```

For  $k = 1, 2, \dots, n$ 
   $a(k, k) = \sqrt{a(k, k)}$ 
   $a(k + 1 : n, k) = \frac{a(k+1:n, k)}{a(k, k)}$ 
   $a(k + 1 : n, k + 1 : n) = a(k + 1 : n, k + 1 : n) - a(k + 1 : n, k)^T a(k + 1 : n, k)$ 
end

```

The entries on and below the diagonal of the resulting matrix are the entries of L . The main step the algorithm is a rank 1 update to an $n - 1 \times n - 1$ block.

Notice that some fill-in may occur when we carry out the decomposition. i.e., L may be significantly less sparse than A . An important problem in direct solution to sparse linear system is to find a “good” ordering of the rows and columns of the matrix to reduce the amount of fill.

As we shown in the previous section that the matrix of the linear system generated by the finite element or finite difference formulation is associated with the graph given by the mesh. In fact, the nonzero structure of each matrix A can be represented by a graph, $G(A)$, where the rows is represented by a vertex and every nonzero element by an edge. Graph theoretically, the graph of the Schur complement after eliminating a row can be obtained from $G(A)$ by deleting the node of the row and connect its graph neighbor by a complete graph. See Figure 14.1.

The fill-in of the Cholesky decomposition can be computed as follows. First form a clique on the neighbors of node 1. Then form a clique on the neighbors of node 2 etc. The edges which are added correspond to entries of the matrix which are filled in. (Of course the filled in entry might be a zero due to cancelation but we ignore this possibility.) In our matrix the filled in entries are given by \times . This calculation of fill-in can be done relatively cheaply.

In the context of parallel computation, an important parameter the height of elimination tree, which is the number of parallel elimination steps need to factor with an unlimited number of processors. The *elimination tree* defined as follows from the fill-in calculation which was described above. Let $j > k$. Define $j >_L k$ if $l_{jk} \neq 0$ where l_{jk} is the (j, k) entry of L , the result of the

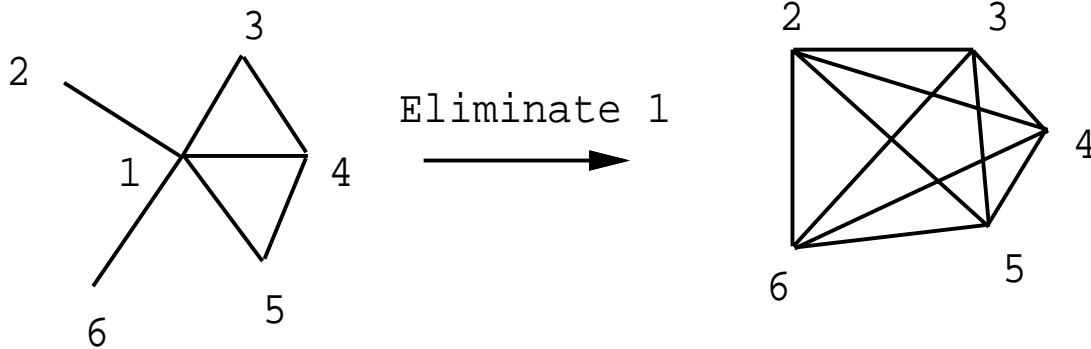


Figure 14.1: Graphical Representation of Elimination

decomposition. Let the parent of k , $p(k) = \min\{j : j >_L k\}$. This defines a tree since if $\beta >_L \alpha$, $\gamma >_L \alpha$ and $\gamma > \beta$ then $\gamma >_L \beta$.

The order of elimination determines both fill and elimination tree height. Unfortunately, but inevitably, finding the best ordering is NP-complete. Heuristics are used to reduce fill-in. The following lists some commonly used ones.

- Ordering by minimum degree (this is SYMMD in Matlab)
- nested dissection
- Cuthill-McKee ordering.
- reverse Cuthill-McKee (SYMRCM)
- ordering by number of non-zeros (COLPERM or COLMMD)

We now examine an ordering method called *nested dissection*, which uses vertex separators in a divide-and-conquer node ordering for sparse Gaussian elimination. Nested dissection [35, 36, 55] was originally a sequential algorithm, pivoting on a single element at a time, but it is an attractive parallel ordering as well because it produces blocks of pivots that can be eliminated independently in parallel [9, 28, 38, 57, 70].

Consider a regular finite difference grid. By dissecting the graph along the center lines (enclosed in dotted curves), the graph is split into four independent graphs, each of which can be solved in parallel.

The connections are included only at the end of the computation in an analogous way to domain decomposition discussed in earlier lectures. Figure 14.3 shows how a single domain can be split up into two roughly equal sized domains **A** and **B** which are independent and a smaller domain **C** that contains the connectivity.

One can now recursively order **A** and **B**, before finally proceeding to **C**. More generally, begin by recursively ordering at the leaf level and then continue up the tree. The question now arises as to how much fill is generated in this process. A recursion formula for the fill F generated for such a 2-dimension nested dissection algorithm is readily derived.

$$F(n) = 4F\left(\frac{n}{2}\right) + \frac{(2\sqrt{n})^2}{2} \quad (14.2)$$

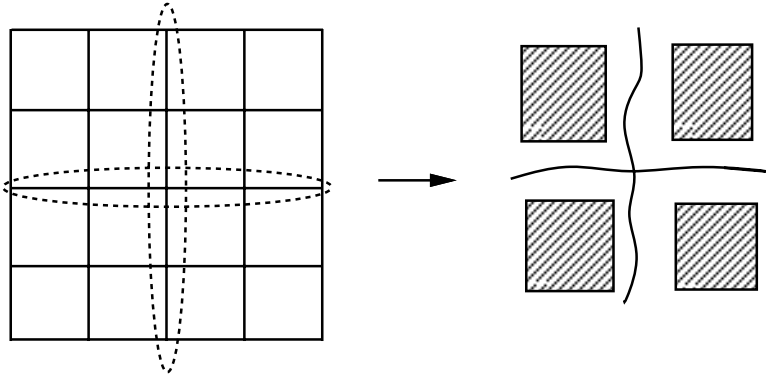


Figure 14.2: Nested Dissection

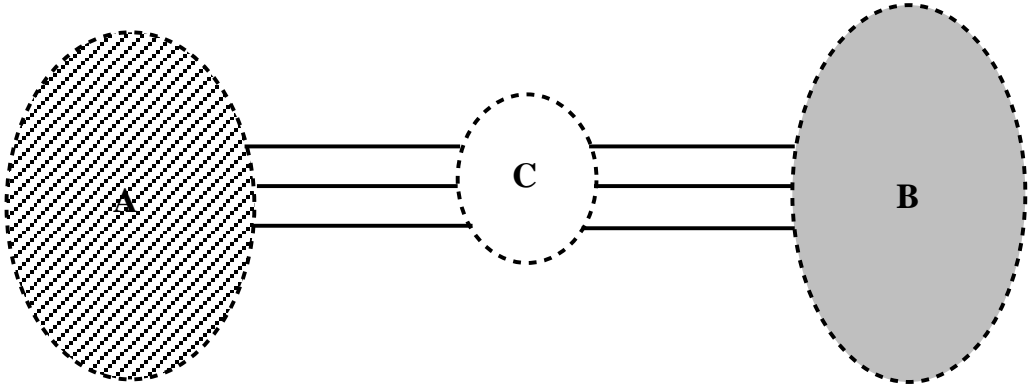


Figure 14.3: Vertex Separators

This yields upon solution

$$F(n) = 2n \log(n) \quad (14.3)$$

In an analogous manner, the elimination tree height is given by:

$$H(n) = H\left(\frac{n}{2}\right) + 2\sqrt{n} \quad (14.4)$$

$$H(n) = \text{const} \times \sqrt{n} \quad (14.5)$$

Nested dissection can be generalized to three dimensional regular grid or other classes of graphs that have small separators. We will come back to this point in the section of graph partitioning.

14.2.2 Parallel Factorization: the Multifrontal Algorithm

Nested dissection and other heuristics give the ordering. To factor in parallel, we need not only to find a good ordering in parallel, but also to perform the elimination in parallel. To achieve better parallelism and scalability in elimination, a popular approach is to modify the algorithm so that we are performing a rank k update to an $n - k \times n - k$ block. The basic step will now be given by

$$A = \begin{pmatrix} D & V^T \\ V & C \end{pmatrix} = \begin{pmatrix} L_D & 0 \\ VL_D^{-T} & I \end{pmatrix} \begin{pmatrix} I & 0 \\ 0 & C - VD^{-1}V^T \end{pmatrix} \begin{pmatrix} L_D^T & L_D^{-1}V^T \\ 0 & I \end{pmatrix}$$

where C is $n - k \times n - k$, V is $n - k \times k$ and $D = L_D L_D^T$ is $k \times k$. D can be written in this way since A is positive definite. Note that $VD^{-1}V^T = (VL_D^{-T})(L_D^{-1}V^T)$.

The elimination tree shows where there is parallelism since we can “go up the separate branches in parallel.” i.e. We can update a column of the matrix using only the columns below it in the elimination tree. This leads to the multifrontal algorithm. The sequential version of the algorithm is given below. For every column j there is a block \bar{U}_j (which is equivalent to $VD^{-1}V^T$).

$$\bar{U}_j = - \sum_k \begin{pmatrix} l_{jk} \\ l_{i_1 k} \\ \vdots \\ l_{i_r k} \end{pmatrix} (l_{jk} \ l_{i_1 k} \ \dots \ l_{i_r k})$$

where the sum is taken over all descendants of j in the elimination tree. j, i_1, i_2, \dots, i_r are the indices of the non-zeros in column j of the Cholesky factor.

For $j = 1, 2, \dots, n$. Let j, i_1, i_2, \dots, i_r be the indices of the non-zeros in column j of L . Let c_1, \dots, c_s be the children of j in the elimination tree. Let $\bar{U} = U_{c_1} \uparrow \dots \uparrow U_{c_s}$ where the U_i 's were defined in a previous step of the algorithm. \uparrow is the extend-add operator which is best explained by example. Let

$$R = \begin{matrix} & 5 & 8 & & 5 & 9 \\ 5 & \begin{pmatrix} p & q \\ u & v \end{pmatrix} & & & 5 & \begin{pmatrix} w & x \\ y & z \end{pmatrix} \end{matrix}$$

(The rows of R correspond to rows 5 and 8 of the original matrix etc.) Then

$$R \uparrow S = \begin{matrix} & & 5 & 8 & 9 \\ 5 & \begin{pmatrix} p+w & q & x \\ u & v & 0 \\ y & 0 & z \end{pmatrix} & & & \end{matrix}$$

Define

$$F_j = \begin{pmatrix} a_{jj} & \dots & a_{ji_r} \\ \vdots & \ddots & \\ a_{i_rj} & \dots & a_{i_ri_r} \end{pmatrix} \updownarrow \bar{U}$$

(This corresponds to $C - VD^{-1}V^T$)

Now factor F_j

$$\begin{pmatrix} l_{jj} & 0 & \dots & 0 \\ l_{i_1j} & & & \\ \vdots & & I & \\ l_{i_rj} & & & \end{pmatrix} \begin{pmatrix} 1 & 0 & \dots & 0 \\ 0 & & & \\ \vdots & & U_j & \\ 0 & & & \end{pmatrix} \begin{pmatrix} l_{jj} & l_{i_1j} & \dots & l_{i_rj} \\ 0 & & & \\ \vdots & & I & \\ 0 & & & \end{pmatrix}$$

(Note that U_j has now been defined.)

We can use various BLAS kernels to carry out this algorithm. Recently, Kumar and Karypis have shown that direct solver can be parallelized efficient. They have designed a parallel algorithm for factorization of sparse matrices that is more scalable than any other known algorithm for this problem. They have shown that our parallel Cholesky factorization algorithm is asymptotically as scalable as any parallel formulation of dense matrix factorization on both mesh and hypercube architectures. Furthermore, their algorithm is equally scalable for sparse matrices arising from two- and three-dimensional finite element problems.

They have also implemented and experimentally evaluated the algorithm on a 1024-processor nCUBE 2 parallel computer and a 1024-processor Cray T3D on a variety of problems. In structural engineering problems (Boeing-Harwell set) and matrices arising in linear programming (NETLIB set), the preliminary implementation is able to achieve 14 to 20 GFlops on a 1024-processor Cray T3D.

In its current form, they algorithm is applicable only to Cholesky factorization of sparse symmetric positive definite (SPD) matrices. SPD systems occur frequently in scientific applications and are the most benign in terms of ease of solution by both direct and iterative methods. However, there are many applications that involve solving large sparse linear systems which are not SPD. An efficient parallel algorithm for a direct solution to non-SPD sparse linear systems will be extremely valuable because the theory of iterative methods is far less developed for general sparse linear systems than it is for SPD systems.

14.3 Basic Iterative Methods

These methods will focus on the solution to the linear system $Ax = b$ where $A \in \mathcal{R}^{n \times n}$ and $x, b \in \mathcal{R}^n$, although the theory is equally valid for systems with complex elements.

Choose some initial guess, x_o , for the solution vector. Generate a series of solution vectors, $\{x_1, x_2, \dots, x_k\}$, through an iterative process taking advantage of previous solution vectors.

Define x^* as the true (optimal) solution vector. Each iterative solution vector is chosen such that the absolute error, $e_i = \|x^* - x_i\|$, is decreasing with each iteration for some defined norm. Define also the residual error, $r_i = \|b - Ax_i\|$, at each iteration. These error quantities are clearly related by a simple transformation through A .

$$r_i = b - Ax_i = Ax^* - Ax_i = Ae_i$$

14.3.1 Jacobi Method

Perform the matrix decomposition $A = D - L - U$ where D is some diagonal matrix, L is some strictly lower triangular matrix and U is some strictly upper triangular matrix.

Any solution satisfying $Ax = b$ is also a solution satisfying $Dx = (L + U)x + b$. This presents a straightforward iteration scheme with small computation cost at each iteration. Solving for the solution vector on the right-hand side involves inversion of a diagonal matrix. Assuming this inverse exists, the following iterative method may be used.

$$x_i = D^{-1}(L + U)x_{i-1} + D^{-1}b$$

This method presents some nice computational features. The inverse term involves only the diagonal matrix, D . The computational cost of computing this inverse is minimal. Additionally, this may be carried out easily in parallel since each entry in the inverse does not depend on any other entry.

14.3.2 Gauss-Seidel Method

This method is similar to Jacobi Method in that any solution satisfying $Ax = b$ is now a solution satisfying $(D - L)x = Ub$ for the $A = D - L - U$ decomposition. Assuming an inverse exists, the following iterative method may be used.

$$x_i = (D - L)^{-1}Ux_{i-1} + (D - L)^{-1}b$$

This method is often stable in practice but is less easy to parallelize. The inverse term is now a lower triangular matrix which presents a bottleneck for parallel operations.

This method presents some practical improvements over the Jacobi method. Consider the computation of the j^{th} element of the solution vector x_i at the i^{th} iteration. The lower triangular nature of the inverse term demonstrates only the information of the $(j + 1)^{\text{th}}$ element through the n^{th} elements of the previous iteration solution vector x_{i-1} are used. These elements contain information not available when the j^{th} element of x_{i-1} was computed. In essence, this method updates using only the most recent information.

14.3.3 Splitting Matrix Method

The previous methods are specialized cases of Splitting Matrix algorithms. These algorithms utilize a decomposition $A = M - N$ for solving the linear system $Ax = b$. The following iterative procedure is used to compute the solution vector at the i^{th} iteration.

$$Mx_i = Nx_{i-1} + b$$

Consider the computational tradeoffs when choosing the decomposition.

- cost of computing M^{-1}
- stability and convergence rate

It is interesting to analyze convergence properties of these methods. Consider the definitions of absolute error, $e_i = x^* - x_i$, and residual error, $r_i = Ax_i - b$. An iteration using the above algorithm yields the following.

$$\begin{aligned}
 x_1 &= M^{-1}Nx_0 + M^{-1}b \\
 &= M^{-1}(M - A)x_0 + M^{-1}b \\
 &= x_0 + M^{-1}r_0
 \end{aligned}$$

A similar form results from considering the absolute error.

$$\begin{aligned}
 x^* &= x_0 + e_0 \\
 &= x_0 + A^{-1}r_0
 \end{aligned}$$

This shows that the convergence of the algorithm is in some way improved if the M^{-1} term approximates A^{-1} with some accuracy. Consider the amount of change in the absolute error after this iteration.

$$\begin{aligned}
 e_1 &= A^{-1}r_0 - M^{-1}r_0 \\
 &= e_0 - M^{-1}Ae_0 \\
 &= M^{-1}Ne_0
 \end{aligned}$$

Evaluating this change for a general iteration shows the error propagation.

$$e_i = (M^{-1}N)^i e_0$$

This relationship shows a bound on the error convergence. The largest eigenvalue, or spectral eigenvalue, of the matrix $M^{-1}N$ determines the rate of convergence of these methods. This analysis is similar to the solution of a general difference equation of the form $x_k = Ax_{k-1}$. In either case, the spectral radius of the matrix term must be less than 1 to ensure stability. The method will converge to 0 faster if all the eigenvalue are clustered near the origin.

14.3.4 Weighted Splitting Matrix Method

The splitting matrix algorithm may be modified by including some scalar weighting term. This scalar may be likened to the free scalar parameter used in practical implementations of Newton's method and Steepest Descent algorithms for optimization programming. Choose some scalar, w , such that $0 < w < 1$, for the following iteration.

$$\begin{aligned}
 x_i &= (1 - w)x_0 + w(x_0 + M^{-1}v_0) \\
 &= x_0 + wM^{-1}v_0
 \end{aligned}$$

14.4 Red-Black Ordering for parallel Implementation

The concept of ordering seeks to separate the nodes of a given domain into subdomains. Red-black ordering is a straightforward way to achieve this. The basic concept is to alternate assigning a "color" to each node. Consider the one- and two-dimensional examples on regular grids..

The iterative procedure for these types of coloring schemes solves for variables at nodes with a certain color, then solves for variables at nodes of the other color. A linear system can be formed with a block structure corresponding to the color scheme.

$$\begin{bmatrix} \text{BLACK} & \text{MIXED} \\ \text{MIXED} & \text{RED} \end{bmatrix}$$

This method can easily be extended to include more colors. A common practice is to choose colors such that no nodes has neighbors of the same color. It is desired in such cases to minimize the number of colors so as to reduce the number of iteration steps.

14.5 Conjugate Gradient Method

The Conjugate Gradient Method is the most prominent iterative method for solving sparse symmetric positive definite linear systems. We now examine this method from parallel computing perspective. The following is a copy of a pseudocode for the conjugate gradient algorithm.

Algorithm: Conjugate Gradient

1. $\underline{x}_0 = 0$, $r_0 = b - A\underline{x}_0 = b$
2. do $m = 1$, to n steps
 - (a) if $m = 1$, then $p_1 = r_0$
 else
 $\beta = r_{m-1}^T r_{m-1} / r_{m-2}^T r_{m-2}$
 $p_m = r_{m-1} + \beta p_{m-1}$
 endif
 - (b) $\alpha_m = r_{m-1}^T r_{m-1} / p_m^T A p_m$
 - (c) $x_m = x_{m-1} + \alpha_m p_m$
 - (d) $r_m = r_{m-1} - \alpha_m A p_m$

When A is symmetric positive definite, the solution of $Ax = b$ is equivalent to find a solution to the following quadratic minimization problem.

$$\min_{\underline{x}} \phi(x) = \frac{1}{2} x^T A x - x^T b.$$

In this setting, $r_0 = -\nabla\phi$ and $p_i^T A p_j = 0$, i.e., p_i^T and p_j are *conjugate* with respect to A .
How many iterations shall we perform and how to reduce the number of iterations?

Theorem 14.5.1 *Suppose the condition number is $\kappa(A) = \lambda_{max}(A)/\lambda_{min}(A)$, since A is Symmetric Positive Definite, $\forall x_0$, suppose x^* is a solution to $Ax = b$, then*

$$\|x^* - x_m\|_A \leq 2\|x^* - x_0\|_A \left(\frac{\sqrt{\kappa} - 1}{\sqrt{\kappa} + 1}\right)^m,$$

where $\|V\|_A = V^T A V$

Therefore, $\|e_m\| \leq 2\|e_0\| \cdot \left(\frac{\sqrt{\kappa}-1}{\sqrt{\kappa}+1}\right)^m$.

Another high order iterative method is Chebyshev iterative method. We refer interested readers to the book by Own Axelsson (Iterative Solution Methods, Cambridge University Press). Conjugate gradient method is a special Krylov subspace method. Other examples of Krylov subspace are GMRES (Generalized Minimum Residual Method) and Lanczos Methods.

14.6 Preconditioning

Preconditioning is important in reducing the number of iterations needed to converge in many iterative methods. Given a linear system $Ax = b$ a parallel preconditioner is an invertible matrix C satisfying the following:

1. The inverse C^{-1} is relatively easy to compute. More precisely, after preprocessing the matrix C , solving the linear system $Cy = b'$ is much easier than solving the system $Ax = b$. Further, there are fast parallel solvers for $Cy = b'$.
2. Iterative methods for solving the system $C^{-1}Ax = C^{-1}b$, such as, conjugate gradient¹ should converge much more quickly than they would for the system $Ax = b$.

Generally a preconditioner is intended to reduce $\kappa(A)$.

Now the question is: *how to choose a preconditioner C?* There is no definite answer to this. We list some of the popularly used preconditioning methods.

- The basic splitting matrix method and SOR can be viewed as preconditioning methods.
- **Incomplete factorization preconditioning:** the basic idea is to first choose a good “sparsity pattern” and perform factorization by Gaussian elimination. The method rejects those fill-in entries that are either small enough (relative to diagonal entries) or in position outside the sparsity pattern. In other words, we perform an approximate factorization L^*U^* and use this product as a preconditioner. One effective variant is to perform block incomplete factorization to obtain a preconditioner.
- **Subgraph preconditioning:** The basic idea is to choose a subgraph of the graph defined by the matrix of the linear system so that the linear system defined by the subgraph can be solved efficiently and the edges of the original graph can be embedded in the subgraph with small congestion and dilation, which implies small condition number of the preconditioned matrix. In other words, the subgraph can “support” the original graph.
- **Block Diagonal Preconditioning:** The observation of this method is that a matrix in many applications can be naturally partitioned in the form of a 2×2 blocks

$$A = \begin{pmatrix} A_{11} & A_{12} \\ A_{21} & A_{22} \end{pmatrix}$$

Moreover, the linear system defined by A_{11} can be solved more efficiently. Block diagonal preconditioning chooses a preconditioner with format

$$C = \begin{pmatrix} B_{11} & 0 \\ 0 & B_{22} \end{pmatrix}$$

with the condition that B_{11} and B_{22} are symmetric and

$$\begin{aligned} \alpha_1 A_{11} &\leq B_{11} \leq \alpha_2 A_{11} \\ \beta_1 A_{22} &\leq B_{22} \leq \beta_2 A_{22} \end{aligned}$$

Block diagonal preconditioning methods are often used in conjunction with domain decomposition technique. We can generalize the 2-block formula to multi-blocks, which correspond to multi-region partition in the domain decomposition,

Other preconditioning methods include Schur complement preconditioning and various heuristics of computing an approximate matrix inverses and use them as preconditioners.

¹In general the matrix $C^{-1}A$ is not symmetric. Thus the formal analysis uses the matrix LAL^T where $C^{-1} = LL^T$ [?].

14.7 Main Issues

The most computational expensive step in conjugate gradient (and the Krylov method in general) is a sparse matrix-vector multiplication. This is true for most iterative methods. We will discuss parallel sparse matrix-vector product in the section of graph partitioning.

Numerically and algorithmically, the important problem is to efficiently construct good preconditioners.

14.8 Efficient sparse matrix algorithms

14.8.1 Scalable algorithms

By a *scalable* algorithm for a problem, we mean one that maintains efficiency bounded away from zero as the number p of processors grows and the size of the data structures grows roughly linearly in p .

Notable efforts at analysis of the scalability of dense matrix computations include those of Li and Coleman [54] for dense triangular systems, and Saad and Schultz [80]; Ostrouchov, *et al.* [69], and George, Liu, and Ng [37] have made some analyses for algorithms that map matrix columns to processors. Rothberg and Gupta [76] is an important paper for its analysis of the effect of caches on sparse matrix algorithms.

Consider any distributed-memory computation. In order to assess the communication costs analytically, it is useful to employ certain abstract lower bounds. Our model assumes that machine topology is given. It assumes that memory consists of the memories local to processors. It assumes that the communication channels are the edges of a given undirected graph $G = (W, L)$, and that processor-memory units are situated at some, possibly all, of the vertices of the graph. The model includes hypercube and grid-structured message-passing machines, shared-memory machines having physically distributed memory (the Tera machine) as well as tree-structured machines like a CM-5.

Let $V \subseteq W$ be the set of all processors and L be the set of all communication links.

We assume identical links. Let β be the inverse bandwidth (slowness) of a link in seconds per word. (We ignore latency in this model; most large distributed memory computations are bandwidth limited.)

We assume that processors are identical. Let ϕ be the inverse computation rate of a processor in seconds per floating-point operation. Let β_0 be the rate at which a processor can send or receive data, in seconds per word. We expect that β_0 and β will be roughly the same.

A distributed-memory computation consists of a set of processes that exchange information by sending and receiving messages. Let M be the set of all messages communicated. For $m \in M$, $|m|$ denotes the number of words in m . Each message m has a source processor $src(m)$ and a destination processor $dest(m)$, both elements of V .

For $m \in M$, let $d(m)$ denote the length of the path taken by m from the source of the message m to its destination. We assume that each message takes a certain path of links from its source to its destination processor. Let $p(m) = (\ell_1, \ell_2, \dots, \ell_{d(m)})$ be the path taken by message m . For any link $\ell \in L$, let the set of messages whose paths utilize ℓ , $\{m \in M \mid \ell \in p(m)\}$, be denoted $M(\ell)$.

The following are obviously lower bounds on the completion time of the computation. The first three bounds are computable from the set of message M , each of which is characterized by its size and its endpoints. The last depends on knowledge of the paths $p(M)$ taken by the messages.

1. (Average flux)

$$\frac{\sum_{m \in M} |m| \cdot d(m)}{|L|} \cdot \beta.$$

This is the total flux of data, measured in word-hops, divided by the machine's total communication bandwidth, L/β .

2. (Bisection width) Given $V_0, V_1 \subseteq W$, V_0 and V_1 disjoint, define

$$sep(V_0, V_1) \equiv \min |\{L' \subseteq L \mid L' \text{ is an edge separator of } V_0 \text{ and } V_1\}|$$

and

$$flux(V_0, V_1) \equiv \sum_{\{m \in M \mid src(m) \in V_i, dest(m) \in V_{1-i}\}} |m|.$$

The bound is

$$\frac{flux(V_0, V_1)}{sep(V_0, V_1)} \cdot \beta.$$

This is the number of words that cross from one part of the machine to the other, divided by the bandwidth of the wires that link them.

3. (Arrivals/Departures (also known as node congestion))

$$\max_{v \in V} \sum_{dest(m) = v} |m| \beta;$$

$$\max_{v \in V} \sum_{src(m) = v} |m| \beta.$$

This is a lower bound on the communication time for the processor with the most traffic into or out of it.

4. (Edge contention)

$$\max_{\ell \in L} \sum_{m \in M(\ell)} |m| \beta.$$

This is a lower bound on the time needed by the most heavily used wire to handle all its traffic.

Of course, the actual communication time may be greater than any of the bounds. In particular, the communication resources (the wires in the machine) need to be scheduled. This can be done dynamically or, when the set of messages is known in advance, statically. With detailed knowledge of the schedule of use of the wires, better bounds can be obtained. For the purposes of analysis of algorithms and assignment of tasks to processors, however, we have found this more realistic approach to be unnecessarily cumbersome. We prefer to use the four bounds above, which depend only on the integrated (i.e. time-independent) information M and, in the case of the edge-contention bound, the paths $p(M)$. In fact, in the work below, we won't assume knowledge of paths and we won't use the edge contention bound.

14.8.2 Cholesky factorization

We'll use the techniques we've introduced to analyze alternative distributed memory implementations of a very important computation, Cholesky factorization of a symmetric, positive definite (SPD) matrix A . The factorization is $A = LL^T$ where L is lower triangular; A is given, L is to be computed.

The algorithm is this:

```

1.   $L := A$ 
2.  for  $k = 1$  to  $N$  do
3.     $L_{kk} := \sqrt{L_{kk}}$ 
4.    for  $i = k + 1$  to  $N$  do
5.       $L_{ik} := L_{ik}L_{kk}^{-1}$ 
6.    for  $j = k + 1$  to  $N$  do
7.      for  $i = j$  to  $N$  do
8.         $L_{ij} := L_{ij} - L_{ik}L_{jk}^T$ 

```

We can let the elements L_{ij} be scalars, in which case this is the usual or “point” Cholesky algorithm. Or we can take L_{ij} to be a block, obtained by dividing the rows into contiguous subsets and making the same decomposition of the columns, so that diagonal blocks are square. In the block case, the computation of $\sqrt{L_{kk}}$ (Step 3) returns the (point) Cholesky factor of the SPD block L_{kk} . If A is sparse (has mostly zero entries) then L will be sparse too, although less so than A . In that case, only the non-zero entries in the sparse factor L are stored, and the multiplication/division in lines 5 and 8 are omitted if they compute zeros.

Mapping columns

Assume that the columns of a dense symmetric matrix of order N are mapped to processors cyclically: column j is stored in processor $map(j) \equiv j \bmod p$. Consider communication costs on two-dimensional grid or toroidal machines. Suppose that p is a perfect square and that the machine is a $\sqrt{p} \times \sqrt{p}$ grid. Consider a mapping of the computation in which the operations in line 8 are performed by processor $map(j)$. After performing the operations in line 5, processor $map(k)$ must send column k to all processors $\{map(j) \mid j > k\}$.

Let us fix our attention on 2D grids. There are $L = 2p + O(1)$ links. A column can be broadcast from its source to all other processors through a spanning tree of the machine, a tree of total length p reaching all the processors. Every matrix element will therefore travel over $p - 1$ links, so the total information flux is $(1/2)N^2p$ and the average flux bound is $(1/4)N^2\beta$.

Only $O(N^2/p)$ words leave any processor. If $N \gg p$, processors must accept almost the whole $(1/2)N^2$ words of L as arriving columns. The bandwidth per processor is β_0 , so the arrivals bound is $(1/2)N^2\beta_0$ seconds. If $N \approx p$ the bound drops to half that, $(1/4)N^2\beta_0$ seconds. We summarize these bounds for 2D grids in Table 14.1.

We can immediately conclude that this is a nonscalable distributed algorithm. We may not take $p > \frac{N\phi}{\beta}$ and still achieve high efficiency.

Mapping blocks

Dongarra, Van de Geijn, and Walker [25] have shown that on the Intel Touchstone Delta machine ($p = 528$), mapping blocks is better than mapping columns in LU factorization. In such a mapping, we view the machine as an $p_r \times p_c$ grid and we map elements A_{ij} and L_{ij} to processor

Type of Bound	Lower bound
Arrivals	$\frac{1}{4}N^2\beta_0$
Average flux	$\frac{1}{4}N^2\beta$

Table 14.1: Communication Costs for Column-Mapped Full Cholesky.

Type of Bound	Lower bound
Arrivals	$\frac{1}{4}N^2\beta\left(\frac{1}{p_r} + \frac{1}{p_c}\right)$
Edge contention	$N^2\beta\left(\frac{1}{p_r} + \frac{1}{p_c}\right)$

Table 14.2: Communication Costs for Torus-Mapped Full Cholesky.

$(mapr(i), mapc(j))$. We assume a cyclic mappings here: $mapr(i) \equiv i \pmod{p_r}$ and similarly for $mapc$.

The analysis of the preceding section may now be done for this mapping. Results are summarized in Table 14.2. With p_r and p_c both $O(\sqrt{p})$, the communication time drops like $O(p^{-1/2})$. With this mapping, the algorithm is scalable even when $\beta \gg \phi$. Now, with $p = O(N^2)$, both the compute time and the communication lower bounds agree; they are $O(N)$. Therefore, we remain efficient with storage per processor is $O(1)$. (This scalable algorithm for distributed Cholesky is due to O’Leary and Stewart [68].)

14.8.3 Distributed sparse Cholesky and the model problem

In the sparse case, the same holds true. To see why this must be true, we need only observe that most of the work in sparse Cholesky factorization takes the form of the factorization of dense submatrices that form during the Cholesky algorithm. Rothberg and Gupta demonstrated this fact in their work in 1992 – 1994.

Unfortunately, with naive cyclic mappings, block-oriented approaches suffer from poor balance of the computational load and modest efficiency. Heuristic remapping of the block rows and columns can remove load imbalance as a cause of inefficiency.

Several researchers have obtained excellent performance using a block-oriented approach, both on fine-grained, massively-parallel SIMD machines [22] and on coarse-grained, highly-parallel MIMD machines [77]. A block mapping maps rectangular blocks of the sparse matrix to processors. A 2-D mapping views the machine as a 2-D $p_r \times p_c$ processor grid, whose members are denoted $p(i, j)$. To date, the 2-D cyclic (also called torus-wrap) mapping has been used: block L_{ij} resides at processor $p(i \pmod{p_r}, j \pmod{p_c})$. All blocks in a given block row are mapped to the same row of processors, and all elements of a block column to a single processor column. Communication volumes grow as the square root of the number of processors, versus linearly for the 1-D mapping; 2-D mappings also asymptotically reduce the critical path length. These advantages accrue even when the underlying machine has some interconnection network whose topology is not a grid.

A 2-D cyclic mapping, however, produces significant load imbalance that severely limits achieved efficiency. On systems (such as the Intel Paragon) with high interprocessor communication bandwidth this load imbalance limits efficiency to a greater degree than communication or want of parallelism.

An alternative, heuristic 2-D block mapping succeeds in reducing load imbalance to a point where it is no longer the most serious bottleneck in the computation. On the Intel Paragon the block mapping heuristic produces a roughly 20% increase in performance compared with the cyclic mapping.

In addition, a scheduling strategy for determining the order in which available tasks are performed adds another 10% improvement.

14.8.4 Parallel Block-Oriented Sparse Cholesky Factorization

In the block factorization approach considered here, matrix blocks are formed by dividing the columns of the $n \times n$ matrix into N contiguous subsets, $N \leq n$. The identical partitioning is performed on the rows. A block L_{ij} in the sparse matrix is formed from the elements that fall simultaneously in row subset i and column subset j .

Each block L_{ij} has an owning processor. The owner of L_{ij} performs all block operations that update L_{ij} (this is the “owner-computes” rule for assigning work). Interprocessor communication is required whenever a block on one processor updates a block on another processor.

Assume that the processors can be arranged as a grid of p_r rows and p_c columns. In a *Cartesian product* (CP) mapping, $map(i, j) = p(RowMap(i), ColMap(j))$, where $RowMap : \{0..N - 1\} \rightarrow \{0..p_r - 1\}$, and $ColMap : \{0..N - 1\} \rightarrow \{0..p_c - 1\}$ are given mappings of rows and columns to processor rows and columns. We say that map is *symmetric Cartesian* (SC) if $p_r = p_c$ and $RowMap = ColMap$. The usual 2-D cyclic mapping is SC.²

14.9 Load balance with cyclic mapping

Any CP mapping is effective at reducing communication. While the 2-D cyclic mapping is CP, unfortunately it is not very effective at balancing computational load. Experiment and analysis show that the cyclic mapping produces particularly poor load balance; moreover, some serious load balance difficulties must occur for any SC mapping. Improvements obtained by the use of nonsymmetric CP mappings are discussed in the following section.

Our experiments employ a set of test matrices including two dense matrices (DENSE1024 and DENSE2048), two 2-D grid problems (GRID150 and GRID300), two 3-D grid problems (CUBE30 and CUBE35), and 4 irregular sparse matrices from the Harwell-Boeing sparse matrix test set [26]. Nested dissection or minimum degree orderings are used. In all our experiments, we choose $p_r = p_c = \sqrt{P}$, and we use a block size of 48. All Mflops measurements presented here are computed by dividing the operation counts of the best known sequential algorithm by parallel runtimes. Our experiments were performed on an Intel Paragon, using hand-optimized versions of the Level-3 BLAS for almost all arithmetic.

14.9.1 Empirical Load Balance Results

We now report on the efficiency and load balance of the method. Parallel efficiency is given by $t_{seq}/(P \cdot t_{par})$, where t_{par} is the parallel runtime, P is the number of processors, and t_{seq} is the

²See [77] for a discussion of *domains*, portions of the matrix mapped in a 1-D manner to further reduce communication.

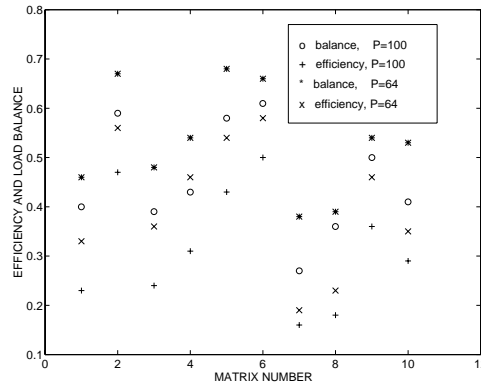


Figure 14.4: Efficiency and overall balance on the Paragon system ($B = 48$).

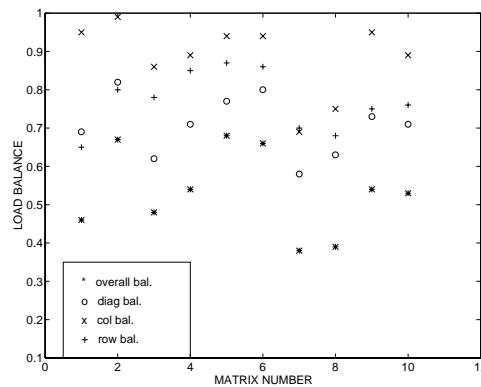


Figure 14.5: Efficiency bounds for 2-D cyclic mapping due to row, column and diagonal imbalances ($P = 64$, $B = 48$).

runtime for the same problem on one processor. For the data we report here, we measured t_{seq} by factoring the benchmark matrices using our parallel algorithm on one processor. The overall balance of a distributed computation is given by $work_{total}/(P \cdot work_{max})$, where $work_{total}$ is the total amount of work performed in the factorization, P is the number of processors, and $work_{max}$ is the maximum amount of work assigned to any processor. Clearly, overall balance is an upper bound on efficiency.

Figure 1 shows efficiency and overall balance with the cyclic mapping. Observe that load balance and efficiency are generally quite low, and that they are well correlated. Clearly, load balance alone is not a perfect predictor of efficiency. Other factors limit performance. Examples include interprocessor communication costs, which we measured at 5% — 20% of total runtime, long critical paths, which can limit the number of block operations that can be performed concurrently, and poor scheduling, which can cause processors to wait for block operations on other processors to complete. Despite these disparities, the data indicate that load imbalance is an important contributor to reduced efficiency.

We next measured load imbalance among rows of processors, columns of processors, and diagonals of processors. Define $work[i, j]$ to be the runtime due to updating of block L_{ij} by its owner. To approximate runtime, we use an empirically calibrated estimate of the form

work = operations + ω · block-operations; on the Paragon, $\omega = 1,000$.

Define $RowWork[i]$ to be the aggregate work required by blocks in row i : $RowWork[i] = \sum_{j=0}^{N-1} work[i, j]$. An analogous definition applies for $ColWork$, the aggregate column work. Define *row balance* by $work_{total}/p_r \cdot work_{rowmax}$, where $work_{rowmax} = \max_r \sum_{i: RowMap[i]=r} RowWork[i]$. This row balance statistic gives the best possible overall balance (and hence efficiency), obtained only if there is perfect load balance within each processor row. It isolates load imbalance due to an overloaded processor row caused by a poor row mapping. An analogous expression gives column balance, and a third analogous expression gives diagonal balance. (Diagonal d is made up of the set of processors $p(i, j)$ for which $(i - j) \bmod p_r = d$.) While these three aggregate measures of load balance are only upper bounds on overall balance, the data we present later make it clear that improving these three measures of balance will in general improve the overall load balance.

Figure 2 shows the row, column, and diagonal balances with a 2-D cyclic mapping of the benchmark matrices on 64 processors. Diagonal imbalance is the most severe, followed by row imbalance, followed by column imbalance.

These data can be better understood by considering dense matrices as examples (although the following observations apply to a considerable degree to sparse matrices as well). Row imbalance is due mainly to the fact that $RowWork[i]$, the amount of work associated with a row of blocks, increases with increasing i . More precisely, since $work[i, j]$ increases linearly with j and the number of blocks in a row increases linearly with i , it follows that $RowWork[i]$ increases quadratically in i . Thus, the processor row that receives the last block row in the matrix receives significantly more work than the processor row immediately following it in the cyclic ordering, resulting in significant row imbalance. Column imbalance is not nearly as severe as row imbalance. The reason, we believe, is that while the work associated with blocks in a column increases linearly with the column number j , the number of blocks in the column *decreases* linearly with j . As a result, $ColWork[j]$ is neither strictly increasing nor strictly decreasing. In the experiments, row balance is indeed poorer than column balance. Note that the reason for the row and column imbalance is not that the 2-D cyclic mapping is an SC mapping; rather, we have significant imbalance because the mapping functions $RowMap$ and $ColMap$ are each poorly chosen.

To better understand diagonal imbalance, one should note that blocks on the diagonal of the matrix are mapped exclusively to processors on the main diagonal of the processor grid. Blocks just below the diagonal are mapped exclusively to processors just below the main diagonal of the processor grid. These diagonal and sub-diagonal blocks are among the most work-intensive blocks in the matrix. In sparse problems, moreover, the diagonal blocks are the only ones that are guaranteed to be dense. (For the two dense test matrices, diagonal balance is not significantly worse than row balance.) The remarks we make about diagonal blocks and diagonal processors apply to *any* SC mapping, and do not depend on the use of a cyclic function $RowMap(i) = i \bmod p_r$.

14.10 Heuristic Remapping

Nonsymmetric CP mappings, which map rows independently of columns, are a way to avoid diagonal imbalance that is automatic with SC mappings. We shall choose the row mapping $RowMap$ to maximize the row balance, and independently choose $ColMap$ to maximize column balance. Since the row mapping has no effect on the column balance, and vice versa, we may choose the row mapping in order to maximize row balance independent of the choice of column mapping.

The problems of determining $RowMap$ and $ColMap$ are each cases of a standard NP-complete problem, *number partitioning* [34], for which a simple heuristic is known to be good³. This

³Number partitioning is a well studied NP-complete problem. The objective is to distribute a set of numbers

heuristic obtains a row mapping by considering the block rows in some predefined sequence. For each processor row, it maintains the total work for all blocks mapped to that row. The algorithm iterates over block rows, mapping a block row to the processor row that has received the least work thus far. We have experimented with several different sequences, the two best of which we now describe.

The **Decreasing Work (DW)** heuristic considers rows in order of decreasing work. This is a standard approach to number partitioning; that small values toward the end of the sequence allow the algorithm to lessen any imbalance caused by large values encountered early in the sequence.

The **Increasing Depth (ID)** heuristic considers rows in order of increasing depth in the elimination tree. In a sparse problem, the work associated with a row is closely related to its depth in the elimination tree.

The effect of these schemes is dramatic. If we look at the three aggregate measures of load balance, we find that these heuristics produce row and column balance of 0.98 or better, and diagonal balance of 0.93 or better, for test case BCSSTK31, which is typical. With ID as the row mapping we have produced better than a 50% improvement in overall balance, and better than a 20% improvement in performance, on average over our test matrices, with $P = 100$. The DW heuristic produces only slightly less impressive improvements. The choice of column mapping, as expected, is less important. In fact, for our test suite, the cyclic column mapping and ID row mapping gave the best mean performance.⁴

We also applied these ideas to four larger problems: DENSE4096, CUBE40, COPTER2 (a helicopter rotor blade model, from NASA) and 10FLEET (a linear programming formulation of an airline fleet assignment problem, from Delta Airlines). On 144 and 196 processors the heuristic (increasing depth on rows and cyclic on columns) again produces a roughly 20% performance improvement over a cyclic mapping. Peak performance of 2.3 Gflops for COPTER2 and 2.7 Gflops for 10FLEET were achieved; for the model problems CUBE40 and DENSE4096 the speeds were 3.2 and 5.2 Gflops.

In addition to the heuristics described so far, we also experimented with two other approaches to improving factorization load balance. The first is a subtle modification of the original heuristic. It begins by choosing some column mapping (we use a cyclic mapping). This approach then iterates over rows of blocks, mapping a row of blocks to a row of processors so as to minimize the amount of work assigned to any one *processor*. Recall that the earlier heuristic attempted to minimize the aggregate work assigned to an entire row of processors. We found that this alternative heuristic produced further large improvements in overall balance (typically 10-15% better than that of our original heuristic). Unfortunately, realized performance did not improve. This result indicates that load balance is not the most important performance bottleneck once our original heuristic is applied.

A very simple alternate approach reduces imbalance by performing cyclic row and column mappings on a processor grid whose dimensions p_c and p_r are relatively prime; this reduces diagonal imbalance. We tried this using 7×9 and 9×11 processor grids (using one fewer processor than for our earlier experiments with $P = 64$ and $P = 100$.) The improvement in performance is somewhat lower than that achieved with our earlier remapping heuristic (17% and 18% mean improvement on 63 and 99 processors versus 20% and 24% on 64 and 100 processors). On the other hand, the mapping needn't be computed.

among a fixed number of bins so that the maximum sum in any bin is minimized.

⁴Full experimental data has appeared in another paper [78].

14.11 Scheduling Local Computations

The next questions to be addressed, clearly, are: (i) what is the most constraining bottleneck after our heuristic is applied, and (ii) can this bottleneck be addressed to further improve performance?

One potential remaining bottleneck is communication. Instrumentation of our block factorization code reveals that on the Paragon system, communication costs account for less than 20% of total runtime for all problems, even on 196 processors. The same instrumentation reveals that most of the processor time not spent performing useful factorization work is spent idle, waiting for the arrival of data.

We do not believe that the idle time is due to insufficient parallelism. Critical path analysis for problem BCSSTK15 on 100 processors, for example, indicates that it should be possible to obtain nearly 50% higher performance than we are currently obtaining. The same analysis for problem BCSSTK31 on 100 processors indicates that it should be possible to obtain roughly 30% higher performance. We therefore suspected that the scheduling of tasks by our code was not optimal.

To that end we tried alternative scheduling policies. They are:

FIFO. Tasks are initiated in the order in which the processor discovers that they are ready.

Destination depth. Ready tasks initiated in order of the destination block's elimination tree depth.

Source depth. Ready tasks initiated in order of the source block's elimination tree depth.

For the FIFO policy, a queue of ready tasks is used, while for the others, a heap is used. We experimented with 64 processors, using BSCCST31, BCSSTK33, and DENSE2048. Both priority-based schemes are better than FIFO; destination depth seems slightly better than source depth. We observed a slowdown of 2% due to the heap data structure on BCSSTK33; the destination priority scheme then improved performance by 15% for a net gain of 13%. For BSCCST31 the net gain was 8%. For DENSE2048, however, there was no gain. This improvement is encouraging. There may be more that can be achieved through the pursuit of a better understanding of the scheduling question.

Chapter 15

Domain Decomposition for PDE

Domain decomposition is a term used by at least two different communities. Literally, the words indicate the partitioning of a region. As we will see in Part ?? of this book, an important computational geometry problem is to find good ways to partition a region. This is not what we will discuss here.

In scientific computing, domain decomposition refers to the technique of solving partial differential equations using subroutines that solve problems on subdomains. Originally, a domain was a contiguous region in space, but the idea has generalized to include any useful subset of the discretization points. Because of this generalization, the distinction between domain decomposition and multigrid has become increasingly blurred.

Domain decomposition is an idea that is already useful on serial computers, but it takes on a greater importance when one considers a parallel machine with, say, a handful of very powerful processors. In this context, domain decomposition is a parallel divide-and-conquer approach to solving the PDE.

To guide the reader, we quickly summarize the choice space that arises in the domain decomposition literature. As usual a domain decomposition problem starts as a continuous problem on a region and is discretized into a finite problem on a discrete domain.

We will take as our model problem the solution of the elliptic equation $\nabla^2 u = f$ on a region Ω which is the union of at least subdomains Ω_1 and Ω_2 . Domain decomposition ideas tend to be best developed for elliptic problems, but may be applied in more general settings.

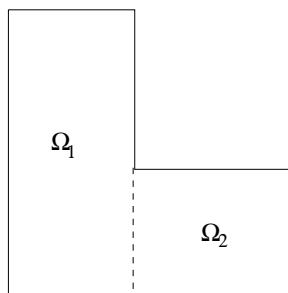


Figure 15.1: Domain divided into two subdomains without overlap

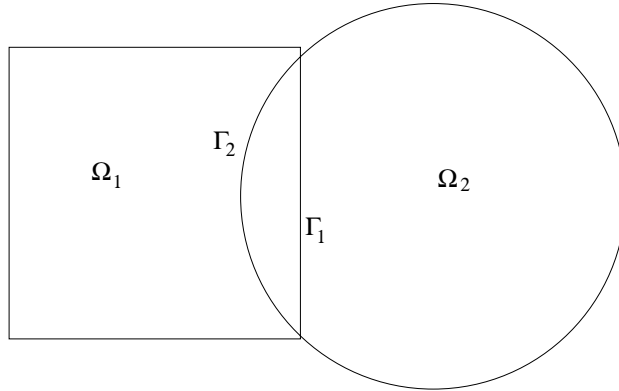


Figure 15.2: Example domain of circle and square with overlap

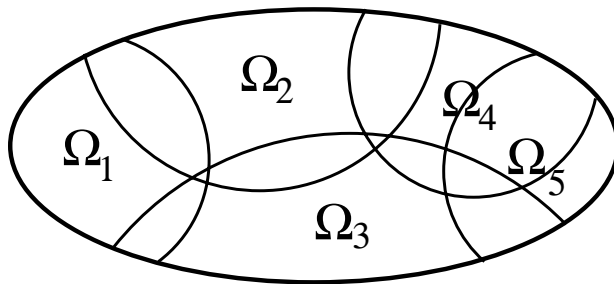


Figure 15.3: Example domain with many overlapping regions

DOMAIN DECOMPOSITION OUTLINE

1. Geometric Issues

- Overlapping or non-overlapping regions

- Geometric Discretization

- Finite Difference or Finite Element

- Matching or non-matching grids

2. Algorithmic Issues

- Algebraic Discretization

- Schwarz Approaches: Additive vs Multiplicative

- Substructuring Approaches

- Accelerants

- Domain Decomposition as a Preconditioner

- Course (Hierarchical/Multilevel) Domains

3. Theoretical Considerations

15.1 Geometric Issues

The geometric issues in domain decomposition are 1) how are the domains decomposed into subregions, and 2) how is the region discretized using some form of grid or irregular mesh. We consider these issues in turn.

15.1.1 Overlapping vs Non-overlapping regions

So as to emphasize the issue of overlap vs non-overlap, we can simplify all the other issues by assuming that we are solving the continuous problem (no discretization) exactly on each domain (no choice of algorithm). The reader may be surprised to learn that domain decomposition methods divide neatly into either being overlapping or nonoverlapping methods. Though one can find much in common between these two methods, they are really rather different in flavor. When the methods overlap, the methods are sometimes known as Schwarz methods, while when there is no overlap, the methods are sometimes known as substructuring. (Historically, the former name was used in the continuous case, and the latter in the discrete case, but this historical distinction has been, and even should be, blurred.)

We begin with the overlapping region illustrated in Figure 15.2. Schwarz in 1870 devised an obvious alternating procedure for solving Poisson's equation $\nabla^2 u = f$:

1. Start with any guess for u_2 on Ω_1 .
2. Solve $\nabla^2 u = f$ on Ω_1 by taking $u = u_2$ on $\partial\Omega_1$. (i.e. solve in the square using boundary data from the interior of the circle)
3. Solve $\nabla^2 u = f$ on Ω_2 by taking $u = u_1$ on $\partial\Omega_2$ (i.e. solve in the circle using boundary data from the interior of the square)
4. Goto 2 and repeat until convergence is reached

One of the characteristics of elliptic PDE's is that the solution at every point depends on global conditions. The information transfer between the regions clearly occurs in the overlap region.

If we “choke” the transfer of information by considering the limit as the overlap area tends to 0, we find ourselves in a situation typified by Figure 15.1. The basic Schwarz procedure no longer works? Do you see why? No matter what the choice of data on the interface, it would not be updated. The result would be that the solution would not be differentiable along the interface.

One approach to solving the non-overlapped problem is to concentrate directly on the domain of intersection. Let g be a current guess for the solution on the interface. We can then solve $\nabla^2 u = f$ on Ω_1 and Ω_2 independently using the value of g as Dirichlet conditions on the interface. We can define the map

$$T : g \rightarrow \frac{\partial g}{\partial n_1} + \frac{\partial g}{\partial n_2}.$$

This is a map from functions on the interface to functions on the interface defined by taking a function to the jump in the derivative. The operator T is known as the Steklov-Poincaré operator.

Suppose we can find the exact solution to $Tg = 0$. We would then have successfully decoupled the problem so that it may be solved independently into the two domains Ω_1 and Ω_2 . This is a “textbook” illustration of the divide and conquer method, in that solving $Tg = 0$ constitutes the “divide.”

15.1.2 Geometric Discretization

In the previous section we contented ourselves with formulating the problem on a continuous domain, and asserted the existence of solutions either to the subdomain problems in the Schwarz case, or the Steklov-Poincaré operator in the continuous case.

Of course on a real computer, a discretization of the domain and a corresponding discretization of the equation is needed. The result is a linear system of equations.

Finite Differences or Finite Elements

Finite differences is actually a special case of finite elements, and all the ideas in domain decomposition work in the most general context of finite elements. In finite differences, one typically imagines a square mesh. The prototypical example is the five point stencil for the Laplacian in two dimensions. An analog computer to solve this problem would consist of a grid of one ohm resistors. In finite elements, the prototypical example is a triangulation of the region, and the appropriate formulation of the PDE on these elements.

Matching vs Non-matching grids

When solving problems as in our square-circle example of Figure 15.2, it is necessary to discretize the interior of the regions with either a finite difference style grid or a finite element style mesh. The square may be nicely discretized by covering it with Cartesian graph-paper, while the circle may be more conveniently discretized by covering it with Polar graph-paper. Under such a situation, the grids do not match, and it becomes necessary to transfer points interior to Ω_2 to the boundary of Ω_1 and vice versa.

15.2 Algorithmic Issues

Once the domain is discretized, numerical algorithms must be formulated. There is a definite line drawn between Schwarz (overlapping) and substructuring (non-overlapping) approaches.

15.2.1 Schwarz approaches: additive vs multiplicative

A procedure that alternates between solving an equation in Ω_1 and then Ω_2 does not seem to be parallel at the highest level because if processor 1 contains all of Ω_1 and processor 2 contains all of Ω_2 then each processor must wait for the solution of the other processor before it can execute. Such approaches are known as multiplicative approaches because of the form of the operator applied to the error. Alternatively, approaches that allow for the solution of subproblems simultaneously are known as additive methods. The difference is akin to the difference between Jacobi and Gauss-Seidel. We proceed to explain this in further detail.

Classical Iterations and their block equivalents

Let us review the basic classical methods for solving pde's on a discrete domain.

1. Jacobi - At step n , the neighboring values used are from step $n - 1$
2. Gauss-Seidel - Values at step n are used if available, otherwise the values are used from step $n - 1$
3. Red Black Ordering - If the grid is a checkerboard, solve all red points in parallel using black values at $n - 1$, then solve all black points in parallel using red values at step n

Analogous *block* methods may be used on a domain that is decomposed into a number of multiple regions. Each region is thought of as an element used to solve the larger problem. This is known as block Jacobi, or block Gauss-Seidel.

1. Gauss-Seidel - Solve each region in series using the boundary values at n if available.
2. Jacobi - Solve each region on a separate processor in parallel and use boundary values at $n - 1$. (Additive scheme)
3. Coloring scheme - Color the regions so that like colors do not touch and solve all regions with the same color in parallel. (Multiplicative scheme)

The block Gauss-Seidel algorithm is called a multiplicative scheme for reasons to be explained shortly. In a corresponding manner, the block Jacobi scheme is called an additive scheme.

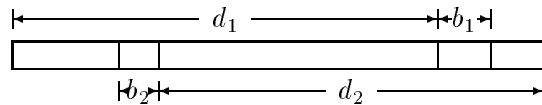
Overlapping regions: A notational nightmare?

When the grids match it is somewhat more convenient to express the discretized PDE as a simple matrix equation on the gridpoints.

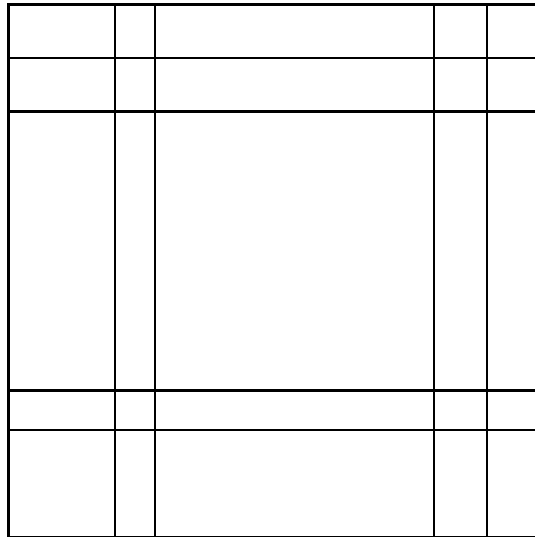
Unfortunately, we have a notational difficulty at this point. It is this difficulty that is probably the single most important reason that domain decomposition techniques are not used as extensively as they can be. Even in the two domain case, the difficulty is related to the fact that we have domains 1 and 2 that overlap each other and have internal and external boundaries. By setting the boundary to 0 we can eliminate any worry of external boundaries. I believe there is only one reasonable way to keep the notation manageable. We will use subscripts to denote subsets of indices. d_1 and d_2 will represent those nodes in domain 1 and domain 2 respectively. b_1 and b_2 will represent those nodes in the boundary of 1 and 2 respectively that are not external to the entire domain.

Therefore u_{d_1} denotes the subvector of u consisting of those elements interior to domain 1, while A_{u_1, b_1} is the rectangular subarray of A that map the interior of domain 1 to the internal boundary

of domain 1. If we were to write u^T as a row vector, the components might break up as follows (the overlap region is unusually large for emphasis:)



Correspondingly, the matrix A (which of course would never be written down) has the form



The reader should find A_{b_1, b_1} etc., on this picture. To further simplify notation, we write 1 and 2 for d_1 and $d_2, 1_b$ and 2_b for b_1 and b_2 , and also use only a single index for a diagonal block of a matrix (i.e. $A_1 = A_{11}$).

Now that we have leisurely explained our notation, we may return to the algebra. Numerical analysts like to turn problems that may seem new into ones that they are already familiar with. By carefully writing down the equations for the procedure that we have described so far, it is possible to relate the classical domain decomposition method to an iteration known as *Richardson iteration*. Richardson iteration solves $Au = f$ by computing $u^{k+1} = u^k + M(f - Au^k)$, where M is a “good” approximation to A^{-1} . (Notice that if $M = A^{-1}$, the iteration converges in one step.)

The iteration that we described before may be written algebraically as

$$A_1 u_1^{k+1/2} + A_{1,1_b} u_{1_b}^k = f_1$$

$$A_2 u_2^{k+1} + A_{2,2_b} u_{2_b}^{k+1/2} = f_2$$

Notice that values of $u^{k+1/2}$ updated by the first equation, specifically the values on the boundary of the second region, are used in the second equation.

With a few algebraic manipulations, we have

$$u_1^{k+1/2} = u_1^{k-1} + A_1^{-1}(f - Au^{k-1})_1$$

$$u_2^{k+1} = u_2^{k+1/2} + A_2^{-1}(f - Au^{k+1/2})_2$$

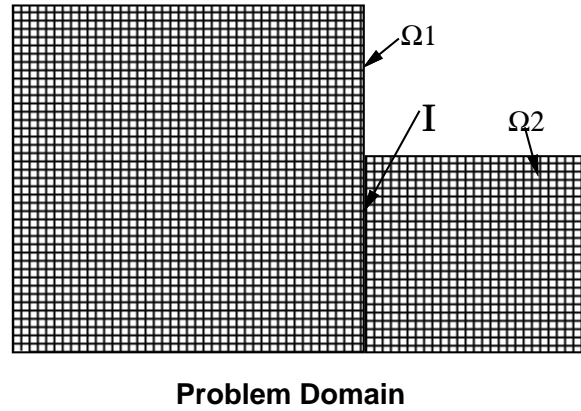


Figure 15.4: Problem Domain

This was already obviously a Gauss-Seidel like procedure, but those of you familiar with the algebraic form of Gauss-Seidel might be relieved to see the form here.

A roughly equivalent block Jacobi method has the form

$$u_1^{k+1/2} = u_1^{k-1} + A_1^{-1}(f - Au^{k-1})_1$$

$$u_2^k = u_2^{k+1/2} + A_2^{-1}(f - Au^k)_2$$

It is possible to eliminate $u^{k+1/2}$ and obtain

$$u^{k+1} = u^k + (A_1^{-1} + A_2^{-1})(f - Au^k),$$

where the operators are understood to apply to the appropriate part of the vectors. It is here that we see that the procedure we described is a Richardson iteration with operator $M = A_1^{-1} + A_2^{-1}$.

15.2.2 Substructuring Approaches

Figure 15.4 shows an example domain of a problem for a network of resistors or a discretized region in which we wish to solve the Poisson equation, We will see that the discrete version of the Steklov-Poincaré operator has its algebraic equivalent in the form of the Schur complement.

$$\nabla^2 v = g$$

In matrix notation, $Av = g$, where

$$A = \begin{pmatrix} A_1 & 0 & A_{1I} \\ 0 & A_2 & A_{2I} \\ A_{I1} & A_{I2} & A_I \end{pmatrix}$$

One of the direct methods to solve the above equation is to use LU or LDU factorization. We will do an analogous procedure with blocks. We can rewrite A as,

$$A = \begin{pmatrix} I & 0 & 0 \\ 0 & I & 0 \\ A_{I1}A_1^{-1} & A_{I2}A_2^{-1} & I \end{pmatrix} \begin{pmatrix} I & 0 & 0 \\ 0 & I & 0 \\ 0 & 0 & S \end{pmatrix} \begin{pmatrix} A_1 & 0 & A_{1I} \\ 0 & A_2 & A_{2I} \\ 0 & 0 & I \end{pmatrix}$$

where,

$$S = A_I - A_{I1}A_1^{-1}A_{1I} - A_{I2}A_2^{-1}A_{2I}$$

We really want A^{-1}

$$A^{-1} = \begin{pmatrix} A_1^{-1} & 0 & -A_1^{-1}A_{1I} \\ 0 & A_2^{-1} & -A_2^{-1}A_{2I} \\ 0 & 0 & I \end{pmatrix} \begin{pmatrix} I & 0 & 0 \\ 0 & I & 0 \\ 0 & 0 & S^{-1} \end{pmatrix} \begin{pmatrix} I & 0 & 0 \\ 0 & I & 0 \\ -A_{I1}A_1^{-1} & -A_{I2}A_2^{-1} & I \end{pmatrix} \quad (15.1)$$

Inverting S turns out to be the hardest part.

$$A^{-1} \begin{pmatrix} V_{\Omega 1} \\ V_{\Omega 2} \\ V_{Interface} \end{pmatrix} \begin{matrix} \rightarrow \text{Voltages in region } \Omega 1 \\ \rightarrow \text{Voltages in region } \Omega 2 \\ \rightarrow \text{Voltages at interface} \end{matrix}$$

Let us examine Equation 15.1 in detail.

In the third matrix,

A_1^{-1} - Poisson solve in $\Omega 1$

A_{I1} - is putting the solution onto the interface

A_2^{-1} - Poisson solve in $\Omega 2$

A_{I2} - is putting the solution onto the interface

In the second matrix,

Nothing happening in domain 1 and 2

Complicated stuff at the interface.

In the first matrix we have,

A_1^{-1} - Poisson solve in $\Omega 1$

A_2^{-1} - Poisson solve in $\Omega 2$

$A_1^{-1}A_{1I}$ and $A_2^{-1}A_{2I}$ - Transferring solution to interfaces

In the above example we had a simple 2D region with neat squares but in reality we might have to solve on complicated 3D regions which have to be divided into tetrahedra with 2D regions at the interfaces. The above concepts still hold.

Getting to S^{-1} ,

$$\begin{pmatrix} a & b \\ c & d \end{pmatrix} = \begin{pmatrix} 1 & 0 \\ c/a & 1 \end{pmatrix} \begin{pmatrix} a & b \\ 0 & d - bc/a \end{pmatrix}$$

where, $d - bc/a$ is the Schur complement of d.

In Block form

$$\begin{pmatrix} A & B \\ C & D \end{pmatrix} = \begin{pmatrix} 1 & 0 \\ CA^{-1} & 1 \end{pmatrix} \begin{pmatrix} A & B \\ 0 & D - CA^{-1}B \end{pmatrix}$$

We have

$$S = A_I - A_{I1}A_1^{-1}A_{1I} - A_{I2}A_2^{-1}A_{2I}$$

Arbitrarily break A_I as

$$A_I = A_I^1 + A_I^2$$

Think of A as

$$\begin{pmatrix} A_1 & 0 & A_{1I} \\ 0 & 0 & 0 \\ A_{I1} & 0 & A_I^1 \end{pmatrix} + \begin{pmatrix} 0 & 0 & 0 \\ 0 & A_2 & A_{2I} \\ 0 & A_{I2} & A_I^2 \end{pmatrix}$$

Schur Complements are

$$S^1 = A_I^1 - A_{I1}A_1^{-1}A_{1I}$$

$$S^2 = A_I^2 - A_{I2}A_2^{-1}A_{2I}$$

and

$$S = S^1 + S^2$$

$A_1^{-1} \rightarrow$ Poisson solve on Ω_1

$A_2^{-1} \rightarrow$ Poisson solve on Ω_2

$A_{I1} \quad \Omega_1 \rightarrow I$

$A_{21} \quad \Omega_2 \rightarrow I$

$A_{1I} \quad I \rightarrow \Omega_1$

$A_{2I} \quad I \rightarrow \Omega_2$

Sv - Multiplying by the Schur Complement involves 2 Poisson solves and some cheap transferring.

$S^{-1}v$ should be solved using Krylov methods. People have recommended the use of S_1^{-1} or S_2^{-1} or $(S_1^{-1} + S_2^{-1})$ as a preconditioner

15.2.3 Accelerants

Domain Decomposition as a Preconditioner

It seems wasteful to solve subproblems extremely accurately during the early stages of the algorithm when the boundary data is likely to be fairly inaccurate. Therefore it makes sense to run a few steps of an iterative solver as a preconditioner for the solution to the entire problem.

In a modern approach to the solution of the entire problem, a step or two of block Jacobi would be used as a preconditioner in a Krylov based scheme. It is important at this point not to lose track what operations may take place at each level. To solve the subdomain problems, one might use multigrid, FFT, or preconditioned conjugate gradient, but one may choose to do this approximately during the early iterations. The solution of the subdomain problems itself may serve as a preconditioner to the solution of the global problem which may be solved using some Krylov based scheme.

The modern approach is to use a step of block Jacobi or block Gauss-Seidel as a preconditioner for use in a Krylov space based subsolver. There is not too much point in solving the subproblems exactly on the smaller domains (since the boundary data is wrong) just an approximate solution suffices \rightarrow **domain decomposition preconditioning**

Krylov Methods - Methods to solve linear systems : $\mathbf{A}u = \mathbf{g}$. Examples have names such

as the Conjugate Gradient Method, GMRES (Generalized Minimum Residual), BCG (Bi Conjugate Gradient), QMR (Quasi Minimum Residual), CGS (Conjugate Gradient Squared). For this lecture, one can think of these methods in terms of a black-box. What is needed is a subroutine that given u computes Au . This is a matrix-vector multiply in the abstract sense, but of course it is not a dense matrix-vector product in the sense one practices in undergraduate linear algebra. The other needed ingredient is a subroutine to *approximately* solve the system. This is known as a preconditioner. To be useful this subroutine must roughly solve the problem quickly.

Course (Hierarchical/Multilevel) Techniques

These modern approaches are designed to greatly speed convergence by solving the problem on different sized grids with the goal of communicating information between subdomains more efficiently. Here the “domain” is a course grid. Mathematically, it is as easy to consider a contiguous domain consisting of neighboring points, as it is to consider a course grid covering the whole region.

Up until now, we saw that subdividing a problem did not directly yield the final answer, rather it simplified or allowed us to change our approach in tackling the resulting subproblems with existing methods. It still required that individual subregions be composited at each level of refinement to establish valid conditions at the interface of shared boundaries.

Multilevel approaches solve the problem using a coarse grid over each sub-region, gradually accommodating higher resolution grids as results on shared boundaries become available. Ideally for a well balanced multi-level method, no more work is performed at each level of the hierarchy than is appropriate for the accuracy at hand.

In general a hierarchical or multi-level method is built from an understanding of the difference between the damping of low frequency and high components of the error. Roughly speaking one can kill off low frequency components of the error on the course grid, and higher frequency errors on the fine grid.

Perhaps this is akin to the Fast Multipole Method where p poles that are “well-separated” from a given point could be considered as clusters, and those nearby are evaluated more precisely on a finer grid.

15.3 Theoretical Issues

This section is not yet written. The rough content is the mathematical formulation that identifies subdomains with projection operators.

15.4 A Domain Decomposition Assignment: Decomposing MIT

Perhaps we have given you the impression that entirely new codes must be written for parallel computers, and furthermore that parallel algorithms only work well on regular grids. We now show you that this is not so.

You are about to solve Poisson’s equation on our MIT domain:

Notice that the letters MIT have been decomposed into 32 rectangles – this is just the right number for solving

$$\frac{\partial^2 u}{\partial x^2} + \frac{\partial^2 u}{\partial y^2} = \rho(x, y)$$

on a 32 processor CM-5.

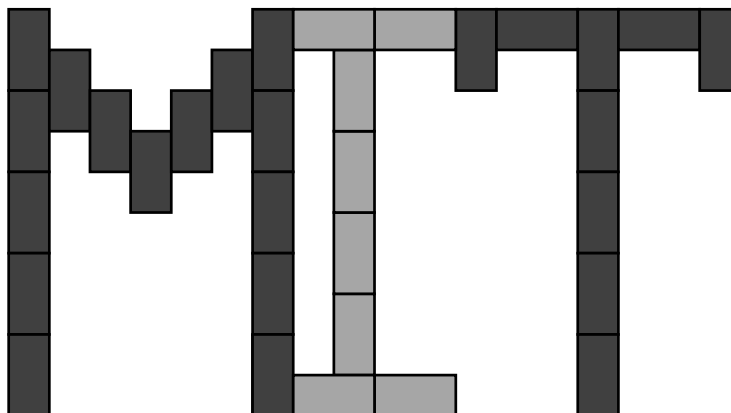


Figure 15.5: MIT domain

To solve the Poisson equation on the individual rectangles, we will use a FISHPACK library routine. (I know the French would cringe, but there really is a library called FISHPACK for solving the Poisson equation.) The code is old enough (from the 70's) but in fact it is too often used to really call it dusty.

[Can you tell that the paragraphs below were written before the web caught on?]

As a side point, this exercise highlights the ease of grabbing kernel routines off the network these days. High quality numerical software is out there (bad stuff too). One good way to find it is via `xnetlib`.

On athena, type

```
athena% add netlib
athena% xnetlib
```

to play with netlib which is actually running off of a machine in Oak Ridge, TN. Click on `Library`, then `fishpack`, then the first routine: `fishpack/hwscrt.f`

Now click `download` on the top bar button, then “Get Files Now” as you watch your gas tank go from empty to full. Xnetlib has now created the directory `xnlFiles` (`x-net-lib-files`). You can `cd xnlFiles/fishpack` to see the routine.

Congratulations, you have just obtained free software over the network. You probably want to have a Friday directory on scout. You can then ftp the code over to scout by typing on athena:

```
ftp scout.lcs.mit.edu
```

and using your userid (`mit-0?`) followed by your password. (If you hit return after your last name it will not work.) If all the directories are set up right you can type `put hwscrt.f` to move the file to scout.

All of the rectangles on the MIT picture have sides in the ratio 2 to 1; some are horizontal while others are vertical. We have arbitrarily numbered the rectangles according to scheme below, you might wish to write the numbers in the picture on the first page.

4				10	21	21	22	22	23	24	24	25	26	26	27
4	5			9	10		20		23			25			27
3	5	6		8	9	11		20				28			
3		6	7	8		11		19				28			

2	7	12	19	29
2		12	18	29
1		13	18	30
1		13	17	30
0		14	17	31
0		14 15 15 16 16		31

In our file `neighbor.data` which you can take from `~edelman/summer94/friday` we have encoded information about neighbors and connections. A copy of the file is included in this handout. You will see numbers such as

```

1 0 0 0 0 0
4 0 0 0 0 0
0 0 0 0
0

```

This contains information about the 0th rectangle. The first line says that it has a neighbor 1. The 4 means that the neighbor meets the rectangle on top. (1 would be the bottom, 6 would be the lower right.) We starred out a few entries towards the bottom. Figure out what they should be.

In the actual code (`solver.f`), a few lines were question marked out for the message passing. Figure out how the code works and fill in the appropriate lines. The program may be compiled with the `makefile`.

Chapter 16

Multilevel Methods

Multilevel methods can be viewed a family of useful methods for solving sparse linear systems defined on spatial domains. It can also be viewed as an extension of our basic numerical methods such as the finite element and finite difference methods. Instead using a single mesh to approximate PDEs on a physical domain as in the finite element and difference method, the multilevel method (or called hierarchical methods) use a gradient (series) of meshes M_0, \dots, M_k , where M_i is a coarsened mesh of M_{i-1} , or equivalently M_{i-1} is a refinement of M_i . Two examples are multigrid (MD) [?] and (multilevel) domain decomposition (DD) [?]. Both methods are iterative in nature. They perform an iterative computation that transforms partial solutions from one mesh to its coarsened mesh or refined mesh (called its neighboring meshes). It uses interpolation or restriction to go from mesh to mesh.

16.1 Multigrids

Originally, multigrid methods were developed to solve boundary value problems posed on a (geometric) physical domain. Therefore, there are two important inputs: the PDEs and the geometric structure of the domain. Such problems are made discrete by choosing a set of grid points.

16.1.1 The Basic Idea

1. Use coarse grids to obtain better initial guesses for the finest grid.
2. Use coarse grids to correct the error of the solution obtained on the finest grid. We call such a scheme a coarse grid correction scheme.

16.1.2 Restriction and Interpolation

For supporting both approach, we need to define

- an operator to transfer a fine grid vector to a coarse grid vector.
- an operator to a coarse grid vector to a fine grid vector.
- the corresponding linear systems for coarse grids.

To move the solution from a coarse grid to a fine one, we use *interpolation*. Conversely, to move the solution from a fine grid to a coarse one we apply *restriction*. Many methods for interpolation

and restriction can be used. Here we discuss some simple ones that are commonly used in multigrid implementation. *These simple ones are quite effective in practice.*

Let I_{2h}^h denote the interpolation operator. It takes a coarse grid vector v^{2h} and return a fine grid vector v^h , i.e., $I_{2h}^h v^{2h} = v^h$. For one dimensional fine grid of $n - 1$ points, the following interpolation vector is the most commonly used one:

$$\begin{aligned} v_{2j}^h &= v_j^{2h} \\ v_{2j+1}^h &= (v_j^{2h} + v_{j+1}^{2h})/2, \end{aligned}$$

where $0 \leq j \leq n/2 - 1$.

Notice that the interpolation operator is an linear operator and can be written as a matrix vector product. We else use I_{2h}^h to denote the transformation matrix.

For two dimensional grids, the interpolation operator can be defined in a similar way. One again, we let I_{2h}^h denote the interpolation operator and hence, $I_{2h}^h v^{2h} = v^h$. The components of v^h are then given by

$$\begin{aligned} v_{2i,2j}^h &= v_{i,j}^{2h} \\ v_{2i+1,2j}^h &= (v_{i,j}^{2h} + v_{i+1,j}^{2h})/2 \\ v_{2i,2j+1}^h &= (v_{i,j}^{2h} + v_{i,j+1}^{2h})/2 \\ v_{2i+1,2j+1}^h &= (v_{i,j}^{2h} + v_{i+1,j}^{2h} + v_{i,j+1}^{2h} + v_{i+1,j+1}^{2h})/4 \end{aligned}$$

where $0 \leq i, j \leq n/2 - 1$.

Because the regular grids used in multigrid are well-nested. The simplest way to transfer vector from a fine grid to a coarse grid is by injection, i.e., by assign $v_j^{2h} = v_{2j}^h$ for one dimensional case. An alternative restriction operator is called *full weighting* and we denoted it by I_h^{2h} . It takes a fine grid vector v^h and return a coarse grid vector v^{2h} , i.e., $I_h^{2h} v^h = v^{2h}$. The components of v^h are given by

$$v_j^{2h} = (v_{2j-1}^h + 2v_{2j}^h + v_{2j+1}^h)/4,$$

where $1 \leq j \leq n/2 - 1$.

As a linear operator, we have $I_{2h}^h = 2(I_h^{2h})^T$, where $(I_h^{2h})^T$ is the transpose of (I_h^{2h}) .

Similarly, we can define the *full weighting restriction* operator for two dimensional regular grid, $I_h^{2h} v^h = v^{2h}$. The components of v^h are given by

$$\begin{aligned} v_j^{2h} &= \{(v_{2i-1,2j-1}^h + 2v_{2i-1,2j+1}^h + v_{2i+1,2j-1}^h + 2v_{2i+1,2j+1}^h) \\ &\quad (v_{2i,2j-1}^h + 2v_{2i,2j+1}^h + v_{2i-1,2j}^h + 2v_{2i+1,2j}^h) + 4v_{2i,2j}^h\} \end{aligned}$$

where $1 \leq i, j \leq n/2 - 1$. Again, we have $I_{2h}^h = 2(I_h^{2h})^T$. Clearly in theory, we can use other convex combination of the values of the neighboring points in the restriction formulation.

Numerically, the interpolation can restriction operator transfer the vector of errors on one grid to another. So its numerical effectiveness and correctness depends on the assumption that the error is "smooth". Notice that if the error is highly oscillatory, then clearly the interpolation and the full weighted restriction may produce an error vector that is not very accurate. Fortunately, for multigrid, the iterative process at each grid eliminates the oscillatory components of the error vector and hence produce an error vector that is much smooth. The process of interpolation, restriction, and local relaxation complement each other. That is the intuition why multigrid can be very effective.

Clearly, for regular grids, the computation in both interpolation and restriction involves values only from nearest neighbors and can be written again as a sparse matrix time a vector. Therefore such operation can be supported efficiently on parallel machines.

16.1.3 The Multigrid Scheme

To simplify our discussion, we introduce some notation.

- Let A^h denote the linear system associated with grid of spacing h .
- For each vector name, say v , let v^h denote a vector for the grid of spacing h .

Therefore, if h is the spacing of the finest grid, then the linear systems associated with the finest grid give as $A^h u^h = f^h$.

The simplest multigrid scheme is the use the coarse grid to relax the error. Such a scheme is referred as a V-cycle scheme in the literature.

Algorithm V-cycle MG(v^h, f^h)
if Ω^h is the coarsest grid, solve $A^h u^h = f^h$ directly (if A^h is small enough),
 or apply an iterative method k times to relax the equation $A^h u^h = f^h$ with
 initial solution v^h to obtain a new v^h .
else

1. apply an iterative method k_1 times to relax the equation $A^h u^h = f^h$
 with initial solution v^h to obtain a new v^h .
2. $r^{2h} = I_h^{2h}(f^h - A^h v^h)$
3. $e^{2h} = 0$
4. $e^{2h} = \text{V-cycle MG}(e^{2h}, r^{2h})$
5. $e^h = I_{2h}^h(e^{2h})$
6. $v^h = v^h + e^h$
7. apply an iterative method k_2 times to relax the equation $A^h u^h = f^h$
 with initial solution v^h to obtain a new v^h .

Suppose u^* is the exact solution to approximation e^h of $e.A^h u^h = f^h$. The basic idea here is to first solve the finest grid linear equation $A^h u^h = f^h$ iteratively with an initial guess v^h to obtain a new v^h . Therefore the error of the solution is $e = u^* - v^h$ and the residual error is $r^h = f^h - A^h v^h$. Therefore $u^* = v^h + e$. We also know that $A^h e = f r^h$. Instead to find e on the finest grid, we transfer r^h to r^{2h} and try to approximate $A^{2h} e^{2h} = r^{2h}$ on the coarse grid (recursively). After obtain an approximation e^{2h} , we transfer e^{2h} back to the finer grid to obtain an approximation of e^h . The new approximation to the linear system is then $v^h + e^h$.

V Graph and Geometric Algo- rithms

Chapter 17

Partitioning and Load Balancing

Handling a large mesh or a linear system on a supercomputer or on a workstation cluster usually requires that the data for the problem be somehow partitioned and distributed among the processors. The quality of the partition affects the speed of solution: a good partition divides the work up evenly and requires as little communication as possible. Unstructured meshes may approximate irregular physical problems with fewer mesh elements, their use increases the difficulty of programming and requires new algorithms for partitioning and mapping data and computations onto parallel machines. Partitioning is also important for VLSI circuit layout and parallel circuit simulation.

17.1 Motivation from the Parallel Sparse Matrix Vector Multiplication

Multiplying a sparse matrix by a vector is a basic step of most commonly used iterative methods (conjugate gradient, for example). We want to find a way of efficiently parallelizing this operation.

Say that processor i holds the value of v_i . To update this value, processor need to compute a weighted sum of values at itself and all of its neighbors. This means it has to first receiving values from processors holding values of its neighbors and then computing the sum. Viewing this in graph terms, this corresponds to communicating with a node's nearest neighbors.

We therefore need to break up the vector (and implicitly matrix and graph) so that:

- We balance the computational load at each processor. This is directly related to the number of non-zero entries in its matrix block.
- We minimize the communication overhead. How many other values does a processor have to receive? This equals the number of these values that are held at other processors.

We must come up with a proper division to reduce overhead. This corresponds to dividing up the graph of the matrix among the processors so that there are very few crossing edges. First assume that we have 2 processors, and we wish to partition the graph for parallel processing. As an easy example, take a simplistic cut such as cutting the 2D regular grid of size n in half through the middle. Let's define the cut size as the number of edges whose endpoints are in different groups. A good cut is one with a small cut size. In our example, the cut size would be \sqrt{n} . Assuming that the cost of each communication is 10 times more than an local arithmetic operation. Then the total parallel cost of perform matrix-vector product on the grid is $(4n)/2 + 10\sqrt{n} = 2n + 10\sqrt{n}$. In general, for p processors, to need to partition the graph into p subgraphs.

Various methods are used to break up a graph into parts such that the number of crossing edges is minimized. Here we'll examine the case where $p = 2$ processors, and we want to partition the graph into 2 halves.

17.2 Separators

The following definitions will be of use in the discussion that follows. Let $G = (V, E)$ be an undirected graph.

- A **bisection** of G is a division of V into V_1 and V_2 such that $|V_1| = |V_2|$. (If $|V|$ is odd, then the cardinalities differ by at most 1). The **cost** of the bisection (V_1, V_2) is the number of edges connecting V_1 with V_2 .
- If $\beta \in [1/2, 1)$, a **β -bisection** is a division of V such that $V_{1,2} \leq \beta|V|$.
- An **edge separator** of G is a set of edges that if removed, would break G into 2 pieces with no edges connecting them.
- A **p -way partition** is a division of V into p pieces V_1, V_2, \dots, V_p where the sizes of the various pieces differ by at most 1. The cost of this partition is the total number of edges crossing the pieces.
- A **vertex separator** is a set C of vertices that break G into 3 pieces A , B , and C where no edges connect A and B . We also add the requirement that A and B should be of roughly equal size.

Usually, we use edge partitioning for parallel sparse matrix-vector product and vertex partitioning for the ordering in direct sparse factorization.

17.3 Spectral Partitioning – One way to slice a problem in half

The three steps to illustrate the solution of that problem are:

- Electrical Networks (for motivating the Laplace matrix of a graph)
- Laplacian of a Graph
- Partitioning (that uses the spectral information)

17.3.1 Electrical Networks

As an example we choose a certain configuration of resistors (1 ohm), which are combined as shown in fig. 17.1. A battery is connected to the nodes 3 and 4. It provides the voltage V_B . To obtain the current, we have to calculate the effective resistance of the configuration

$$I = \frac{V_B}{\text{eff. res.}}. \quad (17.1)$$

This so called *Graph* is by definition a *collection of nodes and edges*.

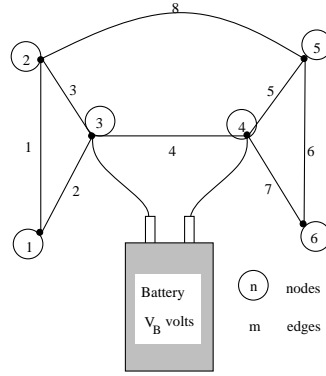


Figure 17.1: Resistor network with nodes and edges

17.3.2 Laplacian of a Graph

Kirchoff's Law tells us

$$\begin{pmatrix} 2 & -1 & -1 & & & \\ -1 & 3 & -1 & & -1 & \\ -1 & -1 & 3 & -1 & & \\ & & -1 & 3 & -1 & -1 \\ & -1 & & -1 & 3 & -1 \\ & & & -1 & -1 & 2 \end{pmatrix} \begin{pmatrix} V_1 \\ V_2 \\ V_3 \\ V_4 \\ V_5 \\ V_6 \end{pmatrix} = \begin{pmatrix} 0 \\ 0 \\ 1 \\ -1 \\ 0 \\ 0 \end{pmatrix} \tag{17.2}$$

The matrix contains the information of how the resistors are connected, it is called the *Laplacian of the Graph*

$$\nabla_G^2 = n \times n \text{ matrix, } \begin{matrix} G \dots \text{graph} \\ n \dots \text{nodes} \\ m \dots \text{edges} \end{matrix} \tag{17.3}$$

$$(\nabla_G^2)_{ii} = \text{degree of node } i \tag{17.4}$$

$$(\nabla_G^2)_{ij} = \begin{cases} 0 & \text{if } \nexists \text{ edge between node } i \text{ and node } j \\ -1 & \text{if } \exists \text{ edge between node } i \text{ and node } j \end{cases} \tag{17.5}$$

Yet there is another way to obtain the Laplacian. First we have to set up the so called *Node-edge Incidence matrix*, which is a $m \times n$ matrix and its elements are either 1, -1 or 0 depending on whether the edge (row of the matrix) connects the node (column of matrix) or not. We find

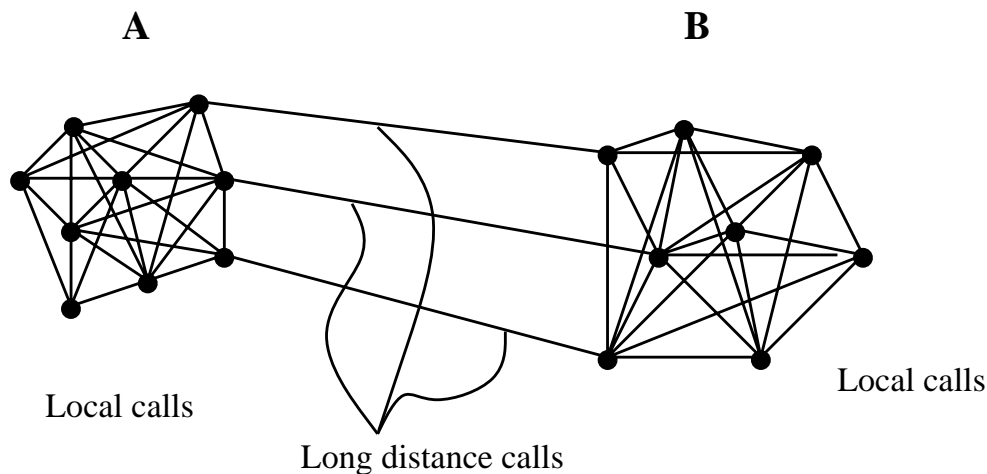


Figure 17.2: Partitioning of a telephone net as an example for a graph comparable in cost

$$\begin{array}{r}
 \text{edges} \\
 \begin{matrix} 1 \\ 2 \\ 3 \\ 4 \\ 5 \\ 6 \\ 7 \\ 8 \end{matrix}
 \end{array}
 \begin{pmatrix}
 & 1 & 2 & 3 & 4 & 5 & 6 \\
 1 & 1 & -1 & & & & \\
 2 & & 1 & -1 & & & \\
 3 & & & 1 & -1 & & \\
 4 & & & & 1 & -1 & \\
 5 & & & & & 1 & -1 \\
 6 & & & & & & 1 & -1 \\
 7 & & & & & & & 1 & -1 \\
 8 & & & & & & & & 1 & -1
 \end{pmatrix}
 \tag{17.6}$$

$$\mathbf{M}_G^T \mathbf{M}_G = \nabla_G^2 \tag{17.7}$$

17.3.3 Spectral Partitioning

Partitioning means that we would like to break the problem into 2 parts A and B, whereas the number of connections between both parts are to be as small as possible (because they are the most expensive ones), see fig. 17.2. Now we define a vector $\mathbf{x} \in \mathcal{R}^n$ having the values $x_i = \pm 1$. +1 stands for *belongs to part A*, -1 means *belongs to part B*. With use of some vector calculus we can show the following identity

$$\sum_{i=1}^n (\mathbf{M}_G \mathbf{x})_i^2 = (\mathbf{M}_G \mathbf{x})^T (\mathbf{M}_G \mathbf{x}) = \mathbf{x}^T \mathbf{M}_G^T \mathbf{M}_G \mathbf{x} = \mathbf{x}^T \nabla_G^2 \mathbf{x} \tag{17.8}$$

$$\mathbf{x}^T \nabla_G^2 \mathbf{x} = 4 \times (\# \text{ edges between A and B}).$$

In order to find the vector \mathbf{x} with the least connections between part A and B, we want to solve the minimization problem:

$$\left. \begin{array}{l} \text{Min. } \mathbf{x}^T \nabla_G^2 \mathbf{x} \\ x_i = \pm 1 \\ \sum x_i = 0 \end{array} \right\} \geq \left\{ \begin{array}{l} \text{Min. } \mathbf{x}^T \nabla_G^2 \mathbf{x} \\ x_i \in \mathcal{R}^n \\ \sum x_i^2 = n \\ \sum x_i = 0 \end{array} \right. \tag{17.9}$$

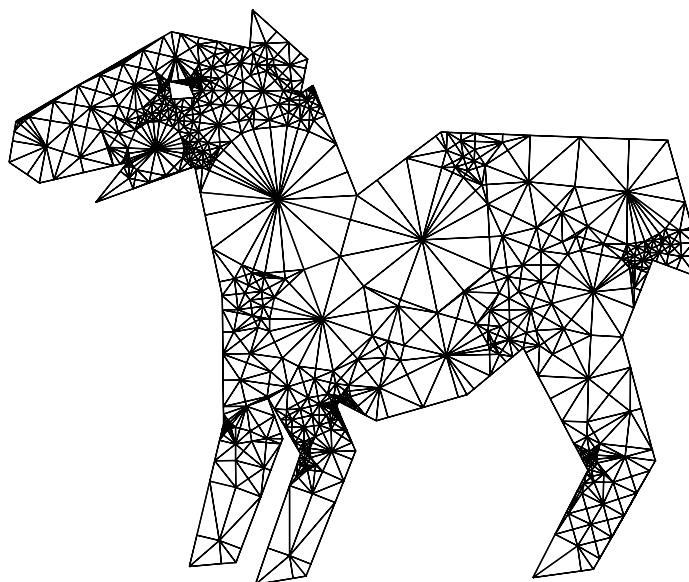


Figure 17.3: Tapir (Bern-Mitchell-Ruppert)

Finding an optimal ± 1 solution is intractable (NP-hard) in general. In practice, we relax the integer condition and allow the solution to be real. We do require the norm square of the solution, like the integer case, equal to n (see RHS of eqn. (17.9)). The relaxation enlarges the solution space, hence its optimal solution is no more than that of its integer counterpart. As an heuristic, we solve the relaxed version of the problem and “round” the solution to give an ± 1 solution.

The solution of the problem on the RHS of eqn. (17.9) gives us the second smallest eigenvalue of the Laplacian ∇_G^2 and the corresponding eigenvector, which is in fact the vector \mathbf{x} with the least connections in the relaxation sense. To obtain a partition of the graph, we can divide its node set according to the vector x . We can even control the ratio of the partition. For example to obtain a bisection, i.e., a partition of each size, we can find the median of x and put those nodes whose x values is smaller than the median on one side and the remaining on the other side. We can also use the similar idea to divide the graph into two parts in which one is twice as big as the another.

Figure 17.3 shows a mesh together with its spectral partition. For those of you as ignorant as your professors, a tapir is defined by Webster as any of several large inoffensive chiefly nocturnal ungulates (family Tapiridae) of tropical America, Malaya, and Sumatra related to the horses and rhinoceroses. The tapir mesh is generated by a Matlab program written by Scott Mitchell based on a non-obtuse triangulation algorithm of Bern-Mitchell-Ruppert. The partition in the figure is generated by John Gilbert’s spectral program in Matlab.

One has to notice that the above method is merely a heuristic. The algorithm does not come with any performance guarantee. In the worst case, the partition may be far from the optimal, partially due to the round-off effect and partially due the requirement of equal-sized partition. In fact the partition for the tapir graph is not quite optimal. Nevertheless, the spectral method, with the help of various improvements, works very well in practice. We will cover the partitioning problem more systematically later in the semester.

The most commonly used algorithm for finding the second eigenvalue and its eigenvector is the Lanczos algorithm though it makes far better sense to compute singular values rather than eigenvalues. Lanczos is an iterative algorithm that can converge quite quickly.

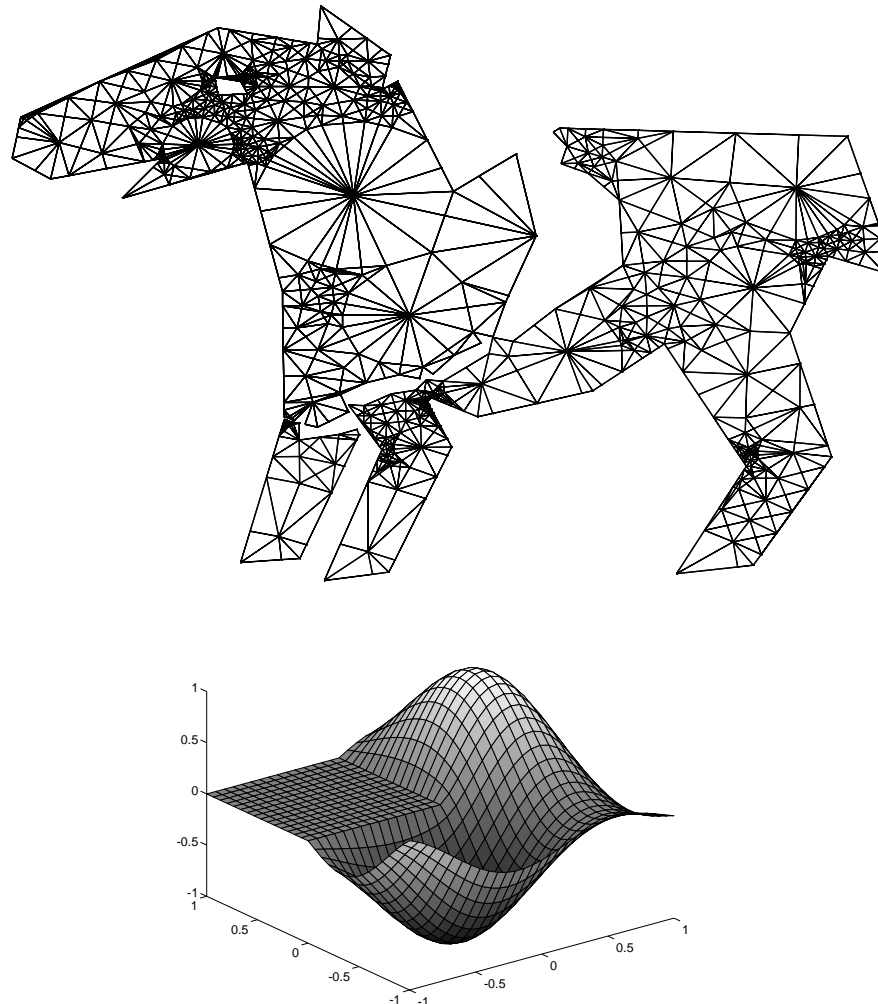


Figure 17.5: The 2nd eigenfunction of MathWork's logo

In general, we may need to divide a graph into more than one piece. The most commonly used approach is to recursively apply the partitioner that divides the graph into two pieces of roughly equal size. More systematic treatment of the partitioning problem will be covered in future lectures.

The success of the spectral method in practice has a physical interpretation. Suppose now we have a continuous domain in place of a graph. The Laplacian of the domain is the continuous counterpart of the Laplacian of a graph. The k th eigenfunction gives the k th mode of vibration and the second eigenfunction induce a cut (break) of the domain along the weakest part of the domain. (See figure17.5)

17.4 Geometric Methods

The geometric method developed by Miller, Teng, Thurston, and Vavasis guarantees to find a partitioning of a d -dimensional unstructured mesh of n of cut size $O(n^{1-1/d})$, a bound which is same as the the cut size for regular grid of the same size. Notice that such a bound does not hold for spectral method in general.

The partition of the graph into two pieces is defined by a circle (that is, a sphere in \mathbb{R}^d). The algorithm chooses the separating circle at random, from a distribution that is carefully constructed

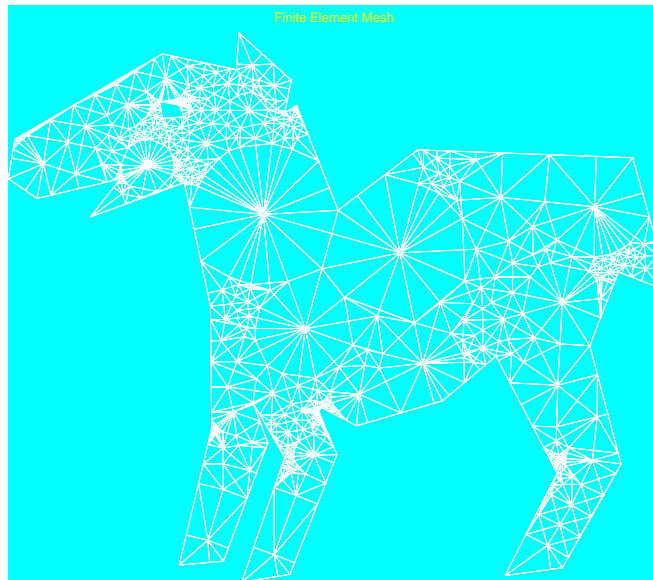


Figure 17.6: The input is a mesh with specified coordinates. Every triangle must be "well-shaped", which means that no angle can be too small. **Remarks:** The mesh is a subgraph of the intersection graph of a set of disks, one centered at each mesh point. Because the triangles are well-shaped, only a bounded number of disks can overlap any point, and the mesh is an "alpha-overlap graph". This implies that it has a good separator, which we proceed to find.

so that the separator will satisfy the $O(n^{1-1/d})$ bound with high probability. The distribution is described in terms of a stereographic projection and conformal mapping on the surface of a sphere of one dimension higher, in \mathbb{R}^{d+1} . To motivate the software development aspect of this approach, we use the following figures (Figures 17.6 – 17.13) generated by a Matlab implementation (written by Gilbert and Teng) to outline the steps for dividing a well-shaped mesh into two pieces. The algorithm works on meshes in any dimension, but we'll stick to two dimensions for the purpose of visualization.

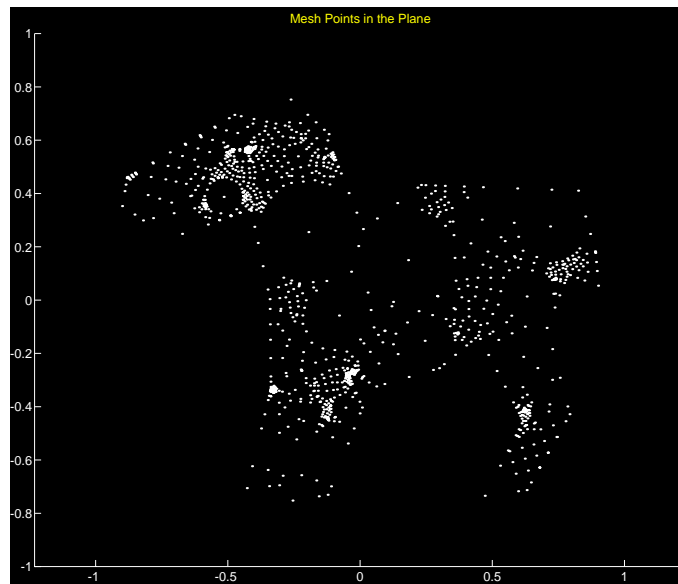


Figure 17.7: Let's redraw the mesh, omitting the edges for clarity.

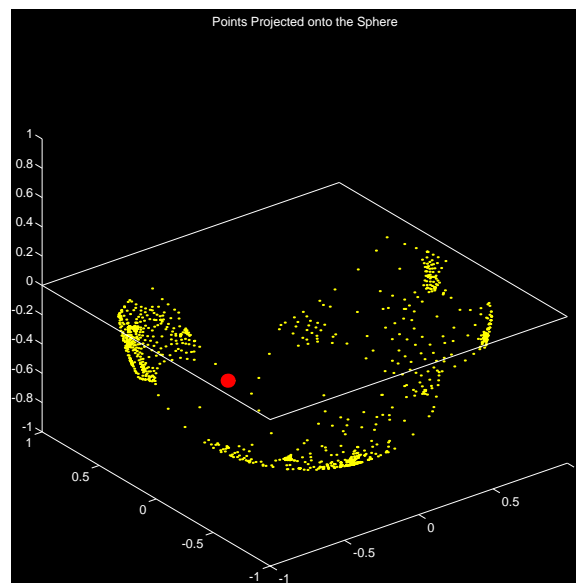


Figure 17.8: First we project the points stereographically from the plane onto a sphere (of one higher dimension than the mesh); Now we compute a "centerpoint" for the projected points in 3-space. Every plane through the centerpoint separates the input points into two roughly equal subsets. (Actually it's too expensive to compute a real centerpoint, so we use a fast, randomized heuristic to find a pretty good approximation.)

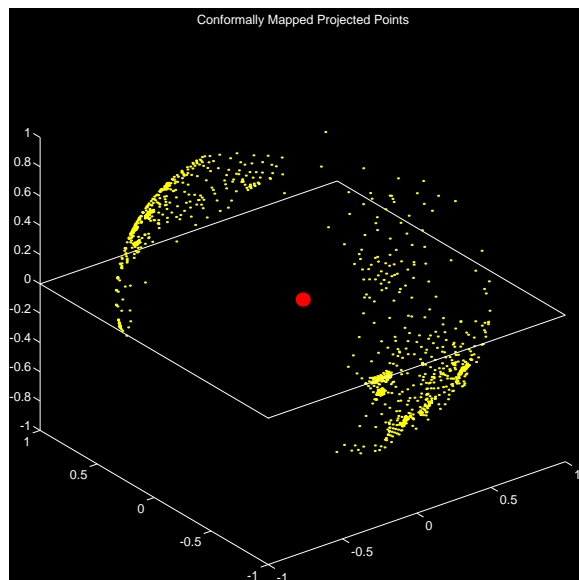


Figure 17.9: Next, we conformally map the points so that the centerpoint maps to the center of the sphere. This takes two steps: First we reflect the points on the sphere so the centerpoint is on the z axis, and then we scale the points in the plane to move the centerpoint along the z axis to the origin. The figures show the final result on the sphere and in the plane.

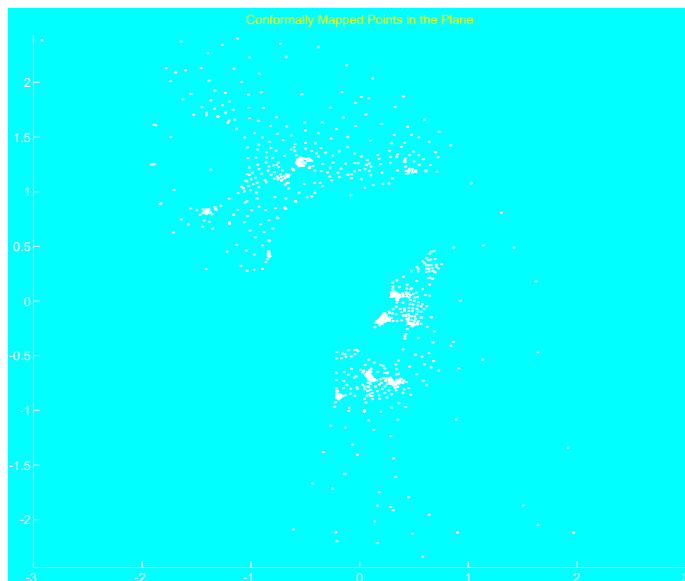


Figure 17.10: Any plane through the origin divides the points roughly evenly. Also, most planes only cut a small number of mesh edges ($O(\sqrt{n})$, to be precise). Thus we find a separator by choosing a plane through the origin, which induces a great circle on the sphere. We shift the circle slightly to make the split exactly even. The second circle is the shifted version.

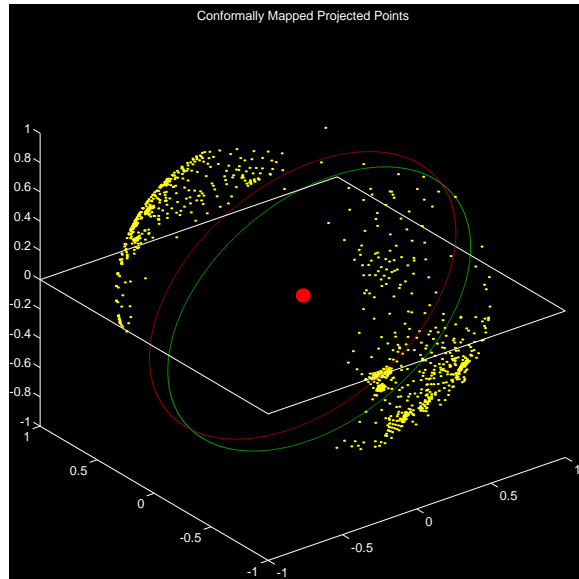


Figure 17.11: To translate this into a separator for the mesh, we first undo the conformal mapping, giving a (non-great) circle on the original sphere ...

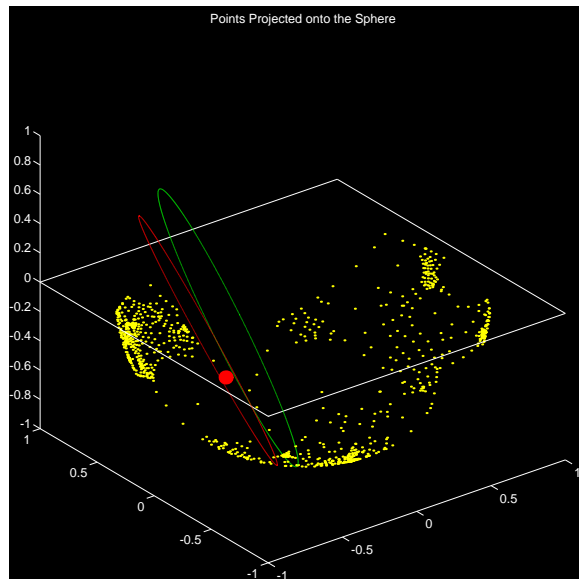


Figure 17.12: ... and then undo the stereographic projection, giving a circle in the original plane.

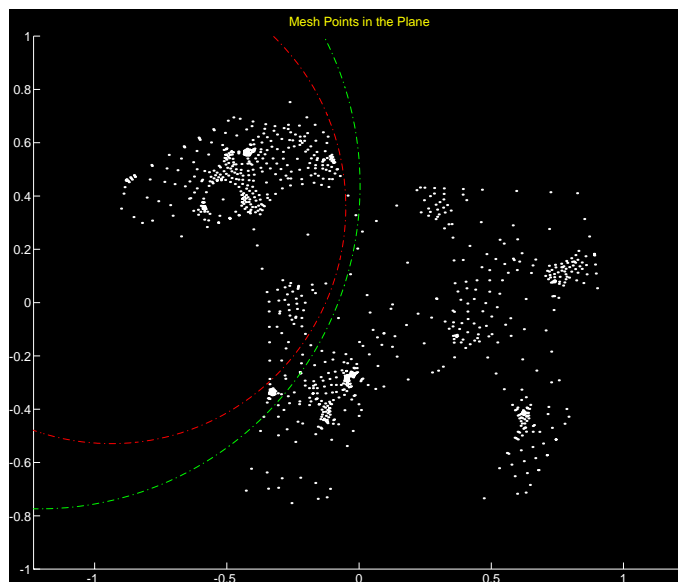


Figure 17.13: This partitions the mesh into two pieces with about $n/2$ points each, connected by at most $O(\sqrt{n})$ edges. These connecting edges are called an "edge separator".

17.4.1 Geometric Graphs

This method applies to meshes in both two and three dimensions. It is based on the following important observation: graphs from large-scale problems in scientific computing are often defined geometrically. They are meshes of elements in a fixed dimension (typically two and three dimensions), that are *well shaped* in some sense, such as having elements of bounded aspect ratio or having elements with angles that are not too small. In other words, they are graphs embedded in two or three dimensions that come with natural geometric coordinates and with structures.

We now consider the types of graphs we expect to run these algorithms on. We don't expect to get a truly random graph. In fact, Erdős, Graham, and Szemerédi proved in the 1960s that with probability = 1, a random graph with cn edges does not have a two-way division with $o(n)$ crossing edges.

Structured graphs usually have divisions with \sqrt{n} crossing edges. The following classes of graphs usually arise in applications such as finite element and finite difference methods (see Chapter ??):

- **Regular Grids:** These arise, for example, from finite difference methods.
- **'Quad'-tree graphs and "Meshes":** These arise, for example, from finite difference methods and hierarchical N-body simulation.
- **k -nearest neighbour graphs in d dimensions** Consider a set $P = \{p_1, p_2, \dots, p_n\}$ of n points in \mathbb{R}^d . The vertex set for the graph is $\{1, 2, \dots, n\}$ and the edge set is $\{(i, j) : p_j \text{ is one of the } k\text{-nearest neighbours of } p_i \text{ or vice-versa}\}$. This is an important class of graphs for image processing.
- **Disk packing graphs:** If a set of non-overlapping disks is laid out in a plane, we can tell which disks are touch. The nodes of a disk packing graph are the centers of the disks, and edges connect two nodes if their respective disks touch:

- **Planar graphs:** These are graphs that can be drawn in a plane without having crossing edges. Note that disk packing graphs are planar, and in fact every planar graph is isomorphic to some disk-packing graph (Andreev and Thurston).

17.4.2 Geometric Partitioning: Algorithm and Geometric Modeling

The main ingredient of the geometric approach is a novel geometrical characterization of graphs embedded in a fixed dimension that have a small *separator*, which is a relatively small subset of vertices whose removal divides the rest of the graph into two pieces of approximately equal size. By taking advantage of the underlying geometric structure, partitioning can be performed efficiently.

Computational meshes are often composed of elements that are *well-shaped* in some sense, such as having bounded aspect ratio or having angles that are not too small or too large. Miller et al. define a class of so-called *overlap graphs* to model this kind of geometric constraint.

An overlap graph starts with a *neighborhood system*, which is a set of closed disks in d -dimensional Euclidean space and a parameter k that restricts how deeply they can intersect.

Definition 17.4.1 *A k -ply neighborhood system in d dimensions is a set $\{D_1, \dots, D_n\}$ of closed disks in \mathbb{R}^d , such that no point in \mathbb{R}^d is strictly interior to more than k of the disks.*

A neighborhood system and another parameter α define an overlap graph. There is a vertex for each disk. For $\alpha = 1$, an edge joins two vertices whose disks intersect. For $\alpha > 1$, an edge joins two vertices if expanding the smaller of their two disks by a factor of α would make them intersect.

Definition 17.4.2 *Let $\alpha \geq 1$, and let $\{D_1, \dots, D_n\}$ be a k -ply neighborhood system. The (α, k) -overlap graph for the neighborhood system is the graph with vertex set $\{1, \dots, n\}$ and edge set*

$$\{(i, j) \mid (D_i \cap (\alpha \cdot D_j) \neq \emptyset) \text{ and } ((\alpha \cdot D_i) \cap D_j \neq \emptyset)\}.$$

We make an overlap graph into a mesh in d -space by locating each vertex at the center of its disk.

Overlap graphs are good models of computational meshes because every mesh of bounded-aspect-ratio elements in two or three dimensions is contained in some overlap graph (for suitable choices of the parameters α and k). Also, every planar graph is an overlap graph. Therefore, any theorem about partitioning overlap graphs implies a theorem about partitioning meshes of bounded aspect ratio and planar graphs.

We now describe the geometric partitioning algorithm.

We start with two preliminary concepts. We let Π denote the *stereographic projection* mapping from \mathbb{R}^d to S^d , where S^d is the unit d -sphere embedded in \mathbb{R}^{d+1} . Geometrically, this map may be defined as follows. Given $\mathbf{x} \in \mathbb{R}^d$, append ‘0’ as the final coordinate yielding $\mathbf{x}' \in \mathbb{R}^{d+1}$. Then compute the intersection of S^d with the line in \mathbb{R}^{d+1} passing through \mathbf{x}' and $(0, 0, \dots, 0, 1)^T$. This intersection point is $\Pi(\mathbf{x})$.

Algebraically, the mapping is defined as

$$\Pi(\mathbf{x}) = \begin{pmatrix} 2\mathbf{x}/\chi \\ 1 - 2/\chi \end{pmatrix}$$

where $\chi = \mathbf{x}^T \mathbf{x} + 1$. It is also simple to write down a formula for the inverse of Π . Let \mathbf{u} be a point on S^d . Then

$$\Pi^{-1}(\mathbf{u}) = \frac{\bar{\mathbf{u}}}{1 - u_{d+1}}$$

where $\bar{\mathbf{u}}$ denotes the first d entries of \mathbf{u} and u_{d+1} is the last entry. The stereographic mapping, besides being easy to compute, has a number of important properties proved below.

A second crucial concept for our algorithm is the notion of a *center point*. Given a finite subset $P \subset \mathbb{R}^d$ such that $|P| = n$, a *center point* of P is defined to be a point $\mathbf{x} \in \mathbb{R}^d$ such that if H is any open halfspace whose boundary contains \mathbf{x} , then

$$|P \cap H| \leq dn/(d+1). \quad (17.10)$$

It can be shown from Helly's theorem [24] that a center point always exists. Note that center points are quite different from centroids. For example, a center point (which, in the $d = 1$ case, is the same as a median) is largely insensitive to "outliers" in P . On the hand, a single distant outlier can cause the centroid of P to be displaced by an arbitrarily large distance.

Geometric Partitioning Algorithm

Let $P = \{\mathbf{p}_1, \dots, \mathbf{p}_n\}$ be the input points in \mathbb{R}^d that define the overlap graph.

1. Given $\mathbf{p}_1, \dots, \mathbf{p}_n$, compute $P' = \{\Pi(\mathbf{p}_1), \dots, \Pi(\mathbf{p}_n)\}$ so that $P' \subset S^d$.
2. Compute a center point \mathbf{z} of P' .
3. Compute an orthogonal $(d+1) \times (d+1)$ matrix Q such that $Q\mathbf{z} = \mathbf{z}'$ where

$$\mathbf{z}' = \begin{pmatrix} 0 \\ \vdots \\ 0 \\ \theta \end{pmatrix}$$

such that θ is a scalar.

4. Define $P'' = QP'$ (i.e., apply Q to each point in P'). Note that $P'' \subset S^d$, and the center point of P'' is \mathbf{z}' .
5. Let D be the matrix $[(1-\theta)/(1+\theta)]^{1/2}I$, where I is the $d \times d$ identity matrix. Let $P''' = \Pi(D\Pi^{-1}(P''))$. Below we show that the origin is a center point of P''' .
6. Choose a random great circle S_0 on S^d .
7. Transform S_0 back to a sphere $S \subset \mathbb{R}^d$ by reversing all the transformations above, i.e., $S = \Pi^{-1}(Q^{-1}\Pi(D^{-1}\Pi^{-1}(S_0)))$.
8. From S compute a set of vertices of G that split the graph as in Theorem ???. In particular, define C to be vertices embedded "near" S , define A be vertices of $G - C$ embedded outside S , and define B to be vertices of $G - C$ embedded inside S .

We can immediately make the following observation: because the origin is a center point of P''' , and the points are split by choosing a plane through the origin, then we know that $|A| \leq (d+1)n/(d+2)$ and $|B| \leq (d+1)n/(d+2)$ regardless of the details of how C is chosen. (Notice that the constant factor is $(d+1)/(d+2)$ rather than $d/(d+1)$ because the point set P' lies in \mathbb{R}^{d+1} rather than \mathbb{R}^d .) Thus, one of the claims made in Theorem ??? will follow as soon as we have shown that the origin is indeed a center point of P''' at the end of this section.

We now provide additional details about the steps of the algorithm, and also its complexity analysis. We have already defined stereographic projection used Step 1. Step 1 requires $O(nd)$ operations.

Computing a true center point in Step 2 appears to a very expensive operation (involving a linear programming problem with n^d constraints) but by using random (geometric) sampling, an approximate center point can be found in random constant time (independent of n but exponential in d) [91, 45]. An *approximate* center point satisfies 17.10 except with $(d + 1 + \epsilon)n/(d + 2)$ on the right-hand side, where $\epsilon > 0$ may be arbitrarily small. Alternatively, a deterministic linear-time sampling algorithm can be used in place of random sampling [61, 90], but one must again compute a center of the sample using linear programming in time exponential in d [63, 39].

In Step 3, the necessary orthogonal matrix may be represented as a single Householder reflection—see [40] for an explanation of how to pick an orthogonal matrix to zero out all but one entry in a vector. The number of floating point operations involved is $O(d)$ independent of n .

In Step 4 we do not actually need to compute P'' ; the set P'' is defined only for the purpose of analysis. Thus, Step 4 does not involve computation. Note that the \mathbf{z}' is the center point of P'' after this transformation, because when a set of points is transformed by any orthogonal transformation, a center point moves according to the same transformation (more generally, center points are similarly moved under any affine transformation). This is proved below.

In Step 6 we choose a random great circle, which requires time $O(d)$. This is equivalent to choosing plane through the origin with a randomly selected orientation. (This step of the algorithm can be made deterministic; see [?].) Step 7 is also seen to require time $O(d)$.

Finally, there are two possible alternatives for carrying out Step 8. One alternative is that we are provided with the neighborhood system of the points (i.e., a list of n balls in \mathbb{R}^d) as part of the input. In this case Step 8 requires $O(nd)$ operations, and the test to determine which points belong in A , B or C is a simple geometric test involving S . Another possibility is that we are provided with the nodes of the graph and a list of edges. In this case we determine which nodes belong in A , B , or C based on scanning the adjacency list of each node, which requires time linear in the size of the graph.

Theorem 17.4.1 *If M is an unstructured mesh with bounded aspect ratio, then the graph of M is a subgraph of a bounded overlap graph of the neighborhood system where we have one ball for each vertex of M of radius equal to half of the distance to its nearest vertices. Clearly, this neighborhood system has ply equal to 1.*

Theorem 17.4.1 (Geometric Separators [63]) *Let G be an n -vertex (α, k) -overlap graph in d dimensions. Then the vertices of G can be partitioned into three sets A , B , and C , such that*

- *no edge joins A and B ,*
- *A and B each have at most $(d + 1)/(d + 2)$ vertices,*
- *C has only $O(\alpha k^{1/d} n^{(d-1)/d})$ vertices.*

Such a partitioning can be computed by the geometric-partitioning-algorithm in randomized linear time sequentially, and in $O(n/p)$ parallel time when we use a parallel machine of p processors.

17.4.3 Other Graphs with small separators

The following classes of graphs all have small separators:

- Lines have edge-separators of size 1. Removing the middle edge is enough.
- Trees have a 1-vertex separator with $\beta = 2/3$ - the so-called centroid of the tree.

- Planar Graphs. A result of Lipton and Tarjan shows that a planar graph of bounded degree has a $\sqrt{8n}$ vertex separator with $\beta = 2/3$.
- d dimensional regular grids (those are used for basic finite difference method). As a folklore, they have a separator of size $n^{1-1/d}$ with beta $\beta = 1/2$.

17.4.4 Other Geometric Methods

Recursive coordinate bisection

The simplest form of geometric partitioning is recursive coordinate bisection (RCB) [86, 92]. In the RCB algorithm, the vertices of the graph are projected onto one of the coordinate axes, and the vertex set is partitioned around a hyperplane through the median of the projected coordinates. Each resulting subgraph is then partitioned along a different coordinate axis until the desired number of subgraphs is obtained.

Because of the simplicity of the algorithm, RCB is very quick and cheap, but the quality of the resultant separators can vary dramatically, depending on the embedding of the graph in \mathbb{R}^d . For example, consider a graph that is “+”-shaped. Clearly, the best (smallest) separator consists of the vertices lying along a diagonal cut through the center of the graph. RCB, however, will find the largest possible separators, in this case, planar cuts through the centers of the horizontal and vertical components of the graph.

Inertia-based slicing

Williams [92] noted that RCB had poor worst case performance, and suggested that it could be improved by slicing orthogonal to the principal axes of inertia, rather than orthogonal to the coordinate axes. Farhat and Lesoinne implemented and evaluated this heuristic for partitioning [31].

In three dimensions, let $v = (v_x, v_y, v_z)^t$ be the coordinates of vertex v in \mathbb{R}^3 . Then the inertia matrix I of the vertices of a graph with respect to the origin is given by

$$I = \begin{pmatrix} I_{xx} & I_{xy} & I_{xz} \\ I_{yx} & I_{yy} & I_{yz} \\ I_{zx} & I_{zy} & I_{zz} \end{pmatrix}$$

where,

$$I_{xx} = \sum_{v \in V} v_y^2 + v_z^2, \quad I_{yy} = \sum_{v \in V} v_x^2 + v_z^2, \quad I_{zz} = \sum_{v \in V} v_x^2 + v_y^2$$

and, for $i, j \in \{x, y, z\}, i \neq j$,

$$I_{ij} = I_{ji} = - \sum_{v \in V} v_i v_j$$

The eigenvectors of the inertia matrix are the principal axes of the vertex distribution. The eigenvalues of the inertia matrix are the principal moments of inertia. Together, the principal axes and principal moments of inertia define the inertia ellipse; the axes of the ellipse are the principal axes of inertia, and the axis lengths are the square roots of the corresponding principal moments. Physically, the size of the principal moments reflect how the mass of the system is distributed with respect to the corresponding axis - the larger the principal moment, the more mass is concentrated at a distance from the axis.

Let I_1 , I_2 , and I_3 denote the principal axes of inertia corresponding to the principal moments $\alpha_1 \leq \alpha_2 \leq \alpha_3$. Farhat and Lesoinne projected the vertex coordinates onto I_1 , the axis about which the mass of the system is most tightly clustered, and partitioned using a planar cut through the median. This method typically yielded a good initial separator, but did not perform as well recursively on their test mesh - a regularly structured “T”-shape.

Farhat and Lesoinne did not present any results on the theoretical properties of the inertia slicing method. In fact, there are pathological cases in which the inertia method can be shown to yield a very poor separator. Consider, for example, a “+”-shape in which the horizontal bar is very wide and sparse, while the vertical bar is relatively narrow but dense. I_1 will be parallel to the horizontal axis, but a cut perpendicular to this axis through the median will yield a very large separator. A diagonal cut will yield the smallest separator, but will not be generated with this method.

Gremban, Miller, and Teng show how to use moment of inertia to improve the geometric partitioning algorithm.

17.4.5 Partitioning Software

- **Chaco** written by Bruce Hendrickson and Rob Leland. To get code send email to bahendr@cs.sandia.gov (Bruce Hendrickson).
- **Matlab Mesh Partitioning Toolbox**: written by Gilbert and Teng. It includes both edge and vertex separators, recursive bipartition, nested dissection ordering, visualizations and demos, and some sample meshes. The complete toolbox is available by anonymous ftp from machine ftp.parc.xerox.com as file /pub/gilbert/meshpart.uu.
- **Spectral code**: Pothen, Simon, and Liou.

17.5 Load-Balancing N-body Simulation for Non-uniform Particles

The discussion of Chapter ?? was focused on particles that are more or less uniformly distributed. However, in practical simulations, particles are usually not uniformly distributed. Particles may be highly clustered in some regions and relatively scattered in some other regions. Thus, the hierarchical tree is adaptively generated, with smaller box for regions of clustered particles. The computation and communication pattern of a hierarchical method becomes more complex and often is not known explicitly in advance.

17.5.1 Hierarchical Methods of Non-uniformly Distributed Particles

In this chapter, we use the following notion of non-uniformity: We say a point set $P = \{\mathbf{p}_1, \dots, \mathbf{p}_n\}$ in d dimensions is μ -non-uniform if the hierarchical tree generated for P has height $\log_{2^d}(n/m) + \mu$. In other words, the ratio of the size of smallest leaf-box to the root-box is $1/2^{\log_{2^d}(n/m) + \mu}$. In practice, μ is less than 100.

The Barnes-Hut algorithm, as an algorithm, can be easily generalized to the non-uniform case. We describe a version of FMM for non-uniformly distributed particles. The method uses the box-box interaction. FMM tries to maximize the number of FLIPs among large boxes and also tries to FLIP between roughly equal sized boxes, a philosophy which can be described as: let parents do as much work as possible and then do the left-over work as much as possible before passing to the next

generation. Let $\mathbf{c}_1, \dots, \mathbf{c}_{2^d}$ be the set of child-boxes of the root-box of the hierarchical tree. FMM generates the set of all *interaction-pairs* of boxes by taking the union of Interaction-pair($\mathbf{c}_i, \mathbf{c}_j$) for all $1 \leq i < j \leq 2^d$, using the Interaction-Pair procedure defined below.

Procedure Interaction-Pair ($\mathbf{b}_1, \mathbf{b}_2$)

- If \mathbf{b}_1 and \mathbf{b}_2 are β -well-separated, then $(\mathbf{b}_1, \mathbf{b}_2)$ is an interaction-pair.
- Else, if both \mathbf{b}_1 and \mathbf{b}_2 are leaf-boxes, then particles in \mathbf{b}_1 and \mathbf{b}_2 are near-field particles.
- Else, if both \mathbf{b}_1 and \mathbf{b}_2 are not leaf-boxes, without loss of generality, assuming that \mathbf{b}_2 is at least as large as \mathbf{b}_1 and letting $\mathbf{c}_1, \dots, \mathbf{c}_{2^d}$ be the child-boxes of \mathbf{b}_2 , then recursively decide interaction pair by calling: Interaction-Pair($\mathbf{b}_1, \mathbf{c}_i$) for all $1 \leq i \leq 2^d$.
- Else, if one of \mathbf{b}_1 and \mathbf{b}_2 is a leaf-box, without loss of generality, assuming that \mathbf{b}_1 is a leaf-box and letting $\mathbf{c}_1, \dots, \mathbf{c}_{2^d}$ be the child-boxes of \mathbf{b}_2 , then recursively decide interaction pairs by calling: Interaction-Pair($\mathbf{b}_1, \mathbf{c}_i$) for all $1 \leq i \leq 2^d$.

FMM for far-field calculation can then be defined as: for each interaction pair $(\mathbf{b}_1, \mathbf{b}_2)$, letting $\Phi_i^p()$ ($i = 1, 2$) be the multipole-expansion of \mathbf{b}_i , flip $\Phi_1^p()$ to \mathbf{b}_2 and add to \mathbf{b}_2 's potential Taylor-expansion. Similarly, flip $\Phi_2^p()$ to \mathbf{b}_1 and add to \mathbf{b}_1 's potential Taylor-expansion. Then traverse down the hierarchical tree in a preordering, shift and add the potential Taylor-expansion of the parent box of a box to its own Taylor-expansion.

Note that FMM for uniformly distributed particles has a more direct description (see Chapter ??).

17.5.2 The Communication Graph for N-Body Simulations

In order to efficiently implement an N-body method on a parallel machine, we need to understand its communication pattern, which can be described by a graph that characterizes the pattern of information exchange during the execution of the method. The communication graph is defined on basic computational elements of the method. The basic elements of hierarchical N-body methods are boxes and points, where points give the locations of particles and boxes are generated by the hierarchical method. Formally, the communication graph is an edge-weighted directed graph, where the edges describe the pattern of communication and the weight on an edge specifies the communication requirement along the edge.

A Refined FMM for Non-Uniform Distributions

For parallel implementation, it is desirable to have a communication graph that uses small edge-weights and has small in- and out-degrees. However, some boxes in the set of interaction-pairs defined in the last section may have large degree!

FMM described in the last subsection has a drawback which can be illustrated by the following 2D example. Suppose the root-box is divided into four child-boxes A, B, C , and D . Assume further that boxes A, B and C contains less than m (< 100) particles, and most particles, say n of them, are uniformly distributed in D , see Figure 17.14. In FMM, we further recursively divide D by $\log_4(n/m)$ levels. Notice that A, B , and C are not well-separated from any box in D . Hence the FMM described in the previous subsection will declare all particles of D as near-field particles of A, B , and C (and vice versa). The drawback is two-folds: (1) From the computation viewpoint, we cannot take advantage of the hierarchical tree of D to evaluate potentials in A, B , and C . (2) From the communication viewpoint, boxes A, B , and C have a large in-degree in the sense that each

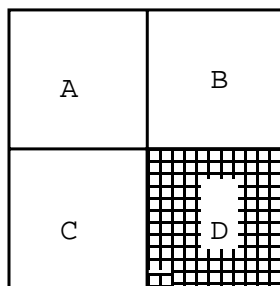


Figure 17.14: A non-uniform example

particle in these boxes need to receive information from all n particles in D , making partitioning and load balancing harder. Notice that in BH most boxes of D are well-separated from particles in A , B , and C . Hence the well-separation condition is different in BH: *because BH uses the particle-box interaction, the well-separation condition is measured with respect to the size of the boxes in D . Thus most boxes are well-separated from particles in A , B , and C . In contrast, because FMM applies the FLIP operation, the well-separation condition must measure up against the size of the larger box. Hence no box in D is well-separated from A , B , and C .*

Our refined FMM circumvents this problem by incorporating the well-separation condition of BH into the Interaction-Pair procedure: if \mathbf{b}_1 and \mathbf{b}_2 are not well-separated, and \mathbf{b}_1 , the larger of the two, is a leaf-box, then we use a well-separation condition with respect to \mathbf{b}_2 , instead of to \mathbf{b}_1 , and apply the FLIP operation directly onto particles in the leaf-box \mathbf{b}_1 rather than \mathbf{b}_1 itself.

We will define this new well-separation condition shortly. First, we make the following observation about the Interaction-Pair procedure defined in the last subsection. We can prove, by a simple induction, the following fact: if \mathbf{b}_1 and \mathbf{b}_2 are an interaction-pair and both \mathbf{b}_1 and \mathbf{b}_2 are not leaf-boxes, then $1/2 \leq \text{size}(\mathbf{b}_1)/\text{size}(\mathbf{b}_2) \leq 2$. This is precisely the condition that FMM would like to maintain. For uniformly distributed particles, such condition is always true between any interaction-pair (even if one of them is a leaf-box). However, for non-uniformly distributed particles, if \mathbf{b}_1 , the larger box, is a leaf-box, then \mathbf{b}_1 could be much larger than \mathbf{b}_2 .

The new β -well-separation condition, when \mathbf{b}_1 is a leaf-box, is then defined as: \mathbf{b}_1 and \mathbf{b}_2 are β -well-separated if \mathbf{b}_2 is well-separated from all particles of \mathbf{b}_1 (as in BH). Notice, however, with the new condition, we can no longer FLIP the multipole expansion of \mathbf{b}_1 to a Taylor-expansion for \mathbf{b}_2 . Because \mathbf{b}_1 has only a constant number of particles, we can directly evaluate the potential induced by these particles for \mathbf{b}_2 . This new condition makes the FLIP operation of this special class of interaction-pairs *uni-directional*: We only FLIP \mathbf{b}_2 to \mathbf{b}_1 .

We can describe the refined Interaction-Pair procedure using modified well-separation condition when one box is a leaf-box.

Procedure Refined Interaction-Pair ($\mathbf{b}_1, \mathbf{b}_2$)

- If \mathbf{b}_1 and \mathbf{b}_2 are β -well-separated and $1/2 \leq \text{size}(\mathbf{b}_1)/\text{size}(\mathbf{b}_2) \leq 2$, then $(\mathbf{b}_1, \mathbf{b}_2)$ is a bi-directional interaction-pair.
- Else, if the larger box, without loss of generality, \mathbf{b}_1 , is a leaf-box, then the well-separation condition becomes: \mathbf{b}_2 is well-separated from all particles of \mathbf{b}_1 . If this condition is true, then $(\mathbf{b}_1, \mathbf{b}_2)$ is a uni-directional interaction-pair from \mathbf{b}_2 to \mathbf{b}_1 .
- Else, if both \mathbf{b}_1 and \mathbf{b}_2 are leaf-boxes, then particles in \mathbf{b}_1 and \mathbf{b}_2 are near-field particles.

- Else, if both \mathbf{b}_1 and \mathbf{b}_2 are not leaf-boxes, without loss of generality, assuming that \mathbf{b}_2 is at least as large as \mathbf{b}_1 and letting $\mathbf{c}_1, \dots, \mathbf{c}_{2^d}$ be the child-boxes of \mathbf{b}_2 , then recursively decide interaction-pairs by calling: Interaction-Pair($\mathbf{b}_1, \mathbf{c}_i$) for all $1 \leq i \leq 2^d$.
- Else, if one of \mathbf{b}_1 and \mathbf{b}_2 is a leaf-box, without loss of generality, assuming that \mathbf{b}_1 is a leaf box and letting $\mathbf{c}_1, \dots, \mathbf{c}_{2^d}$ be the child-boxes of \mathbf{b}_2 , then recursively decide interaction pairs by calling: Interaction-Pair($\mathbf{b}_1, \mathbf{c}_i$) for all $1 \leq i \leq 2^d$.

Let $\mathbf{c}_1, \dots, \mathbf{c}_{2^d}$ be the set of child-boxes of the root-box of the hierarchical tree. Then the set of all interaction-pair can be generated as the union of Refined-Interaction-Pair($\mathbf{c}_i, \mathbf{c}_j$) for all $1 \leq i < j \leq 2^d$.

The refined FMM for far-field calculation can then be defined as: for each bi-directional interaction pair $(\mathbf{b}_1, \mathbf{b}_2)$, letting $\Phi_i^p()$ ($i = 1, 2$) be the multipole expansion of \mathbf{b}_i , flip $\Phi_1^p()$ to \mathbf{b}_2 and add to \mathbf{b}_2 's potential Taylor-expansion. Similarly, flip $\Phi_2^p()$ to \mathbf{b}_1 and add to \mathbf{b}_1 's potential Taylor-expansion. Then traverse down the hierarchical tree in a preordering, shift and add the potential Taylor-expansion of the parent box of a box to its own Taylor-expansion. For each uni-directional interaction pair $(\mathbf{b}_1, \mathbf{b}_2)$ from \mathbf{b}_2 to \mathbf{b}_1 , letting $\Phi_2^p()$ be the multipole-expansion of \mathbf{b}_2 , evaluate $\Phi_2^p()$ directly for each particle in \mathbf{b}_2 and add its potential.

Hierarchical Neighboring Graphs

Hierarchical methods (BH and FMM) explicitly use two graphs: the *hierarchical tree* which connects each box to its parent box and each particle to its leaf-box, and the *near-field graph* which connects each box with its near-field boxes. The hierarchical tree is generated and used in the first step to compute the multipole expansion induced by each box. We can use a bottom-up procedure to compute these multipole expansions: First compute the multipole expansions at leaf-boxes and then *SHIFT* the expansion to the parent boxes and then up the hierarchical tree until multipole-expansions for all boxes in the hierarchical tree are computed.

The near-field graph can also be generated by the Refined-Interaction-Pair procedure. In Section 17.5.3, we will formally define the near-field graph.

Fast-Multipole Graphs (FM)

The Fast-Multipole graph, FM^β , models the communication pattern of the refined FMM. It is a graph defined on the set of boxes and particles in the hierarchical tree. Two boxes \mathbf{b}_1 and \mathbf{b}_2 are connected in FM^β iff (1) \mathbf{b}_1 is the parent box of \mathbf{b}_2 , or vice versa, in the hierarchical tree; or (2) $(\mathbf{b}_1, \mathbf{b}_2)$ is an interaction-pair generated by Refined-Interaction-Pair defined in Section 17.5.2. The edge is bi-directional for a bi-directional interaction-pair and uni-directional for a uni-directional interaction-pair. Furthermore, each particle is connected with the box that contains the particle.

The following Lemma that will be useful in the next section.

Lemma 17.5.1 *The refined FMM flips the multipole expansion of \mathbf{b}_2 to \mathbf{b}_1 if and only if (1) \mathbf{b}_2 is well-separated from \mathbf{b}_1 and (2) neither the parent of \mathbf{b}_2 is well-separated from \mathbf{b}_1 nor \mathbf{b}_2 is well-separated from the parent of \mathbf{b}_1 .*

It can be shown that both in- and out-degrees of FM^β are small.

Barnes-Hut Graphs (BH)

BH defines two classes of communication graphs: BH_S^β and BH_P^β . BH_S^β models the sequential communication pattern and BH_P^β is more suitable for parallel implementation. The letters S and P , in BH_S^β and BH_P^β , respectively, stand for “Sequential” and “Parallel”.

We first define BH_S^β and show why parallel computing requires a different communication graph BH_P^β to reduce total communication cost.

The graph BH_S^β of a set of particles P contains two sets of vertices: P , the particles, and B , the set of boxes in the hierarchical tree. The edge set of the graph BH_S^β is defined by the communication pattern of the sequential BH. A particle \mathbf{p} is connected with a box \mathbf{b} if in BH, we need to evaluate \mathbf{p} against \mathbf{b} to compute the force or potential exerted on \mathbf{p} . So the edge is directed from \mathbf{b} to \mathbf{p} . Notice that if \mathbf{p} is connected with \mathbf{b} , then \mathbf{b} must be well-separated from \mathbf{p} . Moreover, the parent of \mathbf{b} is not well-separated from \mathbf{p} . Therefore, if \mathbf{p} is connected with \mathbf{b} in BH_S^β , then \mathbf{p} is not connected to any box in the subtree of \mathbf{b} nor to any ancestor of \mathbf{b} .

In addition, each box is connected directly with its parent box in the hierarchical tree and each point \mathbf{p} is connected its leaf-box. Both types of edges are bi-directional.

Lemma 17.5.2 *Each particle is connected to at most $O(\log n + \mu)$ number of boxes. So the in-degree of BH_S^β is bounded by $O(\log n + \mu)$.*

Notice, however, BH_S^β is not suitable for parallel implementation. It has a large out-degree. This major drawback can be illustrated by the example of n uniformly distributed particles in two dimensions. Assume we have four processors. Then the “best” way to partition the problem is to divide the root-box into four boxes and map each box onto a processor. Notice that in the direct parallel implementation of BH, as modeled by BH_S^β , each particle needs to access the information of at least one boxes in each of the other processors. Because each processor has $n/4$ particles, the total communication overhead is $\Omega(n)$, which is very expensive.

The main problem with BH_S^β is that many particles from a processor need to access the information of the same box in some other processors (which contributes to the large out-degree). We show that a combination technique can be used to reduce the out-degree. The idea is to *combine* the “same” information from a box and send the information as one unit to another box on a processor that needs the information. We will show that this combination technique reduces the total communication cost to $O(\sqrt{n \log n})$ for the four processor example, and to $O(\sqrt{pn \log n})$ for p processors. Similarly, in three dimensions, the combination technique reduces the volume of messages from $\Omega(n \log n)$ to $O(p^{1/3} n^{2/3} (\log n)^{1/3})$.

We can define a graph BH_P^β to model the communication and computation pattern that uses this combination technique. Our definition of BH_P^β is inspired by the communication pattern of the refined FMM. It can be shown that the communication pattern of the refined FMM can be used to guide the message combination for the parallel implementation of the Barnes-Hut method!

The combination technique is based on the following observation: Suppose \mathbf{p} is well-separated from \mathbf{b}_1 but not from the parent of \mathbf{b}_1 . Let \mathbf{b} be the largest box that contains \mathbf{p} such that \mathbf{b} is well-separated from \mathbf{b}_1 , using the well-separation definition in Section 17.5.2. If \mathbf{b} is not a leaf-box, then $(\mathbf{b}, \mathbf{b}_1)$ is a bi-directional interaction-pair in the refined FMM. If \mathbf{b} is a leaf-box, then $(\mathbf{b}, \mathbf{b}_1)$ is a uni-directional interaction-pair from \mathbf{b}_1 to \mathbf{b} . Hence $(\mathbf{b}, \mathbf{b}_1)$ is an edge of FM^β . Then, any other particle \mathbf{q} contained in \mathbf{b} is well-separated from \mathbf{b}_1 as well. Hence we can combine the information from \mathbf{b}_1 to \mathbf{p} and \mathbf{q} and all other particles in \mathbf{b} as follows: \mathbf{b}_1 sends its information (just one copy) to \mathbf{b} and \mathbf{b} forwards the information down the hierarchical tree, to both \mathbf{p} and \mathbf{q} and all other particles

in \mathbf{b} . This combination-based-communication scheme defines a new communication graph BH_P^β for parallel BH: The nodes of the graph are the union of particles and boxes, i.e., $P \cup B(P)$. Each particle is connected to the leaf-box it belongs to. Two boxes are connected iff they are connected in the Fast-Multipole graph. However, to model the communication cost, we must introduce a weight on each edge along the hierarchical tree embedded in BH_P^β , to be equal to the number of data units needed to be sent along that edge.

Lemma 17.5.3 *The weight on each edge in BH_P^β is at most $O(\log n + \mu)$.*

It is worthwhile to point out the difference between the comparison and communication patterns in BH. In the sequential version of BH, if \mathbf{p} is connected with \mathbf{b} , then we have to compare \mathbf{p} against all ancestors of \mathbf{b} in the computation. The procedure is to first compare \mathbf{p} with the root of the hierarchical tree, and then recursively move the comparison down the tree: if the current box compared is not well-separated from \mathbf{p} , then we will compare \mathbf{p} against all its child-boxes. However, in terms of force and potential calculation, we only evaluate a particle against the first box down a path that is well-separated from the particle. The graphs BH_S^β and BH_P^β capture the communication pattern, rather than the comparison pattern. The communication is more essential to force or potential calculation. The construction of the communication graph has been one of the bottlenecks in load balancing BH and FMM on a parallel machine.

17.5.3 Near-Field Graphs

The near-field graph is defined over all leaf-boxes. A leaf-box \mathbf{b}_1 is a *near-field neighbor* of a leaf-box \mathbf{b} if \mathbf{b}_1 is not well-separated from some particles of \mathbf{b} . Thus, FMM and BH directly compute the potential at particles in \mathbf{b} induced by particles of \mathbf{b}_1 .

There are two basic cases: (1) if $size(\mathbf{b}_1) \leq size(\mathbf{b})$, then we call \mathbf{b}_1 a *geometric near-field neighbor* of \mathbf{b} . (2) if $size(\mathbf{b}_1) > size(\mathbf{b})$, then we call \mathbf{b}_1 a *hierarchical near-field neighbor* of \mathbf{b} . In the example of Section 17.5.2, A, B, C are hierarchical near-field neighbors of all leaf-boxes in D ; while A, B , and C have some geometric near-field neighbors in D .

We introduce some notations. The *geometric in-degree* of a box \mathbf{b} is the number of its geometric near-field neighbors. The *geometric out-degree* of a box \mathbf{b} is the number of boxes to which \mathbf{b} is the geometric near-field neighbors. The *hierarchical in-degree* of a box \mathbf{b} is the number of its hierarchical near-field neighbors. We will define the *hierarchical out-degree* of a box shortly.

It can be shown that the geometric in-degree, geometric out-degree, and hierarchical in-degree are small. However, in the example of Section 17.5.2, A, B , and C are hierarchical near-field neighbors for all leaf-boxes in D . Hence the number of leaf-boxes to which a box is a hierarchical near-field neighbor could be very large. So the near-field graph defined above can have a very large out-degree.

We can use the combination technique to reduce the degree when a box \mathbf{b} is a hierarchical near-field neighbor of a box \mathbf{b}_1 . Let \mathbf{b}_2 be the ancestor of \mathbf{b}_1 of the same size as \mathbf{b} . Instead of \mathbf{b} sending its information directly to \mathbf{b}_1 , \mathbf{b} sends it to \mathbf{b}_2 and \mathbf{b}_2 then forwards the information down the hierarchical tree. Notice that \mathbf{b} and \mathbf{b}_2 are not well-separated. We will refer to this modified near-field graph as the near-field graph, denoted by NF^β . We also define the *hierarchical out-degree* of a box \mathbf{b} to be the number of edges from \mathbf{b} to the set of non-leaf-boxes constructed above. We can show that the *hierarchical out-degree* is also small.

To model the near-field communication, similar to our approach for BH, we introduce a weight on the edges of the hierarchical tree.

Lemma 17.5.4 *The weight on each edge in NF^β is at most $O(\log n + \mu)$.*

17.5.4 N-body Communication Graphs

By abusing notations, let $FM^\beta = FM^\beta \cup NF^\beta$ and $BH_P^\beta = BH_P^\beta \cup NF^\beta$. So the communication graph we defined simultaneously supports near-field and far-field communication, as well as communication up and down the hierarchical tree. Hence by partitioning and load balancing FM^β and BH_P^β , we automatically partition and balance the hierarchical tree, the near-field graph, and the far-field graph.

17.5.5 Geometric Modeling of N-body Graphs

Similar to well-shaped meshes, there is a geometric characterization of N-body communication graphs. Instead of using neighborhood systems, we use box-systems. A *box-system* in \mathbb{R}^d is a set $B = \{B_1, \dots, B_n\}$ of boxes. Let $P = \{\mathbf{p}_1, \dots, \mathbf{p}_n\}$ be the centers of the boxes, respectively. For each integer k , the set B is a *k-ply box-system* if no point $\mathbf{p} \in \mathbb{R}^d$ is contained in more than k of $\text{int}(B_1), \dots, \text{int}(B_n)$.

For example, the set of all leaf-boxes of a hierarchical tree forms a 1-ply box-system. The box-system is a variant of neighborhood system of Miller, Teng, Thurston, and Vavasis [63], where a neighborhood system is a collection of Euclidean balls in \mathbb{R}^d . We can show that box-systems can be used to model the communication graphs for parallel adaptive N-body simulation.

Given a box-system, it is possible to define the *overlap* graph associated with the system:

Definition 17.5.1 *Let $\alpha \geq 1$ be given, and let $\{B_1, \dots, B_n\}$ be a k -ply box-system. The α -overlap graph for this box-system is the undirected graph with vertices $V = \{1, \dots, n\}$ and edges*

$$E = \{(i, j) : B_i \cap (\alpha \cdot B_j) \neq \emptyset \text{ and } (\alpha \cdot B_i) \cap B_j \neq \emptyset\}.$$

The edge condition is equivalent to: $(i, j) \in E$ iff the α dilation of the smaller box touches the larger box.

As shown in [90], the partitioning algorithm and theorem of Miller *et al* can be extended to overlap graphs on box-systems.

Theorem 17.5.1 *Let G be an α -overlap graph over a k -ply box-system in \mathbb{R}^d , then G can be partitioned into two equal sized subgraphs by removing at most $O(\alpha k^{1/d} n^{1-1/d})$ vertices. Moreover, such a partitioning can be computed in linear time sequentially and in parallel $O(n/p)$ time with p processors.*

The key observation is the following theorem.

Theorem 17.5.2 *Let $P = \{\mathbf{p}_1, \dots, \mathbf{p}_n\}$ be a point set in \mathbb{R}^d that is μ -non-uniform. Then the set of boxes $B(P)$ of hierarchical tree of P is a $(\log_{2^d} n + \mu)$ -ply box-system and $FM^\beta(P)$ and $BH_P^\beta(P)$ are subgraphs of the 3β -overlap graph of $B(P)$.*

Therefore,

Theorem 17.5.3 *Let G be an N-body communication graph (either for BH or FMM) of a set of particles located at $P = \{\mathbf{p}_1, \dots, \mathbf{p}_n\}$ in \mathbb{R}^d ($d = 2$ or 3). If P is μ -non-uniform, then G can be partitioned into two equal sized subgraphs by removing at most $O(n^{1-1/d}(\log n + \mu)^{1/d})$ nodes. Moreover, such a partitioning can be computed in linear time sequentially and in parallel $O(n/p)$ time with p processors.*

Chapter 18

Mesh Generation

An essential step in scientific computing is to find a proper discretization of a continuous domain. This is the problem of *mesh generation*. Once we have a discretization or sometimes we just say a “mesh”, differential equations for flow, waves, and heat distribution are then approximated by finite difference or finite element formulations. However, not all meshes are equally good numerically. Discretization errors depend on the geometric shape and size of the elements while the computational complexity for finding the numerical solution depends on the number of elements in the mesh and often the overall geometric quality of the mesh as well.

The most general and versatile mesh is an unstructured triangular mesh. Such a mesh is simply a triangulation of the input domain (e.g., a polygon), along with some extra vertices, called *Steiner points*. A triangulation is a decomposition of a space into a collection of interior disjoint simplices so that two simplices can only intersect at a lower dimensional simplex. We all know that in two dimensions, a simplex is a triangle and in three dimensions a simplex is a tetrahedron. A triangulation can be obtained by triangulating a point set, that form the vertices of the triangulation.

Even among triangulations some are better than others. Numerical errors depend on the *quality* of the triangulation, meaning the shapes and sizes of triangles.

In order for a mesh to be useful in approximating partial differential equations, it is necessary that discrete functions generated from the mesh (such as the piecewise linear functions) be capable of approximating the solutions sought. Classical finite element theory [17] shows that a sufficient condition for optimal approximation results to hold is that the minimum angle or the aspect ratio of each simplex in the triangulation be bounded independently of the mesh used; however, Babuska [4] shows that while this is sufficient, it is not a necessary condition. See Figure ?? for a triangulation whose minimum degree is at least 20 degree.

Automatic mesh generation is a relatively new field. No mathematically sound procedure for obtaining the ‘best’ mesh distribution is available. The criteria are usually heuristic.

The input description of physical domain has two components: the geometric definition of the domain and the numerical requirements within the domain. The geometric definition provides the boundary of the domain either in the form of a continuous model or of a discretized boundary model. Numerical requirements within the domain are typically obtained from an initial numerical simulation on a preliminary set of points. The numerical requirements obtained from the initial point set define an additional local spacing function restricting the final point set.

An automatic mesh generator try to generate an additional points to the internally and boundary of the domain to smooth out the mesh generation and concentrate mesh density where necessary - to optimize the total number of mesh points.

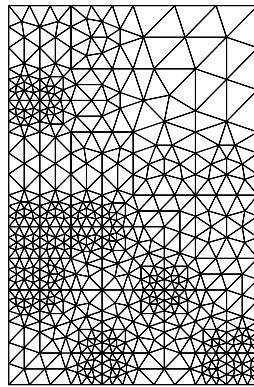


Figure 18.1: A well-shaped triangulation

18.1 How to Describe a Domain?

The most intuitive and obvious structure of a domain (for modeling a scientific problem) is its geometry.

One way to describe the geometry is to use *constructive solid geometry* formula. In this approach, we have a set of basic geometric primitive shapes, such as boxes, spheres, half-spaces, triangles, tetrahedra, ellipsoids, polygons, etc. We then define (or approximate) a domain as finite unions, intersections, differences, and complementation of primitive shapes, i.e., by a well-structured formula of a finite length of primitive shapes with operators that include union, intersection, difference, and complementation.

An alternative way is to discretize the boundary of the domain, and describes the domain as a polygonal (polyhedral) object (perhaps with holes). Often we convert the constructive solid geometry formula into the discretized boundary description for mesh generation.

For many computational applications, often, some other information of a domain and the problem are equally important for quality mesh generation.

The numerical spacing functions, typically denoted by $h(\mathbf{x})$, is usually defined at a point \mathbf{x} by the eigenvalues of the Hessian matrix of the solution u to the governing partial differential equations (PDEs) [4, 89, 65]. Locally, u behaves like a quadratic function

$$u(\mathbf{x} + d\mathbf{x}) = \frac{1}{2}(\mathbf{x}H\mathbf{x}^T) + \mathbf{x}\nabla u(\mathbf{x}) + u(\mathbf{x}),$$

where H is the *Hessian matrix* of u , the matrix of second partial derivatives. The spacing of mesh points, required by the accuracy of the discretization at a point \mathbf{x} , is denoted by $h(\mathbf{x})$ and should depend on the reciprocal of the square root of the largest eigenvalues of H at \mathbf{x} .

When solving a PDE numerically, we estimate the eigenvalues of Hessian at a certain set of points in the domain based on the numerical approximation of the previous iteration [4, 89]. We then expand the spacing requirement induced by Hessian at these points over the entire domain.

For a problem with a smooth change in solution, we can use a (more-or-less) uniform mesh where all elements are of roughly equal size. On the other hand, for problem with rapid change in solution, such as earthquake, wave, shock modeling, we may use much dense gridding in the area of with high intensity. See Fig 18.2. So, the information about the solution structure can be of a great value to quality mesh generation.

Other type of information may come in the process of solving a simulation problem. For example, in adaptive methods, we may start with a much coarse and uniform grid. We then estimate the

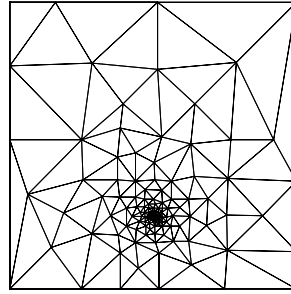


Figure 18.2: Triangulation of well-spaced point set around a singularity

error of the previous step. Based on the error bound, we then adaptively refine the mesh, e.g., make the area with larger error much more dense for the next step calculation. As we shall argue later, unstructured mesh generation is more about finding the proper distribution of mesh point than the discretization itself (this is a very personal opinion).

18.2 Types of Meshes

- **Structured grids** divide the domain into regular grid squares. For examples finite difference gridding on a square grid. Matrices based on structured grids are very easy and fast to assemble. Structured grids are easy to generate; numerical formulation and solution based on structured grids are also relatively simple.
- **Unstructured grids** decompose the domain into simple mesh elements such as simplices based on a density function that is defined by the input geometry or the numerical requirements (e.g., from error estimation). But the associated matrices are harder and slower to assemble compared to the previous method; the resulting linear systems are also relatively hard to solve. Most of finite element meshes used in practice are of the unstructured type.
- **Hybrid grids** are generated by first decomposing the domain into non-regular domain and then decomposing each such domain by a regular grid. Hybrid grids are often used in domain decomposition.

Structured grids are much easy to generate and manipulate. The numerical theory of this discretization is better understood. However, its applications is limited to problems with simple domain and smooth changes in solution. For problems with complex geometry whose solution changes rapidly, we need to use an *unstructured mesh* to reduce the problem size. For example, when modeling earthquake we want a dense discretization near the quake center and a sparse discretization in the regions with low activities. It would be waste to give regions with low activities as fine a discretization as the regions with high activities. Unstructured meshes are especially important for three dimensional problems.

The adaptability of unstructured meshes comes with new challenges, especially for 3D problems. However, the numerical theory becomes more difficult – this is an outstanding direction for future research; the algorithmic design becomes much harder.

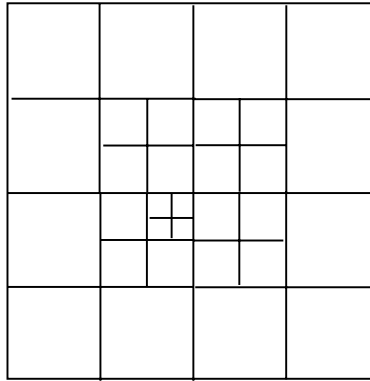


Figure 18.3: A quadtree

18.3 Refinement Methods

A mesh generator usually does two things: (1) it generates a set of points that satisfies both geometric and numerical conditions imposed on the physical domain. (2) it builds a robust and well-shaped meshes over this point set, e.g., a triangulation of the point set. Most mesh generation algorithms merge the two functions, and generate the point set implicitly as part of the mesh generation phase. A most useful technique is to generate point set and its discretization by an iterative refinement. We now discuss *hierarchical refinement* and *Delaunay refinement*, two of the most commonly used refinement methods.

18.3.1 Hierarchical Refinement

The hierarchical refinement uses quadtrees in two dimensions and octtrees in three dimensions. The basic philosophy of using quad- and oct-trees in meshes refinements and hierarchical N-body simulation is the same: adaptively refining the domain by selectively and recursively divide boxes enable us to achieve numerical accuracy with close to an optimal discretization. The definition of quad- and oct-tree can be found in Chapter ?? . Figure 18.3 shows a quad-tree.

In quadtree refinement of an input domain, we start with a square box encompassing the domain and then adaptively splitting a box into four boxes recursively until each box small enough with respect to the geometric and numerical requirement. This step is very similar to quad-tree decomposition for N-body simulation. However, in mesh generation, we need to ensure that the mesh is well-shaped. This requirement makes mesh generation different from hierarchical N-body approximation. In mesh generate, we need to generate a set of smooth points. In the context of quad-tree refinement, it means that we need to make the quad-tree *balanced* in the sense that no leaf-box is adjacent to a leaf-box more than twice its side length.

With adaptive hierarchical trees, we can “optimally” approximate any geometric and numerical spacing function. The proof of the optimality can be found in the papers of Bern, Eppstein, and Gilbert for 2D and Mitchell and Vavasis for 3D. Formal discuss of the numerical and geometric spacing function can be found in the point generation paper of Miller, Talmor and Teng.

The following procedure describes the basic steps of hierarchical refinement.

1. Construct the hierarchical tree for the domain so that the leaf boxes approximate the numerical and geometric spacing functions.

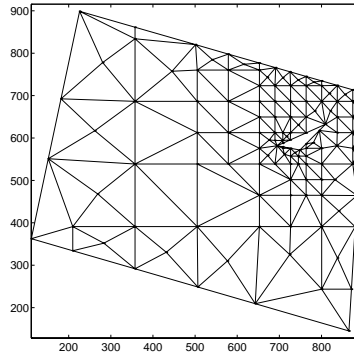


Figure 18.4: A well-shaped mesh generated by quad-tree refinement

2. Balance the hierarchical tree.
3. Warping and triangulation: If a point is too close to a boundary of its leaf box then one of the corners collapses to that point.

18.3.2 Delaunay Triangulation

Suppose $P = \{p_1, \dots, p_n\}$ is a point set in d dimensions. The convex hull of $d+1$ affinely independent points from P forms a *Delaunay simplex* if the circumscribed ball of the simplex contains no point from P in its interior. The union of all Delaunay simplices forms the *Delaunay diagram*, $DT(P)$. If the set P is not degenerate then the $DT(P)$ is a simplex decomposition of the convex hull of P . We will sometimes refer to the Delaunay simplex as a triangle or a tetrahedron.

Associated with $DT(P)$ is a collection of balls, called *Delaunay balls*, one for each cell in $DT(P)$. The Delaunay ball circumscribes its cell. When points in P are in general position, each Delaunay simplex define a Delaunay ball, its circumscribed ball. By definition, there is no point from P lies in the interior of a Delaunay ball. We denote the set of all Delaunay balls of P by $DB(P)$.

The geometric dual of Delaunay Diagram is the *Voronoi Diagram*, which consists a set of polyhedra V_1, \dots, V_n , one for each point in P , called the *Voronoi Polyhedra*. Geometrically, V_i is the set of points $p \in \mathbb{R}^d$ whose Euclidean distance to p_i is less than or equal to that of any other point in P . We call p_i the *center* of polyhedra V_i . For more discussion, see [74, 29].

The DT has some very desired properties for mesh generation. For example, among all triangulations of a point set in 2D, the DT maximizes the smallest angle, it contains the nearest-neighbors graph, and the minimal spanning tree. Thus Delaunay triangulation is very useful for computer graphics and mesh generation in two dimensions. Moreover, discrete maximum principles will only exist for Delaunay triangulations. Chew [16] and Ruppert [79] have developed Delaunay refinement algorithms that generate provably good meshes for 2D domains.

Notice that an internal diagonal belongs to the Delaunay triangulation of four points if the sum of the two opposing angles is less than π .

A 2D Delaunay Triangulation can be found by the following simple algorithm: *FLIP algorithm*

- Find any triangulation (can be done in $O(n \lg n)$ time using divide and conquer.)
- For each edge pq , let the two faces the edge is in be prq and psq . Then pq is not an local Delaunay edge if the interior the circumscribed circle of prq contains s . Interestingly, this

condition also mean that the interior of the circumscribed circle of psq contains r and the sum of the angles prq and psq is greater than π . We call the condition that the sum of the angles of prq and psq is no more than π *the angle condition*. Then, if pq does not satisfy the angle property, we just flip it: remove edge pq from T , and put in edge rs . Repeat this until all edges satisfy the angle property.

It is not too hard to show that if FLIP terminates, it will output a Delaunay Triangulation. A little additional geometric effort can show that the FLIP procedure above, fortunately, always terminates after at most $O(n^2)$ flips.

The following is an interesting observation of Guibas, Knuth and Sharir. If we choose a random ordering π of from $\{1, \dots, n\}$ to $\{1, \dots, n\}$ and permute the points based on π : $p_{\pi(1)} \dots p_{\pi(n)}$. We then incrementally insert the points into the the current triangulation and perform flip if needed. Notice that the initial triangulation is a triangle formed by the first three points. It can be shown that the expected number of flips of the about algorithm is $O(n \log n)$. This gives a randomized $O(n \log n)$ time DT algorithm.

18.3.3 Delaunay Refinement

Even though the Delaunay triangulation maximize the smallest angles. The Delaunay triangulation of most point sets are bad in the sense that one of the triangles is too 'skinny'. In this case, Chew and Ruppert observed that we can refine the Delaunay triangulation to improve its quality. This idea is first proposed by Paul Chew. In 1992, Jim Ruppert gave a quality guaranteed procedure.

- Put a point at the circumcenter of the skinny triangle
- if the circum-center encroaches upon an edge of an input segment, split an edge adding its middle point; otherwise add the circumcenter.
- Update the Delaunay triangulation by FLIPPING.

A point *encroaches* on an edge if the point is contained in the interior of the circle of which the edge is a diameter. We can now define two operations, Split-Triangle and Split-Segment

Split-Triangle(T)

- Add circumcenter C of Triangle T
- Update the Delaunay Triangulation ($P \cup C$)

Split-Segment(S)

- Add midpoint m
- Update the Delaunay Triangulation ($P \cup M$)

The *Delaunay Refinement* algorithm then becomes

- Initialize

- Perform a Delaunay Triangulation on P
- IF some segment, l , is not in the Delaunay Triangle of P , THEN Split-Segment (l)
- Repeat the following until $\alpha > 25^\circ$
 - IF T is a skinny triangle, try to Split(T)
 - IF C of T is 'close' to segment S then Split-Seg(S)
 - ELSE Split Triangle (T)

The following theory was then stated, without proof. The proof is first given by Jim Ruppert in his Ph.D thesis from UC. Berkeley.

Theorem 18.3.1 Not only does the Delaunay Refinement produce all triangles so that $MIN \alpha > 25^\circ$, the size of the mesh it produces is no more than $C * Optimal(size)$.

VI Selected Topics

Chapter 19

The Pentium Bug

19.1 About These Notes on The Pentium Bug

The purpose of these notes is to summarize the 18.337 class on ♡ February 14, 1995 ♡. It includes a brief history on the discovery of the Pentium bug in §2 followed by the details of the Pentium bug flaw in §3. The material appearing in §3 is intended to be a simplification of the proof which appeared in the Coe/Tang paper “It Takes Six Ones to Reach a Flaw.”

19.2 The Discovery of The Bug

The first posting about the Pentium bug was by Professor Nicely at the Lynchburg College of Virginia. It seems that Dr. Nicely was working with twin primes – numbers such as { 11, 13 }, { 29, 31 }, or { 107, 109 }. Specifically, he was going after the sum:

$$S = \frac{1}{5} + \frac{1}{7} + \frac{1}{11} + \frac{1}{13} + \frac{1}{17} + \frac{1}{19} + \dots$$

This sum is mathematically known to be finite. Dr. Nicely had been running his program to compute this sum on several different computers. But when he ran the program on a Pentium machine, he got a different answer than he expected – even though he was using double precision, he was getting worse results than would be expected from single precision numbers. Eventually, Dr. Nicely narrowed the the source of the error to a part of his code that computed the terms in the sum. (i.e. $\frac{1}{p}$) He knew that his code was correct, so on October 10, 1994 he posted his conclusion that the Pentium chip contained a division flaw.

This posting caught the attention of Dr. Timothy Coe at Vitesse, who decided that this was a good opportunity to discover how the chip works. He asked for people to send him examples of the bug, and successfully put together a model of what Intel was doing.

19.3 The Pentium Bug

What Dr. Coe discovered was that Intel was doing division using the Radix-4 version of the Sweeney, Robertson, and Tocher (SRT) algorithm. In order to get an idea of the magnitude of the bug that we will be discussing, consider the following example: The fraction $\frac{4195835}{3145727}$ should evaluate to 1.33382, but a flawed Pentium chip returns 1.33374. This is a relative error of 6.1E-5 or about 61 ppm – roughly twice the concentration of carbon monoxide allowed in ambient air by national

ambient air quality standards¹. It is interesting that some software developers have come up with ways to deal with this annoying bug. For example, there is a patch available for MATLAB which detects at-risk denominators, multiplies the numerator and denominator by $\frac{15}{16}$, and then performs the division. The remainder of this section is devoted to a description of the details of the Radix-4 SRT algorithm and the Pentium Bug.

19.4 Introduction

This is text from an old version of my paper. Better to grab a later version off of my web page, and also see recent work by Kahan.— Alan

Quite properly, the risk to users emerged as the most popular issue in the discussion of the Intel Pentium flaw. Unfortunately, evaluating this risk is probably infeasible. Other popular issues include Intel's public relations policy, the story of how Nicely found the bug, how Coe succeeded in reverse engineering the algorithm based on "bad" numerators and denominators, and those ubiquitous Pentium jokes [14]. Here we cover the one issue that is not very well understood, the bug itself. The contribution of this paper is to supply a simplified explanation of the Coe, Tang [21] result that the at risk divisors have six consecutive ones in positions 5 through 10. Also we explain why the worst case absolute error for arguments in $[1, 2)$ is on the order of $1e-5$.

There have been a number of interesting related works including Kahan's [49] SRT division tester. Kahan's tester chooses arguments more cleverly than random testing, increasing the likelihood of discovering whether an algorithm is somehow broken. His tester concentrates on the fenceposts, which is always a good place to look for difficulties. Randy Bryant [13] shows that binary decision diagrams may be used as a check of the validity of a PD table. His algorithm explicitly checks that partial remainders remain within the critical region. Vaughan Pratt [73], holds the record for the most extensive computational experiments and classifications of the bug.

Sometimes a mistake is itself uninteresting other than that it causes trouble and that it needs to be fixed. For example, a wrong turn while driving in a familiar neighborhood can waste time. On occasion, a mistake is itself inherently interesting. Proceeding with our example, a wrong turn in an unfamiliar neighborhood may lead to interesting discoveries. With all of the media coverage, one message that hardly anyone has noticed is that the bug itself is mathematically interesting.

Suppose the Pentium chip had never been built, but a mathematician had a complete specification of the algorithm including the flaw. Could this mathematician without the aid of a computer readily discover flawed numerators and denominators? My opinion is that the world's leading mathematicians might find them, but I am not so sure. They are difficult to find using traditional non-computer oriented mathematics.

This article is a self-contained mathematical discussion of the bug, and only the bug. Sections 2 through 4 contain a complete mathematical specification of the algorithm which would be sufficient for the reader to try to see if he can devise buggy numerators and denominators without ever touching a Pentium chip.

We begin with a discussion of radix 4 SRT division, and its carry-save implementation. We then give a simplified proof of the Coe/Tang [21] result that it takes six ones to reach a flaw. The first part of the proof begins with a simple analysis of the inequalities that either prevent you or allow you access to an erroneous table entry. The second part of the proof is an arithmetic puzzle not so very different in spirit from the sort found in recreational mathematics, where one has to replace letters with digits to make a correct sum as in this one from a collection by James Fixx [32]

¹National Primary and Secondary Ambient-Air-Quality Standard, 1983

```

  S E N D
+ M O R E
-----
M O N E Y

```

We conclude with an explanation of why the Pentium is always guaranteed to have an absolute error that is bounded by $5e-5$, when the inputs are in the standard interval $[1, 2)$.

19.5 SRT Division

We now present the radix 4 version of the Sweeney, Robertson, and Tocher (SRT) division algorithm. This algorithm computes a radix 4 quotient where the digits are not the set $\{0, 1, 2, 3\}$ as might be expected from base 4, but rather $\{-2, -1, 0, 1, 2\}$. The extra digit introduces a very useful “slack” into the computation. For multiplication, the digits $0, \pm 1$, and ± 2 are also computationally more convenient than the digit 3 would be, say.

Letting p and d denote the numerator and the denominator, we may as well assume that $1 \leq p, d < 2$. The SRT division algorithm may be expressed succinctly in conceptual pseudocode:

RADIX 4 SRT DIVISION

```

 $p_0 := p$ 
for  $k = 0, 1, \dots$ 
  “Lookup” a digit  $q_k \in \{-2, -1, 0, 1, 2\}$  in such a way that
     $p_{k+1} := 4(p_k - q_k d)$ 
  satisfies  $|p_{k+1}| \leq \frac{8}{3}d$ 
end
 $p/d = \sum_{i=0}^{\infty} q_i/4^i$ 

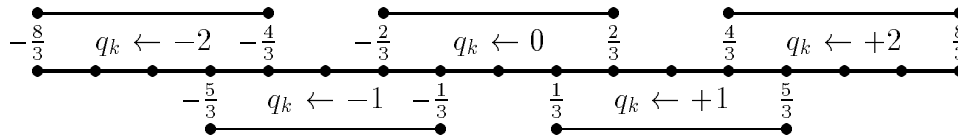
```

The details of the lookup table are intricate and are postponed to Section 19.7. On the Pentium chip, by an accident in the table lookup, it is possible to obtain a q_k which fails to produce a p_{k+1} with absolute value $\leq \frac{8}{3}d$.

We note that if we replace the set $\{-2, -1, 0, 1, 2\}$ with $\{0, \dots, 9\}$, and the 4 with a 10, and finally the inequality $|p_{k+1}| \leq \frac{8}{3}d$ with $p_{k+1} \in [0, 10d)$, then we recover ordinary base 10 long division.

19.6 Understanding why SRT works

It is easy to see that if $|p_k| \leq \frac{8}{3}d$ then at least one of the five values of $p_k - q_k d$ has absolute value $\leq \frac{2}{3}d$. The figure below (with unit length d) shows this clearly. The indicated q_k value translates each interval to the $q_k \leftarrow 0$ interval. Overlap between upper and lower intervals indicates that an arbitrary choice may be made. The $q_k \leftarrow 0$ interval, when scaled up by a factor of 4, remains within the interval $|p| \leq \frac{8}{3}d$.



We therefore may run the algorithm ad infinitum, i.e. we can find a q_k for which

$$p_{k+1} = 4(p_k - q_k d) \tag{19.1}$$

has absolute value $\leq \frac{8}{3}d$.

Since equation (19.1) is equivalent to

$$\frac{p_k}{d} 4^{-k} = \frac{q_k}{4^k} + \frac{p_{k+1}}{d} 4^{-(k+1)},$$

we may prove by induction that

$$\frac{p}{d} = \left(q_0 + \frac{q_1}{4} + \dots + \frac{q_{k-1}}{4^{k-1}} \right) + \frac{p_k}{d} 4^{-k}. \tag{19.2}$$

Letting $k \rightarrow \infty$ in Equation (19.2) proves that the SRT algorithm computes the correct quotient. \square

There is a popular misconception that the SRT algorithm is capable of correcting for “mistakes” by using the redundant set of digits. Though the overlapping in the regions may allow for two choices of digits, if an invalid digit is chosen, the algorithm can never recover.

A consequence of Equation (19.2) is that

$$p_k = d \sum_{i=k}^{\infty} q_i / 4^{i-k} = d \left(q_k + \frac{q_{k+1}}{4} + \frac{q_{k+2}}{4^2} + \dots \right).$$

Summing the geometric progression with the extreme choices of all $q_i = +2$ or all $q_i = -2$ shows that the requirement $|p_k| \leq \frac{8}{3}d$, is not an arbitrary choice, but a necessary ingredient in the algorithm. On the Pentium, for certain values of d and for certain values of p_k just a little smaller than $\frac{8}{3}d$, the chip supplies the value 0 for q_k rather than 2. The value of p_{k+1} would then be nearly $10d$ which is way outside of the range representable by our geometric progression. A consequence is that when the Pentium looks up 0 instead of 2, there is no way to recover.

A small observation that we will use later is

Lemma 19.6.1 *If $q_k = 2$, then $p_{k+1} \leq p_k$.*

Proof This is a simple consequence of the bound $p_k \leq \frac{8}{3}d$. \square

19.7 Quotient digit selection on the Pentium

The Pentium uses a lookup table to obtain q_k . Rather than using p_k and d directly in the lookup table, it uses approximations P_k and D to p_k and d respectively. P_k is a binary number of the form **xxxx.yyy**, i.e. an integer multiple of $1/8$, while D is a binary number of the form **x.yyyy**, i.e. an integer multiple of $1/16$. The number P_k is obtained from the carry-save representation to be explained momentarily. We shall see that we can guarantee that

$$P_k \leq p_k < P_k + \frac{1}{4} \text{ and } D \leq d < D_+ \equiv D + \frac{1}{16}. \tag{19.3}$$

Notice that D and D_+ are defined by the second inequality, but two possible values of P_k are possible given p_k .

The lookup table [21, 85] that computes q_k as a function of P_k and D appears in Figure 19.7 below. The five marked boxes indicate table entries that must be 2 but erroneously return 0 on flawed Pentium chips.

The five bad entries occur for those divisors d for which D has any of the five values $17/16$, $20/16$, $23/16$, $26/16$, $29/16$. For the other D values, there is no algorithm pathology, so there is no independent way to be sure which digits are selected in the overlap regions. Hence the empty area in the lookup table.

For the remainder of this paper, we are only concerned with the five bad columns in the lookup table. In particular, $\frac{2}{3}D_+$ is an integer multiple of $1/8$. Following Coe and Tang [21], a flawed entry exists at the value $P_{\text{Bad}} = \frac{8}{3}D_+ - \frac{1}{8}$. The lookup table is expressed succinctly with thresholds by identifying which of five intervals P_k falls in:

$$P_q^{\text{Min}} \leq P_k \leq P_q^{\text{Max}}. \tag{19.4}$$

The thresholds are

q	P_q^{Min}	P_q^{Max}
-2	$-\frac{8}{3}D_+$	$-\frac{1}{4} - \frac{4}{3}D_+$
-1	$-\frac{1}{8} - \frac{4}{3}D_+$	$[-\frac{1}{4} - \frac{1}{3}D_+]$
0	$[-\frac{1}{8} - \frac{1}{3}D_+]$	$[-\frac{1}{8} + \frac{1}{3}D_+]$
1	$[\frac{1}{3}D_+]$	$-\frac{1}{8} + \frac{4}{3}D_+$
2	$\frac{4}{3}D_+$	$-\frac{1}{8} + \frac{8}{3}D_+$

It is easy to check that the q chosen in this manner satisfies the constraints of the algorithm specified in Section 2.

The computation of P_k : Carry-Save addition

Imagine adding 100 numbers on a calculator. On many calculators after typing $x_1 + x_2$ the sum would be displayed, then folding in x_3 the new sum is obtained, etc. On computers it is convenient to avoid the carry propagation by leaving the result in so-called “carry-save” format (See [23, pp.668–669]). In this format $x_1 + x_2$ is represented as $s_2 + c_2$. When we add in x_3 the result is represented as $s_3 + c_3$, etc. The s_i and c_i are known as the sum and carry word. The basic idea is that when computing the sum of $s_2 + c_2 + x_3$ in binary, every column can add up to 0, 1, 2, or 3 so the modulo 2 sum of the result (0 or 1) is stored in the sum word, and the carry bit is stored in the carry word.

$$\begin{array}{r}
 x_1 \quad 0 \ 1 \ 0 \ 1 \ 1 \\
 x_2 \quad 0 \ 1 \ 1 \ 0 \ 1 \\
 \hline
 s_2 \quad 0 \ 0 \ 1 \ 1 \ 0 \\
 \text{Here is an example: } c_2 \quad 1 \ 0 \ 0 \ 1 \ 0 \\
 x_3 \quad 0 \ 1 \ 1 \ 1 \ 0 \\
 \hline
 s_3 \quad 1 \ 1 \ 0 \ 1 \ 0 \\
 c_3 \quad 0 \ 1 \ 1 \ 0 \ 0
 \end{array}$$

Generally speaking $\text{sum}(\mathbf{a}, \mathbf{b}, \mathbf{c})$ is $a + b = c \pmod 2$ in mathematical language, and $a \oplus b \oplus c$ in a more computer science style language. $\text{carry}(\mathbf{a}, \mathbf{b}, \mathbf{c})$ may be expressed as $a + b + c \geq 2$ in a matlab sort of language, or as $(a \wedge b) \vee (a \wedge c) \vee (b \wedge c)$. The numbers c_k and s_k constitute the carry-save representation of $\sum_{i=1}^k x_k$.

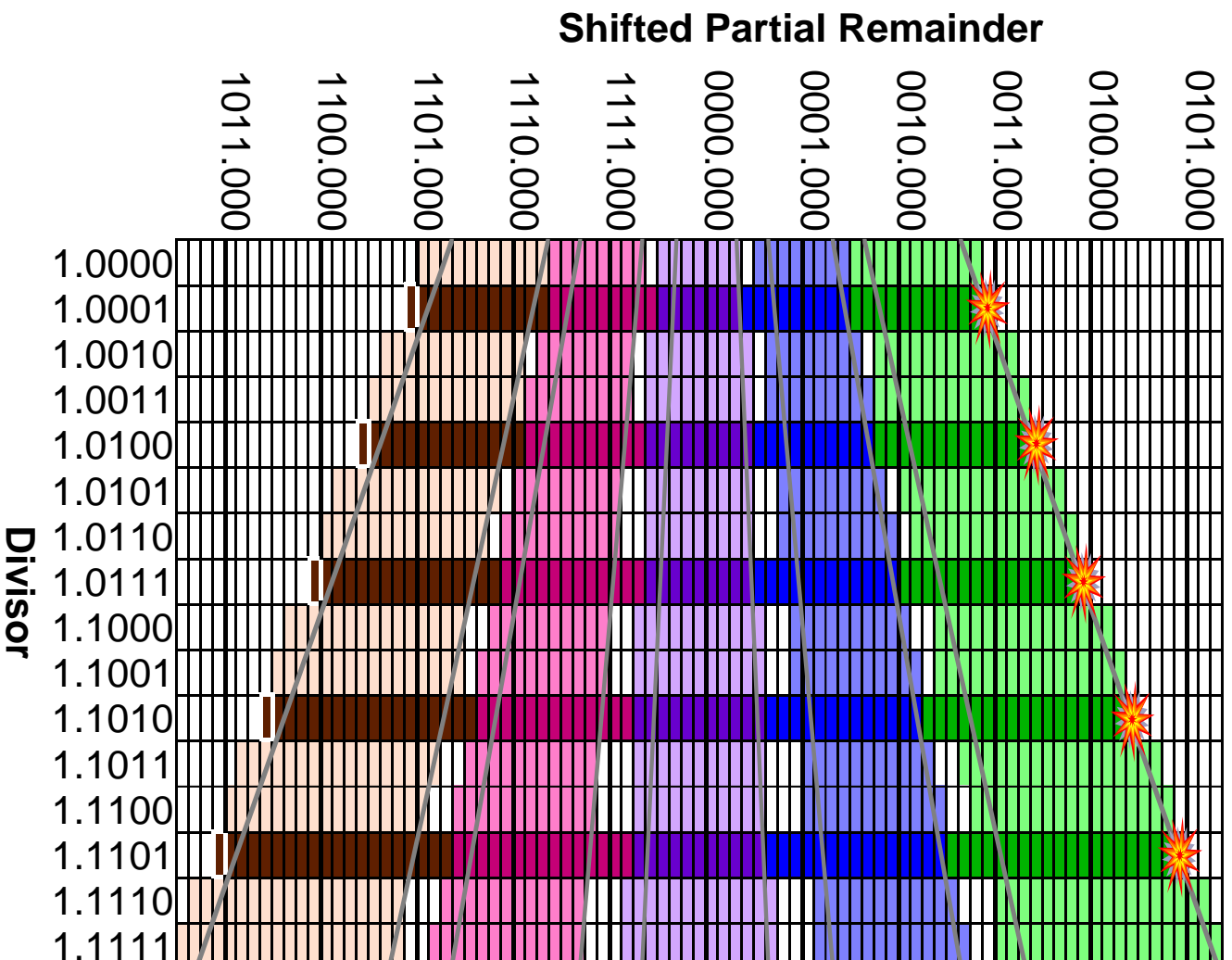


Figure 19.1: The quotient digit $q_k \in \{-2, -1, 0, 1, 2\}$ is a function of P_k and D .

On the Pentium, p_k is represented in the carry-save form $c_k + s_k$ so that the expression $p_{k+1} = p_k - q_k d$ is computed using a carry-save adder. If q_k is positive $-q_k d$ is represented using a ones complement notation. In general $p_k - q_k d$ is obtained from d by a combination of shifting and/or ones complementing or zeroing. Since these are fast operations on a computer, this explains why the digit set $\{-2, -1, 0, 1, 2\}$ is so useful. To perform addition correctly, if a one's complement number is used, a 1 is added in to the least significant carry bit before shifting.

Given that $p_k = c_k + s_k$, it is natural to define $P_K = C_k + S_k$, where C_k and S_k represent c_k and s_k respectively rounded down to the nearest bit. Since

$$C_k \leq c_k < C_k + \frac{1}{8} \text{ and } S_k \leq s_k < S_k + \frac{1}{8},$$

we can conclude that $P_k \leq p_k + \frac{1}{4}$.

The following example illustrates the division of 1.875 by 1.000 using fewer bits than is actually used in the Pentium. Of course, dividing by 1 is trivial, but the important features of the algorithm are illustrated below.

$$\begin{array}{r}
 1.875 = \quad 0001.111 \ 0000000000 \\
 \quad \quad 0000.000 \ 0000000000 \\
 -2 \times 1 = \quad 1101.111 \ 1111111111 \\
 \hline
 \quad \quad 0000.011 \ 1111111100 \\
 \quad \quad 1111.000 \ 0000000100 \\
 -(-1) \times 1 = \quad 0001.000 \ 0000000000 \\
 \hline
 \quad \quad 1001.111 \ 1111110000 \\
 \quad \quad 1000.000 \ 0000010000 \\
 -2 \times 1 = \quad 1101.111 \ 1111111111 \\
 \hline
 \quad \quad 0000.000 \ 00011111100 \\
 \quad \quad 1111.111 \ 11100000100 \\
 -0 \times 1 = \quad 0000.000 \ 0000000000 \\
 \hline
 \quad \quad 1111.111 \ 1111110000 \\
 \quad \quad 0000.000 \ 0000010000 \\
 \quad \quad 0000.000 \ 0000000000 \\
 \hline
 \quad \quad 1111.111 \ 1110000000 \\
 \quad \quad 0000.000 \ 0010000000
 \end{array}$$

19.8 Analyzing the bug

19.8.1 It is not easy to reach the buggy entry

We proceed to prove a lemma which states that the buggy entry P_{Bad} can only be reached from the entry below. This is a subtle phenomenon that may not have been readily guessed from general properties of SRT division. We will also show that the next lower entry, $P_{\text{Bad}} - \frac{1}{8}$, is itself difficult to reach.

In terms of the binary expansion of $d = 1.d_1 d_2 d_3 d_4 d_5 \dots$, we have the following identities for $q_k D_+$:

$$\begin{array}{rcl}
 2D_+ & = & 001 d_1 . d_2 d_3 d_4 \ 0 \quad + \frac{1}{8} \\
 D_+ & = & 000 1. d_1 d_2 d_3 d_4 \quad + \frac{1}{16} \\
 0D_+ & = & 000 0. \ 0 \ 0 \ 0 \ 0 \\
 -D_+ & = & 111 0. \ \bar{d}_1 \ \bar{d}_2 \ \bar{d}_3 \ \bar{d}_4 \\
 -2D_+ & = & 110 \bar{d}_1 . \bar{d}_2 \ \bar{d}_3 \ \bar{d}_4 \ 0
 \end{array}, \tag{19.5}$$

where the negatives numbers are expressed in two's complement notation.² The chopping is a round down process, but D_+ is akin to a round up, hence the existence of the $\frac{1}{8}$ and $\frac{1}{16}$ terms.

Therefore in terms of P_k and D_+ , we have the approximate version of Equation (19.1):

$$P_{k+1} = 4(P_k - q_k D_+) + R_k, \tag{19.6}$$

where R_k is determined by a few higher order bits. To be precise,

$$R_k = 0.0s_4s_5 + 0.0c_4c_5 + \begin{pmatrix} 0.0 & d_5 & d_6 \\ 0.0 & 0 & d_5 \\ 0 & & \\ 0.0 & 0 & \bar{d}_5 \\ 0.0 & \bar{d}_5 & \bar{d}_6 \end{pmatrix} + \frac{1}{8} \times \text{carry-over}(s_6, c_6, \begin{pmatrix} d_7 \\ d_6 \\ 0 \\ \bar{d}_6 \\ \bar{d}_7 \end{pmatrix}) + \begin{pmatrix} -1/2 \\ -1/4 \\ 0 \\ 0 \\ 0 \end{pmatrix}, \text{ if } \begin{cases} q = -2 \\ q = -1 \\ q = 0 \\ q = 1 \\ q = 2 \end{cases}$$

where the s_i , c_i , and d_i are the appropriate bits in the sum, carry, and divisor respectively. The function $\text{carry-over}(b_1, b_2, b_3)$ is 1 if at least two of its arguments are 1. The last correction term of $-1/2$ and $-1/4$ is a direct consequence of Equation (19.5).

Taking the maximum value of the parameters we see that

$$R_k \leq R_k^{\text{Max}} \equiv \begin{cases} 3/4 \\ 3/4 \\ 7/8 \\ 1 \\ 5/4 \end{cases}, \text{ if } \begin{cases} q = -2 \\ q = -1 \\ q = 0 \\ q = 1 \\ q = 2 \end{cases}. \tag{19.7}$$

We assume that D_+ is a multiple of $3/16$ i.e., it corresponds to one of the five flawed table entries. For each value of q_k , we may tabulate the largest possible P_{k+1} that may be reach as a function of the extreme P_k by using equations (19.6) and (19.7). This is our first glimpse at just how difficult it is to reach P_{Bad} .

q_k	P_k	$P_{k+1}^{\text{Max}} = 4(P_k - q_k D_+) + R_k^{\text{Max}}$
-2	$P_{-2}^{\text{Max}} = -\frac{4}{3}D_+ - \frac{1}{4}$	$\frac{8}{3}D_+ - \frac{1}{4} = P_{\text{Bad}} - \frac{1}{8}$
-1	$P_{-1}^{\text{Max}} \leq -\frac{1}{3}D_+ - \frac{1}{4}$	$\frac{8}{3}D_+ - \frac{1}{4} \leq P_{\text{Bad}} - \frac{1}{8}$
0	$P_0^{\text{Max}} \leq \frac{1}{3}D_+$	$\frac{4}{3}D_+ + \frac{7}{8} < P_{\text{Bad}} - \frac{1}{8}$
1	$P_1^{\text{Max}} = \frac{4}{3}D_+ - \frac{1}{8}$	$\frac{4}{3}D_+ + \frac{1}{2} < P_{\text{Bad}} - \frac{1}{8}$
2	$P_{\text{Bad}} - \frac{1}{8} = \frac{8}{3}D_+ - \frac{1}{4}$	$\frac{8}{3}D_+ + \frac{1}{4} > P_{\text{Bad}}$
2	$P_{\text{Bad}} - \frac{1}{4} = \frac{8}{3}D_+ - \frac{3}{8}$	$\frac{8}{3}D_+ - \frac{1}{4} = P_{\text{Bad}} - \frac{1}{8}$

(19.8)

The two “less than” inequalities in the table above are a simple consequence of $D_+ > 1$.

Lemma 19.8.1 *The sequence of P 's and corresponding q 's that lead to the bad entry are given below:*

$$\begin{array}{lcl} P: & P_{-2}^{\text{Max}}/P_{-1}^{\text{Max}} & \longrightarrow \{P_{\text{Bad}} - \frac{1}{8}\}_{m \geq 1} \longrightarrow P_{\text{Bad}} \\ q: & -2/-1 & \longrightarrow \{2\}_{m \geq 1} \longrightarrow (\text{bad entry}) \cdot \\ & R = R^{\text{max}} & R = R^{\text{max}} - \frac{3}{8} \end{array} \tag{19.9}$$

Here the subscript m in the middle column denotes a repetition of the entry $m \geq 1$ times, and the first column indicates that either a P_{-2}^{Max} or P_{-1}^{Max} may start the path to the bug corresponding to either $q = -2$ or $q = -1$ respectively.

²Two's complement represents integers by reducing modulo a power of 2. Add D_+ and $-D_+$ or add $2D_+$ and $-2D_+$ (and multiply by 16 to remove the binary point) to see that the sum is a power of 2.

Proof Our proof goes from right to left. The table in (19.8) shows that we can only reach P_{Bad} from $P_{\text{Bad}} - \frac{1}{8}$. The table also shows that for $q = -2$ or $q = -1$, we can just barely reach $P_{\text{Bad}} - \frac{1}{8}$, but only when $P_k = P_k^{\text{Max}}$ and $R_k = R_k^{\text{Max}}$. $P_{\text{Bad}} - \frac{1}{8}$ may also be reached from $P_{\text{Bad}} - \frac{1}{4}$, but if $P_k = P_{\text{Bad}} - \frac{1}{4}$ then $P_{\text{Bad}} - \frac{1}{4} \leq p_k < P_{\text{Bad}}$, and Lemma 19.6.1 guarantees that while the sequence produces 2's all future p_k will also satisfy $p_k < P_{\text{Bad}}$ which precludes reaching the flawed entry, i.e., reaching k with $P_k = P_{\text{Bad}}$. \square

19.9 The ‘‘Send More Money’’ Puzzle for the Pentium

Theorem 19.9.1 (Coe,Tang) *A flawed table entry can only be reached if the divisor $d = d_1d_2d_3 \dots$ has the property that the six consecutive bits from d_5 to d_{10} are all ones. (Of course $1.d_1d_2d_3d_4$ must be one of the five bad values.)*

Proof

First assume that $m = 1$. (We later show in Lemma 19.9.1 that this is the only possibility.) The table below illustrates the carry-sum addition that leads to the buggy entry. The Greek letter subscripts indicate the alphabetical order in which the entries are filled in. The reasoning behind the entries appears immediately below. Asterisks (*) indicate entries whose values are not of interest. Also of no interest are values to the left of the binary point.

$q = -2$	s_{j-2}	.*	*	*	1_α	1_α	1_ζ	1	1	s_{j-2}	.*	*	*	1_α	1_α	1_ζ	1	1	$q = -1$
$q = -2$	c_{j-2}	.*	*	*	1_α	1_α	1_ζ	1	1	c_{j-2}	.*	*	*	1_α	1_α	1_ζ	1	1	$q = -1$
	$2d$	$.d_2$	d_3	d_4	1_α	1_α	1_ζ	1	1	d	$.d_1$	d_2	d_3	d_4	1_α	1_ζ	1	1	
	s_{j-1}	.*	1_β	1_β	1_ϵ	1_ι	1	1	1	s_{j-1}	.*	1_β	1_β	1_ϵ	1_ι	1	1	1	
$q = 2$	c_{j-1}	$.1_\beta$	1_β	1_γ	1_ϵ	1_ι	1	1	1	c_{j-1}	$.1_\beta$	1_β	1_γ	1_ϵ	1_ι	1	1	1	
	$-2d$	$.d_2$	d_3	d_4	0_δ	0_δ	0_κ	0	0	$-2d$	$.d_2$	d_3	d_4	0_δ	0_ζ	0	0	0	
	s_j	.*	0_η	0_λ	0	0	0	0	0	s_j	.*	0_η	0_λ	0	0	0	0	0	
bug	c_j	$.1_\eta$	1_θ	1_λ	*	*	*	*	*	c_j	$.1_\theta$	1_λ	*	*	*	*	*	*	

- α Since R (Lemma 19.8.1 must equal R^{max} we must have $c_4, c_5, s_4, s_5, d_5, d_6 = 1$. (Only up to d_5 when $q =$
- β Arithmetic from above.
- γ $8(P_{\text{Bad}} - \frac{1}{8})$ is even. (It can be 22, 26, 30, 34, or 38.)
- δ Complement the 1_α since now $q = +2$.
- ϵ $R = R^{\text{max}} - \frac{3}{8}$ (Lemma 19.8.1). Given the 0_δ , if either 1_ϵ were 0, R would be smaller.
- ζ Arithmetic from below.
- η Arithmetic from above.
- θ $8P_{\text{Bad}} \in \{23, 27, 31, 35, 39\}$ is 3 (mod 4).
- ι The 1_θ requires a carry from above.
- κ Complement the d bit 1_ζ .
- λ 0_λ is the result of arithmetic from above. 1_λ since $8P_{\text{Bad}}$ is 3 (mod 4).

The remaining entries follow easily.

The conclusion that we have so far is that if we begin with $q = -2$, we must then have that d_5, d_6, d_7, d_8, d_9 are all 1. If we begin with $q = -1$, then we conclude that d_5, d_6, d_7, d_8 are all 1.

We are almost, but not quite finished. Having all those ones at the $q = -2$ or $q = -1$ step allows us to go back yet another step. A quick analysis shows that the line above s_{j-2} can only be d or $2d$ and that it too has many ones. We can then guarantee that d_9 and d_{10} are also 1. \square

Lemma 19.9.1 *The value for m in Lemma 19.8.1 must be one.*

Proof The results from α to δ are readily seen to be correct, even if $q_{j-2} = 2$. However, checking a few more steps readily yields a contradiction. \square

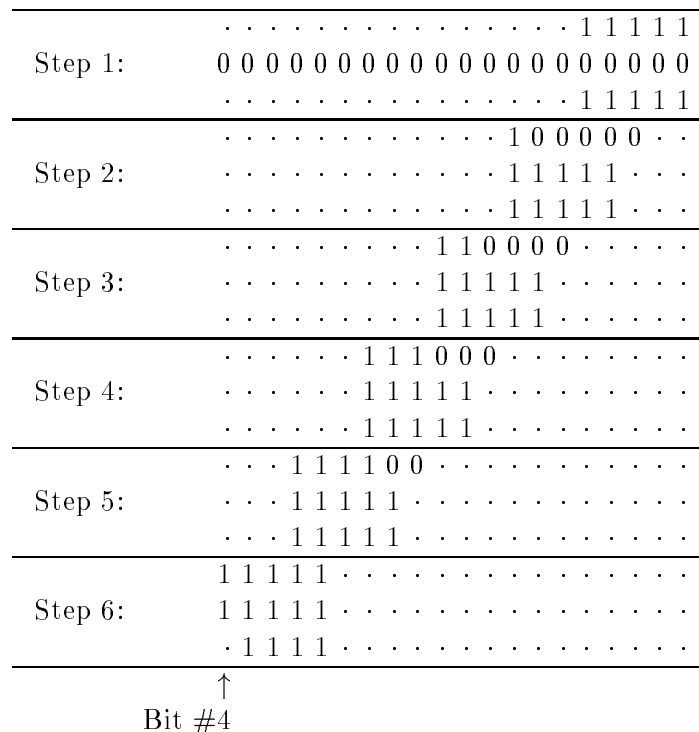
19.10 At least nine steps to failure

Naively, one might have thought that the bad table entries would be hit uniformly at random. If this had been the case, the bug surely have been noticed earlier and would have had the potential to cause more significant damage every instance it went unnoticed.

Even in the worst case of the error, the absolute error in the quotient is roughly $0.00005 = 5e - 5$ when dividing two numbers in the interval $1 \leq x < 2$. This is the worst case, the actual errors can be far smaller. Vaughan Pratt [72] has exhaustively computed all the single precision errors and has found that the quotient $14909255/11009918$ has an absolute error that is roughly $5e - 5$. (In fact it is $4.65e - 5$.) The highest relative error that he reported is roughly $6e - 5$.

The reason the error is bounded is that, no matter what, the Pentium is guaranteed to compute q_0 through q_7 correctly. This is what we will now prove. The result is a straightforward consequence of the results in the previous section.

In particular, if the bug occurs at step 8, then we saw in Section 6 that step 6 must have the form shown in the diagram below which shows the sum, carry, and $q_k d$ bits respectively starting with bit number 4. Taking into account that all the carry bits are 0 at step 1, it is fairly easy to show that the bit patterns must fall as in the diagram below. However, since q_1 is positive, it must follow that all of q_2, \dots, q_6 are positive by observing the overlap in the $q_k d$ row from one step to the next. However, we know that $q_6 < 0$ so we have a contradiction. Therefore the pattern shown below as Step 6, which must occur to trigger the bug, can not appear before the seventh step, and hence the bug appears no earlier than the ninth step.



19.11 Acknowledgement

I owe a great deal to Tim Coe for explaining carefully and patiently the reasoning behind his reverse engineering of the Pentium chip. This paper began life as an extended referee's report for the original version of the Coe, Tang paper [21]. Without this paper, this work would have been impossible. I also thank Velvel Kahan for many interesting discussions during January of 1995, while I was visiting Berkeley, and Vaughan Pratt for reviewing early drafts of this note which had more bugs than the Pentium. Finally, I thank Teddy Slottow for creating the beautiful color figure.

19.12 Conclusions

We have provided a simplified proof the Coe, Tang result that the only divisors at risk are those divisors which six consecutive ones in the fifth through tenth positions. We also explain why the absolute error is bounded by $5e-5$, when dividing two numbers in the standard interval $[1, 2)$. An interesting unexplored question would be: for arbitrary radix SRT division algorithms is it possible to show that every plausible table entry can in fact be reached?

Chapter 20

Network Topologies

Chapter 21

Topology Based Parallel Algorithms

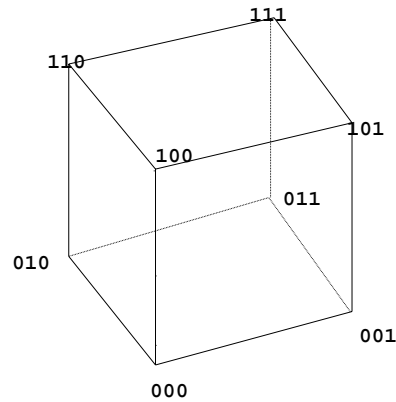
21.1 Overview

- The Gray Code and Other Embeddings of the Hypercube
- Going Beyond Embedded Cycles
- Hypercube theory: Unique Edge-Disjoint Hamiltonian Cycles in a Hypercube
- An Application: Matrix Multiplication on a Grid
- The Direct N-Body problem on a Hypercube
- The Hamming Sum
- Extending Gray Code-directed Body Movement to Multiple Sets of Bodies
- Matrix Multiplication using all Hypercube Wires
- Matrix Multiplication using the Cartesian Product

21.2 Interprocessor Communication and the Hypercube Graph

All parallel supercomputers allow message passing between nodes as a means of communication. This programming model differs from programming in a data-parallel language such as CM-FORTRAN or C*, which has been done previously in this course. The CM-5 was designed primarily for data parallel programming, but may also be used for message passing. In the past, message passing did not give users access to the vector units which make the CM-5 so fast. The latest nodal model allows message passing to take advantage of the vector units.

As research in parallel computation has come to the forefront of computer science in recent years, parallel algorithm designers have had to struggle with the complications imposed by a large network of processors working to solve a single problem. As the number of processors increases, experimental evidence indicates that *communication bandwidth* (throughput), rather than latency, becomes the bottleneck limiting the scalability of parallel algorithms. Thus, choosing the correct communication sub substrate for one's parallel computer is of paramount importance to its performance. Because of the versatility of an interconnection graph known as the *hypercube*, it looked very attractive to machine designers in the recent past, and was used in the CM-2, Cosmic Cube,

Figure 21.1: The Hypercube for $d = 3$

and N-Cube (one is located here at MIT, in the Earth Resources Laboratory).

A Hypercube graph consists of:

1. d Dimensions
2. 2^d Vertices
3. $(b_0 \dots b_{d-1})$ and $(b'_0 \dots b'_{d-1})$ are connected by an edge if *and only if they* differ in exactly one bit.

There are $d2^{d-1}$ edges in a hypercube of dimension d .

A picture of the three-dimensional hypercube may not be as helpful as it would seem, but is included as Figure 21.1.

On a sad note, the hypercube design for the most part has been abandoned. Network routing today is often randomized, taking away the users' control over network communication. Fat trees, consisting of interconnection trees in which the processors are nodes and the links near the root have a proportionately higher bandwidth, are now enjoying acclaim. They have a lower edge count than hypercubes (not counting bandwidth per edge) and win under randomized communication schemes.

21.2.1 The Gray Code and Other Embeddings of the Hypercube

A hypercube is an amazingly versatile medium on top of which familiar and useful topologies can be easily created. Perhaps the most basic such embedding is the *Hamiltonian Path*¹, a topology in which the nodes appear to be in a ring, so that each node has two neighbors and a message traveling along the ring encounters each node exactly once. Finding such a path in a d -dimensional

¹A Hamiltonian Path is one which touches each node of a graph exactly once. Contrast with an Eulerian Path.

hypercube is easy because of the existence of a d -bit *Gray code*.

The Gray Code is named after Frank Gray, who formalized it in the 1940's while working on radar-related engineering problems. Given a rapidly changing binary output from a physical measuring device, sampling accuracy can be improved by using the Gray Code to encode adjacent numbers rather than conventional binary. The code was originally invented by Emile Baudet (1845-1903) for telegraph communication optimization—proper equipment can send several telegraph signals down the same wire to maximize bandwidth under fixed physical constraints.

The Gray Code for $d = 3$ embeds a Hamiltonian path in the three-dimensional hypercube shown above:

GRAY CODE	TRANSITION SEQUENCE
0 0 0	
0 0 1	0
0 1 1	1
0 1 0	0
1 1 0	2
1 1 1	0
1 0 1	1
1 0 0	0

Each time we advance from one element of the Gray Code to the next, we move along a single dimension. The *transition sequence* is merely the sequence of such change directions mapped out as the Gray Code sweeps along its Hamiltonian path. (As a single bit must change at every step, only the dimension of the changed bit, 0, 1, or 2, in this case, must be described.)

To build a Gray Code for d dimensions, one need only take the Gray Code for $d - 1$ dimensions, reflect it top to bottom across a horizontal line just below the last element, and add a leading one to each new element below the line of reflection. Given that, you can see how the Gray Code above was derived easily from the Gray Code for $d = 2$:

GRAY CODE
(LOCATION OF VERTEX)
0 0
0 1
1 1
1 0

21.2.2 Going Beyond Embedded Cycles

We are not limited to cycles; now that the Hamiltonian cycle has been described, we can use it to embed a *grid* inside a hypercube. For example, suppose we have a $d = 5$ hypercube. We can group the bits together like $d_4d_3|d_2d_1d_0$, where the left group is given two bits, and the right group three. By using *two independent Gray Codes* for the two sets of bits, we can index into the total set of nodes using *two numbers*. Each number determines a sequential position in one of the Gray Codes (or, equivalently, along one of the Hamiltonian cycles mapped out by them), so that together they completely specify a unique node. By sweeping through the Gray Code mapped to the top two bits, the position moves up and down a “column,” and by sweeping through the code mapped to

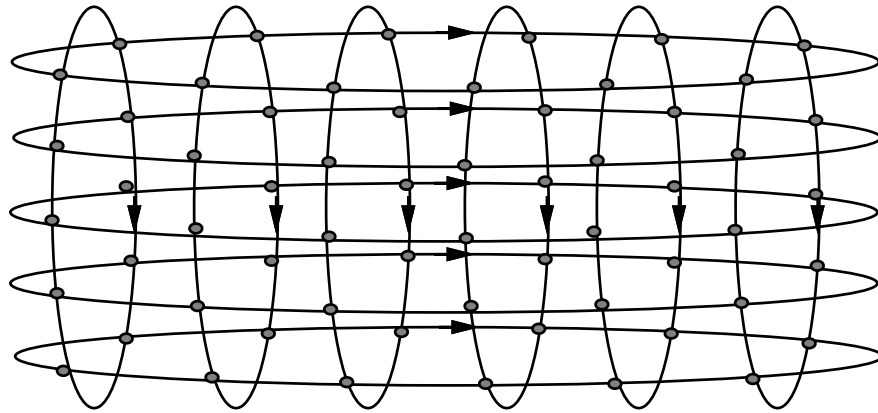


Figure 21.2: Embedding a Two-dimensional Grid in a Hypercube by bit-field partitioning.

Two Distinct Embedded Hamiltonian Paths

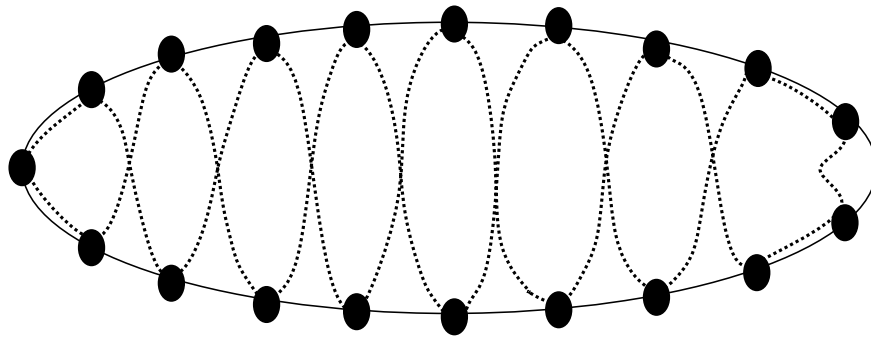


Figure 21.3: Two edge-disjoint Hamiltonian paths spanning a set of nodes.

the lower three, the position moves back and forth in a “row”. The result is a grid like that shown in Figure 21.2. Three dimensional (or even higher dimensional) grids could be generated using this bit-partitioning technique—we are not limited only to two dimensions.

Finally, note that in a hypercube of high dimensionality, several distinct Hamiltonian paths (spanning the entire set of nodes) can exist which have no (directed) edges in common. A set of nodes can thus be spanned by two completely separate loops around which information can be passed without worrying about collisions. An example of this is shown in Figure 21.3.

21.2.3 Hypercube theory: Unique Edge-Disjoint Hamiltonian Cycles in a Hypercube

Consider in more detail the question of how many edge-disjoint Hamiltonian cycles exist for a hypercube in d dimensions. (If two Hamiltonian cycles traverse an edge in opposite directions, they will be considered edge-disjoint for our purposes.)

For hypercubes of even dimension, there are exactly d edge-disjoint Hamiltonian paths. This is not surprising, since from above we know that a hypercube of dimension d has exactly $d2^{d-1}$ edges. Doubling this number to account for both directions of an edge and dividing it by the number of

edges in a Hamiltonian path (2^d , since that's the total number of nodes) *also yields* d . The match tells us that *all edges* can be part of the set of edge-disjoint Hamiltonian paths in a hypercube of even dimensionality.

Strangely, for hypercubes of odd dimension, *there are only $d - 1$ edge-disjoint Hamiltonian paths.*² Since the same edge-use analysis applies as did in the case of hypercubes of even dimension, we conclude some edges must not be used.

We can prove the assertion in the case of $d = 3$. Let's consider a single Hamiltonian cycle embedded in the hypercube of dimension three, as depicted in flattened form in Figure 21.4(a). It should be clear that in three dimensions, any Hamiltonian path can be rotated onto the one shown, so that there is no loss of generality in assuming the presence of the particular path shown. To see this, simply note that each two-dimensional slice of the $d = 3$ cycle must be a cycle in two dimensions (lacking one edge). The cycle in two dimensions is unique except for direction. Furthermore, it can be combined with another such cycle only in one way to form the three-dimensional Hamiltonian cycle. Given this pre-existing cycle in a hypercube of dimension 3, we assume that two additional edge-disjoint Hamiltonian cycles exist in the same hypercube, and produce a contradiction.

The proof is quite simple. Consider in turn the lower-left and upper-left corners of Figure 21.4(a). In the lower-left corner, there are two possibilities for edges entering the corner, and two possibilities for edges leaving. These can be combined to form segments of two paths in a unique way³, so we have determined the behavior at that point of the two additional edge-disjoint Hamiltonian cycles which we assumed existed. See Figure 21.4(b). A similar analysis can be made for the upper-left corner; we again are led to a unique pair of path segments which must belong to the two new edge-disjoint Hamiltonian cycles, as shown in Figure 21.4(c). The only logical way to connect the segments found in Figures 21.4(b) and 21.4(c) is shown in Figure 21.4(d).

We are almost done. Look at the point marked X on Figure 21.4(d). When the path we have just connected gets to this point, it cannot go to the right, for that edge has already been used for rightward travel by the original Hamiltonian cycle. It certainly can't go back out the way it came in. Thus, it must go down, to the point marked Y. *However, this would form a closed loop consisting of four nodes!* Such a loop might be part of larger loop, but then it wouldn't be *Hamiltonian*, since it would pass through two nodes twice.

Since we have reached a contradiction, we conclude there are not two additional edge-disjoint Hamiltonian paths in the three dimensional hypercube, and in fact only one additional such path. Just reverse the direction of the original Hamiltonian path to find it.

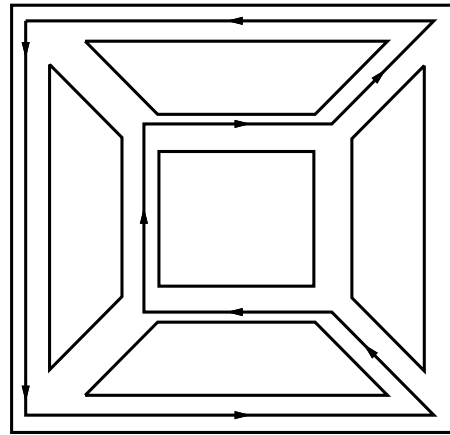
21.2.4 An Application: Matrix Multiplication on a Grid

The first algorithm for matrix multiplication on a grid is Canon's. This algorithm is designed for two dimensional grids. It still can run very fast on the CM-5 using CSHIFTS, which will be shown later.

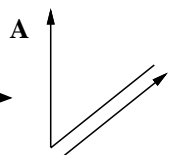
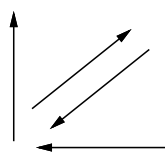
The goal is to find \mathbf{C} where $\mathbf{C} = \mathbf{A} * \mathbf{B}$ and \mathbf{A} , \mathbf{B} and \mathbf{C} are all matrices. Canon's algorithm involves two steps: a skewing step and a Systolic step. In the skewing step, the rows of \mathbf{A} are slid to the left (with wraparound), such that each row is slid to the left a number of slots equal to its row number, with the first row not moving at all. The *columns* of \mathbf{B} are, analogously, each slid upwards a number of slots equal to their column number, with the first column not moving at all. These movements are an effort to achieve a special configuration of the data which will be used by

²I am reminded of the famous vector-field theorem which states that a vector field can exist on the surface of a ball in n dimensions without a singular point iff n is even. Could these two results be related?

³A Hamiltonian cycle in no case immediately backtraces an edge it has just traversed; this provides the uniqueness.

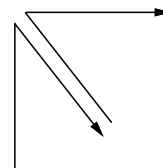


(a) A single Hamiltonian cycle in the $d = 3$ hypercube

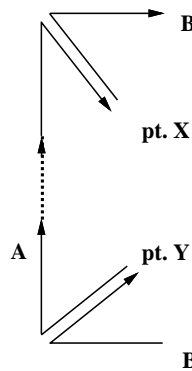


B

(b) The set of legal incoming and outgoing directed edges at the lower left corner for new Hamiltonian paths



(c) The set of legal Hamiltonian cycle segments at the upper-left corner



(d) Path segment A cannot go right at pt. X because of the original Ham. cycle. But if it goes down it forms a closed loop of 4 nodes!

Figure 21.4: Proof that for the $d = 3$ hypercube there are only 2, not 3, edge-disjoint Hamiltonian cycles.

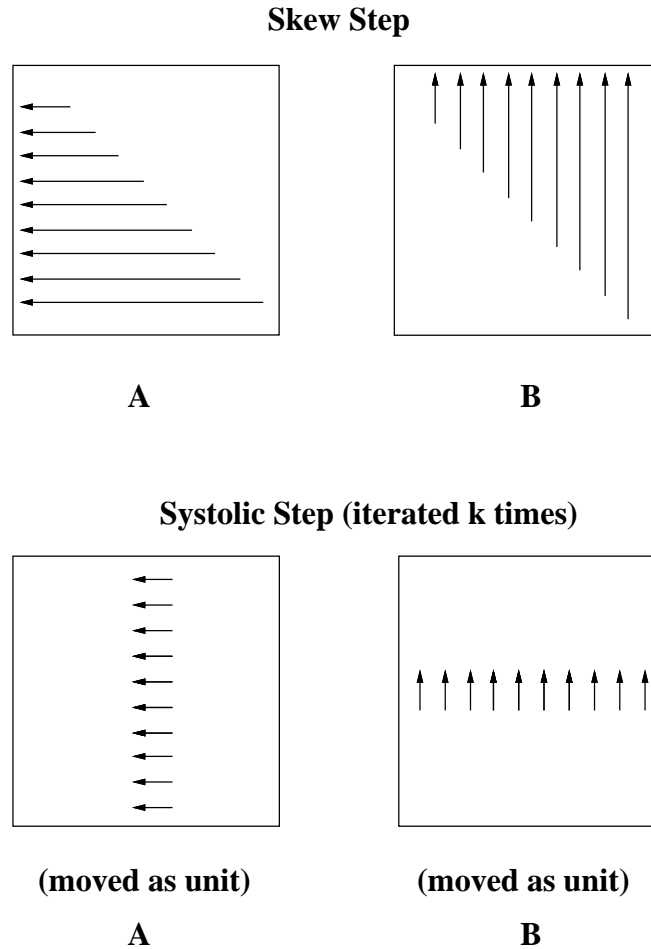


Figure 21.5: Geometry of Canon's Algorithm

the following Systolic step. In the systolic step, we perform k iterations, moving **A** horizontally one slot (as a whole) and **B** vertically one slot (also as a whole) in each iteration. As the iterations go by, the products of the elements of **A** and **B** that pass by a location are accumulated into that location, and at the end the product **C** has been computed in each row and column position.

1. Skewing Step

$$A_{i,j} \leftarrow A_{i,i+j} \quad (\text{modulo } n)$$

$$B_{i,j} \leftarrow B_{i+j,j} \quad (\text{modulo } n)$$

2. Systolic Step

$$C_{(i,j)} = \sum_{k=0}^{n-1} A_{i,j+k} B_{i+k,j}$$

This algorithm is depicted symbolically in Figure 21.5.

Another method for matrix multiplication involves broadcasts on a grid. Thinking about this algorithm on a grid of n^2 processors reduces a matrix multiply to $O(n)$ time (Ref. Bertsekas 77).

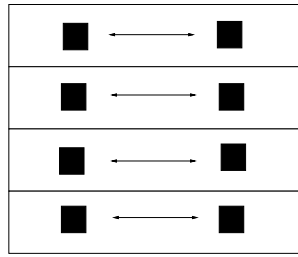


Figure 21.6: Multiple Row Sends

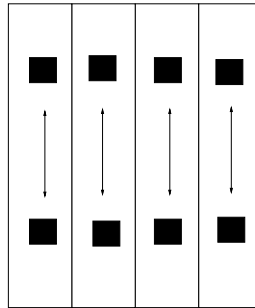


Figure 21.7: Multiple Column Sends

Imagine a $n * n$ processor machine with a block of matrix \mathbf{A} and matrix \mathbf{B} on each node (you can imagine one element on each node, just don't tell Prof. Edelman).

1. Each processor sends $a_{i,j}$ to all the other processors in the i^{th} row. ($a_{i,j}$ is the (row i , column j) element of matrix \mathbf{A}). On a graph this operation looks like Figure 21.6.
2. Each processor sends $b_{i,j}$ to the processors in the j th column. This operation is shown in Figure 21.7.
3. The matrix \mathbf{C} is formed on each node by

$$\sum_1^n a_{i,j} b_{i,j}$$

This algorithm can also be implemented using C-SHIFTS. This can be easily pictured in Figure 21.6 and Figure 21.7.

Another way of improving Canon's algorithm (systolic step) can be easily pictured. In the original implementation, each element of a block in \mathbf{A} was sent to the left (to its western neighbor), and

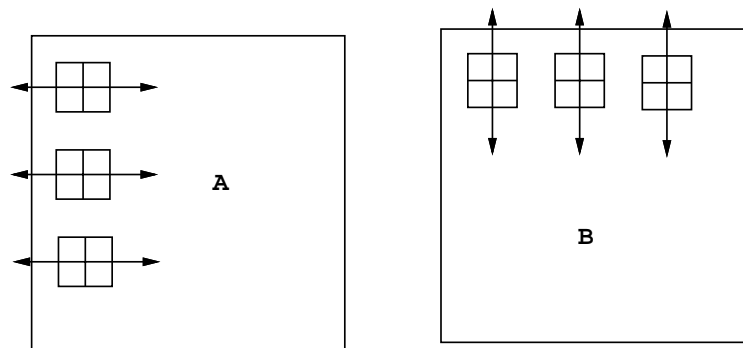


Figure 21.8: Two Direction Matrix Multiply

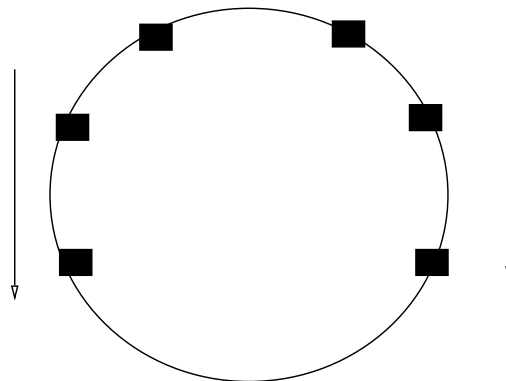


Figure 21.9: Two Direction Ring

each element of a block in \mathbf{B} was sent up (to its northern neighbor). Thus, in each dimension, the ring of connections was only used unidirectionally. The improvement consists in allowing each ring to be used *bidirectionally*. Each block of the \mathbf{A} matrix can be divided into left and right halves while each block of the \mathbf{B} matrix can be divided into top and bottom halves. Matrix \mathbf{A} can simultaneously send information east and west while \mathbf{B} can simultaneously send information north and south. In such an operation, the elements of a block in \mathbf{A} in the block's right half are sent east, and the elements of a block in \mathbf{A} in the block's left half are sent west. Similarly, the elements of a block in \mathbf{B} in the block's top half are sent north, while the elements of a block in \mathbf{B} in the block's bottom half are sent south. This does not change the geometry of the information storage in each matrix, and thus the multiplication occurs after much less the communication time. Figure 21.8 describes this operation pictorially.

This method can be best thought of as a ring going in two directions, as is shown in Figure 21.9.

21.2.5 The Direct N-Body problem on a Hypercube

The simplest way to solve the direct N-body problem on a hypercube is to create two copies of the set of bodies, one stationary and one moving, allocated to the nodes spanned by a single large

Hamiltonian cycle. In each step, the moving bodies advance along the fixed Hamiltonian path one unit, and interaction computations occur in parallel at each node adding the effects of the current pair of bodies to the accumulated sum. To increase efficiency, two edge-disjoint Hamiltonian cycles spanning the nodes of a hypercube can be used instead of a single cycle, as was shown in Figure 21.3. The advantage of this approach is that two sets of moving bodies can be present (each set moving along one of the Hamiltonian cycles) so that the effects of two pairs of bodies are accounted for per systolic step.

A faster method for a direct N-Body solution can take advantage of the hypercube graph and the transition sequence (of a Gray Code) described earlier. A dynamic and static copy of each body can be made at every node. The dynamic body will move around the hypercube changing along the dimension dictated by the transition sequence of a fixed Gray Code. Every body will follow the transition sequence, but not necessarily the Hamiltonian Cycle. The body at (0,0,0) will follow the Hamiltonian cycle exactly, while others will follow in a similar sequence, but not right behind on the same path. Each body will be on a different path, but no body will cross another or “step on another body” at the same moment in time.

In order to define how the bodies other than the one at the zeroth node move, we must introduce the concept of the Hamming sum. (The zeroth node moves exactly in a Hamiltonian path, using the transition sequence derived from that path.)

21.2.6 The Hamming Sum

The Hamming sum will help create an optimal matrix multiply algorithm for the hypercube.

The Hamming Sum is defined as

$$b_{d-1} \dots b_0 \oplus b'_{d-1} \dots b'_1 b'_0 = b_{d-1} \oplus b'_{d-1}, \dots, b_1 \oplus b'_1, b_0 \oplus b'_0$$

where \oplus is an *exclusive or* operation. It is essentially just a bitwise exclusive-or operation. (We can now define the **transition sequence** conveniently as the bit position for which $g_i \oplus g_{i+1}$ is 1—the dimension along which the Gray Code changes in that step.)

Let's pick a fixed Gray Code G_0 . Then the direct N-Body algorithm puts the body that starts at vertex v into the vertex $v \oplus g_k$ at the k^{th} step, where g_k is the k^{th} element of G_0 .

21.2.7 Extending Gray Code-directed Body Movement to Multiple Sets of Bodies

Heretofore, we have been discussing a *single set of moving bodies*. The one at the zeroth node moves in a Hamiltonian cycle, and the others move in similar paths derived from the original Hamiltonian cycle using the node's position and the Hamming sum. Now, however, we consider *multiple sets of moving objects*. For the sake of argument, let's assume we have a three-dimensional hypercube and three sets of moving objects—a red set, a blue set, and a green set. We want to move each colored set according to the rules just defined for a single set. Obviously, we can't assign G_0 to be the Gray Code for each of the three colors, since that would cause the objects on the zeroth node to travel the exact same Hamiltonian path at the same time and collide. (Assume only a single object can be sent along a wire at one time.) What can be done to use “all of the wires all of the time”?

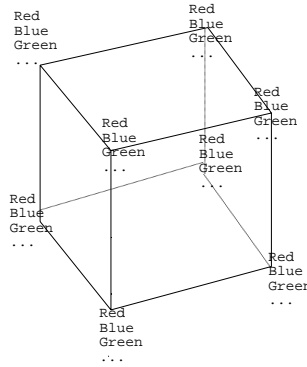


Figure 21.10: N-Body Breakup on a Hypercube

The solution is to note that there are many Gray Codes for a given bit vector length. New Gray Codes can be created from existing ones by *shifting the columns of bits one or more positions to the left, wrapping around when columns move off the left side*. For example, using our previous table, we could make the transformation:

OLD GRAY CODE	OLD TRAN. SEQ.	NEW GRAY CODE	NEW TRAN. SEQ.
LOC. OF VERTEX		LOC. OF VERTEX	
0 0 0		0 0 0	
0 0 1	0	0 1 0	1
0 1 1	1	1 1 0	2
0 1 0	0	1 0 0	1
1 1 0	2	1 0 1	0
1 1 1	0	1 1 1	1
1 0 1	1	0 1 1	2
1 0 0	0	0 0 1	1

Note that the transition sequences of these two Gray Codes are related in a special way. The second can be produced from the first by adding a 1 (modulo 3) to each element of the first's transition sequence. In fact, there is a third unique Gray Code, which can be produced from the first by adding a 2 (modulo 3) to each element of the first's transition sequence. In general, given a hypercube in $d = k$ dimensions, there are k unique Gray Codes. (Gray codes which represent the same path but traversed in an opposite direction are not counted as unique.)

Thus, if in three dimensions we call these different Gray Codes G_0 , G_1 , and G_2 , we know by how their transition sequences can be derived that, *at any given node of the hypercube*, the transition sequence elements of G_0 , G_1 , G_2 are all different. Because of this, if we allow one set of dynamic bodies to be controlled by Gray code G_0 , another by Gray Code G_1 , and the last by Gray Code G_2 , we may safely conclude that at any instant in time the red, blue, and green objects that were at the zeroth node at time $t = 0$ follow the Hamiltonian paths implied by G_0 , G_1 , and G_2 *without colliding*.

You may be asking, "You proved earlier that you can't have 3 edge-disjoint Hamiltonian paths on a hypercube in three dimensions!?! What's going on?!" The question is good one to ask, but is

not difficult to answer. Before, we were talking about *edge-disjoint cycles*—paths which never pass down the same edge going the same direction. Here, we're talking about *time-edge-disjoint* cycles. We don't care whether the red, green, and blue objects that were at the zeroth node at $t = 0$ ever travel down the same wire in the same direction, we only care whether they might do so *at the same time*. As the transition sequences are related by modulo arithmetic in our scheme, a collision is impossible.

Thus, by taking different colored sets of bodies, assigning Gray Codes related by column shifts to those sets, and moving each set around using its assigned Gray Code and the Hamming sum as described above, we can *use all the wires all the time*. In fact, this set up can be used to extend the grid multiplication routine (with the skew and systolic phases) presented earlier so that instead of using only a two-dimensional grid embedded in the hypercube, it uses the hypercube's full connectivity.

21.2.8 Matrix Multiplication using all Hypercube Wires

We can use every connection of the hypercube on every iteration by using the Hamming sum in the calculation of the matrix product. To do so, we require only that the matrices to be multiplied are square, and that the hypercube we are given is of an even dimension. We first split the complete bit-field specifying location in the hypercube into a left and right half, each of which is subsequently addressed as a bit-field of length $d/2$. Using a Gray Code in $d/2$ dimensions, g_k , and the hamming sum on $d/2$ -length bit fields, we can perform a matrix multiply in two phases:

1. Skewing Step

$$\mathbf{A}_{ij} \leftarrow \mathbf{A}_{i,i} \oplus_j$$

$$\mathbf{B}_{ij} \leftarrow \mathbf{B}_i \oplus_{j,j}$$

2. Systolic Step

$$\mathbf{C} = \sum_k \mathbf{A}_{i,j} \oplus_{g_k} \mathbf{B}_i \oplus_{g_k,j}$$

In each case, when a variable is subscripted by two expressions separated by a comma, the left one refers to the left $d/2$ -bit field, and the right one refers to the right $d/2$ -bit field.

21.2.9 Matrix Multiplication using the Cartesian Product

If \mathbf{A} is any graph with the Cartesian product that allows k time-wise edge-disjoint cycles, then the Cartesian product of the graph with itself can be used for matrix multiplication. This is essentially a generalization of the idea we used above when we split the original d -bit field of the hypercube given to us into two $d/2$ -bit fields, and formed a Cartesian product of those fields in order to carry out the matrix multiplication in matrix equations immediately above.

21.3 References

[1] Bertsekas, Dimitri, et al. *Parallel and Distributed Computation*. Prentice hall, New Jersey. 1989.

[2] Leighton, F. Thomson. *Introduction to Parallel Algorithms and Architectures: Arrays, Trees, Hypercubes*. Morgan Kaufmann, San Mateo, California, 1992.

Parts of these notes were taken from last year's notes written by Scott Wallace.

Chapter 22

Scalable Algorithms

22.1 Scalability, Communication Cost, and Matrix-Vector Product

Parallel computation of the product $y = Ax$ of a matrix $A = [a_{ij}]$ and a vector x turns out to be really important. It is the "inner loop" computation in all iterative methods for solving the linear system $Ax = b$. It occurs in the inner loop of all explicit methods for time-dependent PDEs (and in explicit integrators for the linear system of ODEs $y'(t) = Ay(t) + b(t)$). Moreover, from the parallel implementation viewpoint, it is identical to the computation at the heart of a lot of important parallel graph algorithms. For now, we'll restrict our attention to square matrices with symmetric zero structure. Recall that the graph of A , $G = (V, E)$, has a vertex for every row, and an undirected edge from vertex i to vertex j if a_{ij} and a_{ji} are nonzero. Now, since

$$y_i = (Ax)_i = \sum_j a_{ij}x_j = \sum_{(i,j) \in E} a_{ij}x_j,$$

we can view the matrix vector product as a "graph" operation" as follows. Associate x_i and y_i with vertex i of G , and a_{ij} as a weight on edge (i, j) . To compute y_i , communicate the value of x from each neighboring vertex to vertex i , multiply it by the weight of the connecting edge, and add these together with $a_{ii}x_i$.

The parallelism aspects are clear. Each element of Ax can be computed independently of all others. Each of these tasks requires a row of A and an element of y , and some subset of the elements of x , those corresponding to the nonzero elements of the given row of A . If *even more* parallelism is required, one could use several processors per element of Ax , each owning a subset of the corresponding row of A , with a sum-reduction after they compute independently. Such techniques are useful on the Maspar, with its 16,384 processors, but not on mainstream machines with a few hundred processors.

Quite surprising and complex algorithmic ideas are required to produce good efficiency for this computation on distributed memory machines, as we shall see. The issue is communication cost. Matrix-vector is a hard problem because there is not a whole lot of arithmetic to be done: only one flop per element of the matrix. So, unlike the situation with matrix multiplication, we cannot expect to do a lot of flops per datum, unless we map the work to the processors and the data to the processors so that the data needed to do the work are already on the processor doing the work, most of the time.

Let's recall the definitions of speedup and efficiency. If we solve a problem like matrix-vector product, there is a parameter n that describes the size of the problem. Suppose we solve it on one

processor in time $T(n, 1)$ and on p processors in time $T(n, p)$. Then the speedup is

$$S(n, p) = \frac{T(n, 1)}{T(n, p)}$$

and the efficiency is

$$E(n, p) = S(n, p)/p.$$

The goal of parallel algorithm research is algorithms that minimize $T(n, p)$. We've found it useful to consider what happens when we let p get large. In essentially all cases, if we fix the problem size n we find that the efficiency starts to drop, and goes to zero as p grows. So, to deal with the *scalability* of an algorithm, one has to allow n to grow with p . How fast? Well, it should grow fast enough so that the efficiency does not drop off to zeros. In other words, we will ask, for a given parallel algorithm, how fast does the problem have to grow as p grows in order to obtain the bound:

$$E(n(p), p) \geq E_0 > 0 \quad \text{as } p \rightarrow \infty$$

(We're essentially deriving a formula for the contours of the function E in the (n, p) plane — what one wag once called the “isogoodbars”.)

Well, for most algorithms, one can find such a growth rate $n(p)$ that saves the efficiency. So are these algorithms all scalable? What would it mean if n grows so fast that each processor quickly runs out of memory? It would not be too useful. For that reason, I like the definition of scalability that requires that the growth in n required to bound E away from zero be such that the memory required *per processor* be $O(1)$ (for strict scalability) or not more than $O(\log^\alpha p)$ (for a weaker but useful notion of scalability.)

Back to matrix-vector product. One complication is this. We have to map the vectors x and y the same way. That's because they later will participate in operations like the DAXPY, $y \leftarrow \alpha x + y$, or the dotproduct $x^T y$, which require this *alignment* of x and y . So we might as well align them right from the beginning.

Here is the solution. For dense matrices A , the right thing to do is to map blocks of the matrix to a $\sqrt{p} \times \sqrt{p}$ processor grid. For sparse matrices A with a random structure, such as the one used in the NAS parallel conjugate gradient benchmark, the same style of mapping is best. But for sparse matrices coming from PDE applications, it's best to consider the graph of the matrix, map its vertices to the processors using a locality preserving mapping, and then map either the rows or the columns of A using the given mapping.

With dense or random sparse matrices, mapping the matrix rows doesn't lead to a scalable algorithm. Let's analyze the dense $n \times n$ case. Each processor gets n/p rows. WLOG they can be contiguous. The processor that gets a row also gets the corresponding elements of x and y . To compute its part of y it needs *all* of x . Thus, the first step is to communicate x , which begins as a *distributed* and ends up as a *replicated* vector. In message passing parlance this is called a *collect* operation, in MPI it is implemented by `MPI_Allgatherv`, and if we were writing it in HPF, we could express it as a realignment from the original alignment to a replicated alignment:

```

      REAL XDIS(N), XREP(N)
!HPF$ TEMPLATE, DISTRIBUTE(BLOCK) :: T(N)
!HPF$ DISTRIBUTE XDIS(BLOCK)
!HPF$ ALIGN XREP(I) WITH T(*)    ! Replicated alignment
...
      XREP = XDIS    ! Uses MPI_Allgatherv ?

```

Matrix vector product on the SP-2, $n = 2048$

p	Mflops (2D Map)	Mflops (1D Map: $p \times 1$)	Mflops (1D Map: $1 \times p$)
1	60.	60.	60.
2	179.	180.	125.
4	305.	422.	255.
8	665.	805.	432.
16	1120.	1153.	659.
32	2082.	959.	827.

We'll now introduce a very important technique for the analysis and understanding of a distributed memory computation. We can get very useful lower bounds on running time by consider the volume of communication. What does the collect cost? We don't care, for analysis of scalability, about constant factors. By considering the bandwidth with which a processor can send and receive data, we see that it takes $O(n)$ time, regardless of p , to receive all of x . That's because every processor has to accept $n(p-1)/p$ elements of x — the ones it doesn't own — and can only accept data at some fixed rate. Thus, we have a lower bound on communication time that is $O(n)$, independent of p . So, since there is $O(n^2)$ work to do, we can't remain efficient with more than $O(n)$ processors. In other words, as the problem grows in size, we can increase p only as the square root of the required total memory. Thus, each processor will have to store a constant number of columns or rows, and its memory requirement will grow linearly with the machine size! This is not a scalable algorithm.

On the other hand, if we do a two-dimensional mapping of the data:

```
!HPF$ DISTRIBUTE A(BLOCK, BLOCK)
```

onto a $r \times s$ virtual grid of processors, then each processor only needs n/s elements of x and produces part of n/r elements of y . The required collects of x occur within processor columns. (MPI_Allgatherv again.) Then a summation of elements of y that each processor has computed must be done within processor rows. The MPI routine MPI_Reduce_scatter does the trick. (In MPI, we use collective communication routines with a communicator for each processor column and another communicator for each processor row — see Lecture LLLL.) We choose r and s to be $O(\sqrt{p})$. Thus, communication time is $O(n/\sqrt{p})$, much less than with the by-rows mapping. In fact, we can now take p to be $O(n^2)$. If we do this, communication volume is not the limiting factor. Both arithmetic cost and communication volume give $O(1)$ lower bounds on the parallel execution time. But the critical path (for summing the elements in rows) is $O(\log n)$ long, so it dominates. (If we take $p = O(n^2/\log n)$ then we can maintain constant efficiency, with polylog memory growth — yielding a scalable, if not strictly scalable, algorithm.)

Lewis, Payne, and van de Geijn have described a very efficient implementation of the NAS CG benchmark using this idea, and paying careful attention to the mapping of x and y too. They use a (CYCLIC, BLOCK) mapping of A . Element i of x and of y are mapped to the (one and only) processor in the same row as row i of A , and the same column as column i of A . Then a collect of x within processor columns and a distributed sum of y in processor rows produces y in the right place. (Reference: J. G. Lewis, D. G. Payne, and R. A. van de Geijn, "Matrix-Vector Multiplication and Conjugate Gradient Algorithms on Distributed Memory Computers," Scalable High Performance Computing Conference 1994.)

Here are some data from the SP-2. The code is in `MPI_Examples/matvec.c`

Here you see the typical situation. The unscalable algorithm “hits a wall”. On the other hand, there is a region in the (n, p) plane in which the scalable algorithm is as much as 20% slower than the “good” one-dimensional algorithm. Life is not always so simple. You might consider why the (BLOCK, *) mapping is better than the (*, BLOCK) mapping of the matrix.

22.1.1 Sparse Matrices

One idea is to treat sparse matrices the same way as dense, and map the matrix blocks. If we think in terms of the graph of the sparse matrix, then we are mapping subsets of the *edges* rather than the vertices to the processors.

If this is naively done, there may be processors that get no nonzero elements. We’ll have lousy load balance. To correct this, we would first permute the rows and the columns independently to equalize the load. One could use a random permutation (this idea was pushed in A. T. Ogielski and W. Aiello, Sparse matrix computations on parallel processor arrays, *SIAM J. Scient. and Stat. Comput.* 14 (1993), pp. 519–530) which balances the load pretty well with good probability. Or one can choose the permutation by some heuristic load balancing technique. We’ll discuss these in Lecture XXXXX.

The sparse matrices that arise in applications of PDE’s have a property that neither full nor random sparse matrices share. It’s that their graphs have small, balanced separators. This means that the graphs may be partitioned into two roughly equally large subgraphs in such a way that most edges are internal to a subgraph, and only a few connect vertices in different subgraphs. We may recursively partition the subgraphs until we have as many vertex subsets as there are processors. We then assign the subgraphs to the processors, together with the elements of x and y and the rows of A that correspond to its vertices. (An alternative is to map the corresponding columns.) The communication we require is this: each processor gets the elements of x that correspond to vertices adjacent to its vertices but mapped to other processors.

Because of the small separators, this communication is tolerable. Consider a $k \times k$ grid graph. It has $n = k^2$ vertices and can be separated into two $k \times k/2$ subgraphs with an edge separator having $k = \sqrt{n}$ edges. Map each half to one of two processors. If k is big enough, then the per-processor computation time, which is $O(k^2)$ dominates the communication time, which is $O(k)$. Got 2^q processors? No, problem, just recursively bisect the graph q times, to produce a binary tree of subgraphs with the right number of “leaf” subgraphs. If we scale the machine up to more processors, we need only scale the number of grid points proportionally to the number of processors in order to maintain constant efficiency. This is what we mean by a “scalable” algorithm.

What graphs have small separators? A famous theorem of Lipton and Tarjan asserts that any *planar* graph has an $O(\sqrt{n})$ separator into balanced subgraphs. Lots of nonplanar graphs also have $O(n^e)$ separators for $e < 1$; most notably, three dimensional finite element graphs, for which e should be around $2/3$. Some recent theoretical work has characterized some sets of graphs that provably have this property. The trick is to compute those small separators. That’s the topic of another lecture, by Shang-hua Teng.

22.1.2 Parallel iterative Solvers

One can write a book on solving linear systems $Ax = b$ by iterative methods, and another on parallel implementation of these. Here I want to hit on a couple of important points.

First, conjugate gradient methods have become the standard tool. In a CG method, you need to be able to do matrix vector products and vector dot products fast. We’ve discussed the former, and the latter are simple. So what’s left to talk about?

It turns out that the most important thing one can do to efficiently solve $Ax = b$ in practice is the *change the problem!* You pick a matrix B , which has to be nonsingular, and you solve $BAx = Bb$ instead. B is called the *preconditioner*. The trick is to pick B so that fewer iterations are required to get the desired accuracy, and BAx is not much more expensive to compute than Ax . (Some prefer to solve $ABy = b$ for y , and then recover $x = By$. This is “right” preconditioning, while $BAx = Bb$ is “left” preconditioning. $BACy = Bb$ followed by $x = Cy$ is also possible.)

Often, the preconditioner is not explicitly given. For example, B may be $(LU)^{-1}$ where $LU \approx A$ is an approximate triangular factorization of A ; such methods, based on “incomplete” factorization in which the zero structure of L and U is predetermined and very sparse, became quite popular in the 70s and are very effective in practice. Many other possibilities exist. One important one is to use one or more iterations of some simpler iterative method, like SOR or multi-grid, as the preconditioner. For parallel machines, polynomials in A can be used, too.

When B is implicitly given, parallelism may be lost. For example, if A is tridiagonal, and B is given by an LU decomposition, we will have some trouble, even though we converge in one iteration!

Consider SOR as a preconditioner. We need to consider the parallel complexity of the SOR method. Consider the graph of A . In SOR, you visit the vertices in some order, solving for the unknown at each vertex visited while holding fixed the unknowns at the neighboring vertices. For a grid graph (a $k \times k$ mesh) we usually think about a row-by-row sweep over the graph. If we implement this in parallel, we can visit the diagonals of the graph and relax them simultaneously! This reordering of the vertices does not change the result at all. So we can perform the sweep in $O(k)$ parallel steps. On the other hand, suppose we visit first the points (i, j) for which $i + j$ is even, then the points for which $i + j$ is odd. The even points have only odd ones as neighbors, and vice versa. So we could relax all the even points in one parallel step and all the odd ones in a second parallel step. This ordering makes SOR much more parallel. It is known as “red-black” SOR (think of a checkerboard).

How about SOR on other sparse matrices? We need to color the graph of the matrix, assigning colors to vertices so that no adjacent vertices have the same color. (Remember the four-color map theorem?) Once that’s done, all vertices of a given color can be relaxed in parallel, and the number of parallel steps for an SOR sweep is the number of colors we used. (Minimizing this — the minimum is the chromatic number of the graph — is too hard to do in practice. But there is a simple, fast, greedy algorithm that does pretty well.)

What about LU preconditioners. Suppose we require that $L + U$ has the same zero structure as A — i.e. we allow no fill in the incomplete factorization. Then we can parallelize the triangular solvers that implement $B + (LU)^{-1}$ with the same technique of multicoloring. If we order the gridpoints in such a way that all the points of a given color occur consecutively in the ordering, then A , L , and U develop a very nice block structure. For each color, A has a diagonal block that is itself diagonal. Since L and U inherit the structure of A , they have these diagonal blocks as well. I never thought one could use “diagonal” twice in a row in a correct sentence. Now, during the solution of, say, $Ly = f$, one can solve simultaneously for a chunk of the vector x that corresponds to one of the diagonal blocks of L in a single parallel step. The number of steps is the number of colors, again.

The idea of multicolored approximate LU is due to Schreiber and Tang. Plassman, Jones, and Freitag have used these techniques in some very large parallel computations at Argonne, and have produced a parallel solver based on them. The URL for their work is <http://www.mcs.anl.gov/Projects/blocksolve/index.html>

The number of parallel steps can be further reduced by a factor of two. Consider a pair of adjacent diagonal blocks of L , wlog let them be L_{11} and L_{12} . Now consider the whole block two-

by-two submatrix consisting of (in Matlab notation) $[L(1,1), 0; L(2,1), L(2,2)]$. What is its inverse? What is the structure of it? Could it be economically precomputed and used in solving $Ly = g$?

Further ideas about efficient parallel solution of sparse triangular systems can be found in “Highly parallel sparse triangular solution,” by Alvarado, Pothén, and Schreiber, which appears in *Graph Theory and Sparse Matrix Computation*, pp. 141–157. The IMA Volumes in Mathematics and Its Applications, Volume 56, Springer-Verlag, 1993.

Chapter 23

Scheduling on Parallel Machines

Chapter 24

Shared Memory Computations

Chapter 25

Scientific Libraries

25.1 Scientific Libraries

We give an example of scientific library using Thinking Machine CMSSL.

Dense Matrix Computations:

- *Basic Operations* inner product, outer product, matrix vector and vector matrix multiplication, matrix matrix multiplication, various norms of a matrices.
- *Dense Linear Systems*: Gaussian elimination, QR decomposition, matrix inversion and Gauss-Jordan solver.

Sparse Matrix Computations

- *Regular Grid Sparse Operations*: representation, gathering and scattering, permutation.
- *Linear Solvers for Banded systems*:
- *General Sparse Operations*: Sparse gather and scatter.
- *Iterative Solvers*: Krylov-based solvers.
- *Eigenvalue problem*: tridiagonal matrices and reduction to tridiagonal form, dense Hermitian matrices, real symmetric matrices by Jobobi rotations, k -step Lanczos algorithm, etc.

Communication Primitives

- *Polyshift*
- *All-to-All broadcast*
- *SParse communication*: sparse gather and scatter
- *Permutations*
- *Mesh partitioning*

Bibliography

- [1] N. Alon, P. Seymour, and R. Thomas. A separator theorem for non-planar graphs. In *Proceedings of the 22th Annual ACM Symposium on Theory of Computing*, Maryland, May 1990. ACM.
- [2] C. R. Anderson. An implementation of the fast multipole method without multipoles. *SIAM J. Sci. Stat. Comp.*, 13(4):932–947, July 1992.
- [3] A. W. Appel. An efficient program for many-body simulation. *SIAM J. Sci. Stat. Comput.*, 6(1):85–103, 1985.
- [4] I. Babuška and A.K. Aziz. On the angle condition in the finite element method. *SIAM J. Numer. Anal.*, 13(2):214–226, 1976.
- [5] J. Barnes and P. Hut. A hierarchical $O(n \log n)$ force calculation algorithm *Nature*, 324 (1986) pp446–449.
- [6] M. Bern, D. Eppstein, and J. R. Gilbert. Provably good mesh generation. *J. Comp. Sys. Sci.* 48 (1994) 384–409.
- [7] M. Bern and D. Eppstein. Mesh generation and optimal triangulation. In *Computing in Euclidean Geometry*, D.-Z. Du and F.K. Hwang, eds. World Scientific (1992) 23–90.
- [8] M. Bern, D. Eppstein, and S.-H. Teng. Parallel construction of quadtrees and quality triangulations. In *Workshop on Algorithms and Data Structures, Springer LNCS 709*, pages 188–199, 1993.
- [9] G. Birkhoff and A. George. Elimination by nested dissection. *Complexity of Sequential and Parallel Numerical Algorithms*, J. F. Traub, Academic Press, 1973.
- [10] P. E. Bjørstad and O. B. Widlund. Iterative methods for the solution of elliptic problems on regions partitioned into substructures. *SIAM J. Numer. Anal.*, 23:1097–1120, 1986.
- [11] G. E. Blelloch. *Vector Models for Data-Parallel Computing*. MIT-Press, Cambridge MA, 1990.
- [12] J. A. Board, Z. S. Hakura, W. D. Elliott, and W. T. Ranklin. Scalable variants of multipole-based algorithms for molecular dynamic applications. In *Parallel Processing for Scientific Computing*, pages 295–300. SIAM, 1995.
- [13] R. Bryant, *Bit-level analysis of an SRT circuit*, preprint, CMU (See <http://www.cs.cmu.edu:8001/afs/cs.cmu.edu/user/bryant/www/home.html>)
- [14] V. Carpenter, compiler, <http://vinny.csd.my.edu/pentium.html>.

- [15] T. F. Chan and D. C. Resasco. A framework for the analysis and construction of domain decomposition preconditioners. UCLA-CAM-87-09, 1987.
- [16] L. P. Chew. *Guaranteed-quality triangular meshes*. TR-89-983, Cornell, 1989.
- [17] P. G. Ciarlet. *The Finite Element Method for Elliptic Problems*. North-Holland, 1978.
- [18] K. Clarkson, D. Eppstein, G. L. Miller, C. Sturtivant, and S.-H. Teng. Approximating center points with and without linear programming. In *Proceedings of 9th ACM Symposium on Computational Geometry*, pages 91–98, 1993.
- [19] T. Coe, Inside the Pentium FDIV bug, *Dr. Dobb's Journal* 20 (April, 1995), pp 129–135.
- [20] T. Coe, T. Mathisen, C. Moler, and V. Pratt, Computational aspects of the Pentium affair, *IEEE Computational Science and Engineering* 2 (Spring 1995), pp 18–31.
- [21] T. Coe and P. T. P. Tang, *It takes six ones to reach a flaw*, preprint.
- [22] J. Conroy, S. Kratzer, and R. Lucas, Data parallel sparse LU factorization, in *Parallel Processing for Scientific Computing*, SIAM, Philadelphia, 1994.
- [23] T. H. Cormen, C. E. Leiserson, and R. L. Rivest, *Introduction to Algorithms*, MIT Press, Cambridge, MA, 1992.
- [24] L. Danzer, J. Fonlupt, and V. Klee. Helly's theorem and its relatives. *Proceedings of Symposia in Pure Mathematics, American Mathematical Society*, 7:101–180, 1963.
- [25] J. Dongarra, R van de Geijn, and D. Walker, A look at scalable dense linear algebra libraries, in *Scalable High Performance Computer Conference*, Williamsburg, VA, 1992.
- [26] I. S. Duff, R. G. Grimes, and J. G. Lewis, Sparse matrix test problems, *ACM TOMS*, 15 (1989), pp. 1-14.
- [27] A. L. Dulmage and N. S. Mendelsohn. Coverings of bipartite graphs. *Canadian J. Math.* 10, pp 517-534, 1958.
- [28] I. S. Duff. Parallel implementation of multifrontal schemes. *Parallel Computing*, 3, 193–204, 1986.
- [29] H. Edelsbrunner. *Algorithms in Combinatorial Geometry*, volume 10 of *EATCS Monographs on Theoretical CS*. Springer-Verlag, 1987.
- [30] D. Eppstein, G. L. Miller, and S.-H. Teng. A deterministic linear time algorithm for geometric separators and its applications. In *Proceedings of 9th ACM Symposium on Computational Geometry*, pages 99–108, 1993.
- [31] C. Farhat and M. Lesoinne. Automatic partitioning of unstructured meshes for the parallel solution of problems in computational mechanics. *Int. J. Num. Meth. Eng.* 36:745-764 (1993).
- [32] J. Fixx, *Games for the Superintelligent*.
- [33] I. Fried. Condition of finite element matrices generated from nonuniform meshes. *AIAA J.* 10, pp 219–221, 1972.

- [34] M. Garey and M. Johnson, *Computers and Intractability: A Guide to the Theory of NP-Completeness*, Prentice-Hall, Englewood Cliffs, NJ, 1982.
- [35] J. A. George. Nested dissection of a regular finite element mesh. *SIAM J. Numerical Analysis*, 10: 345–363, 1973.
- [36] J. A. George and J. W. H. Liu. *Computer Solution of Large Sparse Positive Definite Systems*. Prentice-Hall, 1981.
- [37] A. George, J. W. H. Liu, and E. Ng, Communication results for parallel sparse Cholesky factorization on a hypercube, *Parallel Comput.* 10 (1989), pp. 287–298.
- [38] A. George, M. T. Heath, J. Liu, E. Ng. Sparse Cholesky factorization on a local-memory multiprocessor. *SIAM J. on Scientific and Statistical Computing*, 9, 327–340, 1988
- [39] J. R. Gilbert, G. L. Miller, and S.-H. Teng. Geometric mesh partitioning: Implementation and experiments. In *SIAM J. Sci. Comp.*, to appear 1995.
- [40] G. H. Golub and C. F. Van Loan. *Matrix Computations, 2nd Edition*. Johns Hopkins University Press, 1989.
- [41] L. Greengard and V. Rokhlin. A fast algorithm for particle simulations. *J. Comp. Phys.* 73 (1987) pp325-348.
- [42] L. J. Guibas, D. E. Knuth, and M. Sharir. Randomized incremental construction of Delaunay and Voronoi diagrams. *Algorithmica*, 7:381–413, 1992.
- [43] R. W. Hackney and J. W. Eastwood. *Computer Simulation Using Particles*. McGraw Hill, 1981.
- [44] G. Hardy, J. E. Littlewood and G. Pólya. *Inequalities*. Second edition, Cambridge University Press, 1952.
- [45] D. Haussler and E. Welzl. ϵ -net and simplex range queries. *Discrete and Computational Geometry*, 2: 127–151, 1987.
- [46] N.J. Higham, The Accuracy of Floating Point Summation *SIAM J. Scient. Comput.* , 14:783–799, 1993.
- [47] Y. Hu and S. L. Johnsson. A data parallel implementation of hierarchical N-body methods. Technical Report TR-26-94, Harvard University, 1994.
- [48] M. T. Jones and P. E. Plassman. Parallel algorithms for the adaptive refinement and partitioning of unstructured meshes. *Proc. Scalable High-Performance Computing Conf.* (1994) 478–485.
- [49] W. Kahan, *A Test for SRT Division*, preprint.
- [50] F. T. Leighton. *Complexity Issues in VLSI*. Foundations of Computing. MIT Press, Cambridge, MA, 1983.
- [51] F. T. Leighton and S. Rao. An approximate max-flow min-cut theorem for uniform multi-commodity flow problems with applications to approximation algorithms. In *29th Annual Symposium on Foundations of Computer Science*, pp 422-431, 1988.

- [52] C. E. Leiserson. *Area Efficient VLSI Computation*. Foundations of Computing. MIT Press, Cambridge, MA, 1983.
- [53] C. E. Leiserson and J. G. Lewis. Orderings for parallel sparse symmetric factorization. in *3rd SIAM Conference on Parallel Processing for Scientific Computing*, 1987.
- [54] G. Y. Li and T. F. Coleman, A parallel triangular solver for a distributed memory multiprocessor, *SIAM J. Scient. Stat. Comput.* 9 (1988), pp. 485–502.
- [55] R. J. Lipton, D. J. Rose, and R. E. Tarjan. Generalized nested dissection. *SIAM J. on Numerical Analysis*, 16:346–358, 1979.
- [56] R. J. Lipton and R. E. Tarjan. A separator theorem for planar graphs. *SIAM J. of Appl. Math.*, 36:177–189, April 1979.
- [57] J. W. H. Liu. The solution of mesh equations on a parallel computer. in 2nd Langley Conference on Scientific Computing, 1974.
- [58] P.-F. Liu. *The parallel implementation of N-body algorithms*. PhD thesis, Yale University, 1994.
- [59] R. Lohner, J. Camberos, and M. Merriam. Parallel unstructured grid generation. *Computer Methods in Applied Mechanics and Engineering* 95 (1992) 343–357.
- [60] J. Makino and M. Taiji, T. Ebisuzaki, and D. Sugimoto. Grape-4: a special-purpose computer for gravitational N-body problems. In *Parallel Processing for Scientific Computing*, pages 355–360. SIAM, 1995.
- [61] J. Matoušek. Approximations and optimal geometric divide-and-conquer. In *23rd ACM Symp. Theory of Computing*, pages 512–522. ACM, 1991.
- [62] G. L. Miller. Finding small simple cycle separators for 2-connected planar graphs. *Journal of Computer and System Sciences*, 32(3):265–279, June 1986.
- [63] G. L. Miller, S.-H. Teng, W. Thurston, and S. A. Vavasis. Automatic mesh partitioning. In A. George, J. Gilbert, and J. Liu, editors, *Sparse Matrix Computations: Graph Theory Issues and Algorithms*, IMA Volumes in Mathematics and its Applications. Springer-Verlag, pp57–84, 1993.
- [64] G. L. Miller, S.-H. Teng, W. Thurston, and S. A. Vavasis. Finite element meshes and geometric separators. *SIAM J. Scientific Computing*, to appear, 1995.
- [65] G. L. Miller, D. Talmor, S.-H. Teng, and N. Walkington. A Delaunay Based Numerical Method for Three Dimensions: generation, formulation, partition. In *the proceedings of the twenty-sixth annual ACM symposium on the theory of computing*, to appear, 1995.
- [66] S. A. Mitchell and S. A. Vavasis. Quality mesh generation in three dimensions. *Proc. 8th ACM Symp. Comput. Geom.* (1992) 212–221.
- [67] K. Nabors and J. White. A multipole accelerated 3-D capacitance extraction program. *IEEE Trans. Comp. Des.* 10 (1991) v11.
- [68] D. P. O’Leary and G. W. Stewart, Data-flow algorithms for parallel matrix computations, *CACM*, 28 (1985), pp. 840–853.

- [69] L.S. Ostrouchov, M.T. Heath, and C.H. Romine, *Modeling speedup in parallel sparse matrix factorization*, Tech Report ORNL/TM-11786, Mathematical Sciences Section, Oak Ridge National Lab., December, 1990.
- [70] V. Pan and J. Reif. Efficient parallel solution of linear systems. In *Proceedings of the 17th Annual ACM Symposium on Theory of Computing*, pages 143–152, Providence, RI, May 1985. ACM.
- [71] A. Pothen, H. D. Simon, K.-P. Liou. Partitioning sparse matrices with eigenvectors of graphs. *SIAM J. Matrix Anal. Appl.* 11 (3), pp 430–452, July, 1990.
- [72] Vaughan Pratt, *personal communication*, June, 1995.
- [73] V. Pratt, Anatomy of the Pentium Bug, *TAPSOFT'95, LNCS 915*, Springer-Verlag, Aarhus, Denmark, (1995), 97–107. <ftp://boole.stanford.edu/pub/FDIV/anapent.ps.gz>.
- [74] F. P. Preparata and M. I. Shamos. *Computational Geometry An Introduction*. Texts and Monographs in Computer Science. Springer-Verlag, 1985.
- [75] A. A. G. Requicha. Representations of rigid solids: theory, methods, and systems. In *ACM Computing Survey*, 12, 437–464, 1980.
- [76] E. Rothberg and A. Gupta, *The performance impact of data reuse in parallel dense Cholesky factorization*, Stanford Comp. Sci. Dept. Report STAN-CS-92-1401.
- [77] E. Rothberg and A. Gupta, An efficient block-oriented approach to parallel sparse Cholesky factorization, *Supercomputing '93*, pp. 503-512, November, 1993.
- [78] E. Rothberg and R. Schreiber, Improved load distribution in parallel sparse Cholesky factorization, *Supercomputing '94*, November, 1994.
- [79] J. Ruppert. A new and simple algorithm for quality 2-dimensional mesh generation. *Proc. 4th ACM-SIAM Symp. Discrete Algorithms* (1993) 83–92.
- [80] Y. Saad and M.H. Schultz, Data communication in parallel architectures, *Parallel Comput.* 11 (1989), pp. 131–150.
- [81] J. K. Salmon. *Parallel Hierarchical N-body Methods*. PhD thesis, California Institute of Technology, 1990. CRPR-90-14.
- [82] J. K. Salmon, M. S. Warren, and G. S. Winckelmans. Fast parallel tree codes for gravitational and fluid dynamical N-body problems. *Int. J. Supercomputer Applications*, 8(2):129–142, 1994.
- [83] H. Samet. The quadtree and related hierarchical data structures. *ACM Computing Surveys*, pages 188–260, 1984.
- [84] K. E. Schmidt and M. A. Lee. Implementing the fast multipole method in three dimensions. *J. Stat. Phys.*, page 63, 1991.
- [85] H.P. Sharangpani and M.L. Barton, *Statistical analysis of floating point flaw in the Pentium™ Processor* (1994). <http://www.intel.com/product/pentium/white11.ps>

- [86] H. D. Simon. Partitioning of unstructured problems for parallel processing. *Computing Systems in Engineering* 2:(2/3), pp135-148.
- [87] H. D. Simon and S.-H. Teng. How good is recursive bisection? *SIAM J. Scientific Computing*, to appear, 1995.
- [88] J. P. Singh, C. Holt, T. Tsucha, A. Gupta, and J. L. Hennessey. Load balancing and data locality in hierarchical N-body methods. Technical Report CSL-TR-92-505, Stanford, 1992.
- [89] G. Strang and G. J. Fix. *An Analysis of the Finite Element Method*. Prentice-Hall, Englewood Cliffs, New Jersey, 1973.
- [90] S.-H. Teng. *Points, Spheres, and Separators: a unified geometric approach to graph partitioning*. PhD thesis, Carnegie-Mellon University, School of Computer Science, 1991. CMU-CS-91-184.
- [91] V. N. Vapnik and A. Ya. Chervonenkis. On the uniform convergence of relative frequencies of events to their probabilities. *Theory Probab. Appl.*, 16: 264-280, 1971.
- [92] R. D. Williams. Performance of dynamic load balancing algorithms for unstructured mesh calculations. *Concurrency*, 3 (1991) 457
- [93] F. Zhao. An $O(n)$ algorithm for three-dimensional n-body simulation. Technical Report TR AI Memo 995, MIT, AI Lab., October 1987.
- [94] F. Zhao and S. L. Johnsson. The parallel multipole method on the Connection Machines. *SIAM J. Stat. Sci. Comp.*, 12:1420–1437, 1991.